THE UNIVERSITY OF CHICAGO

POLYMERIC DELIVERY APPROACHES FOR THE MODULATION OF HUMORAL IMMUNITY

A DISSERTATION SUBMITTED TO
THE FACULTY OF THE PRITZKER SCHOOL OF MOLECULAR ENGINEERING
IN CANDIDACY FOR THE DEGREE OF
DOCTOR OF PHILOSOPHY

BY
RACHEL PATRICIA WALLACE

CHICAGO, ILLINOIS
MARCH 2023

To my grandmother, Joanna Shaver, for sharing with me her love of science

"I believe that fortitude is key. More than anything, be consistent. Go at it. Go at it. Go at it. When you succeed, don't forget the responsibility of making someone else succeed with you."– Antonia Novello, Former Surgeon General

TABLE OF CONTENTS

LIST OF FIGURES

LIST OF TABLES

ACKNOWLEDGMENTS

As I finish up my graduate school experience, I'm convinced now more than ever that science, as well as life, is infinitely better as part of a team. There are so many people I have been fortunate to have on my team and this PhD would not have been possible without them.

First, I want to thank my advisor Prof. Jeffrey Hubbell. I'm incredibly grateful that you were willing to give me a place in your lab. I am continually inspired by your curiosity and dedication to developing technologies with patients in mind. I have learned so much about innovation, translation and scientific communication from you. Thank you for fostering such an innovative and collaborative space where we are able to be creative, take risks, and forge our own paths. I also want to thank my committee members Prof. Cathryn Nagler and Prof. Aaron Esser-Kahn. Thank you for your guidance and support throughout this process.

The projects I present here were far from a solo effort. Thank you Lisa Volpatti, Shijie Cao and Ruyi Wang for your co-leadership throughout the SARS-CoV-2 project and for being great role models of scientific expertise and collaboration. Large experiment days would not have been possible during COVID without help and I am extremely grateful for Taylor Gray, Aaron Alpar, Nick Mistrousis, Prisci Briquez, Andrew Tremain, Maria Stella Sasso, Erica Budina, Tiffany Marchell and others for the amazing effort of passing off experimental samples across three different work shifts. The p(Man) project would not have been possible without Scott Wilson, the genius behind the glycopolymer conjugate design, or Kym Brunggel's initial work on anti-drug antibodies. Thank you Michal Raczy and Anna Slezak for being my go-to chemists as I continued the project. I am also grateful to Ani Solanki and Mindy Nguyen for being animal whisperers and the hardest working, most reliable people I know.

I would not have become the scientist I am without guidance from many mentors along the way. Thank you Elyse Watkins for taking me under your wing when I was a first-year who could barely pipette, and for teaching me both about idea generation and experimental design, as well as where the best restaurants and cocktails can be found in Chicago. I am

grateful to call you a role model and a friend. Thank you Andrew Tremain for teaching by doing and trusting me with experiments and projects before I trusted myself. Thank you Lisa Volpatti for working with me both as a peer and a mentor, and for being a great role model of a fearless and confident scientist.

The best part about working in the Hubbell lab is the people. I have been so lucky to be surrounded by friends throughout the heart-wrenching up and downs of research. Thank you Aaron for being a friend from the beginning and your generous acceptance when I steal your bench and fridge space. I'll miss working next to you every day and discussing your crazy (genius?) ideas. Thank you Taylor for your never-ending generosity and kindness and for always being up to see a musical. Thank you Jenni for your friendship and collaboration in and out of lab. Thank you Abby and Kirsten for making me a mentor as well as being great friends. Thank you to the entire Hubbell lab throughout the years, it has been a joy to work with you all! Finally, thank you to Suzana Gomes for being a lab mom to all of us. Thank you for making lab feel like a family, listening when I needed to talk, cooking amazing food, and solving any problem I thought was impossible.

Balance is important and I'm extremely grateful to my friends outside of lab for reminding me of this. Thank you Veronica for being my first grad school friend and my partner in crime during the rough beginning. Thank you Ande and Paulina (Misty and Yzmo) for being the best roommates, COVID companions, and brunch buddies. I am so grateful for all the laughs and advice you have given me over the years. Thank you Matt for your endless love and support, everything is better with you by my side. Thank you to my long-distance friends who have been by my side figuratively, if not literally, for over a decade. Erin, Taylor, Anna, Victoria, Mia, Colleen you are my rocks, thank you for letting me crash on your couches when I needed an escape.

I would not be the person I am without my family. Thank you Mom and Dad for raising me with the belief that I could accomplish anything I put my mind to and acting as great role models of hard work and intelligence, as well as selflessness. Thank you Selena, Katie

and Luke, for being both siblings and friends. You all continuously inspire me in your own unique ways. Thank you to my grandparents for their endless love, support and kind words of encouragement. Finally, thank you to Grammy and my aunt Mary, my very first role models of strong women in science.

ABSTRACT

The purpose of this dissertation is to investigate the use of novel polymeric nanomaterials for modulation of the humoral immune system. I focus on developing materials for targeted antigen delivery in order to alter the subsequent antigen-specific antibody response for vaccination and tolerance-inducing therapeutics.

In Chapter 1, I review the immune pathways involved in mounting an antibody response including the roles of antigen presenting cells (APCs), T cell and B cells. I introduce the fields of vaccination and antigen-specific tolerance and highlight the open questions involving antigen delivery and recognition by the immune system. Reflecting on these questions, I discuss the value of engineered nanomaterials as tools for better modulating these responses.

In Chapter 2, I build upon previous work and engineer APC-targeted polymersomes for use as a COVID-19 vaccine. Using the receptor binding domain (RBD) of the SARS-CoV-2 spike protein as the target antigen, I formulate RBD-encapsulated (RBDencap) and RBD-surface decorated (RBDsurf) polymeromes for co-administration with adjuvanting monophosphoryl-lipid A (MPLA)-encapsulted polymersomes. I analyze the resulting immune response to vaccination and compare the effects of encapsulated and surface-bound delivery of RBD to find that vaccination with RBDsurf alone elicited strong neutralizing IgG responses as well as RBD-specific CD8+ T cell responses.

In Chapter 3, I present a mannose glycopolymer conjugate (p(Man)) for increased antigen delivery to the tolerogenic microenvironment of the liver. I investigate the effects of p(Man)-antigen delivery on antigen-specific T and B cell responses. Using uricase as a model immunogenic therapeutic, I demonstrate the capacity of p(Man)-uricase pre-treatment to reduce the uricase-specific antibody response upon future antigen experience. Lastly, I probe the effects of antigen post-translational glycosylation on p(Man)-antigen treatment and discuss the use of the *Uox-/-* mouse as a potential model of anti-drug antibody-mediated loss of therapeutic efficacy.

In Chapter 4, I discuss the conclusions and future directions of both projects.

CHAPTER 1

BACKGROUND AND INTRODUCTION

1.1 The innate and adaptive immune system

The immune system is a complex collection of highly evolved cells and signaling molecules specialized to identify and eliminate invading pathogens from the body. This system can be divided into two main responses: the innate response and the adaptive response. The innate immune response provides a first-line of defense against pathogens, engulfing invaders non-specifically. The innate immune response also recruits the adaptive immune system via signaling molecules to activate a more pathogen-specific response. The adaptive immune response is less immediate, but more specialized. It is composed of T cells and B cells expressing highly variable receptors. These receptors can bind to and recognize antigens, smaller fragments of the invading pathogens, with unique specificity. Antigen-specific adaptive cells help to activate and mount a more efficacious attack against pathogens. Once the response is over, the activated T and B cells differentiate into long-lived memory cells capable of quickly re-activating if the pathogen is encountered again(1).

An important set of cells in the innate immune response are antigen presenting cells (APCs). Dendritic cells, as well as macrophages, and B cells can act as APCs(2). Under steady state conditions, APCs uptake antigens from the surrounding environment and process these antigens into peptide fragments. APCs present the peptide fragments on their surface MHC-II molecules to T cells, which recirculate researching for their cognate peptide:MHC (pMHC) complex specific to their T cell receptor (TCR). A subset of APCs, dendric cells (DCs), play a critical role in the activation of T cells. In order to identify pathogens, DCs highly express receptors specific to evolutionarily conserved features of known pathogens called pathogen-associated molecular patterns (PAMPs), including bacterial flagella and cell wall components, and viral double stranded RNA(3). These receptors are known as pattern recognition receptors (PRRs) and include toll-like receptors (TLRs), c-type lectin re-

ceptors (CLRs), nucleotide oligomerization domain (NOD)-like receptors (NLRs), retinoic acid-inducible gene-I (RIG-I)-like receptors (RLRs), and absent in melanoma-2 (AIM2)-like receptors (ALRs)(4). When DCs and other APCs bind PAMPs through these receptors, they activate and upregulate co-stimulatory surface molecules like CD80 and CD86 and pro-inflammatory cytokines like TNFα and IL-6(5). These signals are required for T cell activation upon its binding to the presented pMHC-II.

The adaptive immune response is mediated by B and T cells. B cells recognize the three-dimensional structure of an antigen through their B cell receptor (BCR) and thus mount responses against specific proteins, polysaccharides and other structures. T cells in contrast do not recognize full antigen, but can recognize a small peptide fragment when it is displayed on a major histocompatibility complex (MHC) on an antigen presenting cell. CD4+ T cells are directors of downstream antigen-specific responses and can recognize exogenously produced extracellular peptides presented on MHC class II on specialized antigen presenting cells (APCs). Cytotoxic CD8+ T cells can recognize endogenously produced peptide presented on MHC class I on nucleated cells. The presentation of extracellularly produced antigen on MHC class I is known as cross-presentation and is limited to a specialized subset of APCs(6).

In order to be activated, T cells need three steps or 'signals'. First, the T cell's TCR binds a pMHC expressed on the surface of a DC. TCR-pMHC binding is known as 'signal 1'. Second, CD28, a co-receptor on T cells, must bind the cognate B-7 family molecules on DCs. These molecules are upregulated on DCs in response to PRR engagement(7). Productive signaling through the TCR and CD28 triggers the phosphorylation of associated immunoreceptor tyrosine-based activation motifs (ITAMs) in the cytoplasm and downstream signaling through the Ras-extracellular signal-related kinase (ERK)-activator protein (AP)-1 pathway, the inositol triphosphate (IP3)-Ca2+-nuclear factor of activated T cells (NFAT) pathway, the protein kinase C (PKC)θ-IκB kinase (I$\kappa\kappa$)-nuclear factor (NF)-κB pathway, and the tuberous sclerosis complex (TSC)1/2-mammalian target of rapamycin (mTOR) pathway(8).

Third, T cells need stimulation by cytokines secreted by the DCs. Once activated, T cells will differentiate into a variety of effector cell fates. CD4+ T cells can differentiate into Th1, Th2, Th17, Tfh or Treg pathways to promote different types of antigen-specific immune responses(9). CD8+ T cells can be activated to become cytotoxic T lymphocytes (CTLs) through effective antigen presentation to CD8+ T cells by APCs on MHC class I(10; 11). The pathway ultimately taken by a T cell will be dependent on the cytokines produced by the DCs and present in the environment(12).

1.2 The humoral immune response

The humoral immune response is a portion of the adaptive immune response first recognized by Ehrlich in 1908(13). Ehrlich theorized that antibodies generated by the immune system in response to invading pathogens and toxins could specifically neutralize these foreign entities upon secondary exposure. Our understanding of how cells generate these highly specific antibodies through proliferation and activation in response to antigen was further refined by Burnet's 1960 theory of clonal selection(14) and by 1987 Tonegawa's discovery of Ig chain gene rearrangement as the molecular mechanism allowing for the wide diversity of antibody molecules(15).

The role of the adaptive immune response is to mount highly specialized attacks against specific pathogen-associated antigens while maintaining tolerance to antigens associated with innocuous self and commensals. An important element in the adaptive immune response is the production of highly specific antibodies capable of recognizing and binding to three-dimensional antigens. The recognition of specific antigens is mediated though their binding to a highly variable region of the antibody. A vast antibody repertoire with the potential to bind a near infinite variety of epitopes is generated through gene rearrangement during B cell development(16; 17). The binding of an antibody to its target can result in several outcomes. The antibody may simply neutralize the function of the antigen, or elicit effector functions through Fc receptor binding. The conserved region of the antibodies, the Fc region,

determines the antibody's isotype and its specificity to different Fc receptors. The antibody isotypes include IgD, IgM, IgA, IgE and IgG. IgD is expressed by naive B cells, but the role of IgD antibodies is still unclear. IgM and IgA are important for mediating complement activation and can localize to mucosal barriers(18). IgE binds FcϵRI on the surface of basophils and mast cells, causing their degranulation upon recognition of its cognate antigen and antibody cross-linking(19). IgG is the most common isotype in serum and binds to a variety of FcγR leading to a variety of functions including antibody-dependent cytotoxicity and opsonization as well as immune-modulatory effects(20).

1.3 The initiation of an antibody response

There are two scenarios in which the immune system can mount an antibody response, one which relies on help from T cells (T cell dependent, TD) and one which does not (T cell independent, TI). Both methods lead to the activation of naïve B cells. B cells are lymphocytes which mature in the bone marrow and express a BCR on their surface. The BCR is a surface-bound form of an antibody immunoglobulin. During the course of maturation the B cells undergo stages of regulatory control to eliminate self-reactive BCR. A mature, naïve B cell will recirculate through the secondary lymphoid organs (SLO) until bound antigen signals through its BCR. Antigens are presented to B cells in the SLO by follicular dentridic cells (FDCs) which localize to the follicle and capture and display antigens on their surface via immune complexes(21; 22).

1.3.1 T cell independent response

B cells can be activated without T cell help if the antigen has sufficient multivalency to cross-link and trigger signaling through the clustering of BCRs, leading to engagement of the cell cycle for differentiation(23). Activating cytokines BAFF and APRIL, produced by innate cells, can also increase the signaling upon antigen recognition as can signaling of

PAMPs though TLRs on the B cell's surface. TI responses typically result in differentiation of B cells into a short-lived antibody-secreting plasmablasts, but can form long lived plasma cells in some cases(24). Additionally, since class-switch recombination (CSR) is necessary for Ig isotype switching occurs in germinal centers, TI responses are characterized by primarily IgM and occasionally carbohydrate-specific IgG3 responses(25; 26).

1.3.2 T cell dependent response

In contrast to TI responses, TD B cell responses can result in longer-lived and higher affinity antibody responses through the differentiation of B cells into long-lived plasma cells and formation of germinal centers where somatic hypermutation (SHM) and class-switch recombination (CSR) can occur. A TD response begins when a naïve CD4+ T cell recognizes its cognate peptide antigen presented by a dendritic cell on MHC-II. The signals encountered by the T cell upon binding of the TCR will determine if it will upregulate Bcl6 and become a T follicular helper (Tfh) cell, primed for B cell activation, or a non-Tfh effector cell such as Th1, Th2, Th17 or Th9(27). IL-2 is the most potent inhibitor of Tfh differentiation, while IL-6 and ICOSL signaling are involved in their differentiation(28; 29). Unlike other effector T cell fates, Tfh cells will stay in the secondary lymphoid organ and migrate to the follicle/ T cell border to interact with B cells(30). In the follicle, B cells encounter antigen displayed on FDCs. An antigen which binds to the BCR with sufficient affinity will be endocytosed and peptide from the antigen will be displayed on the MHC-II molecules for presentation to Tfh cells(31). When a Tfh cell recognizes its cognate pMHC on a B cell, it initiates signals for B cell activation. To activate B cells, Tfh will secrete IL-4 and IL-21 and signal to the B cells through CD40L binding(32). T:B cell interactions generate feed-forward loops as B cells signal through T cells via ICOSL, which subsequently promotes upregulation of CD40L on T cells, upregulating ICOSL on B cells and so on(33).

Once a B cell is activated by a Tfh it can undergo a number of fates including differentiation into an antibody-secreting plasma cell, germinal center B cell, or a memory B

cell(34). The plasma cells arising from early B cell response without the germinal center are short-lived and referred to as extrafollicular, whereas germinal centers give rise to long-lived plasma cells. However, the factors which determine whether a PC is long-lived are not fully understood(35). Entry into the GC response is dependent on the extent of T cell help received(36–38). In the germinal center, the B cells will go through multiple cell cycles of division in the "dark zone" of the follicle away from the T cells and FDCs. During these cell cycles, dark zone B cells have high expression of AID and the error prone DNA polymerase η which induce double-stranded breaks and point mutations in the variable regions of their BCR leading to a wide diversity of resulting B cell clones(34). CSR can also occur at this point as the subtype of BCR can be changed from IgM to IgG (including IgG1, IgG2, IgG3 and IgG4 (in humans)), IgE, or IgA. After a specified number of divisions and mutations, the B cells will migrate back to the "light zone" near the T cells and FDCs(39). These B cells then compete against each other in a Darwinian manner for survival. There are two potential mechanisms for germinal center selection of B cells. One potential mechanism, based on the demonstrated importance of the BCR, is that higher affinity B cells will outcompete other B cells for the antigen displayed by FDCs and undergo stronger signaling through the BCR, favoring their survival(40; 41). Another, more supported, mechanism is that higher affinity B cells will outcompete the others for antigen, leading to more antigen-specific peptide displayed on their surface MHC-II and more T cell help, which ultimately favors their survival and return to the dark zone(42–45). At this point, B cells that do not receive survival signals will undergo apoptosis(46). The intensity of the T cell response correlates with the speed and number of cell cycles a B cell experiences in the dark zone leading to a clonal expansion of high affinity B cells(44; 47). In this manner GCs select for higher affinity B cells, leading to the development of a higher affinity B cell response.

After undergoing SHM and CSR in the GC, various B cells will differentiate into memory B cells or antibody-secreting plasma cells. The factors that determine this differentiation are actively under investigation. Higher affinity of the BCR to antigen gives rise to a stronger

PC response(40). Lower affinity B cells may become memory B cells. These cells are long-lived and relatively quiescent, however they can be rapidly reactivated by subsequent antigen exposure(48; 49). After re-exposure, a subset of memory B cells will differentiate into PCs and migrate to the blood to then become LLPCs, while others return to germinal centers for further affinity maturation.

1.3.3 Non-traditional B cells

Herein we have focused our discussion on B2 B cells. Another important subset of B cells are the B1 B cells. These B cells develop during fetal and neonatal periods and are self-renewing(50). After development they become enriched in the peritoneal and pleural cavities(51). B1 B cells are considered to be innate-like and exist in a pre-activated state(52). Upon exposure to their cognate antigen they can rapidly differentiate into antibody-secreting cells. Unlike the wide diversity of B2 BCRs, B1 repertoires are enriched for the recognition of specific carbohydrates and lipids commonly expressed on life-threatening microbes(53). The IgM antibodies expressed by B1 cells are the dominant contributors to natural IgM circulating antibodies that act as a first line of defense against pathogens and can augment follicular B cell responses(54).

Regulatory B cells (Bregs) are a family of B cells that secrete predominantly IL-10, but also other immunoregulatory cytokines such as TGF-β and IL-35(55). The role of these cells is an active area of investigation. Genetic models have shown that mice lacking B cells, and specifically IL-10-producing B cells, result in excessive inflammation(56; 57). Bregs have also been shown to suppress inflammation in colitis, experimental autoimmune encephalitis (EAE) and arthritis(57–59). Bregs have been identified among B cells at different stages of maturation and differentiation including early transitional B cells and highly differentiated plasmablasts and plasma cells(60–62). There is strong evidence that Breg cells differentiate in response to increased inflammation(58; 63).

1.3.4 Antigen-specific immunogenicity

Factors contributing to the strength and duration of an antibody response are still under investigation. Differences between antigens and their trafficking are known to result in different extents of immunogenicity. Antigen valency, density and duration of antigen exposure all contribute to the magnitude of the B cell response(64–69). Self-assembling protein nanoparticles have been used to increase the magnitude and quality of an antibody response in vaccination through multivalent antigen presentation(70–74). This approach has proved effective for promoting antibody responses against antigens such as influenza(75), and RSV(71), however it has also been shown to mount antibody responses to the scaffold itself rather than the antigen of interest(74; 76). This is dependent on the relative immunodominance of the different antigen epitopes. In circumstances when the scaffold antigens are immunodominant, methods to mask these antigens such as pegylation to prevent recognition by BCRs have been shown to be effective at mounting the antibody response to the antigen of interest(70; 77). The relative immunodominance of an antigen ultimately depends on a combination of variables such as B cell precursor frequency, B cell receptor affinity for antigen, and antigen avidity(78).

1.4 Regulation of autoreactive B cell responses

Regulatory checkpoints exist throughout the B cell development and activation processes to ensure that a B cell/antibody response is not mounted against self or commensal antigens. These include both B cell intrinsic(79–83) and B cell extrinsic mechanisms(84–87). The B cell intrinsic mechanisms prevent self-reactive pre-mature B cells from becoming fully mature and are dependent on BCR and TLR signaling(88). B cells will encounter antigen during development in the spleen and will as a result tune the responsiveness of their BCR signaling by downmodulating surface expression of IgM but not IgD and modifying basal calcium levels(89). Autoreactive B cells thus still exist in the mature repertoire and their

functional unresponsiveness acts along a continuum to regulate them(90). In the GC and in the periphery, B cell extrinsic mechanisms predominantly prevent activated B cells from becoming self-reactive. Pro-apoptotic receptor Fas is expressed on B cells in the GC and is required to prevent rogue B cells from differentiating into autoreactive antibody-secreting PCs(91). Self-antigen binding can censor GC output but only when these antigens are expressed in or near the GCs and not in tissue-specific areas like the kidney or liver(92). Other mechanisms to suppress autoreactive B cells in the periphery are largely T cell-dependent and specifically require regulatory Tregs(93). T cell intrinsic mechanisms such as deletion, anergy, and exhaustion also prevent the activation of self-reactive Tfh cells thus preventing T cell help and strong autoreactive antibody responses. A subset of regulatory Tfh cells (Tfr) can also inhibit the GC and temper the activating Tfh effect by competitng with Tfh cells for B cell binding and producing anti-inflammatory cytokines such as IL-10.

1.5 T cell intrinsic tolerance mechanisms

The aberrant activation of T cells against self or innocuous foreign antigen can have disastrous consequences leading to autoimmunity, allergy and other disease states. This damage is compounded via the critical role of T cells in B cell activation. Therefore the mechanisms of T cell tolerance are critical for the development of healthy T cell, B cell and antibody responses. T cell tolerance occurs in two stages; central tolerance occurs during thymocyte development in the thymus, and peripheral tolerance occurs once mature thymocytes encounter their cognate antigen in the periphery(94).

1.5.1 Central tolerance

T cell development begins when bone marrow-derived precursor cells home to the outer portion of the thymus, the cortex. In the cortex developing thymocytes will become CD4+ CD8+ double-positive (DP)thymocytes and undergo somatic recombination of TCR genes,

resulting in a broad repertoire of distinct TCRs with random specificity(94). These DP TCRs will interact with self-peptide MHC presented on the surface of APCs. If binding is not sufficient to signal through the TCR, the T cells will die(95). This positive selection ensures that the resulting T cell compartment will be able to recognize antigens presented on self-MHC. However, if the binding of the TCR to self-peptide MHC is too strong, the T cells will also die, in a process called negative selection or clonal deletion to remove highly self-reactive TCRs from the repertoire(96; 97). The self-antigens presented on MHC for positive and negative selection in the cortex is limited to ubiquitously expressed antigens. Self-antigens expressed in a tissue-specific manner outside of the thymus will not be present in the cortex(98). These tissue-specific antigens can, however, be expressed by unique thymic endothelial cells (mTECs) in the inner medulla of the thymus(99). Once DP thymocytes are positively selected they commit to either CD4+ or CD8+ single-positive (SP) thymocytes and migrate into the medulla. In the medulla they encounter tissue-specific self-antigens expressed by mTECs and if the affinity is too high they can undergo deletion(100; 101). An alternative fate for thymocytes that recognize peptide MHC is to differentiate into regulatory T cells(102; 103). The signals that determine if a self-reactive thymocyte will undergo deletion or differentiation into Tregs have not yet been fully elucidated. TCR signaling strength does play an important role(104–106). Some data suggest that high affinity TCR-pMHC interactions lead to deletion while intermediate affinity interactions lead to Treg differentiation(107; 108). There may also be a propensity for DP thymocytes in the cortex to undergo deletion upon recognition of self-peptide MHC while SP thymocytes in the medulla favor a Treg fate(109; 110). Alternatively mathematical models suggest that clonal deletion is the result of a single strong TCR signaling event, whereas Treg differentiation is the result of multiple weaker signaling events over time(110).

1.5.2 Peripheral tolerance

Within the thymus it is impossible for T cells to self-select against all harmless antigens they could encounter. In the periphery additional regulatory checkpoints are required to establish tolerance against antigens such as food antigens, developmental antigens and commensal microbial antigens. Tolerogenic T cell fates in the periphery include anergy, exhaustion, and death(111). Regulatory T cells can also be induced in the periphery and provide dominant tolerogenic control of other immune cells.

Anergy is a dysfunctional T cell state that is the direct result of TCR signaling in a naïve cell in the absence of co-stimulation. T cell activation requires recognition of its cognate pMHC to initiate TCR signaling along with a second signal mediated by CD28 ligation. In the absence of a second signal, defective RAS-mitogen-activated protein kinase (MAPK) signaling impairs translation of AP-1 into the nucleus and results in partner-less NFAT signaling(112–115). These signaling pathways result in differentiation into an anergic state. Hallmark functional changes of anergy include reduced production of IL-2, IFNγ and TNFα in response to TCR stimulation, and defects in cell cycle progression(116–118). Anergic CD4+ T cells can be identified as CD44hi CD73hi FR4hi and in mice are found to express Lag3 and 4-1BB(119; 120). Anergy is long-lasting but reversible. Maintenance of anergy requires prolonged exposure to the antigen, in the absence of antigen T cells will slowly recover their functional responsiveness(116–118).

Whereas anergy is a tolerogenic T cell state arising from naive T cells, exhaustion is a tolerogenic T cell state arising from activated T cells. Exhaustion occurs when a T cell is activated by chronic signaling through its TCR along with appropriate co-stimulation. As the stimulation persists, memory T cells fail to develop properly and are functionally compromised(121–123). Features of exhausted T cells include decreased cytokine production and high levels of inhibitory receptor expression including PD-1, Lag3, TIGIT, CD38, CD39 and TIM3(123). Exhausted T cells also exhibit altered metabolic and transcriptional states

and express transcription factor TOX(124; 125).

Aberrantly activated T cells can also undergo deletion in the periphery. Similarly to anergy, deletion is the result of TCR stimulation in the absence of co-stimulation(126). The factors determining whether a T cell will become anergic or undergo deletion are not fully elucidated. After initial TCR activation without co-stimulation, T cells will rapidly proliferate and the majority will undergo apoptosis while a minority become anergic(127; 128). Cell death via deletion is mediated by an intrinsic pro-apoptotic family member BIM and is distinct from extrinsic pathways of apoptosis such as FAS and other death receptors(129; 130).

1.5.3 Regulatory T cells

The previous T cell tolerance mechanisms discussed can be classified as "recessive" tolerance mechanisms whereby the self-reactive T cells are removed or impaired before they can induce an immune response. Conversely, the differentiation of self-reactive T cells into Treg fates is a "dominant" tolerance mechanism. These cells have the capacity to actively suppress immune responses against their cognate antigen. There are two types of Tregs: thymic-derived nTregs and peripherally-derived pTregs. Both Tregs require FoxP3 as the lineage master-regulator for Treg cell development and suppressive activity(131). nTregs develop initially in the thymus after stimulation with self-antigen along with signaling from cytokines and co-stimulatory molecules in the thymus. pTregs, in comparison, differentiate from naïve T cells in the presence of TGF-β in the periphery(132). Both classes of Tregs employ a number of mechanisms of suppression against both conventional T cells as well as APCs. Tregs can directly suppress conventional T cells through the production of inhibitory cytokines including IL-10, TGF-β and IL-35(133; 134). They can also use metabolic disruption mechanisms including IL-2 sequestration through their high expression of CD25(135) and employ endonucleases such as CD73, and CD39 to convert extracellular ATP, an inflammatory signal, into adenosine triphosphate into adenosine(136). Adenosine then binds the surface of target

cells, leading to the increase of intracellular cAMP and triggering of downstream suppressive mechanisms. Tregs can also perform cytolysis of target cells through their production of granzymes A and B(137). Mechanisms by which Tregs suppress DCs include CTLA-4 and PD-1 receptor engagement to down-regulate CD80 and CD86 on the surface of DCs as well as depleting cognate peptide-MHC class II from the surface of DCs.

Using the suppressive mechanisms described above Tregs can effectively control a humoral immune response by suppressive the activation of APCs and other T cells, limiting available T cell help to B cells. They can also directly suppress B cells. Treg cells can be found in the T-B border of follicles and within germinal enters and suppress both the Tfh cells and the B cells directly in order to control antibody responses(138; 139). Furthermore, studies have also shown that Treg depletion leads to dysregulated antibody production(140) and Treg transfer reduces autoantibody responses in autoimmune models(141).

1.6 Antibodies in health and disease

Our understanding of antibody biology has important implications for human health and is essential for development of novel vaccines and therapeutics. The principle of vaccination was discovered in parts of China and India when it was noticed that inoculation with smallpox pustules could induce a mild infection and prevent more severe disease(142). Since that time, vaccines against deadly diseases such as polio, diphtheria, measles, mumps, pertussis, rubella and tetanus have led to the eradication or extensive reduction of these diseases worldwide(143). There are currently vaccines against 32 different diseases licensed by the FDA and new vaccines are actively under development(144). Antibodies play a large role in the efficacy of such vaccines. High levels of serum antibodies have been a hallmark of protective immunity following vaccination(145). The development of neutralizing antibodies capable of binding a virus in a manner that prevents its invasion into host cells is particularly protective against many viral infections. Duration of an antibody response also impacts vaccine efficacy. Ideally antibodies would be long-lasting to impart life-long protection. Long-lasting protection is

the combined result of the generation of long-lived plasma cells, which persist for years in the bone marrow, continuously secreting high levels of antibodies, and memory B cells, which retain the ability to quickly differentiate into antibody secreting cells upon recognition of their antigen(146). To generate a lasting, high affinity, neutralizing, antibody response is the goal of many vaccines, however the mechanisms by which vaccines prevent infection are not necessarily the same by which infection is resolved. Recovery from infection relies heavily on the induction of both a cellular immune response and a humoral one. In recent years, more effort has been placed on generating a strong T cell response alongside a strong antibody response to vaccinate against highly mutating viruses as well as cancer(147).

The diverse repertoire of antibody specificity enables valuable protection against pathogens, but can also be pathogenic and lead to autoimmunity, allergy and hypersensitivity when the specificity is directed against a self-antigen. Autoimmune diseases are caused by self-recognizing antibodies in a number of ways. Antibodies can interfere with the function of the target molecule such as the acetylcholine receptor (AChR) and muscle-specific tyrosine kinase (MuSK), leading to myasthenia gravis(148), or aquaporin 4 (AQP4) leading to neuromyelitis optica spectrum disorders (NMOSD)(149). Alternatively, systemic lupus erythematosus (SLE) is a disease resulting in the formation of antibodies specific to nucleic acids and their associated proteins(150). Binding of these antibodies leads to the formation of immune complexes which deposit in organs to induce inflammation and tissue damage. B cells can also play a role in disease progression without directly generating pathogenic antibodies. Type 1 diabetes is associated with B cells recognizing self-antigen, which can present self-antigen to T cells on MHC-II leading to activation of a T cell response(151).

Antibody responses against non-self-antigens can also result in pathology. Food allergy, allergic rhinitis and allergic asthma are caused by allergen-specific IgE, which upon binding of its antigen and cross-linking of cell-surface bound IgE leads to the degranulation of basophils and mast cells which secrete pro-inflammatory molecules and proteases, leading to inflammation and anaphylaxis. Pathogenic antibody responses can also be generated against

protein-based therapeutics or biologics. Unlike traditional small molecule drugs, novel protein and viral vector based therapeutics can be recognized by the immune system as foreign and elicit an immune response. This immune response primarily manifests itself as an anti-drug antibody (ADA) response(152). The presence of ADAs leads to a number of adverse effects including loss of therapeutic efficacy, hypersensitivity reactions upon administration and even life-threatening anaphylaxis.

In order to develop novel treatments to mitigate these antibody-mediated pathologies of autoimmunity, allergy, and hypersensitivity as well as develop next generation vaccines against deadly diseases such as HIV, it is important to understand the factors leading to different types of humoral immune responses and ways to engineer them.

1.7 Engineering strategies for vaccination and tolerance

As collective understanding of the factors which dictate the activation and suppression of antibody responses has developed, a variety of engineering strategies have also emerged to fine-tune these responses. These technologies, which seek to increase the epitope-specificity, strength, and duration of an antibody response, have been employed to design more effective vaccines. A similar but distinct class of technologies have been employed to activate the regulatory elements of the humoral response to prevent or diminish an unwanted antibody response to prevent ADAs and treat autoimmune diseases.

1.7.1 Vaccines

The development of vaccines and mass vaccination programs has been one of the greatest achievements of public health to date. The development of vaccines against smallpox, polio, measles, and other deadly diseases has saved more than 10 million lives since the mid-1960s(153; 154). In this time the technology used to develop new vaccines has progressed from simple attenuation and inactivation of a pathogen to new technologies such as

nanoparticle and nucleic-acid based platforms. Certain types of pathogens, however, have evaded humanity's best vaccination efforts. Pathogens that resist sterilizing immunity after natural infection, that mutate frequently with high variability, and that contain intracellular lifecycles necessitate the development of novel vaccination strategies(155).

1.7.1.1 History of vaccine design

The first vaccines developed in the mid 20th century were developed using either attenuated or inactivated forms of the pathogen. Attenuated vaccines contain a live strain of the virus or bacteria that has been extensively cultured *in vitro* until it mutates sufficiently and is no longer harmful or infectious in humans. Examples of attenuated vaccines include those against influenza(156) and the Sabin vaccine against polio(157). These vaccines are advantageous, because, while no longer virulent, the pathogens maintain their native antigens and capacity to activate an immune response. Attenuated vaccines, however, contain a live pathogen and cannot be administered to immunocompromised individuals. Furthermore the culturing required to generate a sufficiently attenuated pathogen can be time-consuming or impossible if a pathogen is not amenable to *in vitro* cell culture(155). To address these concerns, inactivated pathogens were also used in traditional vaccines. These pathogens were inactivated after exposure to chemicals or elevated temperatures such that they can no longer replicate. Inactivated vaccines are safer to administer than attenuated vaccines, however they are substantially less immunogenic and may require multiple booster administrations to generate a protective immune response(158; 159). The Salk polio vaccine(160), hepatitis(161), and rabies(162) vaccines are examples of inactivated vaccines. Inactivated vaccines can be challenging to develop as the method of inactivation must eliminate replication capacity while maintaining the native antigen integrity. If the antigens are somehow denatured or slightly altered, they may illicit an immune response that is not specific to the native pathogen, limiting efficacy.

To ensure safety and incorporate greater control over the immune response to a pathogen,

subunit vaccine development became an area of active research. Subunit vaccines do not contain an entire intact pathogen, but instead are composed of specific antigens to more narrowly target the immune response. Powerful tools have been developed to aid in antigen selection and design. Genomic sequencing of pathogens and bioinformatic techniques have enabled researchers to identify conserved antigens on the surface of viral and bacterial genomes that would be unlikely to mutate and evade protective responses(163; 164). Machine learning tools have been developed to identify potential T cell and B cell epitopes to maximize the immunogenicity(165–167). The specific antigens identified using these tools can be reliably produced and purified due to the development of recombinant protein production techniques. Structural analysis of these antigen epitopes along with antibodies generated against them can be used to determine the best antigens to use for generating neutralizing antibody responses(168; 169).

The isolated antigens engineered for subunit vaccines lack PAMPs and are often much less immunogenic than the intact pathogen. Therefore, successful immune activation requires co-administration with an adjuvant molecule which can signal to pro-inflammatory immune mechanisms. Aluminum salts such as aluminum hydroxide, aluminum phosphate and alum precipitated materials have been the most extensively used adjuvants. TLRs are the targets of most novel adjuvant development due to their role in increasing the antigen presentation to and activation of T cells(170). An example of a clinically successful subunit vaccine is the HepB vaccine which is composed of hepatitis B surface antigen (HBsAg) along with either an aluminum adjuvant or a TLR9-activating cytidine-phosphate-guanosine oligodeoxynucleotide (CpG)(171).

1.7.1.2 Nanomaterials as emerging strategies for antigen delivery

Subunit vaccines are much safer and faster to develop than traditional attenuated pathogens. Removing an antigen of interest from the native context of its pathogen, however, dramatically changes how the immune system encounters the antigen. In the native context, antigens

are displayed in a highly repetitive fashion, whereas in a subunit vaccine, antigens are often monomeric. Native pathogens provide many endogenous PAMPs, whereas subunit vaccines typically employ a singular adjuvant. Uptake of a native pathogen often results in endosomal escape signaling, whereas phagocytosis of subunit vaccine antigens creates no such help. Combined, these factors limit subunit vaccine immunogenicity.

To mitigate these concerns, novel delivery approaches are used to mimic the immune system's encounter of a native pathogen. Nanomaterials are a promising strategy for antigen and adjuvant delivery and improve the efficacy of subunit vacccines through three main advantages. First, nanomaterial carriers can encapsulate antigens, maintaining their integrity and stability. Decoration of a nanomaterial's surface with antigen can also mimic highly repetitive epitopes found on viruses. Second, nanomaterial carriers can co-encapsulate immunostimulatory adjuvants with the antigen to ensure the immune system encounters the appropriate pro-inflammatory signals upon uptake. Third, nanomaterials allow targeting of the antigen and adjuvant to target organs such as lymph notes, cells such as APCs, and subcellular locations such as the cytosol. This targeting is achieved through tuning nanoparticle biophysical properties like size and charge. The following is a description of a variety of nanoparticle carriers and their use in vaccination.

1.7.1.2.1 Liposomes

Liposomes have been extensively studied for their use in vaccination. They have been shown to be clinically safe and biocompatible as well as easy to manufacture(172). Antigen delivery via cationic liposomes leads to depot effect due to the electrostatic interactions between the liposomes and negatively charged cell membranes, enabling prolonged antigen release at the site of injection(173). The extent of this depot can be tuned through surface decoration with PEG moieties to disrupt some electrostatic interactions and improve accumulation into the lymph nodes(174). Cationic lipids that have been investigated include 1,2-Dipalmitoyl-sn-glycero-3-phosphocholine (DPPC) and acationic lipid component Dimethyl dioctadecyl-

ammonium (DDA), 1,2-Dipalmitoyl-3-trimethylammonium-propane (DPTAP), 1,2-Diacyl-sn-glycero-3 -ethylphosphocholine (eDPPC), or 3β[N-(N',N'-Dimethylaminoethane)-carbamoyl] cholesterol (DC-Chol). Delivery via DC-Chol led to the most pronounced antibody titers and DC maturation(175). The size of liposomes can also be tuned to alter immune responses. The modification of liposomes with octarganine (R8), a cell-penetrating peptide along with pegylation increased particle size from 98 to 273nm and led to a 4 fold increase in localization to the spleen and resulted in strong IFNγ production(176). Additionally immunization with liposomes greater than 400nm in diameter led to stronger Th1-skewed anti-viral response compared to 100nm liposomes(177).

In addition to their tunable physical properties, liposomes are advantageous due to their capacity to co-deliver both adjuvant and antigen. Adsorption of polyinosinic-polycytidylic acid (Poly:IC), a synthetic analog of double stranded RNA, onto DOTAP and R8-liposomes led to TLR3-dependent DC activation and a high frequency of CD8+ T cells(176). Furthermore, vaccine components can be directly targeted to the cytosol through variation in the lipid composition. Delivery of antigen via the fusogenic lipid DOPE and R8 lead to an increased amount of antigen in the cytosol and increased antigen presentation on MHCI for cross-presentation(178).

Several liposome-based vaccines have been approved for clinical trials against intracellular pathogens such as M tuberculosis(179). Their development and use in vaccination may be hindered, however, due to their weak stability under physiological conditions, specifically in the presence of serum components(180). Their administration *in vivo* often results in rapid leakage of encapsulated antigens leading to premature vesicle rupture and reduced delivery efficacy.

1.7.1.2.2 Lipid nanoparticles (LNPs)

Lipid nanoparticles were developed in order to maintain the favorable safety and biocompatibility of liposomes, while improving their stability. They are composed of three components,

a cationic lipid or polymer core, a phospholipid biolayer and an outer PEG-lipid bilayer. Macromolecules such as proteins and nucleic acids can be effectively encapsulated in the inner core. The cationic lipids in the core enable extremely efficient encapsulation of negatively charged macromolecules such as nucleic acids(181). The lipid bilayer provides biocompatibility and biomimetic properties while the PEG coating provides steric stabilization and prolongs the *in vivo* circulation time of particles. LNPs consisting of poly-(beta-amino ester)(PBAE) were shown to be efficient delivery vehicles for mRNA-based vaccines. The pH-responsive PBAE promotes endosomal disruption. Thus, the fragile mRNA is both protected from nucleases *in vivo* and the lipid vesicle is effectively taken up into the endosome and subsequently releases the mRNA into the cytosol for translation(182).

The development of LNPs was rapidly accelerated during the COVID-19 pandemic as LNP-based vaccines carrying the mRNA for SARS-CoV2 spike protein were developed and FDA approved in less than 1 year(183; 184). These LNP-based vaccines generate strong humoral and cellular immune responses that persist for more than 6 months(185; 186). However, after 6 months, they begin to wane and booster administrations are required. LNPs offer many advantages including their efficient delivery of mRNA, their controlled particle size and surface functionality, and their good serum stability. Additionally, LNP-based mRNA vaccines are self-adjuvanting and do not require any additional proinflammatory molecules. The mechanism underlying the adjuvanting properties of LNPs is not fully elucidated but appears to be dependent on the ionizable lipid component and the release of pro-Tfh cytokine IL-6(187). Due to the structure of the lipids and the amphiphilic nature of the phospholipids, they are capable of encapsulating both hydrophobic and hydrophilic payloads. Disadvantages of LNPs include the relative difficulty of incorporating larger molecular surface modifications. Conjugating targeting moieties or antigens to the surface of the LNPs can often affect their stability and delivery efficiency. Careful evaluation and consideration of the entire fluid structure is required as additional components are incorporated.

1.7.1.2.3 Synthetic polymeric nanoparticles

Commonly used synthetic polymers for biocompatible nanoparticles include aliphatic polyesters such as poly(lactic acid), poly(glycolic acid), poly(ϵ-caprolactone), poly(hydroxybutyrate) and poly(lactic-co-glycolic acid) (PLGA). PLGA has been explored extensively including in the clinic due to its safety and biodegradability *in vivo*(188). Upon hydrolysis it breaks down into lactic acid and glycolic acid which can be readily metabolized(189). PLGA has been used to deliver a wide variety of antigens(190–194). One advantage of PLGA nanoparticles in vaccination is their capacity to release antigen for several weeks and months, or in different phases. The sustained release of antigen enhances immune stimulation as well as avoids the need for multiple booster administrations(195–197). Additionally PLGA nanoparticles have been used successfully to co-deliver antigen and adjuvant. Oral administration of PLGA vaccines containing OVA + MPLA induced significantly higher titers of IgG and IgA antibodies(198) and co-encapsulating BSA and imiquimod prevented their enzymatic degradation and promoted intracellular release and TLR activation(191). A major disadvantage of antigen delivery using PLGA nanoparticles is that conventional loading techniques involve the formulation of nanoparticles using a single or double emulsion and solvent evaporation. This manufacturing process exposes protein antigens to harsh organic solvents and oil-water interfaces which risks denaturation and loss of antigenicity.

PEI is a cationic polymer widely used for non-viral gene delivery. Due to its cationic nature, electrostatic interactions with negatively charged nucleic acids such as DNA lead to the formation of nanoscale polyplexes(199). These polyplexes can bind heparan sulfate proteoglycans on the surface of cells such as APCs, leading to their endocytosis(200). Once in the endosome, the PEI demonstrates a proton sponge effect leading to osmotic rupture of the endosome and cytosolic delivery of the cargo for gene expression(201). This endosomal escape makes it a promising delivery vehicle for DNA vaccines. Delivery of antigen via PEI-DNA vaccine increased levels of gene expression by 20-400 fold and enhanced antigen-specific CD8+ T cell responses by 10-25 fold(202). Delivery of OVA antigen via PEI-DNA has been

shown to increase rates of OVA cross-presentation on MHC class I(203). A major drawback, however, of widespread use of such vaccines is high levels of associated cytotoxicity likely due to membrane disruption(204).

Another family of biocompatible polymers used in vaccine delivery are acrylic acid based polymers including polymethylmethacrylate (PMMA), poly(ethylacrylic acid), poly(propylacrylic acid) (PPAA) and poly(butylacrylic acid). These polymers are shown to induce an adjuvant effect *in vivo*(205; 206). They are easy to synthesize, biodegradable and demonstrate a good safety record. In one case, PPAA was formulated to include pH-sensitive and membrane disruptive properties(207). Its protonation at low pH in the endosome destabilizes the membranes and mimics membrane fusion induced by pathogenic proteins such as hemagglutinin, likely increasing the associated immune response. Delivery of OVA via PPAA lead to increased intracellular accumulation, enhanced MHC I presentation and CTL activation(208).

Polypropylene sulfide (PPS) nanoparticles offer an additional tunable, biodegradable material for antigen delivery. These nanoparticles can be precisely engineered at the surface to display chemical moieties or antigens in a disulfide-sensitive manner(209). Solid core PPS nanoparticles can be formulated for vaccination through conjugating antigens to the surface, displaying repetitive epitopes amenable for BCR cross-linking and activation. Alternatively, polymers composed of a di-block PEG-PPS can be formulated into hollow polymersomes(210). These polymersomes consist of a amphiphilic bilayer polymer shell surrounding an aqueous core. They are stable and can self-assemble to encapsulate hydrophobic adjuvants in the polymer shell or hydrophilic antigens in the aqueous core without exposing protein antigens to any harsh organic solvents(211; 212). Mice immunized with polymersomes exhibited enhanced induction of IFNγ producing CD4+ T cells while PPS nanoparticles containing surface-displayed OVA enhanced the clonal expansion of antigen-specific CD8+ T cells. PEG-PPS nanoparticles and polymersomes offer a biocompatible, non-toxic antigen delivery system demonstrated to efficiently deliver antigen to DCs for T cell activation(213).

1.7.1.2.4 Inorganic nanoparticles

Biocompatible inorganic materials have also been explored for vaccine delivery, though to a lesser extent. Conjugation of antigens to nanoparticles formulated from gold, carbon and silica have shown to be biocompatible and protect antigen from degradation. Gold nanoparticles conjugated to M2e were found to induce robust immune responses against influenza(214). Single-walled carbon nanotubes were used to deliver peptide antigen to DCs and enhance IgG responses(215). The clinical translation of inorganic nanoparticles is currently limited by the lack of data regarding excretion routes, biodegradation behavior and long-term toxicity.

1.7.1.2.5 Biological nanoparticles

Biological nanoparticles are composed on naturally self-assembling proteins and include virus-like particles (VLPs), outer membrane vesicles (OMVs) and non-viral derived protein nanocages such as ferritin. VLPs are derived from single-stranded RNA viruses such as MS2 bacteriophage, AP205 and Qβ, which due to their small genomes, are easily modified to generate new surface antigens(216). The antigen of interest can either be fused to the VLP protein during production or chemically conjugated to the surface. The particles form through self-assembly of the surface proteins but lack internal viral machinery enabling replication or infection, thus ensuring their clinical safety. Non-enveloped VLPs such as these can be expressed quickly and economically in bacterial expression systems and form highly repetitive, dense and rigid structures on the surface enabling them to efficiently cross-link BCRs and activate lasting T cell independent responses(217). MS2 coat protein was successfully fused to L2 surface protein of HPV to produce a vaccine eliciting a strong antibody response that lasted over 9 months(218). Alternatively if fusion proteins do not express properly, antigens can be chemically conjugated to VLP surface. For example, the zika antigen was conjugated to the surface of Qβ nanoparticles using a heterobifunctional crosslinker SMPH(219). The utility of VLPs has been demonstrated through their successful

clinical translation. There are currently 4 FDA approve VLP vaccines including Cervarix® and Engerix® from GSK, Gardasil® and Recombivax® from Merck&Co(216). Outer membrane vesicles naturally bud from the outer membrane of gram-negative bacteria and archaea in a similar manner to extracellular vesicles. They contain the same PAMPs associated with the native bacteria including LPS, periplasmic component, nucleic acids, lipoproteins and outer membrane proteins and thus are self-adjuvating. They can be produced directly from target pathogens or from safer bacterial hosts engineered to recombinantly express the antigens from the target pathogen(216). The use of recombinant pathogens lowers the level of containment practices necessary in the manufacturing process, however reliable purification methods are required and uniformity among the vesicles is difficult to ensure. One risk of OMVs is that they can contain high amounts of LPS which upon injection *in vivo* leads to fever, uncontrolled inflammation and even sepsis(220). Despite these risks, OMV vaccines have been developed successfully for influenza(221; 222) malaria(223), pertussis(224; 225), Lyme disease(226), plague(227; 228) and SARS-Cov-2(229–231). There are currently 2 FDA approved OMV vaccines; Novartis's Bexero® and Merck's PedVaxHIB®.

Protein nanocages are made up of non-viral protein subunits that self-assemble to form macromolecular structures. In a similar manner to VLPs, antigens can be fused to protein nanocages recombinantly or chemically conjugated to the surface. These structures mimic the surface properties of pathogens but may require additional boosting or adjuvant due to their natural lack of PAMPs. Ferritin is an example of a protein nanocage which is composed of 24 subunits assembled into a 12nm diameter spherical cage(232). Various ferritin-based vaccines are in clinical trials including 2 influenza trials (NCT03186781,NCT03814720), a SARS-CoV2 trial (NCT04784767) and a trial for Epstein-Barr virus (NCT04645147).

Engineered viral vectors are another biological delivery system that has emerged in the course of the COVID-19 pandemic for delivering specific pathogen antigens. Non-pathogenic, replication-deficient viruses such as adenovirus and adeno-associated virus are genetically engineered to express pathogen-specific antigens on the surface(233). Due to their nature as

functional viruses, viral vector vaccines elicit strong immune responses through the activation of PPRs, while maintaining strong safety profiles. The ChAdOx1 nCoV-19 Covid vaccine developed by AstraZeneca(234) and Merck's Ervebo vaccine against Ebola virus(235) are examples of successful viral vector vaccines. While promising, viral vector based vaccines suffer from manufacturing challenges associated with large scale production.

The emergence of the SARS-CoV-2 virus and the COVID-19 pandemic demonstrated the importance of modular, effective vaccine platforms for reducing the spread of novel pathogens and maintaining public health. In Chapter 2 I will investigate the efficacy of a PEG-PPS polymersome vaccine platform to generate B and T cell responses against SARS-CoV-2 antigen and I will elicidate how the delivery of surface-conjugated vs encapsulated antigen results in distinct immunological changes.

1.7.2 Antigen-specific immune tolerance

1.7.2.1 Current standards-of-care in antibody-mediated pathologies

Autoimmune diseases affect millions globally and arise due to poorly understood interactions between environmental triggers and polymorphous genetic elements. Each disease shows distinct pathologies, but all lead to a complex, self-perpetuating immune response against self-antigens. The resulting immune responses damage specific cell types, tissues and organs. A subset of these autoimmune diseases are antibody-mediated. The development of antibodies against self-antigens in these diseases directly leads to the resulting damage and pathology. Antibody-mediated autoimmune diseases include rheumatoid arthritis, systemic lupus erythematosus, myasthenia gravis and pemphigus vulgaris. The current standard of care for these diseases offers only broad immunosuppression to dampen these antibody responses. Broadly suppressive medications such as methotrexate are used as a first line treatment for rheumatoid arthritis. However, many people do not achieve remission or low-disease activity(236; 237). The next line of therapy offers a range of immune-modulating biolog-

ics including TNFα, IL-6, IL-1 inhibitors and B cell depletion treatments. These broadly immune-active biologics, however, are associated with an increase in the number of serious infections(238). Both treatment with rituximab or methotrexate is associated with decreased response to vaccination(239; 240). Similarly, the first line treatment for SLE is to administer broadly suppressive corticosteroids and immunosuppressive agents including hydroxychloroquine, methotrexate, azathioprine, cyclophosphamine and mycophenolate mofetil(241; 242). More targeted biologics for SLE are an active area of investigation, but currently Belimumab is the only biologic approved for treatment of SLE, it targets B cell activating factor (BAFF), a costimulatory molecule essential for B cell activation. B cell depletion via rituximab showed promise, but ultimately failed in clinical trials(243). Myasthenia gravis and pemphigus vulagaris are also predominantly treated using immunosuppressants including glucocorticoids. These diseases have shown promise in treatment with anti-CD20 B cell depletion, but often long-lived antibody secreting cells remain and require antibody-depleting strategies such as IVIg.

Overall non-steroidal anti-inflammatory drugs offer an inexpensive first line therapy but are often not sufficient to control disease progression necessitating the use of stronger immunosuppressants such as methotrexate, azathioprine and mycophenolate mofetil. None of these treatments are disease-specific in mechanism and expose patients to a higher risk of infection, malignancy and other adverse effects. Recently biologics such as rituximab for B cell depletion have offered a more disease-specific immunosuppression, but failure to deplete long-lived antibody secreting cells limits their therapeutic utility.

Food allergies and allergic asthma are associated with the development of IgE antibodies specific to food or airborn antigens. Food allergy rates are estimated to be more than 10% amongst adults(244), however avoidance combined with the use of an epi-pen in the case of exposure has remained the current standard of care(245). This treatment approach does not address any of the underlying mechanisms of the disease and does nothing to alleviate the patients' anxiety of accidental exposure. Allergic asthma is primarily managed through

administration of antihistamines and corticosteroid inhalers. For severe cases new biologics such as anti-IgE and anti-IL4Rα monoclonal antibodies (mAbs) have shown promise in the treatment of severe, persistent allergic asthma and atopic dermatitis(246; 247). The only available disease-modifying treatments for both food allergy and allergic asthma is allergen immunotherapy (AIT). AIT involves the incremental increase of either subcutaneous, oral, or sublingual antigen over time and has been shown to reduce a patient's severity of allergic response upon a low-dose allergen exposure and decrease the risk of severe anaphylaxis (248). However, food allergen immunotherapy does not induce lasting tolerance to the antigen. There are also side effects associated with AIT including hypersensitivity reactions, and anaphylaxis(249).

The formation of antibodies against therapeutics is an increasing clinical problem. The development of recombinant biologics in the past several decades has resulted in improved therapeutics for a variety of diseases including genetic disorders, cancer and autoimmunity. However, the protein composition of these drugs makes them vulnerable to recognition by the patient's immune system, leading to the development of an anti-drug antibody (ADA) response that can lead to loss of therapeutic function, hypersensitivity and anaphylaxis if untreated. The development of ADAs is most detrimental in genetic disorders such as hemophilia and various glycogen storage disorders in which the patient requires treatment with a functional protein they do not endogenously produce. These proteins will not have undergone central tolerance during development, increasing the immunogenicity of the therapeutic in these patients. Often the development of ADAs or 'inhibitors' against these therapeutics leave patients with limited therapeutic alternatives. Current clinical management of ADAs for these diseases includes an optimized "tolerizing" dosing schedule. These schedules were empirically designed and differ across therapeutic antigens. In some cases such as hemophilia this involves beginning treatment with high doses of factor VIII before scaling down(250). In others, such as treatment for PKU, dosing is begun with very small amounts before scaling up to a therapeutic dose(251). Co-administration with immunosuppressive

agents has also shown promise in limiting the development of ADAs(252–254). In patient populations requiring chronic treatment with mAbs co-administration of methotrexate has increased long-term therapeutic efficacy of the drugs. In severe cases, B cell depletion can be used to try an broadly suppress the B cell and antibody response to a life-saving therapeutic. However, plasma cells do not express CD20 or CD19 and are thus not depleted. If the ADA response is generated by LLPCs, B cell depletion will have no effect on the overall efficacy. Plasma cell depletion strategies such as treatment with bortezomib has been explored in the treatment of Pompe disease(255). These strategies, while effective at lowering ADAs and increasing treatment duration and long-term efficacy leave patients at an unacceptable risk of infection and malignancy(256–259). Therefore, the development of antigen-specific treatments to lower antigen-specific antibody responses is a critical unmet need and active area of research.

1.7.2.2 Emerging strategies in immune tolerance

The current standards of care to treat antibody-mediated autoimmune disease, allergy and drug hypersensitivity rely on broadly suppressing a patient's immune system. These treatments do not address underlying disease mechanism or offer a cure and can increase a patient's risk of developing infection and malignancy. The next generation of treatments aim to induce immune tolerance instead of immune suppression and include regulatory T cell therapies, antigen-specific protein and peptide therapies and engineered CAR-T cell therapies.

Many autoimmune diseases, including antibody-mediated autoimmune diseases, are associated with genetic polymorphisms in regulatory T cell function(260; 261). Due to their capacity to broadly control inflammation as well as other T and B cell responses, increasing the Treg compartment has been the goal of several tolerance treatments. In one instance isolated CD4+CD25$^{\text{intermediate}}$ FoxP3$^{\text{low}}$ cells from patients' blood were expanded *in vitro* and demonstrated to persist for longer than 1 year and show promise in type 1 diabetes and

graft-vs-host-disease(262–264). *In vivo* Treg induction has been attempted through treatment with low doses of IL-2. Due to the high level of surface expression of IL-2 receptor CD25 on the surface of Tregs, they can be expanded using levels of IL-2 below the threshold which would be required to activate pro-inflammatory conventional T cells or NK cells. Low dose IL-2 can prevent autoimmunity in mouse models and is shown to be even more effective when used in combination with an IL-2Rβ blocking antibody to further avoid activation of non-Treg cells(265; 266). These therapies are reliable methods to expand Tregs broadly, however, since they lack antigen-specificity they may still leave patients more immunocompromised than a healthy individual or risk off-target effects. In order to promote a more targeted immune response, genetic engineering approaches have been used to generate T cells with antigen-specificity. CARs composed of an autoantigen fused to the CD3ζ signaling domain have been used to target autoantigen-specific B cells to treat mouse models of pemphigus vulgaris(267). Auto-antigen pMHC complexes are expressed on a similar CAR in order to target and kill antigen-specific T cells recognizing that pMHC. CAR-Tregs have also been developed with a pMHC conjugated to their signaling domain, but alongside expression of FoxP3 to induce their suppressive function. These CAR-T cells have shown therapeutic efficacy in mouse models of autoimmune diseases(268–270). Engineered cell therapies such as these offer great promise in that they offer an powerful antigen-specific targeted strategy for the treatment of unwanted immune responses. However these therapies are complex, costly and time consuming. The use of cells increases the complexity of the possible interactions and therapeutic mechanisms. Exhaustion of the transfused CAR-T cells and safety issues associated with the potential toxicity of cytokine release syndrome may limit the wide-spread adoption of cell therapies for non-life-threatening conditions(271).

Alternative non-cellular antigen-specific treatments utilize the delivery of peptide and protein for immune-modulation. Early studies delivering T cell-specific peptide epitopes or pMHC complexes found that they were able to activate and induce deletion of antigen-specific disease-causing CD8+ T cells(272; 273). While several peptide antigen therapeu-

tic approaches have progressed to clinical trials, these responses were found to be highly dependent on antigen, dose, and route of administration(274–277). This variability combined with the risks of peptide therapy including disease exacerbation(278), hypersensitivity reactions(279) and anaphylaxis(280), have hindered successful clinical translation.

Due to the unreliable tolerance induced by peptide therapy alone, nanomaterials were developed to co-deliver peptide along with immunomodulatory components. Liposomes co-delivering arthritis antigen and NFκb inhibitors were found to inhibit joint inflammation(281). Similarly polymeric nanoparticles delivering both antigens and rapamycin were found to suppress T cell responses in EAE, promote tolerogenic DC formation, and induce factor VIII-specific tolerance in a mouse model of hemophilia(282; 283). While these delivery methods have proven to be more reliable than peptide therapy alone, future clinical trials will determine if their immunomodulatory agents can generate lasting antigen-specific tolerance and if they lead to more broad immunosuppressive features.

One strategy to improve efficacy is to increase targeting of the peptide and protein antigen to tolerogenic APCs. Specialized splenic APCs are essential for the uptake and tolerogenic processing of apoptotic erythrocytes(284). Strategies to deliver antigen to these cells via injection of *ex vivo* antigen-loaded splenocytes(285; 286) or conjugating antigen to glycophorinA binding ERY1(287) was sufficient to induce tolerance in mouse models of autoimmunity as well as prevent antibodies to immunogenic protein antigens(288). The liver has also been used as a target for antigen therapy due to its tolerogenic microenvironment and specialized pro-tolerogenic APCs(289). Nanoparticles coated in poly(maleic anhyedride-alt-1-ocadecene) were found to accumulate in liver sinusoidal endothelial cells (LSECs), known to induce FoxP3+ Tregs(290). Antigen delivery using these nanoparticles was found to block progression of MOG-induced EAE when administered early in disease progression(289).

The Hubbell lab has previously developed a liver-targeted antigen delivery platform. In order to target the asialoglycoprotein receptor(ASGPR), a receptor expressed highly on hepatocytes, they developed a polymer chain of repeating GalNAc (p(GalNAc)) to bind ASGPR

and other c-type lectins expressed on other APCs in the liver with high avidity(291–293). When injected intravenously, antigen conjugated to p(GalNAc) was found to target the liver, increase the frequency of antigen-specific Tregs and inhibit the onset of the BDC2.5 murine model of type 1 diabetes(294). These antigen-specific platforms have investigated the effects of antigen-therapy predominantly on T cell driven diseases. However, more investigation is needed to understand how tolerance induced through liver targeting can impact antibody responses and if inducing T cell tolerance in this manner is sufficient to prevent the progression of a T cell dependent antibody response. In Chapter 3 I will describe a novel glycopolymer to increase antigen delivery to the tolerogenic microenvironment of the liver and investigate its potential to prevent antigen-specific antibody responses to an immunogenic protein drug.

CHAPTER 2

POLYMERSOMES DECORATED WITH SARS-COV-2 SPIKE PROTEIN RECEPTOR BINDING DOMAIN ELICIT ROBUST HUMORAL AND CELLULAR IMMUNITY

2.1 Abstract

A diverse portfolio of SARS-CoV-2 vaccine candidates is needed to combat the evolving COVID-19 pandemic. Here, we developed a subunit nanovaccine by conjugating SARS-CoV-2 Spike protein receptor binding domain (RBD) to the surface of oxidation-sensitive polymersomes. We evaluated the humoral and cellular responses of mice immunized with these surface-decorated polymersomes (RBDsurf) compared to RBD-encapsulated polymersomes (RBDencap) and unformulated RBD (RBDfree), using monophosphoryl lipid A-encapsulated polymersomes (MPLA PS) as an adjuvant. While all three groups produced high titers of RBD-specific IgG, only RBDsurf elicited a neutralizing antibody response to SARS-CoV-2 comparable to that of human convalescent plasma. Moreover, RBDsurf was the only group to significantly increase the proportion of RBD-specific germinal center B cells in the vaccination-site draining lymph nodes. Both RBDsurf and RBDencap drove similarly robust CD4+ and CD8+ T cell responses that produced multiple Th1-type cytokines. We conclude that multivalent surface display of Spike RBD on polymersomes promotes a potent neutralizing antibody response to SARS-CoV-2, while both antigen formulations promote robust T cell immunity.[1]

1. This chapter and the accompanying figures are adapted "Polymersomes decorated with SARS-CoV-2 spike protein receptor binding domain elicit robust humoral and cellular immunity L. R. Volpatti, R. P. Wallace, S. Cao, M. M. Raczy, R. Wang, L. T. Gray, A. T. Alpar, P. S. Briquez, N. Mitrousis, T. M. Marchell, M. S. Sasso, M. Nguyen, A. Mansurov, E. Budina, A. Solanki, E. A. Watkins, M. R. Schnorenberg, A. C. Tremain, J. W. Reda, V. Nicolaescu, K. Furlong, S. Dvorkin, S. Yu, B. Manicassamy, J. L. LaBelle, M. V. Tirrell, G. Randall, M. Kwissa, M. A. Swartz, J. A. Hubbell. ACS Central Science 2021 7 (8), 1368-1380 DOI: 10.1021/acscentsci." This work was contributed to by multiple authors. R.P.W., L.R.V., S.C., M.M.R., R.W., S.S.Y., M.K., M.A.S., and J.A.H. conceived the project and designed the research strategy. R.P.W., L.R.V., S.C., M.M.R., R.W., L.T.G., A.T.A., P.S.B., N.M., T.M.M., M.S.S., M.N., A.M., E.B., A.S., E.A.W.,

2.2 Introduction

COVID-19, the disease caused by the novel coronavirus SARS-CoV-2, emerged in late 2019 and was declared a pandemic by the World Health Organization in March 2020. Since its emergence, researchers across the world have sought to rapidly develop vaccine candidates, some of which have received Emergency Use Authorization by the U.S. Food and Drug Administration(295; 296). While the first vaccines that entered the clinic were based on nucleic acid technologies, subunit vaccines are gaining attention and have also shown promise in clinical trials(297; 298). The primary antigens used in preclinical and clinical vaccine candidates are the Spike protein and its constituent receptor-binding domain (RBD). The RBD of the Spike protein binds to the ACE-2 receptor on host cell surfaces, enabling viral entry into the host cell(299; 300). Several highly potent neutralizing antibodies have been isolated that target RBD and prevent viral binding and uptake, making it an attractive vaccine target(301–304). Since RBD is smaller (25 kDa) and more stable than the full homotrimeric Spike fusion protein (180 kDa), it is also advantageous from a manufacturing and distribution perspective(305). However, RBD has been shown to have lower immunogenicity than the full Spike protein or its RBD-containing S1 domain(306; 307). Materials science and engineering approaches, particularly strategies involving nanotechnology, may improve RBD immunogenicity and thus aid in the development of next-generation vaccines(77; 308; 309). Indeed, several approaches of self-assembling RBD into virus-like particles have resulted in potent neutralizing antibody responses(310–313). In order to offer robust protection from infection, cellular in addition to humoral responses are needed(314–316). Almost all convalescent individuals show T cell immunity, and the majority have both CD4+ and CD8+ SARS-CoV-2-specific T cells(317–320). Conversely, severe disease is associated with lymphopenia and reduced T cell function(321–323). Furthermore, T cell immunity may

A.C.T., and J.W.R. performed experiments. R.P.W., L.R.V., S.C., M.M.R., A.T.A., P.S.B., T.M.M., and M.S.S. performed data analysis. P.S.B., V.N., K.F., S.D., and G.R. performed or advised on SARS-CoV-2 neutralization assays. M.R.S., J.L.L., and M.V.T. advised on surface modification of polymersomes. B.M. contributed the HEK-293-hACE2 cell line.

be more durable than humoral responses, and T cells are expected to play an important role in immune memory(316; 321; 324). Therefore, the goal of this study was to improve both humoral and cellular immunogenicity of RBD and compare the efficacy of engineered nanoparticle formulations in order to inform the design of next-generation nanovaccines. We have previously reported the development of polymersomes (PS) that self-assemble from the oxidation-responsive block copolymer poly(ethylene glycol)-bl-poly(propylene sulfide) (PEG-PPS)(325) and shown their efficacy in delivering antigen and adjuvant to dendritic cell endosomes(213). In endolysosomal compartments, the PPS block becomes oxidized, which initiates the restructuring of the PS into micelles and concurrent release of encapsulated payload(213; 326). These vaccine nanocarriers have been shown to activate dendritic cells, induce robust T cell immunity, and elicit high antibody titers with broad epitope coverage(210; 213; 327). In this study, we hypothesized that we could further improve the humoral responses elicited by PS while retaining their ability to induce T cell immunity by engineering them to mimic the physical form of a viral particle through multivalent surface display of antigen. We envisaged that multivalent surface display of RBD would result in enhanced crosslinking and clustering of B cell receptors (BCRs) and subsequent production of neutralizing antibodies. Here, we report on the development and preclinical evaluation of PS displaying surface-bound RBD (RBDsurf) and PS encapsulating RBD (RBDencap) adjuvanted with monophosphoryl lipid A-encapsulated PS (MPLA PS). We show that mice vaccinated with RBDsurf in combination with MPLA PS in a prime-boost schedule develop high titers of SARS-CoV-2-neutralizing antibodies with robust germinal center responses as well as CD4+ and CD8+ T cell immunity, thus meeting our design criteria.

2.3 Methods

2.3.1 RBD production and purification

For production of the Spike protein RBD (Spike319-541; GenBank: MN908947.3), we obtained expression plasmids on pCAGGS backbone containing mammalian codon-optimized sequences for this gene from Florian Krammer's laboratory (Icahn School of Medicine at Mount Sinai, New York, NY)(328). Suspension-adapted HEK-293F cells were maintained in serum-free Free Style 293 Expression Medium (Gibco). On the day of transfection, cells were inoculated into at a concentration of 1×10^6 cells/mL. Plasmid DNA (1 mg/mL) was mixed with linear 25 kDa polyethyleneimine (2 mg/mL ; Polysciences) and co-transfected in OptiPRO SFM medium (4% final concentration; Thermo Fisher). Flasks were cultured in an orbital shaking incubator (135 rpm, 37 °C, 5% CO_2) for 7 days. Culture medium was then collected by centrifugation, filtered, and loaded into a HisTrap HP 5 mL column (GE Healthcare) using an ÄKTA pure 25 (GE Healthcare). After washing the column with wash buffer (20 mM NaH2PO4 and 0.5 M NaCl, pH 8.0), protein was eluted using a gradient of 500 mM imidazole in wash buffer. The protein was further purified by size-exclusion chromatography using a HiLoad Superdex 200PG column (GE Healthcare) with PBS as an eluent. Dimers of RBD were reduced by the addition of dithiothreitol (1 mM) which was subsequently dialyzed against PBS. All purification steps were carried out at 4 °C. The expressed proteins were verified to be >90% pure through SDS–PAGE. The purified proteins were tested for endotoxin using a HEK-BlueTM TLR4 reporter cell line (InvivoGen), and the endotoxin levels were confirmed to be below 0.01 EU /mL. Protein concentration was determined by absorbance at 280 nm using a NanoDrop spectrophotometer (Thermo Scientific). Proteins were stored at a concentration of 4 mg/mL at -80 °C until use.

2.3.2 PS formulation

PEG-PPS polymersomes were formulated by thin film rehydration as previously described(213). In brief, 20 mg of polymer was dissolved in 750 µL dichloromethane (DCM), and DCM was removed by vacuum desiccation overnight. 1 mL of PBS was then added to the vial, which was rotated at room temperature (RT) for 24 h to allow complete dispersal of the polymer. The solution was then sequentially extruded through 0.8, 0.4, 0.2, and 0.1 µm pore membranes (Whatman). To formulate RBD-encapsulated PS, 250 µL of PBS containing 4 mg/mL RBD was added to the polymer thin film for rehydration, and the solution was rotated at 4 °C for 72 h before extrusion as above. After extrusion, RBD-encapsulated polymersomes were passed through a sepharaose size exclusion chromatography (SEC) column to remove unencapsulated free RBD. The RBD content was quantified by SDS-PAGE using mini-protein TGX stain-free precast gels (Bio-Rad). Gels were imaged on a ChemiDoc XRS+ Gel Documentation System (Bio-Rad) and analyzed using ImageJ. RBD-surface-conjugated PS were synthesized by first formulating empty PS as above consisting of 25% N3-PEG-PPS. RBD was conjugated to a sulfo DBCO-Maleimide linker (Click Chemistry Tools) at the molar ratio of 1:5 (RBD:linker) and reacted for 2.5 hours. Unconjugated linker was removed by Zeba spin desalting columns (7K MWCO; ThermoFisher). The resulting RBD-linker was analyzed by MALDI-TOF MS using an α-cyano-4-hydroxycinnamic acid (Sigma-Aldrich) matrix and a Bruker ultrafleXtreme MALDI TOF/TOF instrument. RBD-linker (4 wt% of polymersome) was then incubated with empty N3-PEG-PPS polymersomes overnight at RT. RBD-surface-conjugated PS were then passed through SEC to remove unconjugated RBD-linker. The conjugation was monitored by SDS-PAGE, and the final RBD content was quantified by the CBQCA Protein Quantitation Kit (ThermoFisher). Fluorescently labeled PS were prepared by conjugating AlexaFluor-647 alkyne dye (ThermoFisher) to PS containing 25% N3-PEG-PPS. The dye was mixed with PS at a molar ratio of 1:20 (dye:N3-PEG-PPS), and the solution was stirred overnight at RT. Labeled PS were then passed through SEC to remove

unconjugated dye. To make the fluorescently labeled RBDsurf, labeled PS were prepared as above and conjugated with RBD as described, followed by SEC purification. Final RBD content was quantified by the CBQCA Protein Quantitation Kit (ThermoFisher). MPLA PS were fabricated by flash nanoprecipitation using a 3D printed impingement jets mixer(329). 20 mg PEG-PPS and 2 mg MPLA (PHAD®; Avanti Polar Lipids) were dissolved in 500 µL tetrahydrofuran (THF) and loaded into a 1 mL plastic disposable syringe. 500 µL PBS was loaded into a second syringe, and the two solutions were impinged against one another slowly within the mixer by hand. The impinged solution was immediately vortexed to form a homogenous polymersome solution which was then extruded and purified by SEC as described above. MPLA loading was quantified using a liquid chromatography-tandem mass spectrometry (LC-MS/MS) method as previously described(330) using PHAD®-504 (Avanti Polar Lipids) as an internal standard on an Agilent 6460 Triple Quad MS-MS with 1290 UHPLC.

2.3.3 PS characterization

The size and polydispersity index (PDI) of all the polymersome formulations were measured by dynamic light scattering (DLS) using a Zetasizer Nano ZS90 (Malvern Instruments). Cryogenic electron microscopy (cryoEM) images were obtained on a FEI Talos 200kV cryoEM dedicated electron microscope.

2.3.4 MPLA PS in vitro *activity*

To determine TLR4 activation, HEK-BlueTM TLR4 cells (Invivogen) were incubated with increasing concentrations of MPLA PS for 24 h 37 $4°C$ in a 5% CO_2 incubator. NF-κB-induced SEAP activity was detected using QUANTI-BlueTM (Invivogen) and by reading the OD at 650 nm. For dendritic cell activation experiments, BMDCs were prepared from C57Bl/6 mice (Jackson) as previously described(331). After 9 days of culture, cells were seeded at 2×10^5 cells/well in round-bottom 96-well plates (Fisher Scientific) in IMDM with 10% FBS and 2% penicillin/streptomycin (Life Technologies). Cells were treated with

varying concentrations of MPLA PS or free MPLA and incubated for 24 h at 37 °C in a 5% CO_2 incubator. After 24 h, the supernatant was collected, and cytokine concentration was measured using a multiplexed mouse Th cytokine panel (BioLegend) according to the manufacturer's instructions.

2.3.5 RBDsurf in vitro *activity*

For the cell-based hACE2-binding assay, human embryonic kidney (HEK)-293T cells over-expressing human ACE-2 (HEK-hACE2) were obtained from BEI Resources (NIH NIAID). Fluorescently labeled empty PS, RBDsurf, or RBDfree was incubated at varying concentrations with 5×10^4 HEK-hACE2 cells at 4 °C for 20 min. Cells were then washed three times in PBS with 2% FBS. Binding of RBD to hACE-2 on the cell surface was assessed via the mean fluorescent intensity measured by flow cytometry using BD LSRFortessa (BD Biosciences).

2.3.6 Production of RBD protein multimers

RBD protein expressed with AviTag was purchased from GenScript. Site-specific biotinylation of the AviTag was performed using BirA Biotin-Protein Ligase Reaction kit (Avidity). Next, unconjugated biotin was removed using Zeba spin desalting columns, 7K MWCO (ThermoFisher). The quantification of reacted biotin was performed using the Pierce Biotin Quantification Kit (ThermoFisher). Biotinylated RBD was incubated with either streptavidin-conjugated PE (Biolegend) or streptavidin-conjugated APC fluorophores (Biolegend) for 20 min on ice at a molar ratio of 4:1 of biotin to streptavidin. Streptavidin-conjugated FITC (BioLegend) was reacted with excess free biotin to form a non-RBD-specific streptavidin probe as a control. Multimer formation was confirmed using SDS-PAGE gel. Cells were stained for flow cytometry with all three streptavidin probes at the same time as other fluorescent surface markers at a volumetric ratio of 1:100 for RBD-streptavidin-PE and 1:200 for RBD-streptavidin-APC and biotin-streptavidin-FITC.

2.3.7 Mouse vaccination experiments

All experiments were performed in accordance with the Institutional Animal Care and Use Committee at the University of Chicago. Female 8-week-old C57BL/6 mice (Jackson Laboratory) were randomly assigned to cohorts of n = 5 and vaccinated with 10 μg of antigen and 5 μg of adjuvant s.c. in the hock (either 2 or 4 hocks) and boosted on day 21. On day 7, 14, 20, and 28 post vaccination, 100 μL of blood was collected in EDTA-K2-coated tubes (Milian), and plasma was separated by centrifugation and stored at -80 °C until use. On day 28 after initial vaccination, mice were sacrificed. Splenocytes and lymph node cells from draining lymph nodes were collected. Single-cell suspensions of the lymph node were prepared by digestion in collagenase D for 45 min at 37 °C. Splenocytes and lymph node cells were filtered through a 70 μm cell strainer. Splenocytes were then incubated in ACK lysis buffer to remove red blood cells. Lymph node cells were stained for Tfh cells and RBD-specific B cells using fluorescent probes listed in Tables 2.1-2.2, respectively. Samples were acquired on a BD LSR-Fortessa (BD) and analyzed using FlowJoTM software. Representative gating strategies used to identify the cell populations are shown in Figure 2.1(Tfh cells) and Figure 2.2 (RBD-specific B cells). To assess antigen-specific cytokine production by T cells, 1×10^6 lymph node cells were incubated with pools of 15-mer peptides overlapping by 10 amino acids covering the N-terminus of SARS-CoV-2 Spike protein up to the furin cleavage site (S1 pool; PepMix SARS-CoV-2 Spike Glycoprotein, JPT) for 6 h at 37 °C with 5% CO_2. Monensin (GolgiStop, BD) was added after 2 h of incubation to inhibit cytokine secretion. Cells were stained for surface markers using fluorescent monoclonal antibodies (mAbs). Cells were subsequently fixed and permeabilized using BD Cytofix/CytopermTM, and intracellular cytokines were stained using fluorescent-mAbs listed in Table 2.2. Samples were acquired on a BD LSR-Fortessa (BD) and analyzed using FlowJoTM software. A representative gating strategy used to identify the cell populations is shown in Figure 2.3. To assess antigen-specific cytokine secretion, lymph node cells were plated at 5×10^5 cells/well

were incubated with 100 μg RBD for 3 d at 37 °C with 5% CO_2. After 3 d, the supernatant was analyzed for cytokine concentration via a multiplexed mouse Th cytokine panel (BioLegend) according to the manufacturer's instructions. Samples were aquired on an Attune NxT flow cytometer (ThermoFisher), and analyzed with LEGENDplex v8.0 software. For long-term experiments, mice were not sacrificed but continued to be bled on day 2, 7, 14 and then every 2 weeks for 80 days.

Table 2.1: Tfh panel antibodies

Marker	**Fluorophore**	**Vendor**	**Cat**
Viability Dye	eFluor 780	Invitrogen	65-0865-14
CD4	BV496	BD Horizon	612952
CD3	BUV737	BD Optibuild	741788
CD44	PerCpCy5.5	Invitrogen	45-0441-82
CXCR5	BV421	Biolegend	145512
ICOS	BUV396	BD Horizon	565885
Bcl6	PE-Cy7	Biolegend	358512

Table 2.2: RBD-specific B cell panel antibodies

Marker	**Fluorophore**	**Vendor**	**Cat**
Viability Dye	Violet fluorescent reactive dye	Invitrogen	L34964A
RBD-multimer	PE	-	-
RBD-multimer	APC	-	-
F4/80 (Dump)	FITC	Biolegend	123107
CD11c (Dump)	FITC	Biolegend	117306
Ly6c(Dump)	FITC	Invitrogen	53-5932-82
Ly6g (Dump)	FITC	Invitrogen	11-9668-82
CD4 (Dump)	FITC	Biolegend	100406
CD8a (Dump)	FITC	Biolegend	100706
B220	BUV496	BD Horizon	612950
CD19	BUV396	BD Horizon	565965
CD138	BV605	Biolegend	142531
IgM	BV786	BD Optibuild	743328
IgD	PE-Cy7	Biolegend	405720
CD38	APC-Cy7	Biolegend	102727
GL7	PerCP-Cy5.5	Invitrogen	46-5902-82

Table 2.3: Restimulation panel antibodies

Marker	**Fluorophore**	**Vendor**	**Cat**
Viability Dye	eFluor 455 (UV)	Invitrogen	65-0868-14
CD3	BUV395	BD Horizon	563565
CD4	BV786	BD Horizon	563331
CD8	BV421	BD Horizon	563898
IFNγ	APC	Biolegend	505810
TNFα	BV605	Biolegend	506329
IL-2	PE	BD Pharmigen	554428

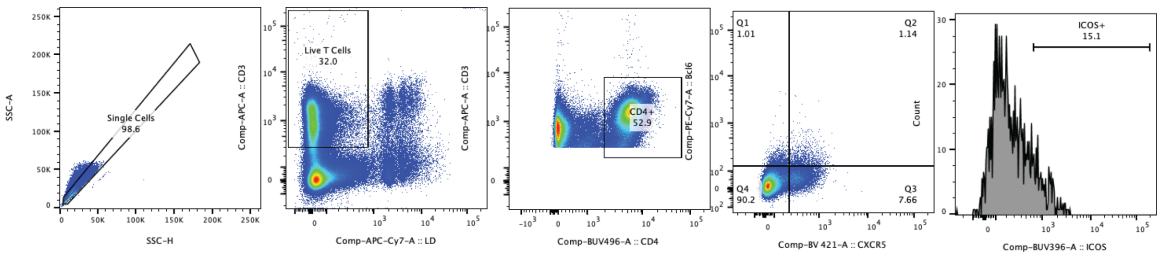

Figure 2.1: Representative T follicular helper cell gating strategy.

2.3.8 RBD-binding ELISA

Plasma was assessed for anti-RBD IgG by ELISA. 96-well ELISA plates (Costar high-bind flat-bottom plates, Corning) were coated with 10 μg/mL RBD in carbonate buffer (50 mM sodium carbonate/sodium bicarbonate, pH 9.6) overnight at 4 °C. The following day, plates were washed three times in PBS with 0.05% Tween 20 (PBS-T) and then blocked with 1x casein (Sigma) for 1 h at RT. Following blocking, wells were washed three times with PBS-T and further incubated with six 10-fold dilutions of plasma in 1x casein for 2 h at RT. Wells were then washed five times with PBS-T and incubated for an additional hour at RT with horseradish peroxide (HRP)-conjugated antibodies against mouse IgG, IgG1, IgG2b, or IgG3 (Southern Biotech). After five washes with PBS-T, bound RBD-specific Ig was detected with tetramethylbenzidine (TMB) substrate. Stop solution (3% H2SO4 + 1% HCl) was added after 18 min of TMB incubation at RT, and the OD was measured at 450 and 570 nm on an Epoch Microplate Spectrophotometer (BioTek). Background signal at 570 nm was subtracted from the OD at 450 nm. Fold-change over the average of blank wells was

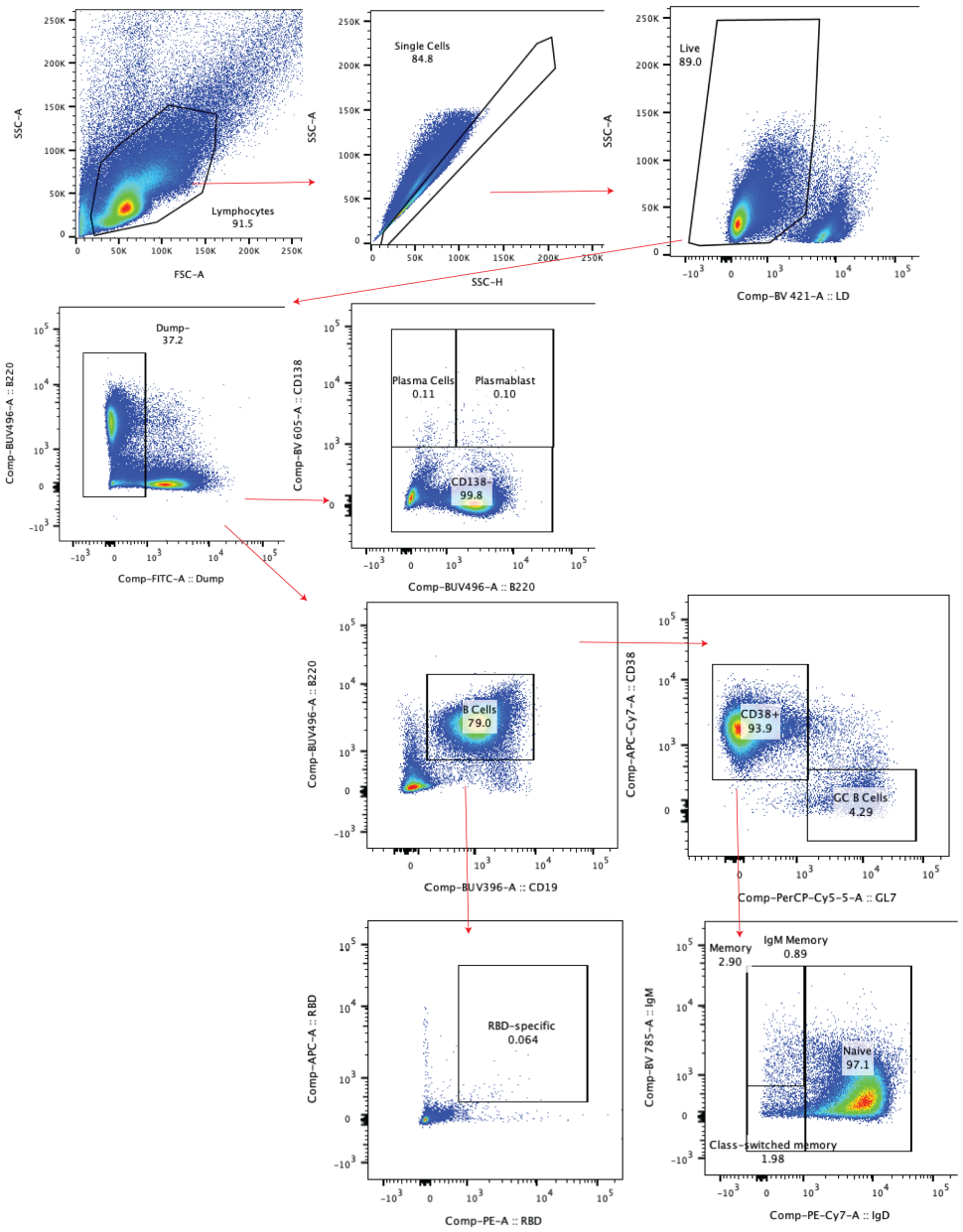

Figure 2.2: Representative B cell gating strategy.

then calculated and log-transformed. The area under the curve (AUC) of log-transformed fold change versus log-transformed dilution was then calculated.

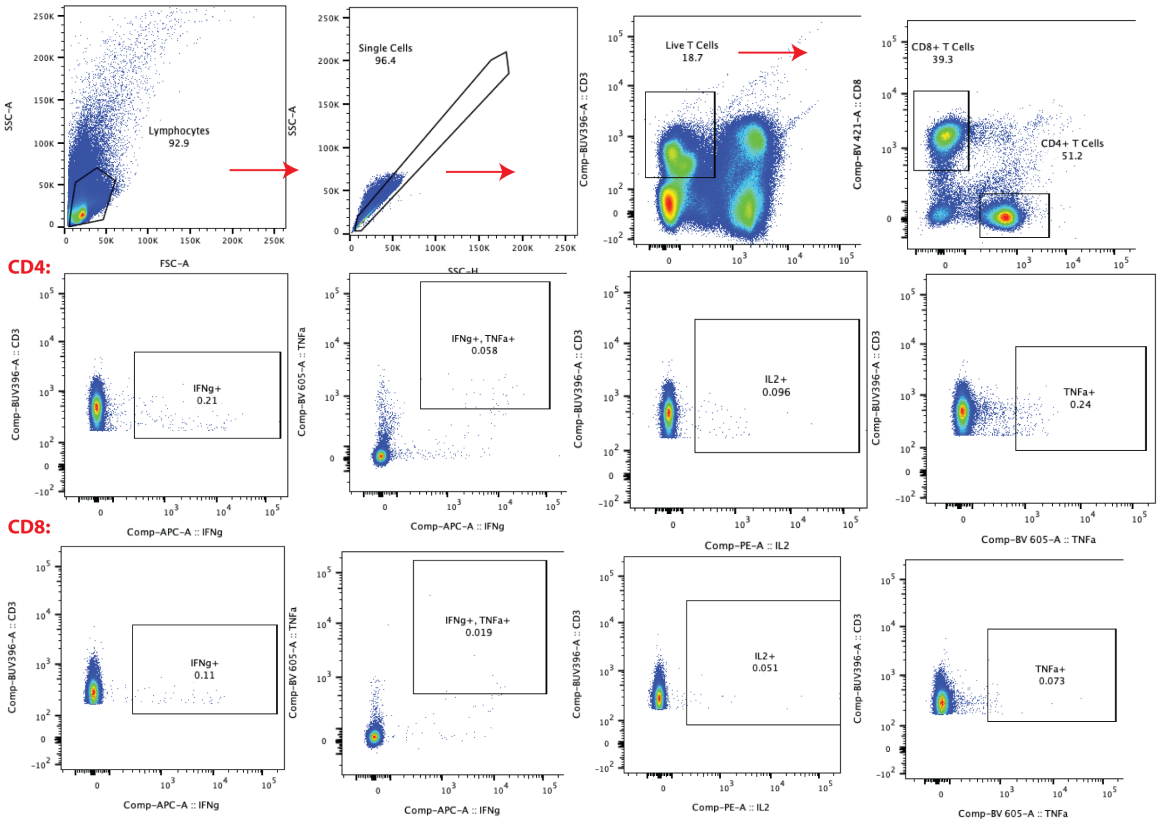

Figure 2.3: Representative intracellular cytokine gating strategy.

2.3.9 RBD-binding IgG ELISpot assay

ELISpot plates (Millipore IP Filter plate) were coated with 20 μg/mL RBD in sterile PBS overnight at 4 °C. Plates were then blocked using ELISpot Media (RPMI 1640, 1% glutamine, 10% fetal bovine serum, 1% penicillin-streptomycin) for 2 hours at 37 °C. Splenocytes from vaccinated mice were seeded in triplicate at a starting concentration of 6.75 $\times$ 10^5 cell/well and diluted seven times in 3-fold serial dilutions. Plates were incubated for 18 hours at 37 °C and 5% CO2 after which the cells were washed five times in PBS. Wells were incubated with 100 μL IgG-biotin HU adsorbed (Southern Biotech) for 2 h at RT. Next, plates were washed four times in PBS followed by the addition of 100 μL HRP-conjugated streptavidin/well for 1 h at RT. Plates were washed again and incubated with 100 μL TMB/well for 5 minutes until distinct spots emerged. Finally, plates are then washed three times with distilled water

and left to dry completely in a laminar flow hood. A CTL ImmunoSpot Analyzer was used to image plates, count spots, and perform quality control.

2.3.10 SARS-CoV-2 virus neutralization assay

SARS-CoV-2 viruses (400 plaque forming units; strain nCov/Washington/1/2020, provided by the National Biocontainment Laboratory, Galveston TX, USA) were incubated with 4-fold serial dilutions of heat-inactivated plasma from vaccinated or control mice and for 1 h at 37 °C in DMEM with 2% fetal bovine serum, penicillin-streptomycin (100 U/mL penicillin, 100 μg/mL streptomycin), and non-essential amino acids (10 mM, glycine, L-alanine, L-asparagine, L-aspartic acid, L-glutamic acid, L-proline, L-serine; Gibco). The pre-incubated viruses were then applied to Vero-E6 cell monolayers, and the cells were maintained until $>$ 90% cell death for the negative control (4-5 d). Cells were then washed with PBS, fixed with 10% formalin, stained with crystal violet, and quantified with a Tecan infinite m200 microplate reader (excitation/emission 592 nm/636 nm). Neutralization titer is measured as the greatest dilution that inhibits 50% of SARS-CoV-2 induced cell death (EC50). To determine the EC50, data were fit using a least squares variable slope four-parameter model. To ensure realistic EC50 values, we considered a dilution (1/X) of X = 10^{-1} to be 100% neutralizing and a dilution of X = 10^{8} to be 0% neutralizing and constrained EC50 $>$ 0. Plasma from convalescent human COVID-19 patients were provided by Ali Ellebedy (Washington University School of Medicine, St. Louis, MO; Catalog # NR-53661, NR-53662, NR-53663, NR-53664, and NR-53665).

2.3.11 Peptide array analysis

Antibody specificity to linear epitopes of the spike protein was analyzed using a CelluSpots™ Covid19hullB Peptide Array (Intavis Peptide Services, Tubingen, Germany) according to the manufacturer's protocol. The array comprises 254 peptides spanning the full-length sequence of the Spike protein (NCBI GenBank accession # QHD43416.1), with each 15-mer peptide

offset from the previous one by 5 amino acids. Briefly, peptide arrays were blocked in 1x casein solution at 4 °C overnight. Arrays were then incubated with pooled serum diluted 1:200 in 1x casein for 6 h at RT on an orbital shaker (60 rpm). After 6 h, arrays were washed four times with PBS-T and incubated for an addition 2 h at RT, 60 rpm with goat anti-mouse IgG conjugated to HRP (Southern Biotech) diluted 1:5000 in 1x casein. Arrays were washed another four times with PBS-T. Spots were detected with ClarityTM Western ECL Substrate (Bio-Rad), and chemiluminescence was measured using a ChemiDoc XRS+ Gel Documentation System (Bio-Rad). Spots were analyzed using Spotfinder software (version v3.2.1).

2.3.12 Software packages and statistical analysis

Statistical analysis was performed using GraphPad Prism 9 (GraphPad). Data were analyzed using one-way ANOVA with Dunn's or Tukey's post-hoc correction for multiple hypothesis testing unless otherwise stated. All flow cytometry data were analyzed using FlowJov10.7.2 software (FlowJo LLC, BD Biosciences). Figures 2.4 and 2.13 were created using BioRender (https://biorender.com) as part of an Academic License through the Chicago Immunoengineering Innovation Center.

2.4 Results

2.4.1 Formulated polymersomes exhibit long-term stability and in vitro *activity*

Having previously encapsulated antigen into PS as nanovaccines(213), here we developed a conjugation strategy to attach antigens to their surface. To create a modular platform that could be generalized to any antigen, we synthesized N3-PEG-PPS (Figure 2.5), which, when formulated into PS, yields particles displaying clickable surface moieties (Figure 2.4a).

Upon the addition of RBD conjugated to a DBCO-containing linker, we generated PS

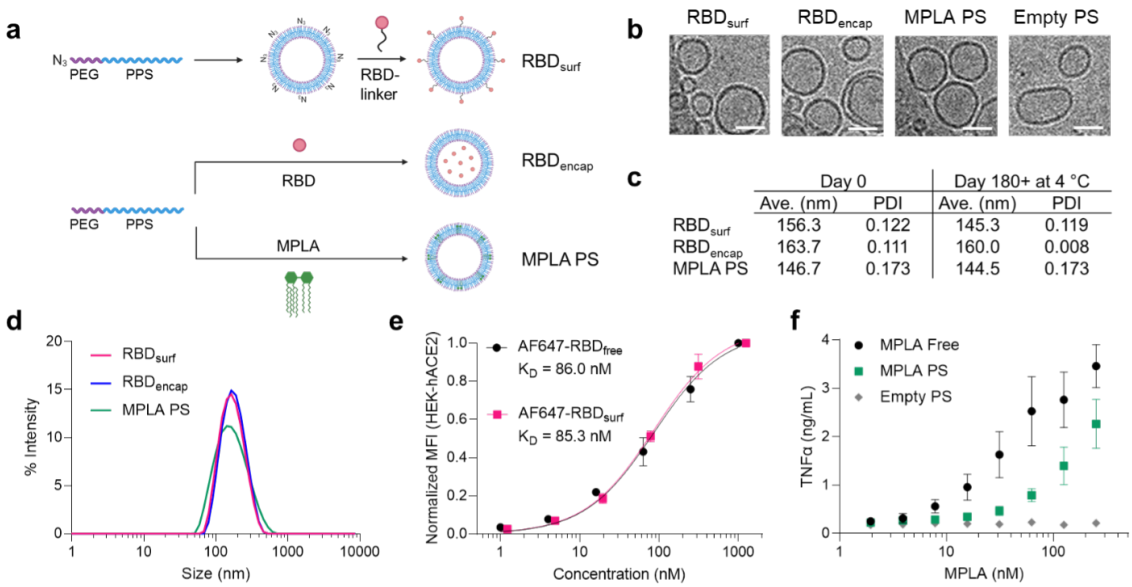

Figure 2.4: RBD and MPLA are formulated into stable, biologically active polymersomes. a, Schematic of formulation of PS. RBD was conjugated to the surface (RBDsurf) or encapsulated inside (RBDencap) of PS, and MPLA was encapsulated in the vesicle membrane (MPLA PS) due to its hydrophobicity. b, Representative cryo-electron microscopy images of PS, depicting vesicle structure. Scale = 50 nm. c, Size and polydispersity index (PDI) from dynamic light scattering (DLS) measurements of PS upon formulation and after > 6 months at 4 °C. d, Representative DLS curves of PS. e, Normalized mean fluorescence intensity (MFI) of AF647 conjugated to free RBD or RBDsurf by flow cytometry showing concentration-dependent binding to HEK-293 cells that express human ACE-2 (HEK-hACE2). Nonlinear regression was used to model data assuming specific binding to one site to determine equilibrium dissociation constants. f, Dose-dependent secretion of TNFα from cultured murine bone marrow-derived dendritic cells (BMDCs) stimulated by free MPLA, MPLA PS, or empty PS. Data represent mean ± SD for n = 2 (e) or 3 (f) replicates.

decorated with RBD (RBDsurf, Figure 2.6). We also synthesized PEG-PPS (Figure 2.7) and formulated PS encapsulating RBD (RBDencap) or adjuvant (MPLA PS, Figure 2.4a).

The loading capacities of RBDsurf and RBDencap were 1.57% and 1.75%, respectively, comparable to previous reports of encapsulated ovalbumin(210; 213), while the loading capacity of MPLA PS was 6.46% (Table 2.4). We confirmed the vesicular structure of PS through cryo-electron microscopy (cryoEM) and demonstrated that the different formulations have similar sizes and morphologies (Figure 2.4b, Figure 2.8).

According to dynamic light scattering (DLS) measurements, the average PS diameter is

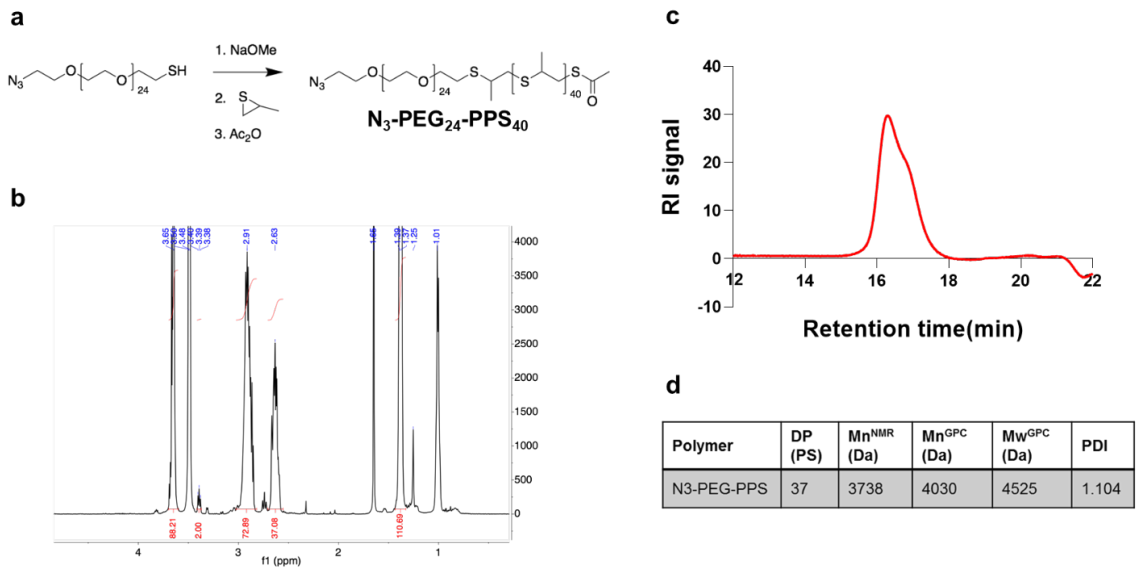

Polymer	DP (PS)	Mn^{NMR} (Da)	Mn^{GPC} (Da)	Mw^{GPC} (Da)	PDI
N3-PEG-PPS	37	3738	4030	4525	1.104

Figure 2.5: Synthesis and characterization of N3-PEG-PPS. a, Synthetic route, b, 1H NMR spectrum, c, gel permeation chromatography (GPC) trace, and d, summary of physiochemical properties of N3-PEG-PPS.

Table 2.4: Summary of loading capacities of PS

	Polymer(mg $mL^{-}1$)	**Cargo (mg $mL^{-}1$)**	**Loading(wt%)**
RBDsurf	7.96	0.127	1.57
RBDencap	7.00	0.125	1.75
MPLA PS	3.49	0.241	6.46

around 150 nm (Figure 2.4c,d), which is similar to the reported size of SARS-CoV-2 particles (60-140 nm)(332).The polydispersity index (PDI) of each formulation was < 0.2, indicative of a relatively homogenous population of nanoparticles. As indicated by their consistent size and PDI, in addition to the absence of free RBD released into solution, PS remain stable at 4°C for at least 180 days, which can be beneficial for distribution and shelf-life considerations (Figure 2.4c, Figure 2.9).

We next characterized the biological activity of the PS formulations *in vitro*. To confirm that RBD structure is not substantially altered upon conjugation to the PS surface, we quantified its ability to bind to HEK-293 cells that express human ACE-2 (HEK-hACE2, Figure 2.4e). The normalized mean fluorescence intensity (MFI) versus RBD concentration curves were used to calculate the equilibrium dissociation constants (KD) for free RBD and

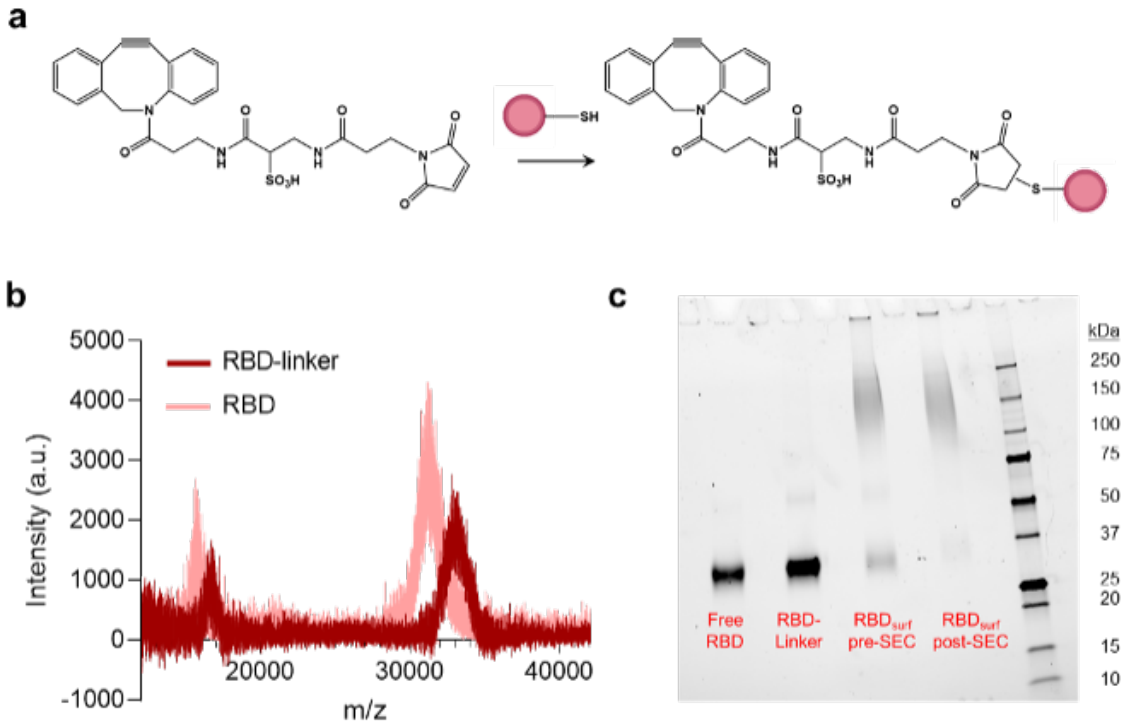

Figure 2.6: Synthesis and characterization of RBD-linker. a, Synthetic route, b, MALDI of RBD-linker and free RBD, c, SDS PAGE of free RBD, RBD-linker, RBDsurf before size exclusion chromatography (SEC) and purified RBDsurf post-SEC.

RBDsurf conjugated to AF647 (AF647-RBDfree and AF647-RBDsurf, respectively). The curves and KD values are in excellent agreement, indicating that surface conjugation to PS did not impact ACE-2 binding of RBD. Empty PS conjugated to AF647 did not bind to HEK-hACE2, and neither PS formulation bound to HEK-293 cells lacking hACE-2 (Figure 2.10).

Next, we confirmed that MPLA retained its ability to serve as a TLR4 agonist upon formulation in PS with a HEK-BlueTM TLR4 reporter cell line (Figure 2.11). To further validate MPLA PS activity in a more physiologically-relevant model, we stimulated murine bone marrow-derived dendritic cells (BMDCs) with free MPLA, MPLA PS, or empty PS, and we measured the subsequent secretion of the pro-inflammatory cytokines TNFα, IL-6, IL-1α, and IL-1β (Figure 2.4f, Figure 2.12).

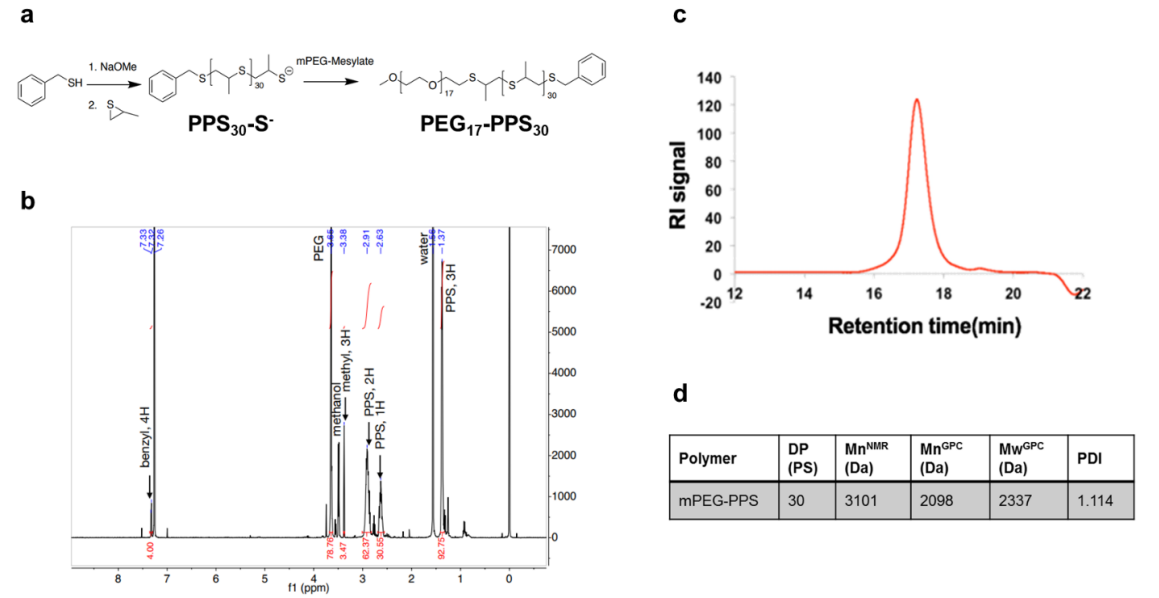

Polymer	DP (PS)	Mn^{NMR} (Da)	Mn^{GPC} (Da)	Mw^{GPC} (Da)	PDI
mPEG-PPS	30	3101	2098	2337	1.114

Figure 2.7: Synthesis and characterization of PEG-PPS. a, Synthetic route, b, 1H NMR spectrum, c, gel permeation chromatography (GPC) trace, and d, summary of physiochemical properties of PEG-PPS.

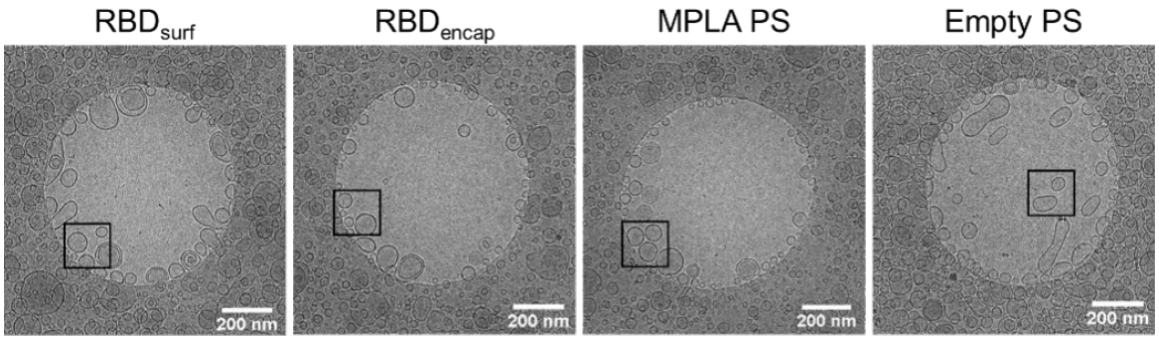

Figure 2.8: Additional cryoEM images of PS. Black box indicates magnified region in Figure 1b.

For each cytokine, there was a dose-dependent increase in secretion for free MPLA and MPLA PS with only background levels of secretion for empty PS, indicating that MPLA PS successfully activated antigen presenting cells (APCs) *in vitro*. Thus, we successfully synthesized two RBD formulations of PS in addition to MPLA PS and showed that they are homogenous vesicular structures with long-term stability and *in vitro* biological activity.

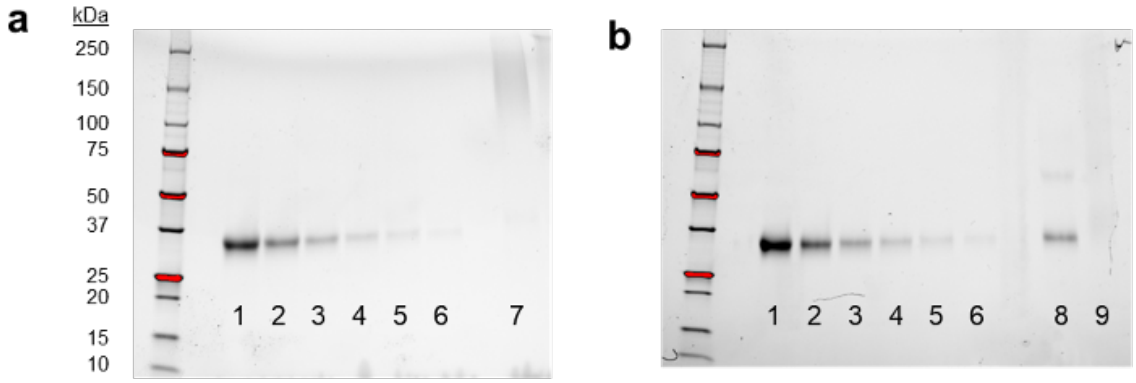

Figure 2.9: PS stability by SDS PAGE after > 180 d at 4°C. SDS PAGE of a, RBDsurf and b, RBDencap. Lanes 1-6 represent RBD standard curve values of 400, 200, 100, 50, 25, and 12.5 μg/mL. Lane 7 contains of RBDsurf disrupted with Triton X. Lane 8 contains of RBDencap disrupted with Triton X, and Lane 9 contains undisrupted RBDencap.

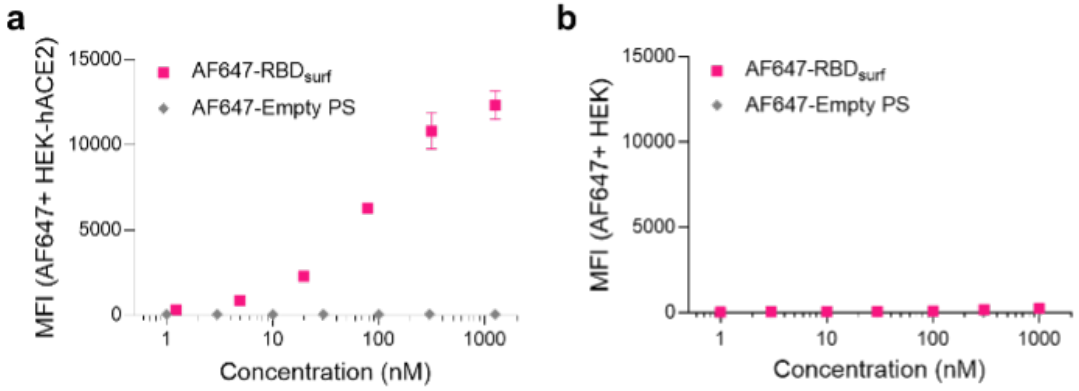

Figure 2.10: RBD binding to HEK-hACE2 and HEK-293 cells. a, Mean fluorescence intensity (MFI) of AF647-labeled RBDsurf and empty PS bound to HEK-hACE2 cells characterized by flow cytometry. b, MFI of AF647-labeled RBDsurf and empty PS indicating an absence of binding to control HEK-293 (HEK) cells. Data plotted as mean ± SD for n = 2 replicates.

2.4.2 All adjuvanted formulations elicit RBD-specific IgG responses

Having confirmed that antigen- and adjuvant-loaded PS exhibit their expected bioactivity *in vitro*, we next evaluated their ability to enhance humoral and cellular immunity in mice compared to RBDfree. We immunized mice via s.c. injection in the hocks in a prime-boost schedule 3 weeks apart and monitored antibody titers weekly (Figure 2.13a). The total

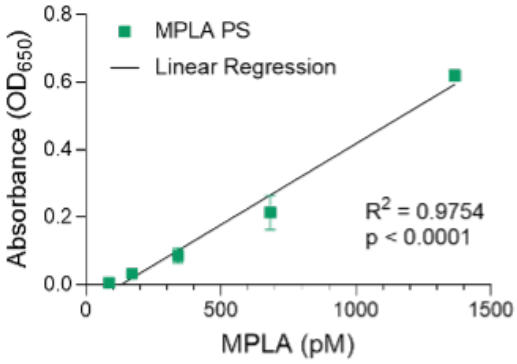

Figure 2.11: MPLA PS as a TLR4 agonist. Linear concentration-dependent stimulation of HEK-BlueTM TLR4 reporter cells with MPLA PS. Data plotted as mean ± SD for n = 3 replicates.

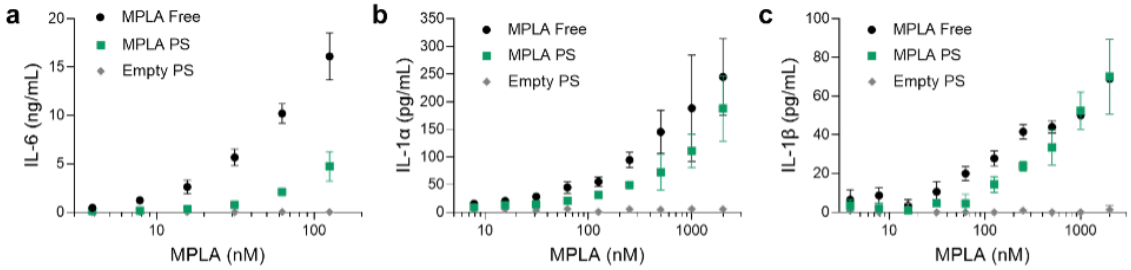

Figure 2.12: *In vitro* activity of MPLA PS. Dose-dependent secretion of a, IL-6, b, IL-1α, and c, IL-1β from cultured murine bone marrow-derived dendritic cells stimulated by free MPLA, MPLA PS, or empty PS. Data plotted as mean ± SD for n = 3 replicates.

RBD-specific IgG is represented by the area under the log-transformed ELISA absorbance curves (AUC), starting at a plasma dilution of 10^{-2} (see Methods, Figure 2.14). All adjuvanted groups had significant anti-RBD binding antibody responses within a week after their first dose, with RBDencap stimulating the highest responses (Figure 2.13b). The antibody responses in adjuvanted groups either increased gradually or remained constant until a week after the booster, when the mean AUC increased 1.3- to 1.6-fold.

In order to explore the humoral response in further detail, we then evaluated IgG subtypes of induced antibodies at the study endpoint (d28, 1 week post-boost). While plasma antibody levels of all adjuvanted groups were similar for IgG1 and IgG3, RBDsurf elicited significantly lower IgG2b and IgG2c antibody responses (Figure 2.13c). The ratio of IgG2b/IgG1 was

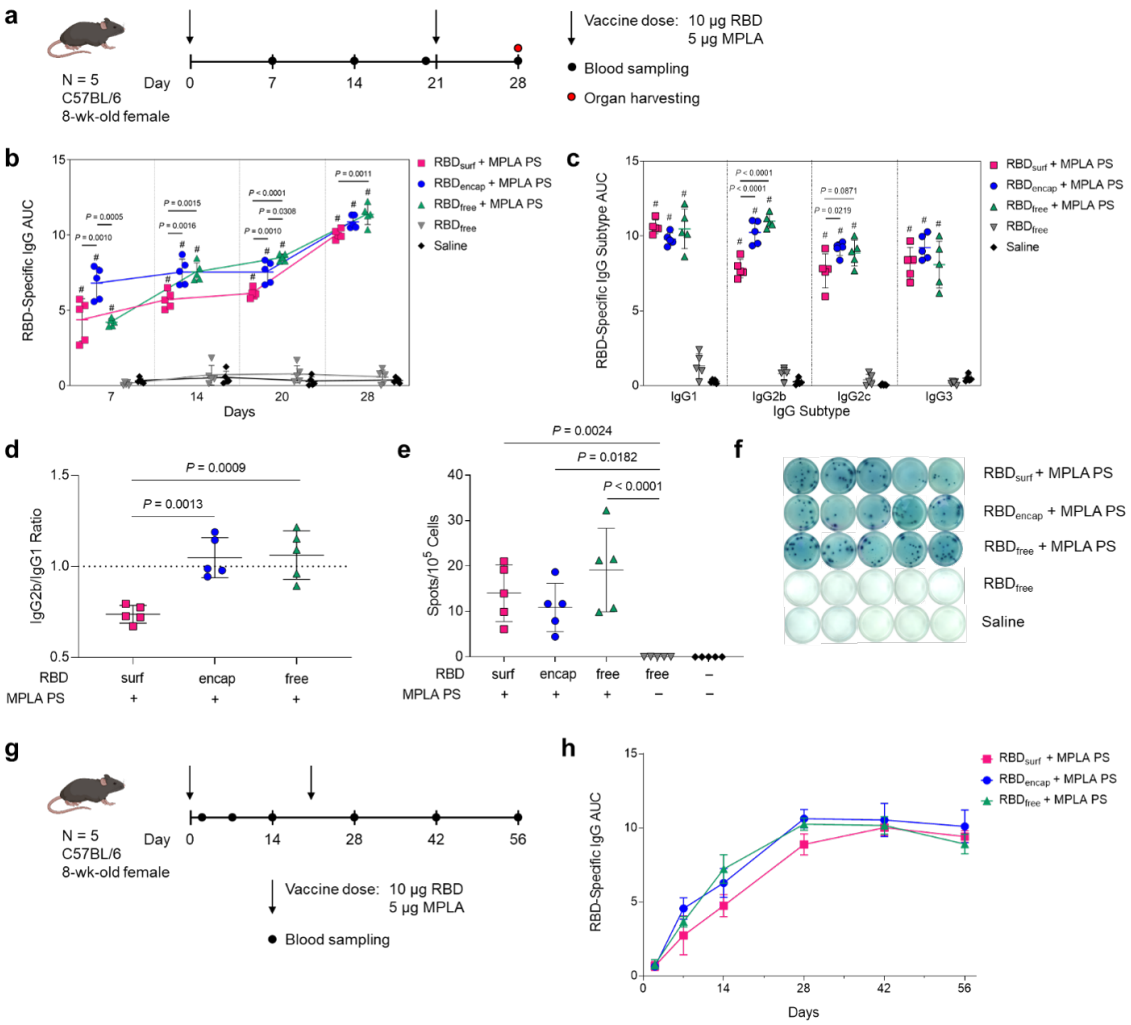

Figure 2.13: High levels of RBD-specific IgG antibodies are produced upon PS vaccination. a, Vaccination schedule consisting of a priming dose followed by a booster 3 weeks later. b, Total RBD-specific IgG antibodies over time reported as the area under the log-transformed curve (AUC) of absorbance vs. dilution. c, Comparison of RBD-specific IgG isotypes (IgG1, IgG2b, IgG2c, IgG3) on day 28. d, Ratio of AUCs of IgG2b:IgG1 isotypes. e, Quantification of RBD-specific IgG+ antibody secreting cells by ELISpot of splenocytes (Dunn's post-test compared to unadjuvanted RBDfree). f, Representative ELISpot wells from (e). Data plotted as mean ± SD and represent 1 of 2 experiments with n = 5 mice each. Symbols represent individual mice. g, Vaccine and blood sampling schedule of long-term kinetics study. h, Total RBD-specific IgG antibodies over time for the vaccination schedule in (g). Data represent mean ± SD for n = 5 mice. Comparisons were made using one-way ANOVA with Tukey's post-test unless stated otherwise. # $P < 0.0001$ compared to unadjuvanted RBDfree.

then taken as an indication of a Th1/Th2-mediated response(333). While RBDencap and RBDfree + MPLA PS have a ratio of around 1, indicating a balanced Th1/Th2 response,

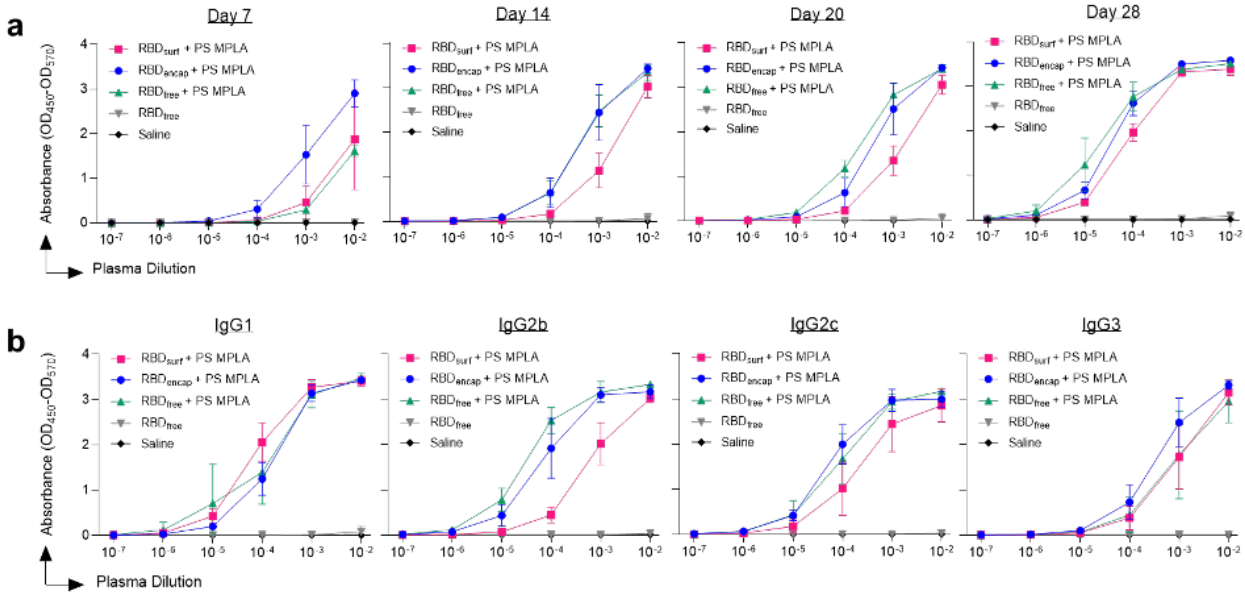

Figure 2.14: ELISA absorbance vs. dilution curves. Absorbance vs. dilution for RBD-specific ELISAs for a, total IgG over time and b, IgG subtypes on d28. Log-transformed curves were quantified by AUC in Figure 2. Data plotted as mean ± SD and represent 1 of 2 experiments with n = 5 mice each.

RBDsurf shows a lower ratio of IgG2b to IgG1 indicating a slightly Th2-skewed response (Figure 2.13d).

Next, to determine if the higher antibody responses of adjuvanted groups stemmed from an expanded number of RBD-specific antibody secreting cells (ASCs), we performed an *ex vivo* RBD enzyme-linked immunosorbent spot (ELISpot) assay with splenocytes harvested 1 week post-boost. All groups receiving adjuvanted RBD showed significantly higher RBD-specific IgG+ ASCs compared to unadjuvanted RBDfree, consistent with plasma antibody levels (Figure 2.13e,f). Finally, we evaluated the kinetics and durability of the humoral response to demonstrate the persistence of elicited antibodies (Figure 2.13g). The RBD-specific IgG AUC for all adjuvanted groups increased until 1 week post-boost and then remained constant over the subsequent 4 weeks, indicating that the antibody responses stimulated by these vaccine formulations persist for at least 2 months in mice after the initial dose. Taken together, MPLA PS-adjuvanted RBDsurf, RBDencap, and RBDfree all

stimulated persistent anti-RBD antibodies and increased the frequencies of RBD-specific ASCs in the spleen.

2.4.3 RBD-surface-decorated polymersomes, but not RBD-encapsulated polymersomes, induce neutralizing antibodies

After analyzing the quantity of RBD-specific antibodies produced by the vaccine candidates, we next sought to determine their neutralizing capacity and breadth of epitope recognition. Neutralizing antibodies were assessed against SARS-CoV-2 infection of Vero E6 cells *in vitro*. Although all adjuvanted groups elicited similarly high titers of RBD-binding IgG antibodies (10^5-10^7, Figure 2.15a), only RBDsurf neutralized the virus to a greater extent than unadjuvanted RBDfree at a plasma dilution of $10^{-2.11}$ (Figure 2.16a).

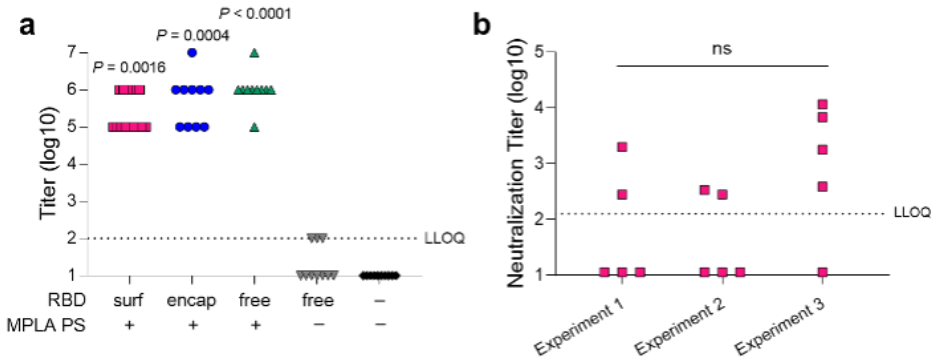

Figure 2.15: IgG antibody and viral neutralization titers. a, Aggregate RBD-specific IgG antibody titers 1 week post-boost based on ELISA. Values below the LLOQ (= 2) are plotted as LLOQ/2. Titers were determined as the -log of the lowest plasma dilution for which (OD450-OD570) – (average of blanks + 4 × standard deviation of blanks) > 0.01. P values represent comparisons to unadjuvanted RBDfree. b) Viral neutralization titers for RBDsurf + MPLA PS across three different cohorts of n = 5 mice, indicating experiment reproducibility. Values below the LLOQ (= 2.11) are plotted as LLOQ/2.; ns p = 0.11. Symbols represent individual mice. Comparisons were made using a Kruskal-Wallis nonparametric test with Dunn's post-test.

We then quantified the viral neutralization titer (VNT) as the dilution at which 50% of SARS-CoV-2-mediated cell death is neutralized. There was no significant difference between

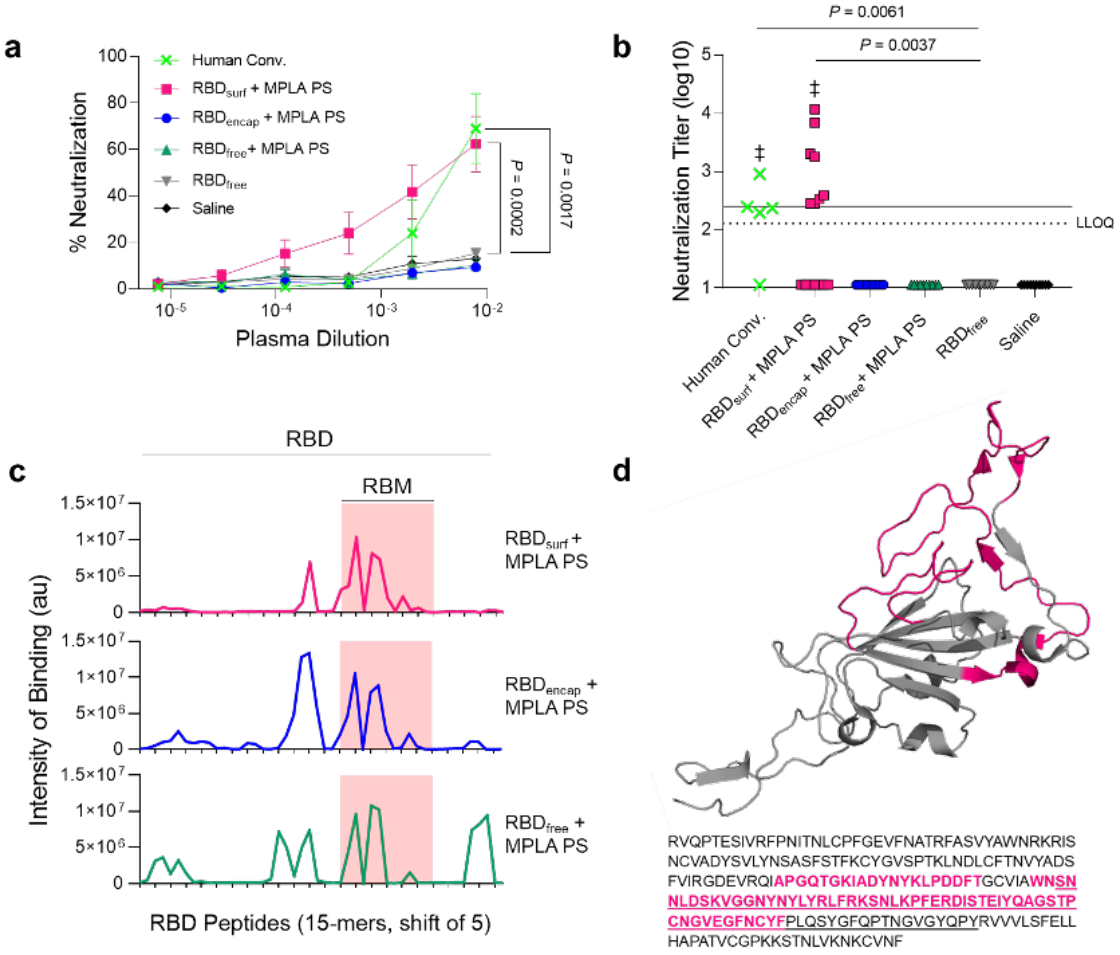

Figure 2.16: Antibodies induced by vaccination with RBDsurf + MPLA PS are neutralizing and localized to the receptor binding motif. a, Plasma from mice 1 week post-boost was tested for its ability to neutralize SARS-CoV-2 infection of Vero E6 cells *in vitro*. Percent neutralization for multiple plasma dilutions normalized to cells without virus (100%) or without plasma (0%). Data plotted as mean ± SEM for n = 5 convalescent human samples (human conv.) or 10-15 mice. Comparisons to unadjuvanted RBDfree were made for lowest dilution (10-2.11) using one-way ANOVA with Dunnett's post-test. b, Viral neutralization titers, representing the plasma dilution at which 50% of SARS-CoV-2-mediated cell death is neutralized. Dashed line: lower limit of quantification (LLOQ = 2.11). (Continued on the following page.)

VNTs of human convalescent individual samples and RBDsurf plasma, and both groups induced higher VNTs compared to unadjuvanted RBDfree (Figure 2.16b). Furthermore, the median VNT elicited by RBDsurf was 2.45, which falls within the FDA classification of "high titer" for convalescent plasma therapy (>2.40)(334). To ensure reproducibility, the neutral-

Figure 2.16, continued: For values below the LLOQ, LLOQ/2 values were plotted. Solid line: FDA recommendation for "high titer" classification (= 2.40). Comparisons were made using Kruskal-Wallis nonparametric test with Dunn's post-test or Wilcoxon signed rank test (‡ ns, $P > 0.05$ compared to hypothetical value of 2.40). Symbols represent individual mice. c, Pooled plasma was then tested for antibody binding to linear epitopes using overlapping 15-amino-acid peptides with 5-amino-acid offsets, spanning the entire RBD sequence. X-axis represents sequential peptide number within the RBD amino acid sequence, and y-axis represents average luminescence for each peptide epitope. d, 3D structure of RBD with the receptor binding motif (RBM) underlined and main peptide sequences recognized by mouse plasma highlighted in pink (Protein Data Bank Entry 7DDD).

ization assay was repeated with 3 different cohorts of n = 5 mice each, and no significant differences were observed between the resulting VNTs (Figure 2.15b). We next aimed to determine whether differences in neutralizing ability resulted from the epitope recognition breadth elicited by each vaccine formulation. To test this, we mapped the epitopes recognized by vaccine-elicited antibodies using a linear peptide array from the full-length RBD sequence. While IgG antibodies elicited by RBDsurf primarily recognized linear epitopes concentrated within the receptor binding motif of RBD (RBM; aa 438-508), RBDencap and RBDfree + MPLA PS exhibited broader linear epitope diversity (Figure 2.16c,d, Figure 2.17). Within RBD, the RBM is particularly critical for interacting with ACE-2, so antibodies specific for this region may have potent neutralizing potential(335; 336).

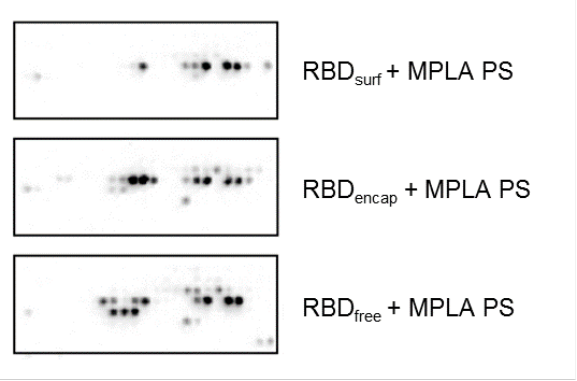

Figure 2.17: Representative peptide array images. Boxes represent region of peptide array specific to the RBD of the Spike protein. Peptide arrays quantified in Figure 3c.

Because RBDsurf appeared to offer the advantage of improved neutralizing activity, while RBDencap offered epitope diversity, we asked if co-administration would synergize to further

enhance protection. To test this, we mixed RBDsurf and RBDencap (with total RBD dose remaining constant) with MPLA PS and treated mice using the same vaccination schedule. As an additional control, we also investigated the humoral response of RBDfree adjuvanted with free MPLA. While both groups produced high RBD-specific IgG AUCs, neither exhibited neutralizing potential against the SARS-CoV-2 virus above background levels (Figure 2.18a,b). Analysis of the peptide arrays for these groups shows the presence of high-intensity-binding antibodies outside of the RBM (Figure 2.18c).

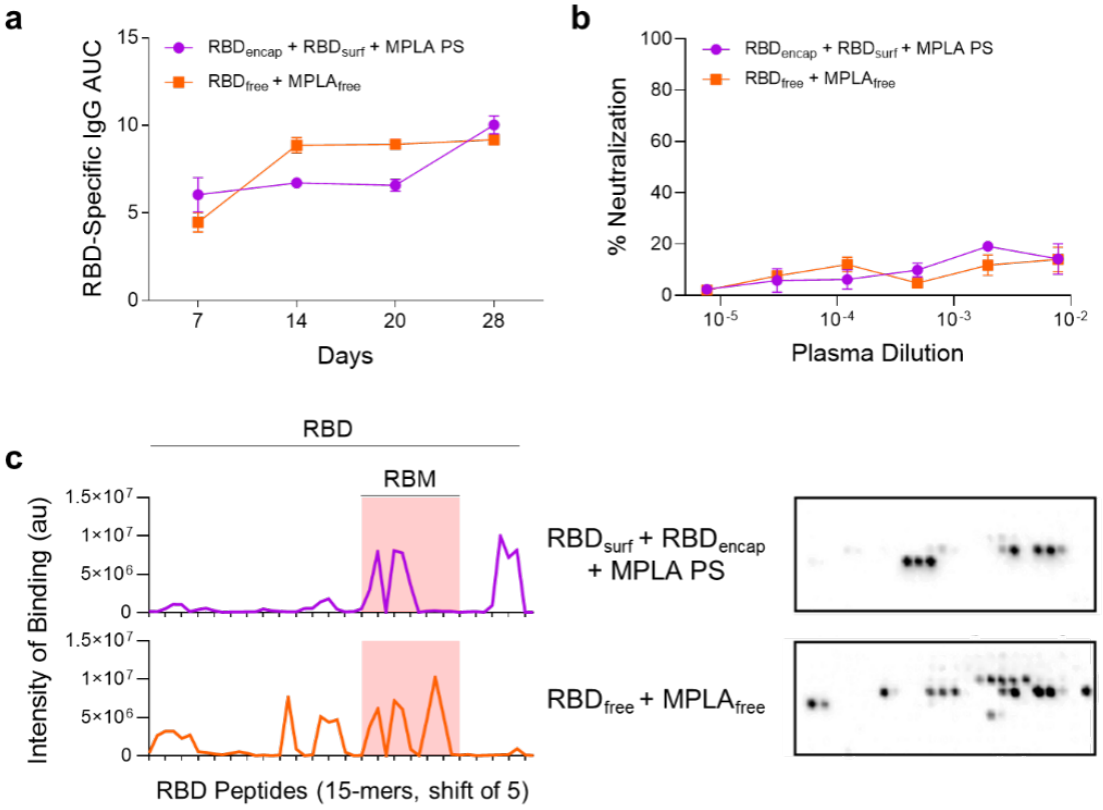

Figure 2.18: Analysis of plasma by mice vaccinated with RBDsurf + RBDencap + MPLA PS and RBDfree + MPLAfree. Mice received a priming dose on day 0 with a boost on day 21, and plasma was taken weekly to monitor production of RBD-specific antibodies. a, AUC of absorbance curve of RBD-specific IgG ELISAs for mice vaccinated with either 5 μg RBDencap + 5 μg RBDsurf + MPLA PS or 10 μg RBDfree + MPLAfree. Data plotted as mean $\pm$ SD for n = 5 mice. b, Neutralization of SARS-CoV-2 infection of Vero E6 cells *in vitro*. Data plotted as mean $\pm$ SEM for n = 5 mice. c, Epitope mapping using 15-amino-acid peptides with a 5-amino-acid shift, spanning the entire RBD sequence with representative images of peptide arrays.

In summary, while all adjuvanted groups elicit high titers of RBD-specific antibodies, only RBDsurf generated neutralizing antibodies against SARS-CoV-2 at titers comparable to human convalescent plasma. Additionally, these antibodies uniquely bound to linear epitopes localized within the RBM, while all other groups produced antibodies with greater epitope breadth.

2.4.4 All adjuvanted formulations increase Tfh and B cell activation in the dLN

Given the differences in antibody responses and neutralizing activity elicited by RBDsurf versus RBDencap vaccination, we further investigated the phenotypes of the B and T cells involved in the initiation of the humoral immune response. All adjuvanted groups showed trends of higher frequencies of T follicular helper cells (Tfh; CD4+CXCR5+BCL6+) in the injection site-draining lymph nodes (dLNs) 1 week post-boost compared to unadjuvanted RBDfree (Figure 2.19a, Figure 2.1), although differences were only statistically significant for RBDfree + MPLA PS.

Interestingly, a greater percentage of Tfh cells in all adjuvanted groups highly upregulated expression of ICOS, a co-stimulatory receptor important in Tfh activation and maintenance (Figure 2.19b)(337).

Following activation by Tfh cells, naïve B cells can either undergo a germinal center (GC)-dependent response in which they become GC B cells and undergo cycles of class-switching and somatic hypermutation (SHM) before differentiation into LLPCs and class-switched memory B cells, or they can differentiate into short-lived plasmablasts or IgM memory cells in a GC-independent response(338). A stronger GC response is valuable in vaccination because it results in higher affinity and longer-lived antibody production(339). Overall frequencies of B cells (CD19+B220+) were unaffected across groups, but there were significantly lower frequencies of naïve IgD+ B cells in the adjuvanted groups compared to unadjuvanted RBDfree (Figure 2.2, Figure 2.20).

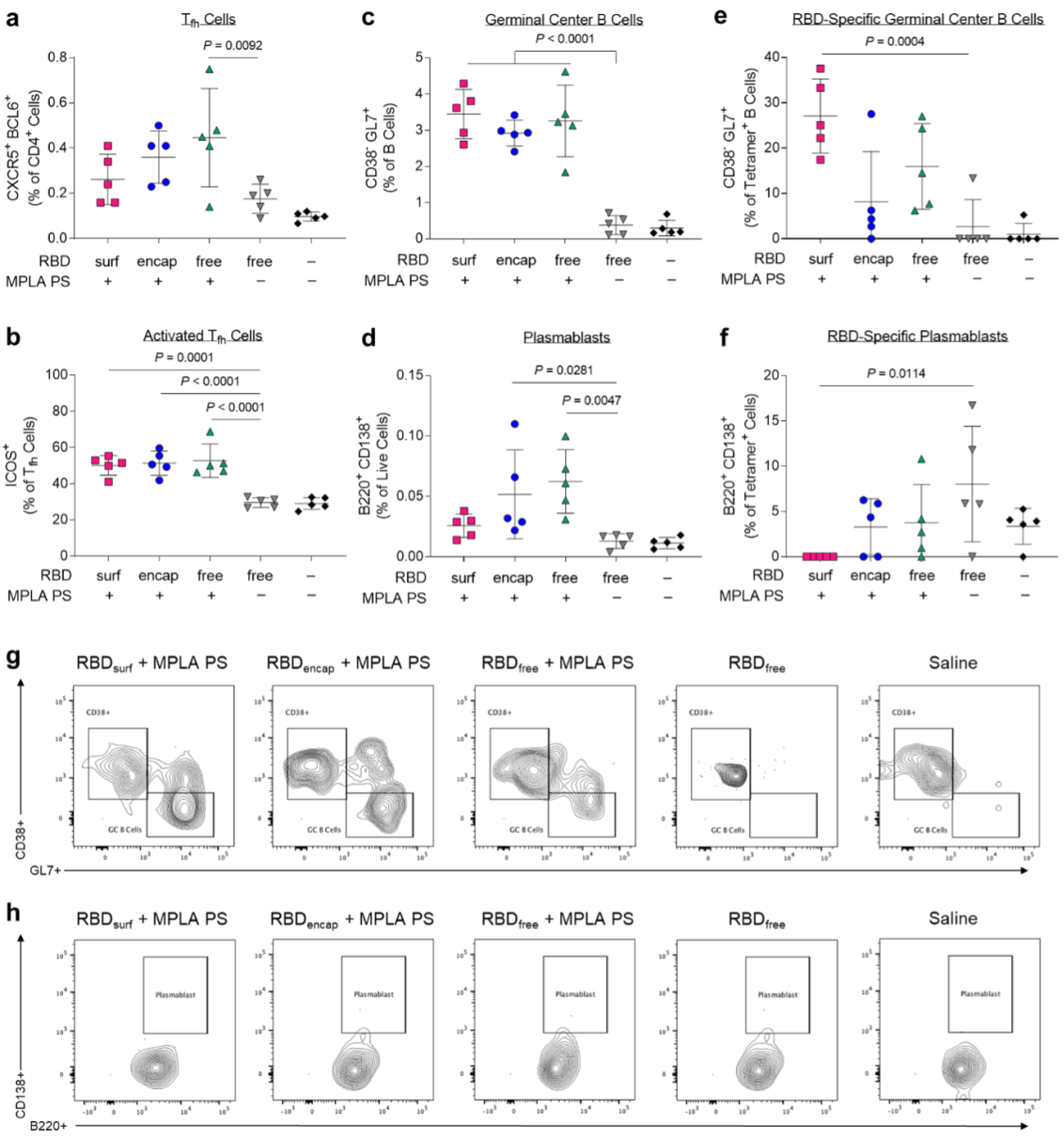

Figure 2.19: CD4+ T follicular helper cell (Tfh) and B cells are activated by PS vaccine 1 week post-boost in the injection site-draining lymph nodes (dLN). a, Tfh cells (CXCR5+ BCL6+) of vaccinated mice quantified via flow cytometry as a percent of live CD4+ T cells. b, Highly activated ICOS+ Tfh cells quantified as percent of Tfh cells. c, Germinal center B cells (CD38- GL7+) quantified as a percentage of total B cells (B220+ CD19+). (Continued on the following page.)

All adjuvanted groups generated GC responses, characterized by increased frequencies of GC B cells (CD38-GL7+) in the dLN compared to unadjuvanted RBDfree (Figure 2.19c). Both RBDencap and RBDfree + MPLA PS formulations, but not RBDsurf, significantly

Figure 2.19, continued: d, Plasmablasts (B220+ CD138+) quantified as a percentage of total dLN cells. e, Germinal center B cells quantified as a percentage of RBD-specific B cells. f, Plasmablasts quantified as a percentage of RBD-specific dLN cells. g-h, Concatenated flow cytometry contour plots for n = 5 mice/group showing RBD-specific GC B cells (g) or plasmablasts (h). Data plotted as mean ± SD and represent 1 of 2 experiments with n = 5 mice each. Symbols represent individual mice. Comparisons to unadjuvanted RBDfree were made using one-way ANOVA with Dunn's post-test.

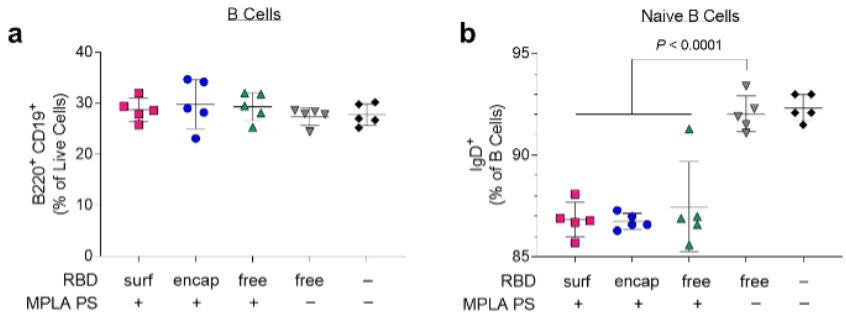

Figure 2.20: Total and naïve B cells in vaccinated mice 1 week post-boost. a, Total B cells (B220+ CD19+) and b, naïve B cells in dLNs. Data plotted as mean ± SD and represent 1 of 2 experiments with n = 5 mice each. Symbols represent individual mice. Comparisons to unadjuvanted RBDfree were made using one-way ANOVA with Dunn's post-test.

increased the frequencies of plasmablasts (B220+CD138+) in the dLN compared to unadjuvanted RBDfree (Figure 2.19d). To determine the antigen-specificity of the B cells, we developed a set of fluorescent RBD protein multimeric probes. To ensure selectivity, B cells were considered RBD-specific if they were double-positive for both PE- and APC-conjugated RBD-multimers and negative for the non-specific control protein multimer (Figure 2.21). RBDfree + MPLA PS was the only formulation to significantly increase the frequency of RBD-specific B cells in the dLN (Figure 2.22).

We next sought to further determine the phenotype of these RBD-specific B cells. RBD-surf , unlike the other adjuvanted formulations, led to a significantly higher fraction of RBD-specific B cells with GC B cell phenotype, suggesting a more robust GC response to RBD (Figure 2.19e). RBDsurf was also the only formulation with a significantly lower fraction of plasmablasts within the RBD-specific B cell subset compared to unadjuvanted RBDfree (Figure 2.19f). These differences are also visually apparent in pooled flow cytometry plots

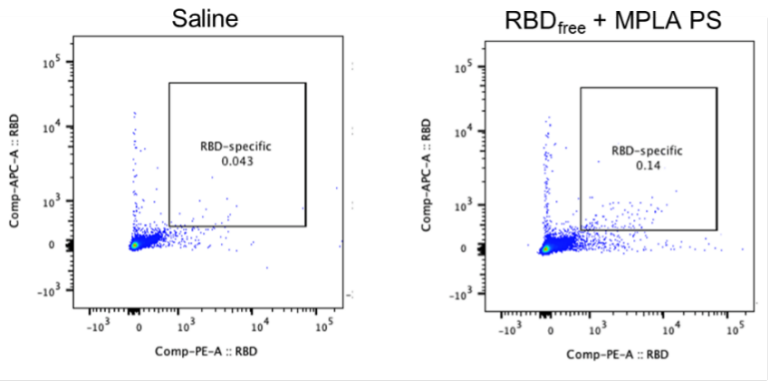

Figure 2.21: Representative multimer staining.

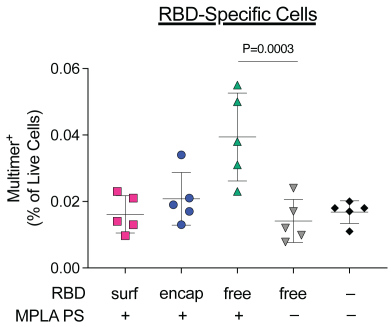

Figure 2.22: RBD-specific cells in vaccinated mice 1 week post-boost. Multimer+ cells in dLNs on d28. Data plotted as mean ± SD and represent 1 of 2 experiments with n = 5 mice each. Symbols represent individual mice. Comparisons to unadjuvanted RBDfree were made using one-way ANOVA with Dunn's post-test.

for RBD-specific GC B cells (Figure 2.19g) and plasmablasts (Figure 2.19h). In summary, all adjuvanted formulations of RBD increased activation of Tfh cells and GC B cells in the dLN, but within the RBD-specific B cell population, only RBDsurf generated a higher fraction of GC B cells and a lower fraction of plasmablasts.

2.4.5 Vaccination with polymersome-formulated RBD generates RBD-specific Th1 T cell responses

Having demonstrated that our PS vaccines can generate strong humoral responses, we next sought to determine their capacity to generate robust CD8+ and CD4+ T cell immunity. In order to assess the RBD-specific T cell response, we isolated cells from the dLNs of vaccinated

mice 1 week post-boost. Prior to intracellular staining, cells were restimulated with RBD peptide pools for 6 hours. The RBD-specific response was quantified by subtracting the signal from cells incubated in media alone from those incubated with RBD peptide pools (Figure 2.3).

Only PS-formulated RBD groups RBDsurf and RBDencap generated significantly higher frequencies of IFNγ+, bifunctional IFNγ+TNFα+, and IL-2+ secreting CD8+ T cells compared to unadjuvanted RBDfree (Figure 2.23a).

Similar trends were seen in the CD4+ T cell compartment. Treatment with RBDsurf and RBDencap but not RBDfree + MPLA PS led to significantly higher frequencies of IFNγ+ and IL-2+ secreting CD4+ T cells, although the increase in bifunctional IFNγ+TNFβ+ was not statistically significant (Figure 2.23b). The production of these cytokines implies a Th1 T cell response, which is correlated with less severe cases of SARS-CoV infection(314). For further validation of the cytokine response, cells from the dLN isolated from the same vaccinated mice were restimulated with full RBD protein *ex vivo* for 3 days, followed by quantification of cytokines in the supernatant. The RBD-specific response was quantified by subtracting unstimulated signal from stimulated signal as above. The levels of Th1-type cytokines detected were consistent with intracellular staining data. Levels of IFNγ and IL-2 were modestly but not significantly increased in the RBDsurf and RBDencap groups compared to the RBDfree group, while cells from RBDencap-treated mice produced TNFα at significantly higher levels than unadjuvanted RBDfree (Figure 2.23c). RBDencap also led to increased production of IL-6 and IL-10, which are pleiotropic cytokines known to be secreted during Th1 responses (Figure 2.23c)(340; 341). Levels of secreted Th2-type cytokines were also measured. More IL-4 was produced in the supernatant of samples treated with RBDsurf and RBDencap compared to RBDfree, albeit at an overall low concentration. There was no significant elevation of IL-5 secretion across any of the treatment groups compared to the saline control and no detectable levels of IL-13 in any sample (Figure 2.24).

In summary, vaccination with RBD delivered via polymersome formulations generated

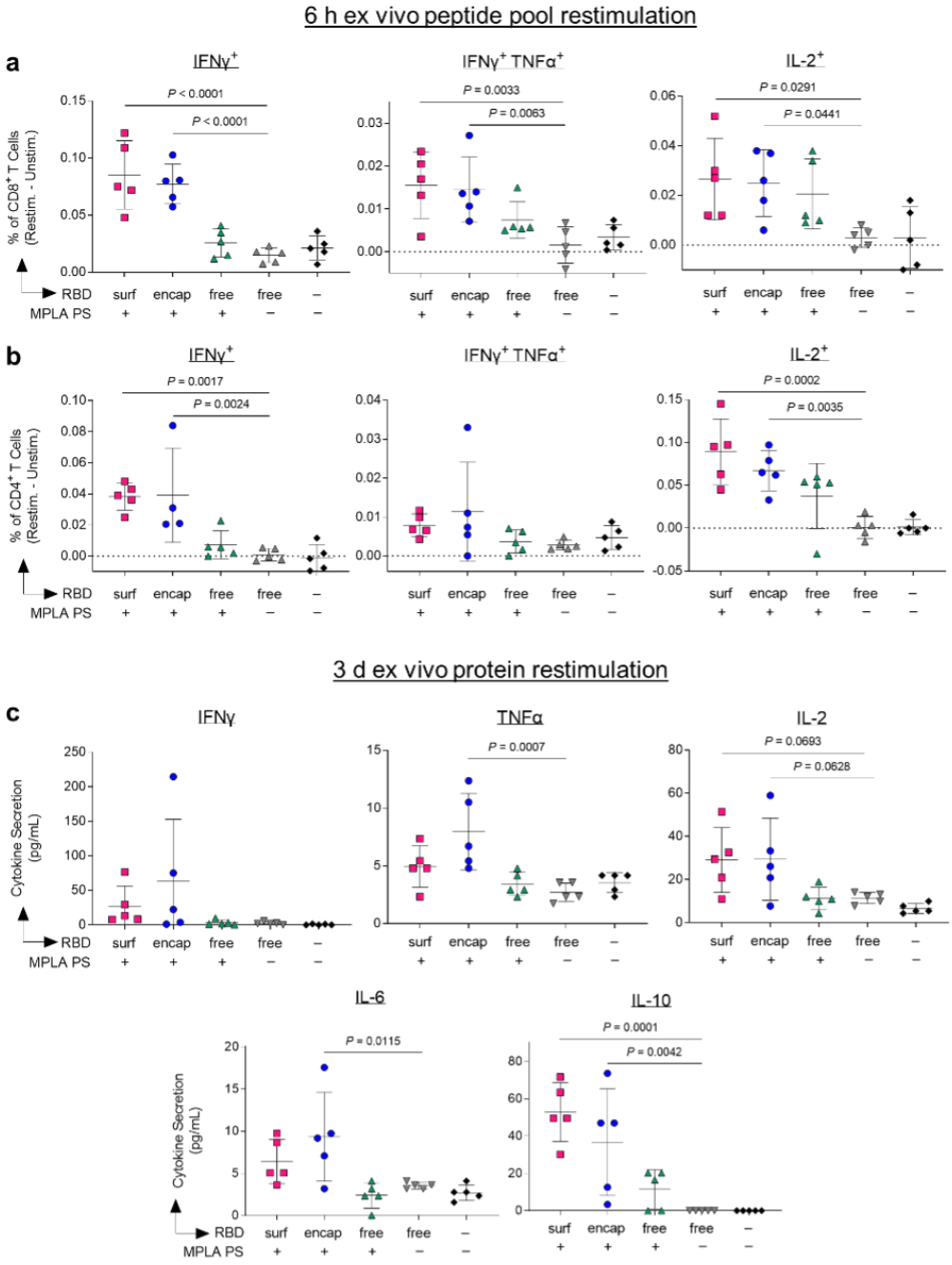

Figure 2.23: Vaccination with polymersome-formulated RBD improves antigen-specific T cell responses in mice. Cells isolated from the injection-site draining lymph nodes of PS-vaccinated mice 1 week post-boost were restimulated *ex vivo* for 6 h with RBD peptide pools or full RBD protein and analyzed by flow cytometry or multiplexed ELISA, respectively. (Continued on the following page.)

Figure 2.23, continued: a-b, percentages of cytokine-positive CD8+ T cells (a) and CD4+ T cells (b) in response to RBD peptide pools, subtracting unstimulated controls. c, Pro-inflammatory cytokine levels released into the supernatant measured after 3 d restimulation with whole RBD protein. Data plotted as mean ± SD and represent 1 of 2 experiments with n = 5 mice each. Symbols represent individual mice. Comparisons to unadjuvanted RBDfree were made using one-way ANOVA with Dunn's post-test.

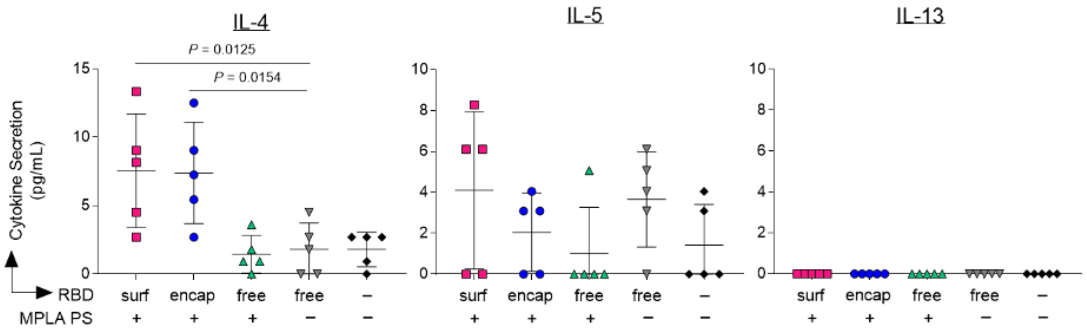

Figure 2.24: Th2-type cytokines secreted upon *ex vivo* stimulation with RBD. Lymph node cells isolated from the dLNs of PS vaccinated mice 1 week post-boost were restimulated *ex vivo* with full RBD protein. After 3 d, levels of IL-4, IL-5, and IL-13 secreted into the supernatant were measured. Data plotted as mean ± SD and represent 1 of 2 experiments with n = 5 mice each. Symbols represent individual mice. Comparisons to unadjuvanted RBDfree were made using one-way ANOVA with Dunn's post-test.

stronger RBD-specific Th1-type CD8+ and CD4+ T cell responses than unadjuvanted RBD-free, while RBDfree + MPLA PS did not.

2.5 Discussion

In this study, we developed antigen-decorated, oxidation-sensitive polymersomes that mimic virus particles as next-generation nanovaccines. While all adjuvanted formulations generated long-lived RBD-binding IgG responses, surface conjugation of antigen was necessary to generate neutralizing antibodies against SARS-CoV-2. More generally, this comparison of antigen formulation on the quality of immune response offers valuable insight into vaccine design, demonstrating the benefits of surface antigen display. The differences in the immune responses elicited by the two PS antigen formulations, RBDsurf and RBDencap, suggest

that surface display of antigen leads to stronger GC responses, while PS-encapsulated antigen elicits more predominantly an extrafollicular response. Though RBD-specific GC B cells are present in the dLN after treatment with both formulations, a much higher percentage of the RBD-specific B cells recovered after vaccination with RBDsurf exhibited a GC B cell phenotype. This higher percentage could be due to the induction of higher numbers of RBD-specific GC B cells after vaccination with RBDsurf or an increase in their affinity, leading to easier detection via RBD protein multimer staining. Both possibilities suggest a more robust GC response, as GC responses are necessary for an efficient SHM leading to increased B cell affinity(342). Evidence for affinity maturation due to SHM also includes the relatively few epitopes on the RBD linear peptide array to which IgG from RBDsurf-treated groups were specific compared to the other adjuvanted groups. Clonal bursts in GC responses can lead to rapid expansion of high-affinity SHM variants and loss of overall clonal diversity(39). A difference in the affinity of RBD-specific IgG generated by these vaccines may also explain the neutralization ability of the plasma after vaccination with RBDsurf but not RBDencap. Further data that suggest that RBDencap elicits a more extrafollicular response include the fast initial antibody response after priming by RBDencap, which resulted in RBD-specific IgG AUC 1 week after the initial prime that was significantly higher than that of RBDsurf. In an extrafollicular B cell response, B cells can differentiate immediately into plasmablasts and begin secreting antibodies after initial T cell help, whereas B cells that enter GCs delay the antibody response by several days(338). The preferential differentiation into plasmablasts rather than GC B cells was also evident in the increased fraction of plasmablasts within the RBD-specific B cell population generated by RBDencap. In vaccine development, the generation of robust GC reactions is preferable to extrafollicular responses because GC formation will usually result in higher affinity B cells, increased memory B cells and increased long-lived plasma cells in the bone marrow(338). The difference in mechanism of B cell activation by these two RBD formulations may be explained by previous studies on multimerization of antigen and use of virus-like particles in vaccination. Virus-like

particles are multi-protein supra-molecular structures constructed of many identical protein copies. Their multimeric nature has been associated with the induction of potent antibody responses due to BCR crosslinking in the presence of CD4+ T cell help(343). Mechanistic studies by Kato et al. demonstrated that increasing antigen valency can enhance the early activation and proliferation of antigen-specific B cells as well as increase B cell accumulation at the T-B border leading to increased differentiation of antigen-specific B cells into GC B cell and plasma cells(69). Furthermore, in contrast to RBDencap, RBDsurf most likely efficiently exposes for BCR interaction the conformational epitopes of RBD reported to be targeted by neutralizing antibodies in plasma of convalescent or vaccinated individuals(301–304). Thus, the multimerization of RBD on the PS surface in addition to its increased availability to B cells led to an improved functional quality of humoral response compared to encapsulated or unformulated RBD. The type of immune response to SARS-CoV-2 may have important implications in how the infection is cleared and should be considered in vaccine design(314). Less severe cases of the original SARS-CoV were associated with increased Th1-type cell responses(344; 345). In contrast, Th2-type responses were associated with increased pathology due to antibody-dependent enhancement, and several vaccine formulations against SARS-CoV tested in animal models showed signs of immunopathology due to Th2 cell-mediated eosinophil infiltration(346; 347). In this study, we measured the ratio of IgG1/IgG2b and the cytokine profile of dLN cells restimulated with RBD protein in order to characterize the type of immune responses generated by our vaccine formulations. RBDencap and RBDfree + MPLA PS generated IgG2b/IgG1 ratios around 1, suggesting a balance between type 1 and type 2 immunity, whereas RBDsurf generated a response with a slightly IgG1-bias, suggestive of a Th2-skewed response. However, both RBDsurf and RBDencapf generated significant levels of the Th1-type cytokines IFNγ, TNFα and IL-2. This Th1-type response is likely induced by the MPLA PS, as MPLA has been shown to generate strong type-1 immunity(348). Although RBDsurf generated a slightly IgG1-biased antibody response, it did not result in an increase in Th2-type cytokines upon restimula-

tion compared to RBDencap. Combined with the evidence of Th1-type cytokine production upon restimulation, we believe the risk of adverse events related to Th2-type responses is low. The PS-formulated RBD vaccines were able to generate stronger Th1-driven CD4+ and CD8+ T cell responses compared to RBDfree. We previously demonstrated that as an antigen delivery vehicle, PEG-PPS polymersomes could improve cross-presentation to CD8+ T cells(213). This increased T cell response likely occurs because of both enhanced APC targeting as well as rapid endosomal antigen release(213). APCs are able to accumulate membrane-impermeable nanocarriers such as PS more efficiently than other cell types due to their constitutive macropinocytosis(349). Once endocytosed, PEG-PPS polymersomes require only a small amount of oxidation to release encapsulated antigen, and payload delivery to the cytosol is not restricted to endosomal compartments with reductive or acidic conditions(213). Unlike antigen-encapsulated PS, however, acidification may be important for proteolytic degradation of RBDsurf and translocation to the cytosol, as evidenced by studies on VLPs(350; 351). Additionally, peptides derived from large antigen particles have been found to enter the cross-presentation pathways more efficiently than those derived from soluble antigens, which may provide rationale for the enhanced CD8+ response of RBDsurf, whereas no such benefit was seen for adjuvanted RBDfree(352). Therefore, antigen formulation using PS to improve T cell responses could be beneficial in the engineering of future vaccines against cancer or other infectious diseases for which T cell immune responses are thought to be necessary for protection, such as herpesviruses, human immunodeficiency virus, and hepatitis C virus(353). In summary, we have demonstrated that a polymersome-based antigen and adjuvant delivery system generates robust humoral immunity and neutralizing antibody titers, as well as T cell responses, against a key SARS-CoV-2 vaccine target, the RBD of Spike. This platform technology is amenable to a wide variety of antigens and formulated or soluble adjuvants. Once the type and dose of adjuvant has been optimized for a given application, a single particle could be used to deliver both antigen and adjuvant to APCs in the injection site-draining lymph node. Additionally, multiple antigens, for example

from different viruses or different strains or variants of the same virus, could be conjugated to the same particle as a strategy to induce cross-reactive neutralizing antibodies(314). Importantly, both surface-decorated and antigen-encapsulated polymersomes remained stable at 4 °C for at least 6 months, as indicated by consistent particle size and absence of antigen released into solution. Vaccines that exhibit long-term stability without requiring sub-zero temperatures will likely be important for widespread vaccine distribution, for example to rural populations or developing nations with poor cold chain network. The evaluation of RBD-decorated polymersomes presented here could thus provide insight into the next generation of stable formulations of nanovaccines to combat the current COVID-19 pandemic as well as future viral outbreaks.

CHAPTER 3

SYNTHETICALLY MANNOSYLATED ANTIGENS CAN REDUCE ANTIGEN-SPECIFIC ANTIBODY RESPONSES TO IMMUNOGENIC PROTEIN DRUGS

3.1 Abstract

Immunogenic protein drugs trigger an anti-drug antibody (ADA) response in patients which reduce efficacy and increase adverse reactions. Our lab has previously shown that targeting antigen to the liver microenvironment can reduce antigen-specific T cell responses; herein, we present a novel strategy to deliver antigen to the liver via conjugation to a synthetically mannosylated polymer (p(Man)). This delivery leads to reduced antigen-specific T follicular helper cell and B cell responses resulting in diminished ADA production which is maintained throughout subsequent administrations of the native biologic. We found that p(Man) treatment impairs the antibody response against recombinant uricase, a highly immunogenic biologic, without a dependence on hapten-skewing or control by Tregs. We identify increased TCR signaling and increased apoptosis and exhaustion in T cells as effects of p(Man)-antigen treatment via transcriptomic analyses. This modular platform may enhance tolerance to current and future biologics, enabling long-term therapeutic solutions for an ever-increasing healthcare problem.[2]

2. This chapter and accompanying figures are adapted from "Synthetically mannosylated antigens induce antigen-specific humoral tolerance and prolong the therapeutic efficacy of immunogenic protein drugs Rachel P. Wallace, Andrew C. Tremain, Kym Brunggel, Jennifer T. Antane, Michal R. Raczy, Aaron T. Alpar, Mindy Nguyen, Ani Solanki, Anna J. Slezak, Shijie Cao, Abigail Lauterbach, Elyse A. Watkins, D. Scott Wilson, Jeffrey A. Hubbell. *in preparation*. This work was contributed to by multiple authors. R.P.W. wrote the manuscript, R.P.W., D.S.W., K.B., A.C.T, and J.A.H. conceived the project and designed the research strategy. R.P.W., A.C.T, K.B., J.T.A., M.R.R, A.T.A., M.N., A.S., A.L., E.A.W., and D.S.W. performed experiments. R.P.W., J.T.A., and D.S.W. performed data analysis. M.R.R., A.J.S., and D.S.W., synthesized materials.

3.2 Introduction

The development of therapeutic proteins or biologics in the 1990s revolutionized the pharmaceutical industry. Novel therapeutic classes such as monoclonal antibodies and enzyme replacement therapies enabled increasingly precise ways to treat debilitating genetic diseases, cancer, and autoimmunity. Biologics such as these accounted for 20% of the FDA approvals in 2020 and are expected to increase(354). Compared to traditional small-molecule therapeutics, the protein composition of biologics enables them to directly interact with native pathways and mimic endogenous molecules to improve efficacy, but it also makes them vulnerable to recognition by the immune system. The immune response primarily manifests as a T cell-dependent antibody response against the drug(355; 356). At high levels these anti-drug antibodies (ADAs) generated in response to the therapeutic cause a large number of complications including neutralization of the drug's therapeutic function, increased clearance resulting in reduced efficacy, hypersensitivity and life-threatening anaphylaxis reactions upon administration(357–361). The extent to which a protein activates an ADA response is known as immunogenicity. A biologic's immunogenicity is determined by a variety of factors including characteristics of the protein such as its homology to native human proteins, the number of subunits, and post-translational modifications, as well as genetic factors and dose route, quantity, and frequency(356). The pharmaceutical industry has employed a number of strategies to reduce the immunogenicity throughout the development of a biologic including selecting sequences with maximum homology to human proteins, and expression in mammalian systems, however immunogenicity remains a hurdle for regulatory approval(362; 363). Strategies to design less immunogenic proteins using MHC associated peptide proteomics, predictive algorithms and machine learning(165; 364–368) are under development, but the only treatments currently available to patients who require immunogenic drugs is to co-administer broad immunosuppressants such as methotrexate and thiopurines, which leave patients at an unacceptably increased risk for infection and malignancy(256–

259; 261). There is a critical need for an antigen-specific approach to reduce immunogenicity to these biologics. Here we present a modular polymeric delivery platform to reduce the immunogenicity of any protein therapeutic.

Our lab has previously developed liver-targeted amine-reactive glycopolymers and demonstrated that antigen therapy with these polymer conjugates leads to tolerogenic antigen-specific T cell signatures after both prophylactic and therapeutic administration(293; 294). The polymeric GalNAc moieties utilized in previous studies were designed to target C-type lectins containing the QPD binding motif in the tolerogenic microenvironment of the liver to promote antigen-specific tolerance. Mannose is a similar but more ubiquitous surface glycosylation on foreign antigens from yeast and bacteria, thus many immune cells have evolved to recognize mannosylated structures for uptake and presentation via binding to EPN motif containing lectins(369; 370). We sought to develop a novel mannose glycopolymer to act as a ligand for a broader range of mannose-binding lectins and investigate its potential as a tolerogenic therapy to reduce both T cell and B cell-mediated ADA responses to immunogenic therapeutics. We will show that our p(Man) polymer targets antigen to the liver more effectively than previously published glycopolymers, resulting in reduced antigen specific T cell, B cell and antibody responses to a variety of immunogenic proteins. Finally we will show through depletion studies and transcriptional analysis that this reduction in antibody response likely occurs due to a reduced activated T cell response and is independent of regulatory T cells or hapten immunodominance.

3.3 Methods

3.3.1 Study Design

The purposes of this study were to test the feasibility of pMan-antigen therapy to induce humoral tolerance and lessen an antigen-specific antibody response when administered before treatment with an immunogenic protein. We used OVA as a model protein along with

TCR transgenic OT-I and OT-II to study antigen-specific T cell phenotypes and responses using flow cytometry and RNA-seq readouts. N = 5 mice were used per group in OVA experiments. We next tested pMan antigen pre-treatment to reduce antibodies against immunogenic therapeutic protein uricase from Candida (Sigma). Pre-immune mice with an initial antigen-specific antibody titer >2 prior to antigen experience were excluded from the study. N = 8 mice were used per group in immunogenic challenge experiments. In the *Uox-/-* mice we investigated the ability of pre-treatment with p(Man)-uricase to increase the therapeutic effects of a bi-weekly uricase injection. Two experiments were pooled to include N=6-8 mice per group. Each experiment was repeated at least twice.

3.3.2 Mice

Mice were maintained in a specific pathogen-free facility at the University of Chicago. The experiments in this study were performed in accordance with the Institutional Animal Care and Use Committee. For OT-I and OT-II adoptive transfer experiments, 9 week old C57BL/6 mice were purchased from The Jackson Laboratory. OT-I (stock no: 003831) and OT-II (stock no: 004194) were crossed to CD45.1 mice (stock no: 002014) to yield congenic labeled OT-I and OT-II. For the immunogenic protein challenge experiments 9 week old female Balb/c mice were purchased from Charles River Laboratory. Mice used in the *Uox-/-* experiments were initially purchased from the Jackson Laboratory (stock no: 002223) and breed at the University of Chicago.

3.3.3 Transgenic T cell adoptive transfer

Spleens and lymph nodes (axillary, brachial, inguinal, and popliteal) were isolated from TCR transgenic mice. OT-I and OT-II T cells were isolated by negative magnetic bead selection using a CD8 and CD4 (Stemcell) negative selection kit, respectively. Cell purity was assessed by flow cytometry. OT-I and OT-II cells in DMEM were injected through the tail vein.

3.3.4 Immunogenic antigens

All OVA injections were performed with 15μg Endofit OVA (Sigma). All uricase injections were performed with 0.5U *S. Candida* uricase expressed in *E. Coli* (Sigma) measured via Amplex red uricase activity assay (Thermo Fisher). *S. Candida* uricase was purchased from Sigma and purified via FPLC on the Äkta system (Cytiva). Uricase was reconstituted in 50mM Sodium Phosphate pH 6.4 and purified via anion exchange chromatography on a Sepharose Q FF column (Cytiva) followed by buffer exchange into 50 mM Sodium Carbonate Bicarbonate pH 9.2 and size exclusion chromatography via HiLoad^{TM} 16/600 Superdex^{TM} 200pg (Cytiva). Injections were administered once per week intravenously in the tail vein.

3.3.5 p(Man) polymer synthesis

Unless otherwise stated, chemicals were reagent grade and purchased from Sigma–Aldrich. All NMR spectra were collected on a Bruker Avance-II 400 MHz NMR and analyzed with MnovaNMR (Mestrelab). GPC characterization was performed on Tosoh EcoSEC size exclusion chromatography System using Tosoh SuperAW3000 column at 50°C, with the eluent DMF with 0.01 M LiBr. Refractive index (RI) detector was used to detect polymers, and mass values were determined by column calibration with PMMA standards. Mannose monomer and azide-terminated RAFT chain transfer agent were synthesized as previously described(294; 371). Full synthesis schema with structures provided in supplementary information. For RAFT polymerization, mannose monomer (300 mg, 1.027 mmol) and HEMA (Combi Blocks, 300 mg, 2.326 mmol) were dissolved in dry DMF in a Schlenk tube. To that solution, azide CTA (17 mg, 0.029 mmol) and free radical initiator AIBN (1 mg, 0.0061 mmol) were added. The reaction vessel was degassed via four freeze-pump-thaw cycles and then heated to 70°C to initiate polymerization. After 14 h, the reaction vessel was immersed in liquid nitrogen to stop the reaction. The polymer was the precipitated in cold diethyl ether three times. The final product was dried under reduced pressure. The product was

white powder (550 mg, yield 89%). The polymer was characterized by 1H-NMR and GPC (Supplemental Figures 1-3) Resulting polymer had a number average molecular weight of 18 kDa.

3.3.6 p(Man) antigen constructs

Azido -terminated pMan polymer was conjugated to lysine residues on the antigen via click chemistry using a self-immolative heterobifunction linker, as previously described(291). Conjugation was verified through an increase in molecular weight visible on SDS-PAGE separation (BioRad) which was reduced upon addition of 0.05% β-mercaptoethanol in the loading buffer. Mice were treated weekly for 2-3 weeks with 2.5-5μg pMan-antigen intravenously in the tail vein.

3.3.7 Antigen biodistribution

C57BL/6 mice were treated by tail-vein injection with fluorescently labelled OVA in the form of free OVA (OVA_{649}),OVA_{649}–p(Man), OVA_{649}–p(GalNAc), or OVA_{649}-p(GlcNAc); the subscripts indicate the fluorophores Dy-649 from Dyomics. After 3 h, the livers of mice treated with OVA_{649}, OVA_{649}–p(Man), OVA_{649}-p(GalNAc) or OVA_{649}–p(GlcNAc) were perfused via the hepatic portal vein with 5–10 ml of 42°C Krebs–Ringer modified buffer (KRB) supplemented with 0.5 mM EDTA. The perfused livers and spleens were collected, placed in 4°C PBS, then analysed for total fluorescence using an IVIS Spectrum in vivo imaging system (PerkinElmer).

3.3.8 Preparation of single-cell suspensions

Draining lymph nodes (inguinal, popliteal, inginal, axillary) and/or spleens were collected and filtered through a 70μm filter. Lymph nodes were mechanically disrupted and digested at 37°C for 45 min in collagenase D. Digested lymph nodes and spleens were processed

into single-cell suspensions via mechanical disruption and passage through a sterile 70 μm strainer. Red blood cells in splenocyte suspensions were lysed in ACK lysing buffer (Gibco) for 5 min before quenching with 15 mL DMEM. The single cell suspensions were then resuspended in IMDM + 10% FBS + 1% pen/strep.

3.3.9 Flow cytometry

For phenotypic analysis of cells, 1.5x10^6 cells were stained in PBS with 1:200 CD16/CD32 Fc Block (Biolegend) and 1:500 Live/Dead fixable dye (ThermoFisher) at $4°C$ for 15 min. Cells were washed then stained with 1:200 surface antibodies and multimers at $4°C$ for 30 min. Cells were washed then fixed in 2% paraformaldehyde. For intracellular staining, Cytofix/Cytoperm (BD Biosciences) was used at $4°C$ for 20 min, and cells stained intracellularly in Perm Wash Buffer (Biolegend) with 1:200 antibodies at $4°C$ for 30 min. For transcription factor stain, FoxP3 Transcription Factor Kit (eBioscience) was used per manufactures protocol. For complete antibody panel see Table 3.1-3.3. Representative gating found in Figure 3.1.

Table 3.1: 19 Day Adoptive Transfer Antibodies

Marker	**Fluorophore**	**Vendor**	**Cat**
CD45.1	BV421	Biolegend	110731
CD8	BV510	BD	563068
CD4	BV786	BD	563727
CXCR5	BV650	Biolegend	145517
Bcl6	PE Cy7	Biolegend	358512
Viability dye	e780	Invitrogen	65-0865-14
CD3	BUV395	BD	563585
PD-1	PerCP-Cy5.5	Biolegend	135208
CD25	PE	Biolegend	101904
FoxP3	AF488	BD	560403

Table 3.2: B Cell Panel Antibodies

Marker	**Fluorophore**	**Vendor**	**Cat**
Viability dyet	BV421	Invitrogen	L34955
CD11c	FITC	BD	557400
GR-1	FITC	Biolegend	108406
CD4	FITC	Biolegend	100406
CD8a	FITC	Biolegend	100706
B220	BUV496	BD Horizon	612950
CD19	BUV395	BD Horizon	563557
CD138	BV605	Biolegend	142531
IgM	BV786	BD Optibuild	743328
CD38	APC-Cy7	Biolegend	102728
IgD	PE-Cy7	Biolegend	405720
GL7	PerCP-Cy5.5	Biolegend	144609

Table 3.3: T Cell Panel Antibodies

Marker	**Fluorophore**	**Vendor**	**Cat**
Viability dye	e7801	Invitrogen	65-0865-14
ICOS	BUV395	BD Horizon	565885
CD3	BUV737	BD Horizon	612803
CXCR5	BV421	Biolegend	145512
CD4	BUV496	BD Horizon	612952
CD44	PerCP-Cy5.5	BD Horizon	563058
PD-1	BV605	Biolegend	135219
Bcl6	PE-Cy7	Biolegend	358512
FoxP3	AF647	BD	560402
CD25	PE	Biolegend	101904
CD44	PerCP-Cy5.5	Biolegend	103032

3.3.10 Antigen-specific multimer production

Uricase was biotinylated using EZ-link NHS-biotin (Thermo Scientific). Unreacted NHS-biotin was removed using Zeba spin desalting columns, 7K MWCO (Thermo Scientific). The extent of biotinylation was measured using the QuantTag Biotin Quantification kit (Vector Laboratories) to ensure 1:1 molar ratio of uricase and biotin. Biotinylated uricase was reacted for 20 min on ice with 4:1 molar ratio of biotin to streptavidin-conjugated PE or streptavidin-conjugated APC (Biolegend). Streptavidin-conjugated FITC (BioLegend) was reacted with excess free biotin to form a non-antigen-specific streptavidin probe as a

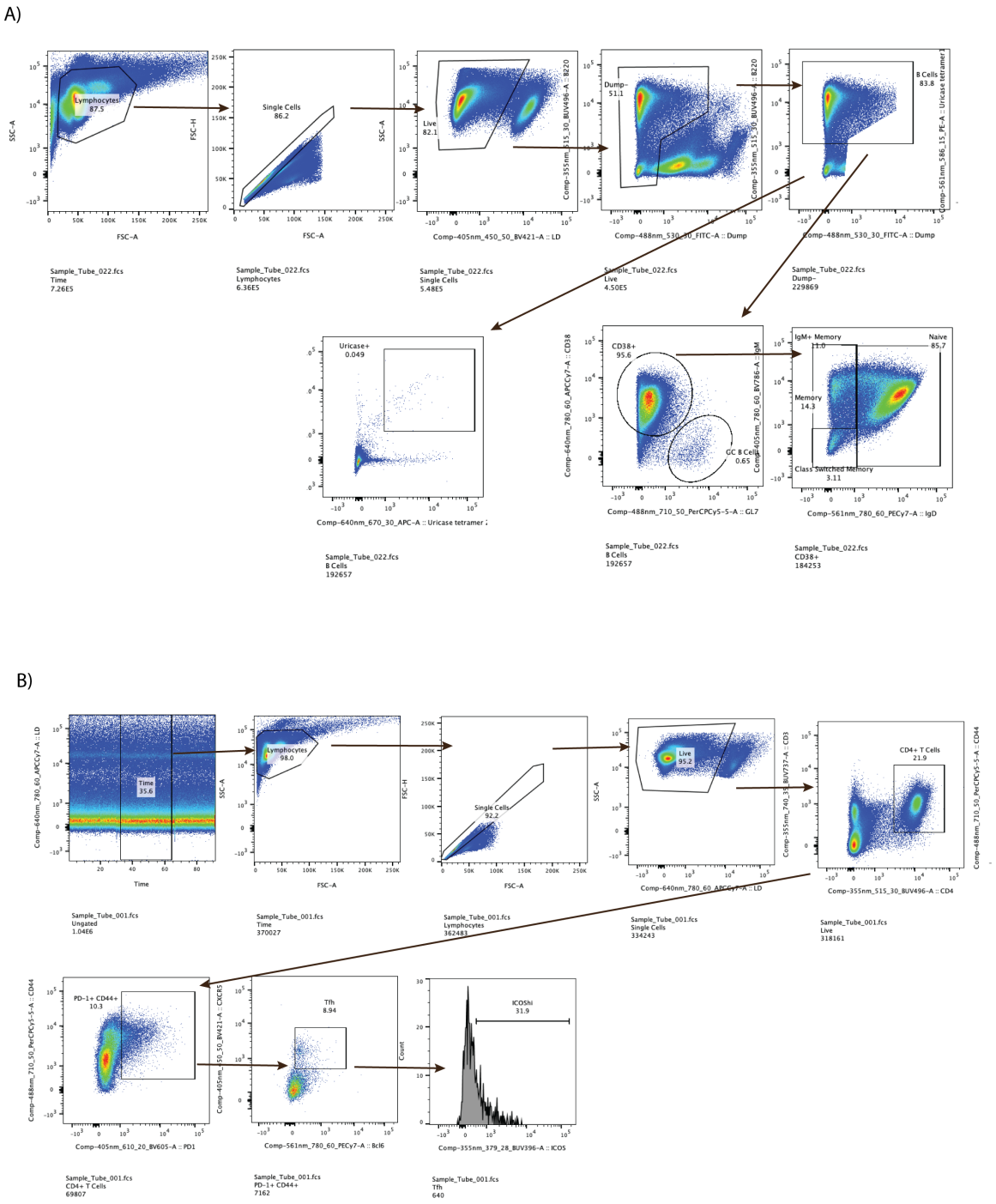

Figure 3.1: Flow cytometry gating strategy. (A) Gating strategy for the identification of Dump- B220+ B cell subsets and uricase-specific multimer-double-positive B cells. (B) Gating strategy for the identification of CD3+ CD4+ CD44+ PD1+ CXCR5+ Bcl6+ T follicular helper (Tfh) cells.

control. Multimer formation was confirmed using SDS-PAGE gel. Cells were stained for flow cytometry with all three streptavidin probes at the same time as other fluorescent surface markers at a volumetric ratio of 1:200. The antigen-specific staining of B cells with multimer was verified by staining with and without 5M uricase on splenocytes from vaccinated and antigen-naive mice.

3.3.11 Antigen-binding ELISA

Plasma was assessed for antigen-specific IgG by ELISA. 96-well ELISA plates (Costar high-bind flat-bottom plates, Corning) were coated with 10 μg/mL antigen in carbonate buffer (50 mM sodium carbonate/sodium bicarbonate, pH 9.6) overnight at $4°C$. The following day, plates were washed three times in PBS with 0.05% Tween 20 (PBS-T) and then blocked with 1x casein (Sigma) for 2 h at RT. Following blocking, wells were washed three times with PBS-T and further incubated with six 10-fold dilutions of plasma in 1x casein for 2 h at RT. Wells were then washed five times with PBS-T and incubated for an additional 1 h at RT with horseradish peroxide (HRP)- conjugated antibodies against mouse IgG, IgG1, IgG2b, IgG2c, or IgG3 (Southern Biotech). After five washes with PBS-T, bound RBD-specific Ig was detected with tetramethylbenzidine (TMB) substrate. Stop solution (3% H2SO4 + 1% HCl) was added after 18 min of TMB incubation at RT, and the OD was measured at 450 and 570 nm on an Epoch Microplate Spectrophotometer (BioTek). Background signal at 570 nm was subtracted from the OD at 450 nm. The area under the curve (AUC) of background-subtracted absorbance versus log-transformed dilution was then calculated. Titer was determined as the log-transformed dilution at which the background-subtracted absorbance was greater than 0.01.

3.3.12 Uricase-binding IgG ELISpot assay

Uricase was inactivated by heating at $98°C$ for 5 min. ELISpot plates (Millipore IP Filter plate) were coated with 20 μg/mL heat inactivated uricase in sterile PBS overnight at $4°C$.

Plates were then blocked using ELISpot Media (RPMI 1640, 1% glutamine, 10% fetal bovine serum, 1% penicillin-streptomycin) for 2 h at $37°C$. Splenocytes from vaccinated mice were seeded in triplicate at a starting concentration of 6.75×10^5 cell/well and diluted seven times in 3-fold serial dilutions. Plates were incubated for 18 h at $37°C$ and 5% CO_2 after which the cells were washed five times in PBS. Wells were incubated with 100 μL IgG-biotin HU adsorbed (Southern Biotech) for 2 h at RT. Next, plates were washed four times in PBS followed by the addition of 100 μL HRP-conjugated streptavidin/well for 1 h at RT. Plates were washed again and incubated with 100 μL TMB/well for 5 minutes until distinct spots emerged. Finally, plates were then washed three times with distilled water and left to dry completely in a laminar flow hood. A CTL ImmunoSpot Analyzer was used to image plates, count spots, and perform quality control.

3.3.13 RNAseq Data Collection

Mice were adoptively transferred with 750k OTIs and OTIIs at day 0. At day 1, mice received i.v. saline, 5 μg pMan-OVA, or equimolar OVA. Four days later, mice were sacrificed and spleens and liver and peripheral lymph nodes were pooled. OT-II were sorted into Trizol using fluorescence activated cell sorting (FACS) and frozen at $-80°C$. RNA was extracted (Qiagen, RNeasy Micro), and three mice were pooled per replicate. RNA integrity was measured by the Agilent 2100 Bioanalyzer. RNA was converted to cDNA using SmartSeq-v4 (Takara, cat no. R400752). The library was prepared using Nextera XT DNA library preparation kit (Illumina, cat no. FC-131-1096). For each setting, all samples were pooled and sequenced using Illumina HiSeq 4000 (2x100 paired end). The complete RNA-seq analysis approach is detailed in the Supplementary Materials.

3.3.14 RNAseq Analysis

The RNA-seq analysis was performed under the R programming and software environment for statistical computing and graphics version 3.6 (R Core Team, 2019). We assessed the

quality of FastQ files using the FastQC tool (version 0.11.5). Raw reads were aligned to the GRCh38 primary genome assembly using Spliced Transcripts Alignment to a Reference (STAR) aligner (version 2.7.2a) 1-pass algorithm(372). Bam files were sorted in lexicographical order with the sambamba program (v0.5.4). Reads were assigned to exon features annotated in Ensembl Mus musculus GRCm38 annotation (release 97) using the FeatureCounts tool from the subread package (version 1.5.2) and the read counts were summarized by genes(373; 374). Picard tools (version 2.18.7) was used for post alignment quality control. Alignment-free transcriptome quantification method kallisto (v0.46.1) was used to estimate the transcript abundance of each sample(375). Transcript-level estimates were summarized for gene-level analysis using R package tximport. Genes with zero read counts across all samples were removed. Raw library sizes were scaled using normalization factors calculated with the calcNormFactors function in the edgeR R package with trimmed mean of M-values (TMM) option enabled(376). The normalized count per million (CPM) values were log2-transformed. We used the voomWithQualityWeights function from the limma package to remove heteroscedascity from the count data. A linear model for each gene was fit with the limma algorithm, adjusted for any batch effects, and the genes were ranked by differential expression using the empirical Bayes method. Differentially expressed genes were identified with the Benjamini-Hochberg procedure for multiple testing correction. Significance was set at an adjusted P-value threshold of 0.05. We used the Ingenuity Pathway Analysis Fall 2020 release (Qiagen) to identify canonical pathways, causal networks, and upstream regulators that related to significant differentially expressed genes in the pMan-OVA to OVA comparisons.

3.3.15 T cell depletion study

Mice were treated weekly for 3 weeks with 500μg αCD4 and αCD8 depleting antibodies or IgG2b isotype control antibodies (BioXCell). 4 days after initial depletion mice were administered 1U of uricase or saline i.v. weekly for 3 weeks. Serum was collected for

antibody measurement.

3.3.16 CD25 depletion study

Mice were treated weekly for 3 weeks with either p(Man)-uricase or saline. Two weeks following last treatment, mice were intravenously given 500μg of either anti-CD25 depletion antibody of the IgG21 isotype control (BioXCell). Two weeks following depletion mice were challenged weekly intravenously with 0.5U uricase for 4 weeks.

3.3.17 Uox-/- mice

Uox-/- mice are administered 45μg/mL Allopurinol (Spectrum) in the drinking water from birth to prevent mortality. At 10-12 weeks mice were treated intravenously weekly for 3 weeks with p(Man)-uircase. One week after the last injection, mice were placed on standard drinking water and administered 0.8U uricase twice weekly for 9 weeks. Plasma and urine were collected weekly. Plasma uric acid levels, and urine uric acid and creatinine levels were determined via ACE Axcel Clinical Chemistry System (Alfa Wassermann).

3.3.18 Kidney histology

At endpoint, kidneys were collected and fixed for 24-48 hours in 2% PFA and embedded in paraffin for HE and Periodic acid-Schiff staining. The slides were stained on Leica Bond RX Automated Stainer.

3.3.19 Statistical Analysis

Statistically significant differences between experimental groups were determined using Prism software (v9, GraphPad). All statistical analyses are stated specifically in the figure legends for all experiments. For most experiments, unless otherwise specified in figure legend, one-way ANOVA was performed with a Tukey's test to correct for multiple comparisons. For

showing statistical significance ***P≤0.001; **P≤0.01; *P≤0.05, unless otherwise stated. For the RNA-seq experiment, a detailed description of the statistical analysis can be found in Methods. Analyses were performed using R and GraphPad Prism V.7 software. The threshold for statistical significance was fixed at $p < 0.05$.

3.4 Results

3.4.1 Conjugation to p(Man) increases antigen uptake and prolongs presentation in the liver

We sought to develop a novel glycopolymer to act as a ligand for a broad range of mannose-binding C-type lectins and investigate its potential as a tolerogenic therapy. Therefore we developed a linear mannose polymer (Figure 3.2, Figure 3.3, Figure 3.4, Figure 3.5A). The polymer was successfully conjugated to ovalbumin via a self-immolative DBCO linker which releases the polymer in reducing conditions (Figure 3.6A). To measure the biodistribution effects of p(Man) conjugation compared to previous glycopolymers, p(Man)-OVA_{647}, p(GlcNAc)-OVA_{647}, p(GalNAc)-OVA_{647}, unconjugated OVA_{647} or saline was injected intravenously (iv) into mice. Organs were collected 3 hours after injection and measured via IVIS. Conjugation to p(Man) alone significantly increased the quantity of OVA antigen in the liver compared to the unconjugated control (Figure 3.5B-C). There was no off-target OVA_{647} signal detected in other organs (3.6B).

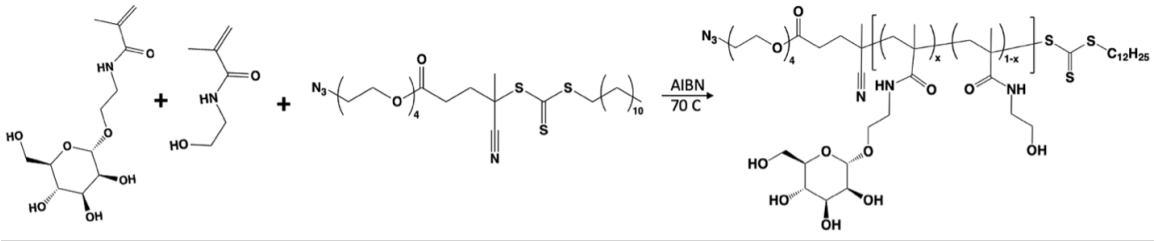

Figure 3.2: Schema of p(Man) polymerization

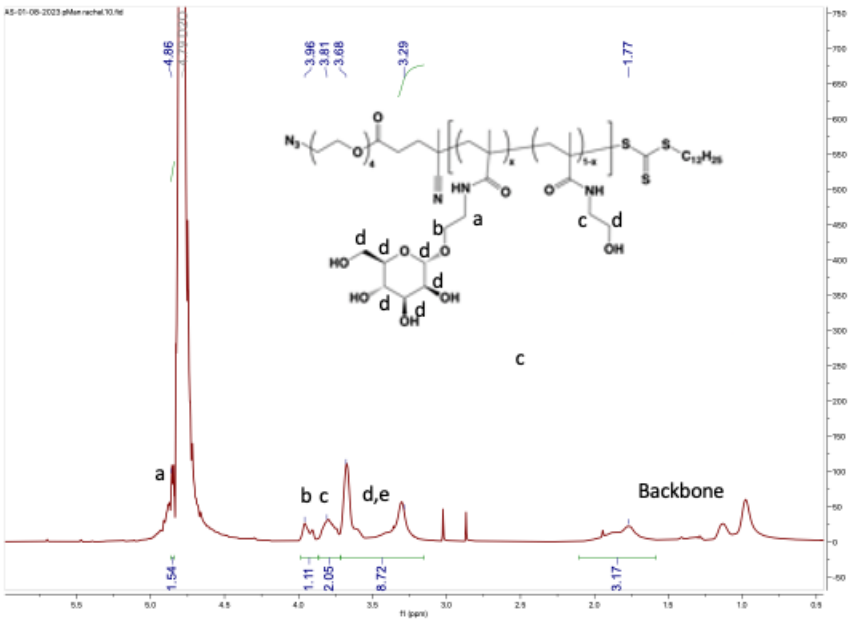

Figure 3.3: p(Man) NMR

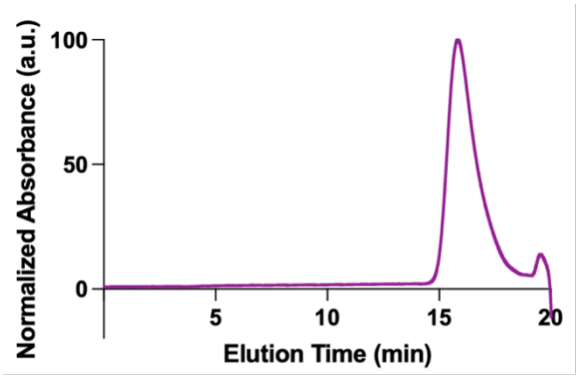

Figure 3.4: p(Man) GPC trace

3.4.2 Pre-treatment with p(Man)-OVA results in decreased antigen-specific Tfh cells and prevents an anti-OVA antibody response

We next investigated the effects of p(Man)-antigen therapy on antigen-specific T cell phenotypes using an OT-I/ OT-II vaccination model (Figure 3.5D). When mice were given prophylactic treatment with p(Man)-OVA we saw impaired expansion of OVA-specific CD4+ T cells upon vaccination compared to the OVA-treated mice (Figure 3.5E). Specifically we found the greatest reduction in CD4+PD-1hiCD44+CXCR5+Bcl-6+ T follicular helper (Tfh) cells

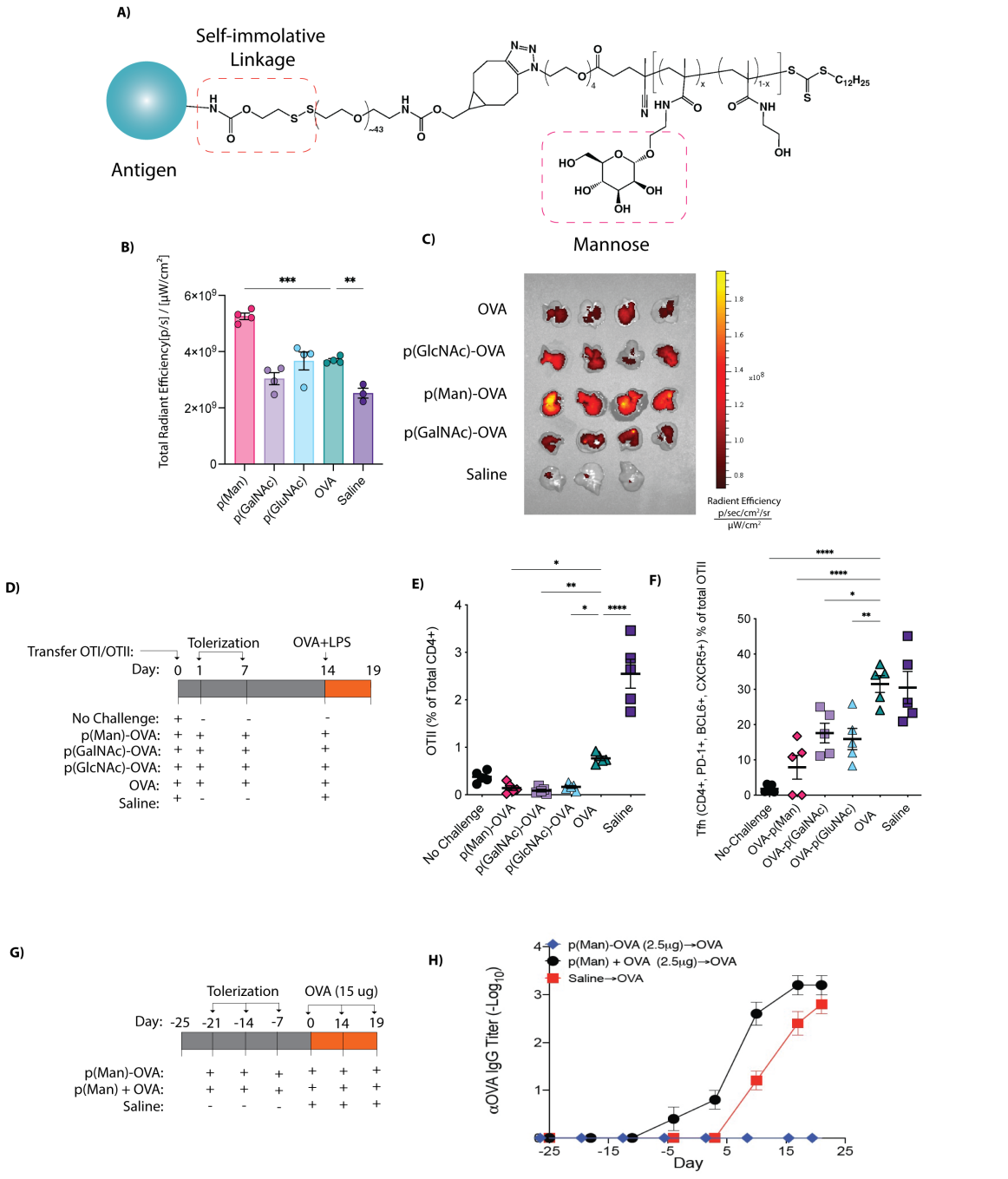

Figure 3.5: p(Man) conjugation increases delivery of antigen to the liver and impairs the activation of CD4+ antigen-specific T follicular helper cells. (A) Structure of the p(Man) polymer conjugated to protein antigen. (B) N=4 C57Bl/6 mice were administered saline, free OVA_{647} or OVA_{647} conjugated to glycopolymers p(Man), p(GluNAc), and p(GalNAc). 3 hours after injection organs were isolated to measure radiant efficiency of the fluorescent antigen in the livers. (Continued on the following page.)

Figure 3.5, continued: (C) Representative IVIS images of the liver compared to spleen, heart, lung, kidney and lymph nodes. (D) 500,000 CD45.1 congenitally labeled OTI and OTII T cells were adoptively transferred into n=5 C57Bl/6 mice. Mice were then treated with saline, free OVA, or OVA conjugated to p(Man), p(GalNAc) or p(GluNAc) before vaccination with OVA+ LPS. OTII cells were isolated on day 19 for phenotypic analysis. (E) Frequency of OTII in the dLN after vaccination. (F) Frequency of PD-1+ Bcl6+ CXCR5+ T follicular helper (Tfh) cells within the OTII population after vaccination. (G) Balb/c mice were treated weekly with p(Man)-OVA, a mixture of unconjugated p(Man) and OVA or saline for three weeks followed by a weekly challenge of high dose OVA. (H) Time course of OVA-specific IgG response represented as $\log_{10}$ titer. Symbols represent mean across n=8 mice. Data are shown as mean ± SEM. Unless otherwise stated symbols represent individual mice and statistical differences in all graphs were determined by one-way ANOVA with Tukey's *p<0.05, **p<0.01 and ***p<0.001.

within the OT-II compartment after p(Man)-antigen treatment (Figure 3.5F). The reduction in Tfh cells prompted us to investigate the effects of p(Man)-antigen therapy on humoral immune responses. We treated mice i.v. weekly with p(Man)-OVA, followed by weekly i.v. challenges of high doses of unmodified OVA (Figure 3.5G). We found that p(Man)-OVA antigen therapy prevented an antibody response to OVA, while treatment with p(Man) and unconjugated OVA seemed to amplify the response (Figure 3.5H).

3.4.3 Pre-treatment with p(Man)-conjugated antigen prevents anti-drug antibody response to immunogenic therapeutic, uricase

Once we established that p(Man)-OVA treatment can prevent antibody responses to OVA, we sought to investigate whether these tolerogenic effects would hold for a more immunogenic antigen like uricase. Uricase is an enzyme approved for the short-term treatment of hyperuricemia, however its long-term use is often limited by immunogenicity. Upon exposure to *Candida* uricase mice generate a robust antigen-specific antibody response This antibody response was shown to be T cell dependent and was completely abrogated when αCD4 and αCD8 blocking antibodies were administered (Figure 3.7A,B).

We produced p(Man)-uricase conjugates and verified the reaction and the self-immolative characteristics of the linker via SDS-PAGE (Figure 3.8A). Enzymatic activity of uricase

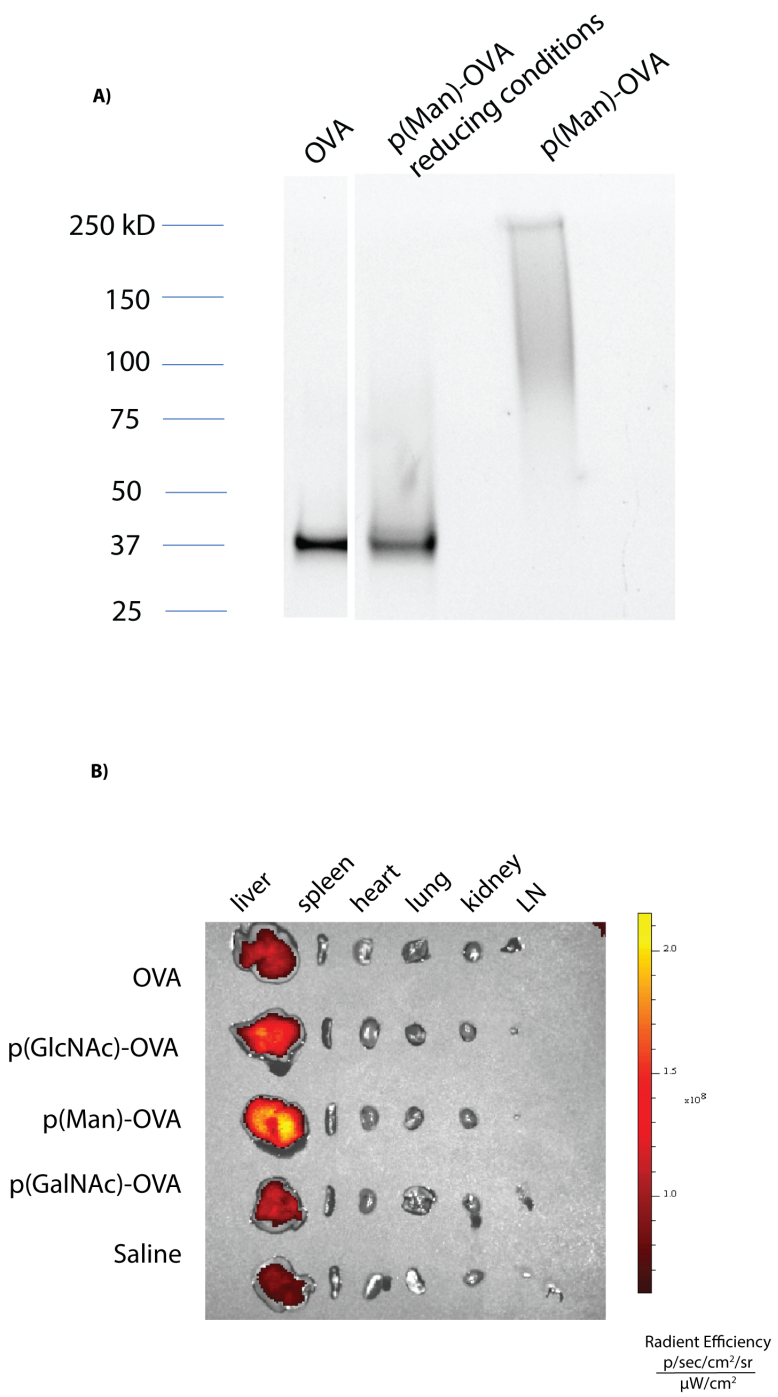

Figure 3.6: p(Man)-OVA characterization and biodistribution. (A) SDS-PAGE of unmodified OVA and p(Man)-OVA with and without β-mercaptoethanol to show self-immolative linker. (B) Representative IVIS image of liver, spleen, heart, lung, kidney and lymph nodes 3 hours after injection with OVA_{647}, p(GlcNAc)-OVA_{647}, p(Man)-OVA_{647}, p(GalNAc)-OVA_{647}, or saline iv.

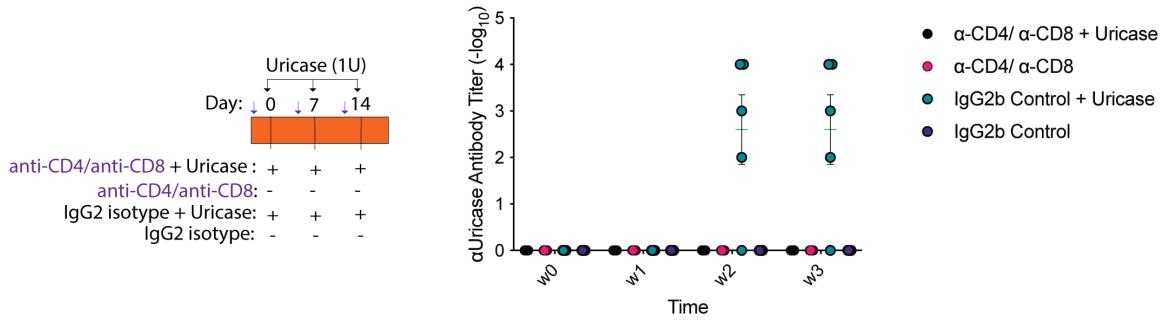

Figure 3.7: Candida uricase elicits a T cell-dependent antibody response in mice. (A) N=4 Balb/c mice were treated weekly i.v. with 1U of Candida uricase along with αCD4 and αCD8 depletion antibodies or an equivalent of IgG2b isotype control. (B) Time-course of uricase-specific IgG antibody response represented as $\log_{10}$ titer. Symbols represent individual mice.

was measured and found to be significantly decreased upon conjugation to p(Man) (Figure 3.8B,C). We administered p(Man)-uricase, unmodified uricase or saline intravenously to mice weekly during a three week tolerization window followed by weekly challenge doses of unmodified uricase (Figure 3.8D). Serum was collected weekly and uricase-specific antibodies were measured via ELISA. The uricase-specific antibody response was represented as the area under the curve of the absorbance over background across a 10-fold log-transformed dilution series. Pre-treatment with p(Man)-uricase was found to significantly decrease the uricase-specific IgG response compared to treatment with unmodified uricase and untreated mice (Figure 3.8E,F). This reduction in antibody response was consistent across all subclasses of IgG (Figure 3.8G). We next quantified the number of uricase-specific antibody secreting cells using ELISpot. Only the untreated group was found to have significantly more uricase-specific antibody secreting cells in the spleen on day 26 after initial uricase challenge, indicative of a smaller plasmablast and plasma cell response after antigen pretreatment (Figure 3.8H).

We next looked at the effect of p(Man)-uricase treatment on the B cell and T cell compartments (Figure 3.1A,B). Fluorescent uricase-streptavidin multimers were used to identify antigen-specific B cells via flow cytometry (Figure 3.10A). Antigen-specificity was verified by incubating splenocytes from uricase-experienced mice with 5mM uricase or OVA prior

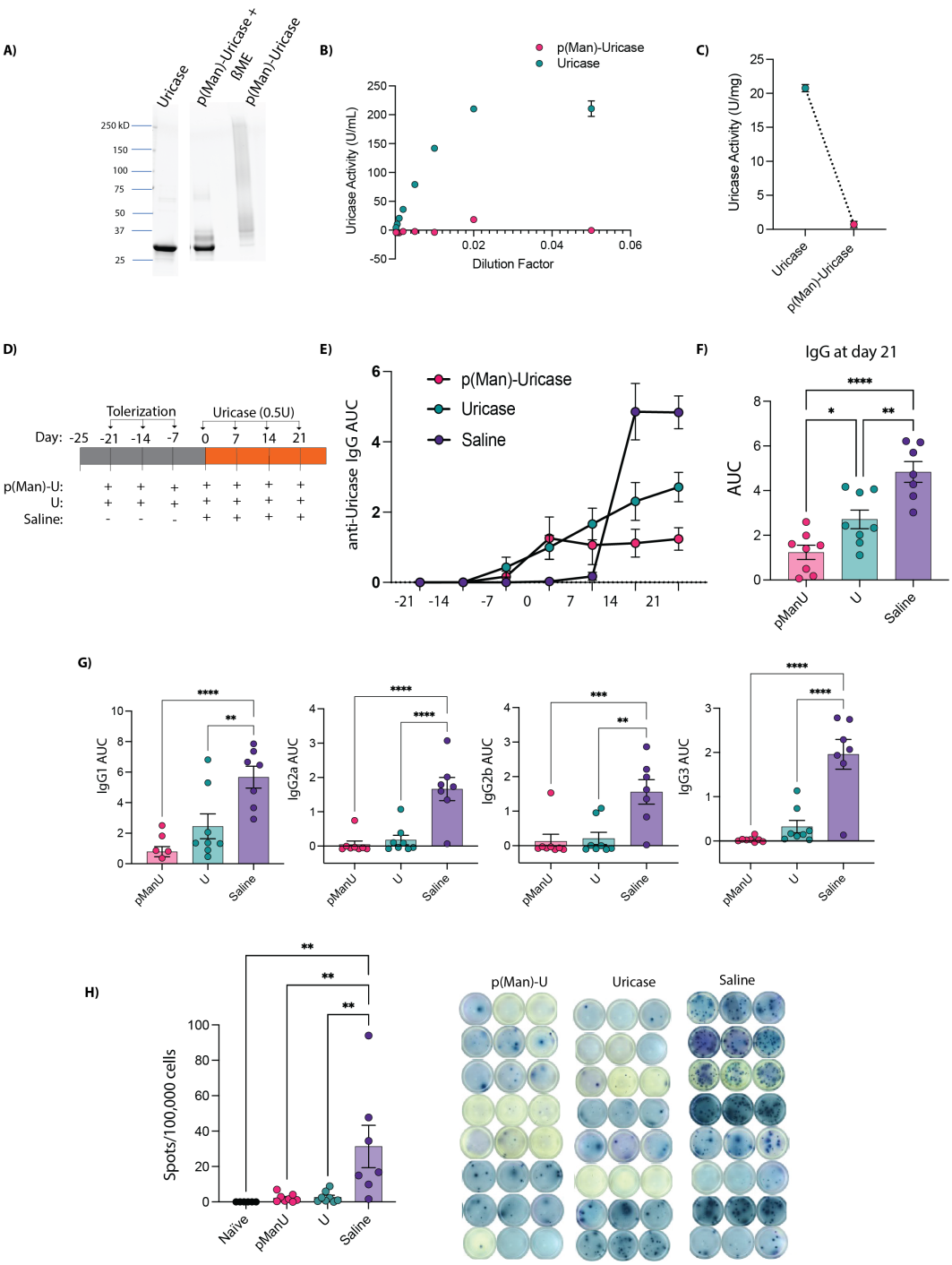

Figure 3.8: Prophylactic administration of p(Man)-antigen, impairs anti-drug antibody responses to immunogenic therapeutic uricase. (A) Structure of the p(Man) polymer conjugated to protein antigen with and without β-mercaptoethanol. (Continued on the following page.)

Figure 3.8, continued: (B) Uricase activity (U/mL) of p(Man)-conjugated and native uricase across dilutions. (C) Uricase activity (U/mg) of p(Man)-conjugated and native uricase. (D) N=8 Balb/c mice were treated 3 times with p(Man)-uricase, free uricase or saline followed by a therapeutic dose of uricase weekly for 4 weeks. (E) Time course of uricase-specific IgG response represented as the area under the curve of absorbance vs log-transformed dilution (AUC). Symbols represent mean across n=8 mice. (F) Uricase-specific IgG response at day 21 represented by AUC. (G) Comparison of uricase-specific IgG subclasses at day 21 represented by AUC. (H) Quantification and representative wells of the uricase-specific IgG-secreting splenocytes by ELISpot. Data are shown as mean±SEM. Unless otherwise stated symbols represent individual mice and statistical differences in all graphs were determined by one-way ANOVA with Tukey's *p<0.05, **p<0.01 and ***p<0.001

to multimer staining. Pre-incubation with uricase, but not OVA resulted in elimination of multimer binding (Figure 3.9).

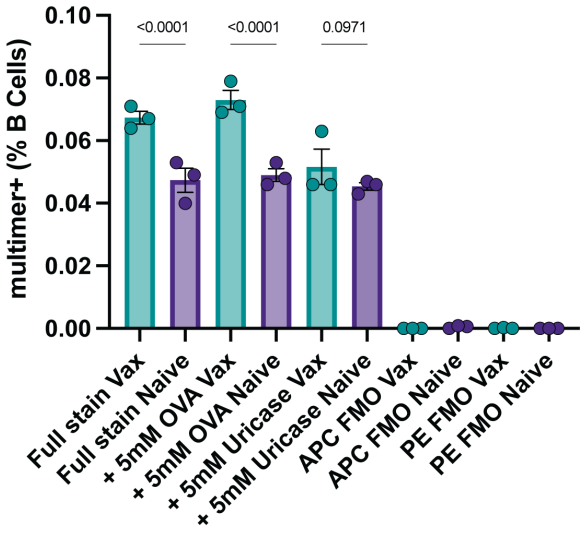

Figure 3.9: Validation of the antigen-specificity of the fluorescent uricase multimers. Splenocytes from naïve Balb/c mice or mice vaccinated with 0.5U i.v. uricase challenge were stained with APC-uricase and PE-uricase multimers with or without pre-incubation with 5mM OVA or uricase. Multimer-double-positive cells were quantified as a percentage of B220+ B cells.

Pre-treatment with p(Man)-uricase but not unmodified uricase prevented a significant rise in uricase-specific B cells in the spleen compared to the naïve controls as well as a note-worthy reduction in CD38+IgD- memory B cells and CD38+IgD-IgM- class-switched memory B cells compared to the saline control treatment which may indicate the potential for long-term B cell tolerance after p(Man)-antigen therapy (Figure 3.10B). We also saw

trends towards reduction in plasmablasts and germinal center B cells, although the response appears bimodal. The phenotype of the corresponding bulk B cell compartment, in contrast, showed no difference between treatment groups indicating that p(Man)-uricase treatment is an antigen-specific therapy without broad non-specific effects on B cells (Figure 3.10C). Similarly, the cell counts of the bulk T cell compartment was consistent across groups, with the exception that all groups exposed to foreign uricase antigen had increased frequency of Tfh cells within the T cell compartment compared to the naïve (Figure 3.11A,B). The p(Man)-uricase treated group was the only group without a significant increase in overall cell numbers of Tfh cells and ICOShi Tfh cells compared to the naïve control (Figure 3.11B,C).

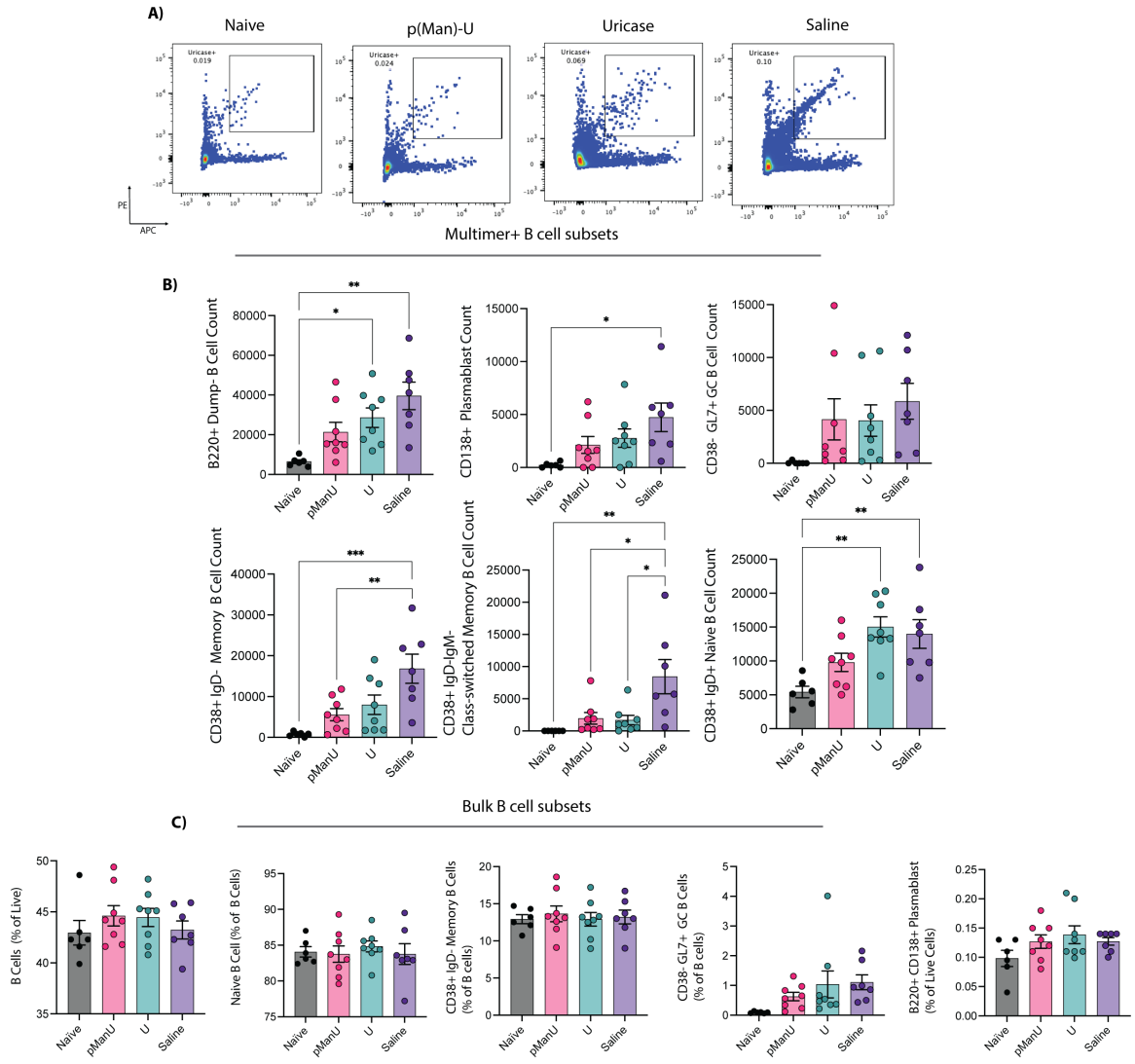

Figure 3.10: Antigen-specific memory B cell responses are impaired after prophylactic p(Man)-uricase treatment. (A) Representative flow plots of antigen-specific uricase-multimer double-positive B cells of naïve mice and uricase-challenged mice on day 25 after treatment with p(Man)-uricase, uricase, or saline. (B) Quantification of uricase-specific B220+ B cells, B220+ CD138+ plasmablasts, B220+ CD38- GL7+ germinal center B cells, CD38+ IgD- memory B cells, CD38+ IgM- IgD- class-switched memory B cells and CD38+ IgD+ naïve B cells in the spleen on day 25 after treatment. (C) Quantification of bulk B220+ B cells as in (B). (D) Quantification of bulk CD3+ T cells, CD4+ CXCR5+ PD-1+ Bcl6+ Tfh cells and ICOShi Tfh cells in the spleen on day 25 after treatment. Data are shown as mean±SEM. Unless otherwise stated symbols represent individual mice and statistical differences in all graphs were determined by one-way ANOVA with Tukey's *p<0.05, **p<0.01 and ***p<0.001.

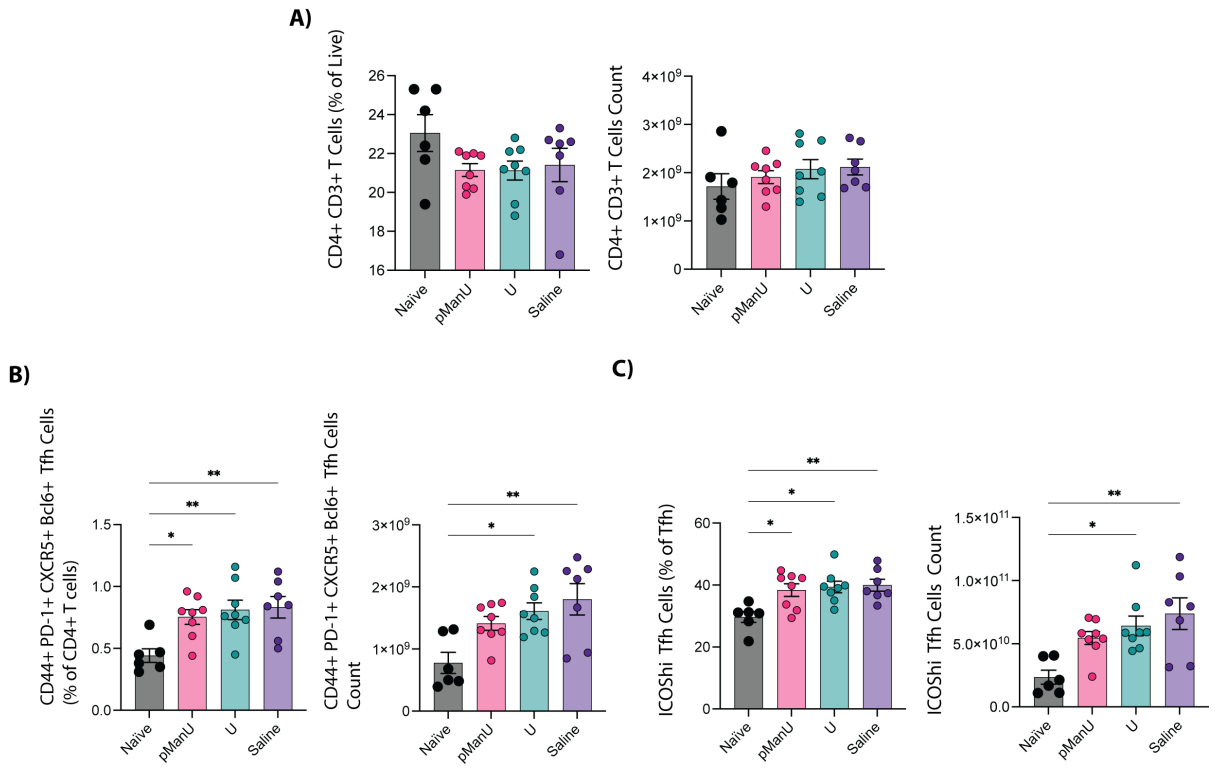

Figure 3.11: T cell compartment after p(Man)-uricase treatment. (A) Frequency of CD3+ T cells as a percentage of live cells after pre-treatment with p(Man)-uricase, uricase or saline as in 2A. (B) Frequency of CD4+CXCR5+PD-1+Bcl6+ Tfh cells as a percentage of T cells after treatment. (C) Frequency of ICOShi Tfh cells as a percentage of Tfh after treatment. Data are shown as mean ±SEM. Unless otherwise stated symbols represent individual mice and statistical differences in all graphs were determined by one-way ANOVA with Tukey's *p<0.05, **p<0.01 and ***p<0.001.

3.4.4 Reduction in antigen-specific antibody response is not due to shift in response to anti-p(Man) antibodies

After we established that pre-treatment with p(Man)-uricase leads to a reduced uricase-specific antibody response, we wanted to probe the potential mechanisms contributing to this effect. One possible mechanism leading to a reduced antigen-specific response is p(Man)-immmunodominance. It may be the case that the B cells are recognizing the p(Man) polymer instead of uricase and out-competing the uricase-specific B cells for T cell help in the germinal center, leading to a strong p(Man)-specific response instead of a uricase-specific response. To test the p(Man)-specific antibody response, we coated ELISA plates with uricase, p(Man)-

uricase, p(Man)-OVA or p(Man) alone and measured antibodies from mice pre-treated with p(Man)-uricase, uricase or saline as in 2A (Figure 3.12A). All of these mice are naïve to the OVA protein. We found the p(Man)-uricase treated mice generated no antibodies that bound p(Man)-OVA or p(Man) and the average antibody response to p(Man)-uricase was not higher than uricase alone in p(Man)-uricase treated mice (Figure 3.12B). These data indicate there was no increased antibody specificity for the p(Man) polymer regardless of treatment.

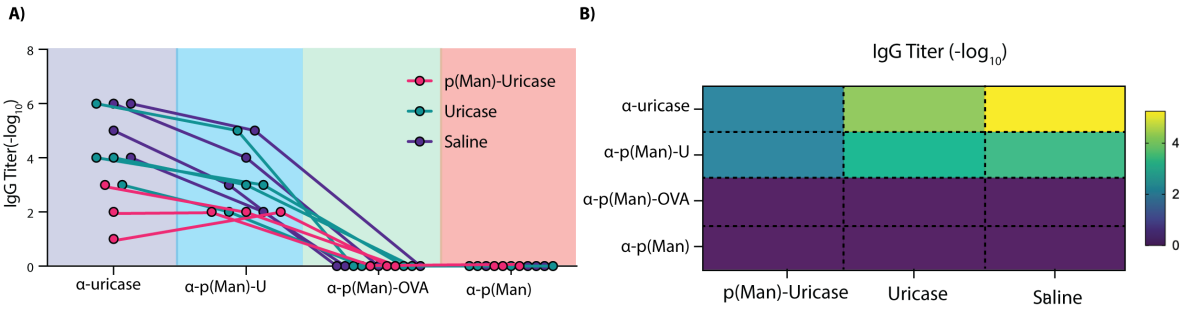

Figure 3.12: (A) Quantification of the antigen-specific antibody response to uricase, p(Man)-uricase, p(Man)-OVA or free p(Man) after treatment as in 3.8D represented as $\log_{10}$ titer. (B) Heatmap representation of the average $\log_{10}$ titer from each treatment group against each antigen as in (A).

3.4.5 Tregs are likely not required to maintain humoral tolerance generated by p(Man)-antigen treatment

We next sought to investigate if p(Man)-antigen treatment resulted in increased antigen-specific T regulatory (Treg) cells. In the OTII vaccination study we found that treatment with p(Man)-OVA resulted in an increased percentage of FoxP3+CD25+ Tregs (Figure 3.13). These cells could be responsible for the reduced antibody response through either Tfh suppression or direct B cell suppression. In order to probe the role of Tregs in the reduced uricase-specific antibody response, we administered αCD25 depleting antibody to the mice after tolerization and waited 2 weeks for the antibody to clear before challenging with uricase (Figure 3.14A). We found that the administration of the depleting antibody was not sufficient

to prevent the reduction in antibody response seen after p(Man)-uricase treatment (Figure 3.14B,C). Therefore, the induction of antigen-specific Tregs is likely not the mechanism by which p(Man)-antigen therapy imparts humoral immune tolerance.

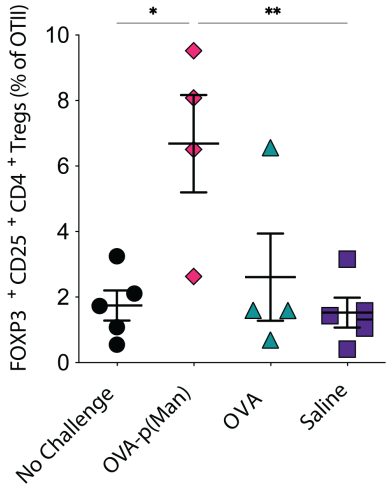

Figure 3.13: p(Man)-OVA treatment results in increased frequency of OVA-specific Tregs. C57Bl/6 mice were treated as in Figure 3.5D. Frequency of OVA-specific CD4+ CD25+ FoxP3+ T regulatory (Treg) cells were quantified as a percentage of OTIIs in the dLN. Data are shown as mean±SEM. Symbols represent individual mice and statistical differences in all graphs were determined by one-way ANOVA with Tukey's *p<0.05, **p<0.01 and ***p<0.001.

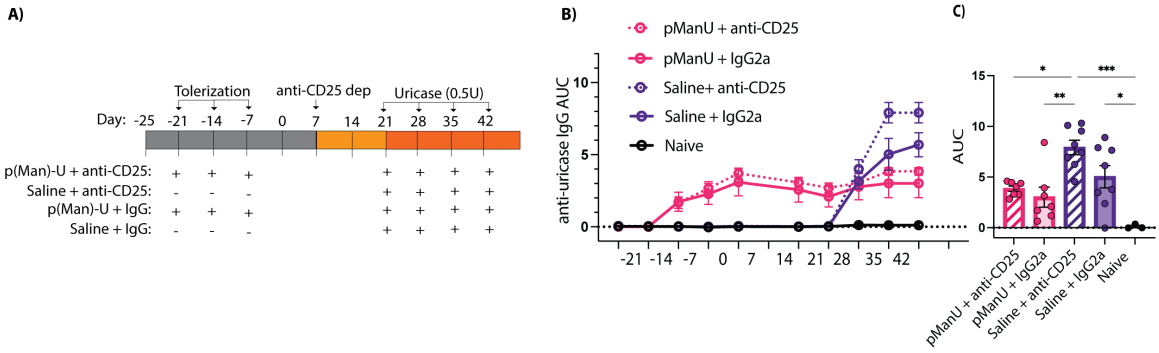

Figure 3.14: (A) N=8 Balb/c mice were treated three times with saline or p(Man)-uricase followed by administration of an isotype control or αCD25. High dose uricase injections were administered 2 weeks after depletion for 4 weeks. (B) Time course of the uricase-specific IgG response represented as AUC. Symbols represent mean across n=8 mice. (C) Uricase-specific IgG at day 45.

3.4.6 p(Man)-OVA treatment results in transcriptionally distinct profiles within OTI/OTII cells

To further investigate the antigen-specific T cell- intrinsic mechanisms by which p(Man)-antigen therapy could result in reduced antibody responses we performed RNAseq on OT-II cells 5 days after antigen treatment (Figure 3.15A). We found the p(Man)-OVA treatment group resulted in 2744 differentially expressed genes (DEGs) compared to the saline control, while OVA resulted in 99 DEGs compared to saline. Of the 2744 DEGs altered by p(Man)-treatment, only 94 were found to also be differentially expressed in the OVA treatment comparison (Figure 3.15B). This indicates that within the antigen-specific CD4+ T cells, p(Man)-OVA treatment is driving transcriptional changes which are distinct from those up-regulated by native antigen presentation. In order to understand which pathways these DEGs may be effecting in the p(Man)-OVA treatment compared to OVA treatment we performed ingeneuity pathway analysis (IPA). We identified 36 immune pathways significantly altered in p(Man)-OVA treated groups compared to OVA alone (Figure 3.15C). The majority of these pathways were found to be associated with T cell activation and TCR signaling. Gene signatures were found for Th1, Th2, Tfh and Th17 pathways, although these pathways shared many activation signatures such as increase in CD3ζ, NFAT, JAK and STAT signaling. Some pathways associated with T cell activation such as Nur77 and TWEAK signaling are also associated with apoptosis and regulation of T cell proliferation. The upregulation of signaling genes after p(Man) treatment is also significantly associated with an increase cytokine signaling pathways such as IL-2, interferons and IL-23. Along with increased T cell signaling and activation, IPA also identified pathways associated with exhaustion and apoptosis. The T cell exhaustion pathway is significantly upregulated due to increases in expression of co-inhibitory receptors CTLA4, EOMES, and PD-1. Upregulation of caspases and Bcl-2 associated agonist of cell death (BAD) are associated with apoptosis pathways, all of which are significantly upregulated in OTIIs after p(Man) treatment. The combination

of T cell activation along with upregulated apoptosis and exhaustion pathways suggest that p(Man)-OVA may lead to a deficient antigen-specific T follicular helper response through the activation of T cells towards different pathways such as Th1, Th2 or Th17 or the increased antigen experience and activation signaling may lead to broad apoptosis and exhaustion of OVA-specific T cells. Both possibilities would result in insufficient T cell help available to drive strong anti-OVA antibody responses.

3.4.7 Native glycosylation of antigen impairs tolerogenic effects of p(Man)-antigen therapy

The majority of the p(Man)-antigen experiments discussed above were performed using a *Candida* uricase sequence expressed in *E Coli*. *E Coli* lack the post-translational modification machinery to add glycosylation and protein expressed recombinantly in *E Coli* are typically aglycosylated(377). One of the native FDA-approved uricases, Rasburicase, is an *A Flavus* sequence expressed recombinantly in yeast. The *A Flavus* uricase sequence contains many potential glycosylation sites, therefore this form of uricase is expected to be extensively glycosylated, unlike uricase expressed in *E Coli*. In order to investigate the role of glycosylation in p(Man)-antigen treatment we compared yeast-expressed Rasburicase to *E Coli* expressed *A Flavus* uricase with the same amino acid sequence. We first compared the glycosylation patterns of each protein using a lectin array (Figure 3.16A). We found that the Rasburicase bound lectins GNA, HHI, NPA, PSA, RCA-1 whereas the *E Coli*-produced *A Flavus* uricase only showed signal in the positive control spots. These lectins bound by Rasburicase are specific for high mannose lectins as well as Galβ4GlcNAc(378), which are likely glycosylations on the Rasburicase protein. We successfully conjugated both proteins to p(Man) as indicated by the increased molecular weight on SDS-PAGE which disappears upon exposure to reducing conditions (Figure 3.16B). There are some larger molecular weight aggregates visible in the p(Man)-Rasburicase conjugate under reducing conditions that are not seen in the *A Flavus* conjugate, but this may be more easily visible due to the increased

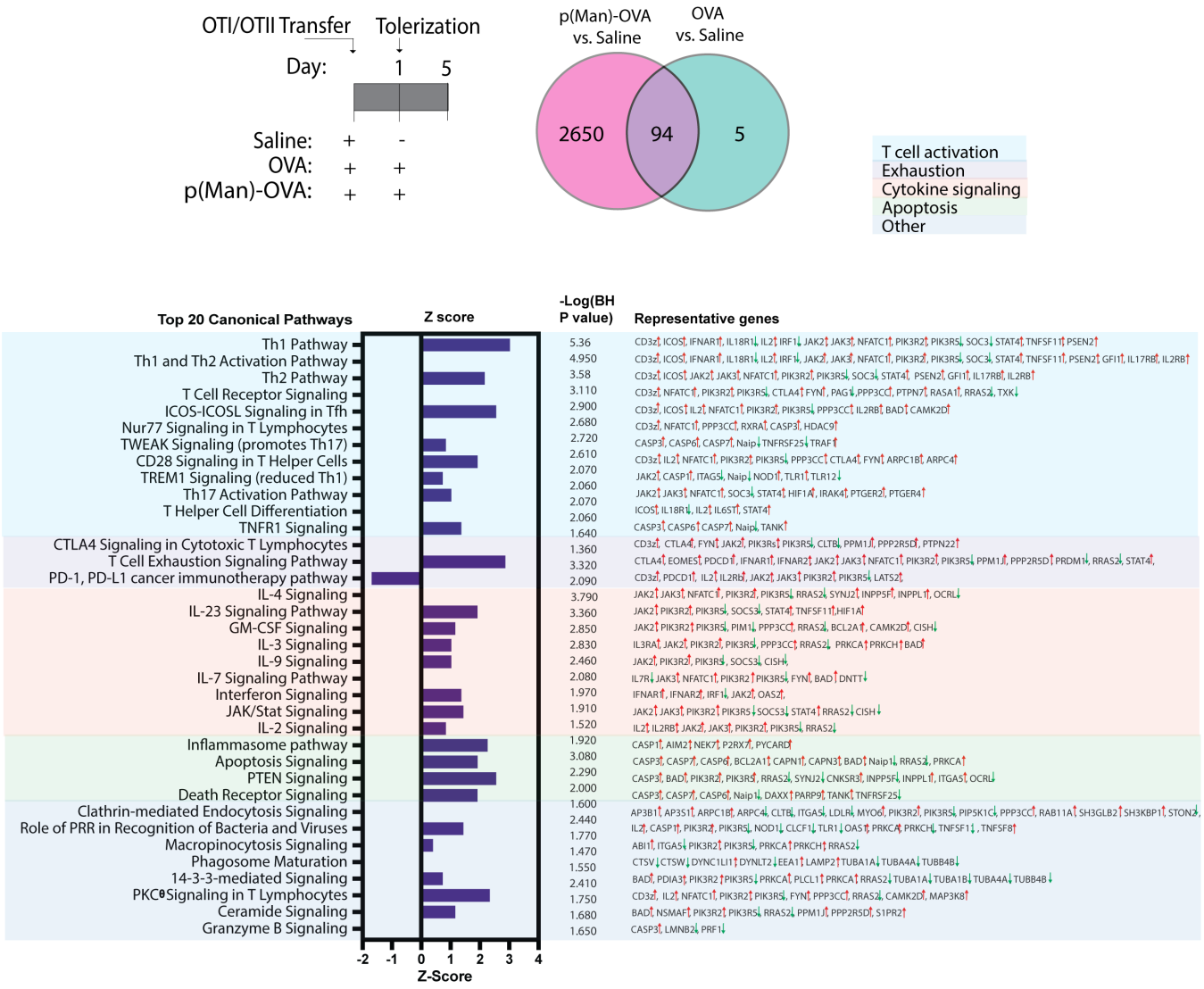

Figure 3.15: p(Man)-OVA treatment results in transciptionally distinct profiles within OTII cells. (A)740,000 CD45.1 congenitally labeled OTI and OTII T cells were adoptively transfered at day 0. One day 1 mice were treated with p(Man)-OVA, OVA or saline. OTII cells were isolated on day 5 for sequencing. (B) Venn diagram displaying the number of distinct and overlapping DEGs in p(Man)-OVA and OVA treatment groups compared to saline control. (C) Significantly up- or down-regulated canonical immune pathways expressed in p(Man)-OVA compared with OVA as identified by ingenuity pathway analysis (IPA). Bars represent calculated z score. The BH-adjusted P value and associated genes are displayed to the right. Up/down arrows indicate gene expression.

concentration of the conjugate in the gel.

We compared the efficacy of p(Man)-Rasburicase (p(Man)-R) and p(Man)-*A Flavus* (p(Man)-AF) to induce tolerance using a similar experimental set up as 3.8D. Balb/c mice

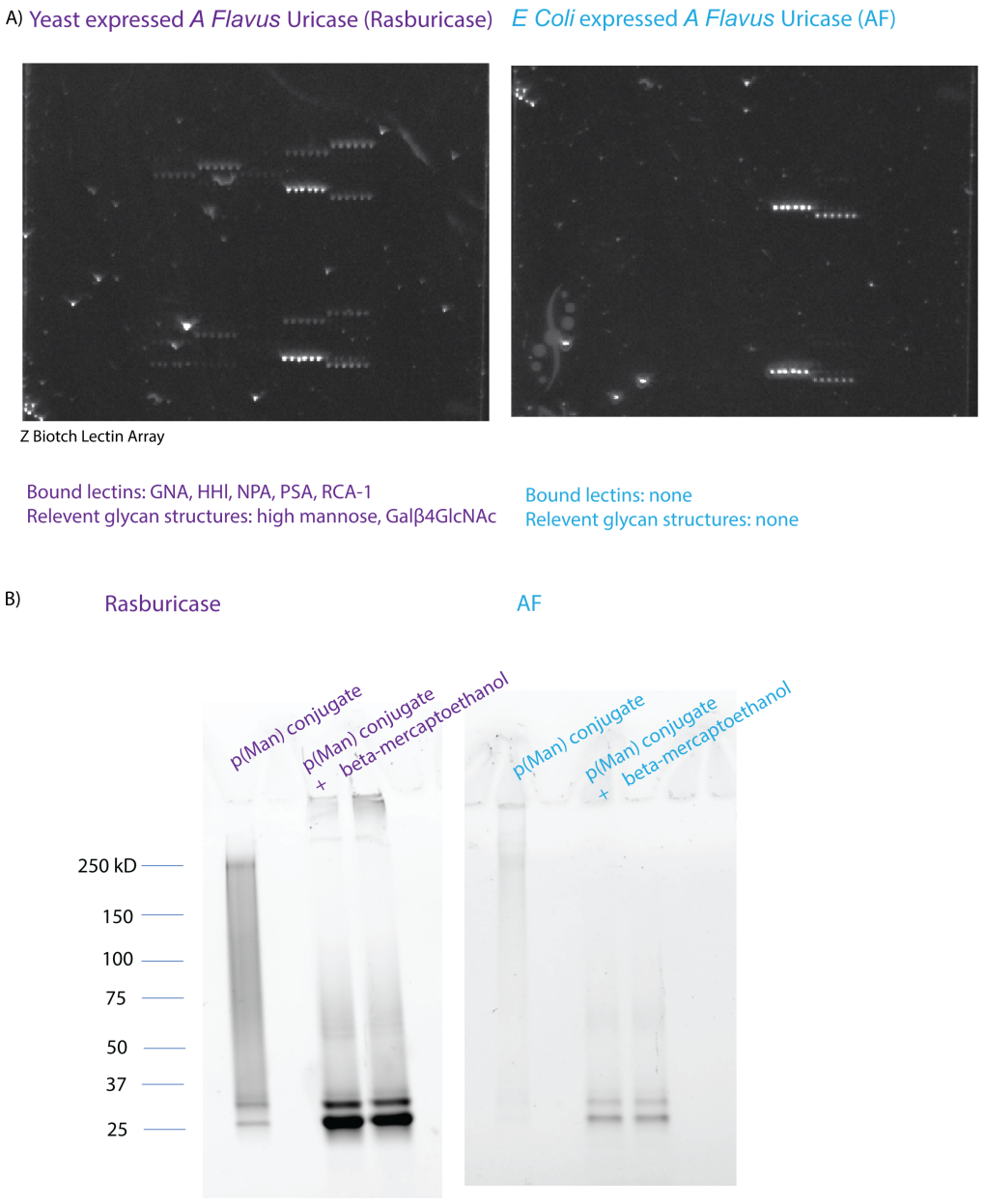

Figure 3.16: Characterization of the p(Man)-Rasburicase and p(Man)-A Flavus uricase constructs. (A) Biotinylated Rasburicase and *A Flavus* uricase were incubated on a lectin array and detected with APC-streptavidin to probe surface glycosylation. Lectins positive for binding are identified along with their reported specificities. (B)SDS-PAGE of p(Man)-conjugated Rasburiacase and *A Flavus* uricase showing expected increase in molecular weight after conjugation and loss of p(Man) after incubation with β-mercaptoethanol.

were treated with either p(Man)-R, p(Man)-AF for saline. The following challenges were done with either Raburicase or *A Flavus* uricase, and the relevant antibody responses were determined in the plasma (Figure 3.17A). We found that p(Man)-R treatment was unable to

abrogate the Rasburicase-specific antibody response, in fact the resulting antibody response trended higher than in the untreated mice. The antibody responses in mice that were pre-treated with p(Man)-AF in contrast trended lower than the untreated mice, although not significantly (Figure 3.17B). A different result was seen in the *A Flavus* challenged mice. p(Man)-AF pre-treatment resulted in a significant reduction in the AF-specific antibody response after challenge compared to the untreated mice (Figure 3.17C). A potential explanation for the unexpected lack of therapeutic efficacy of p(Man)-Rasburicase could be that Rasburicase generates a T cell-independent antibody response. In order to probe this question, we analyzed the subclass of Rasburicase-specific IgG. T cell independent responses can result in IgG3 responses wherase T cell depedent responses to immunogenic therapeutics is predominantly IgG1. We found that the antibody response against Rasburicase was primarily IgG1, similarly to what was seen against *Candida* uricase in Figure 3.8G. p(Man)-R treatment seemed to result in a strong, early IgG1 response and a reduced IgG3 response compared to untreated mice which remains low after high dose challenge (Figure 3.17D). The lack of strong IgG3 response to p(Man)-R make an TI response unlikely to account for the difference in therapeutic efficacy. These data suggest that p(Man)-antigen treatment is most effective when the antigen is aglycosylated, although pre-treatment with an aglycosylated variant of the challenge antigen may result in some level of antibody abrogation, further experimentation is required to better understand these responses.

3.4.8 Uox-/- *mice as a model of pathogenic ADA production*

To best evaluate the potential of p(Man)-antigen therapy to prevent clinically relevant ADAs, we wanted to use a model of anti-drug antibody formation that would result in loss of therapeutic efficacy and increased disease pathology. We selected the uric oxidase knock-out (*Uox-/-*) mouse model. *Uox-/-* mice cannot produce endogenous uricase resulting in the accumulation of insoluble uric acid and kidney damage in untreated mice(379; 380). Mice were kept on allopurinol-supplemented water from birth to inhibit the native enzyme

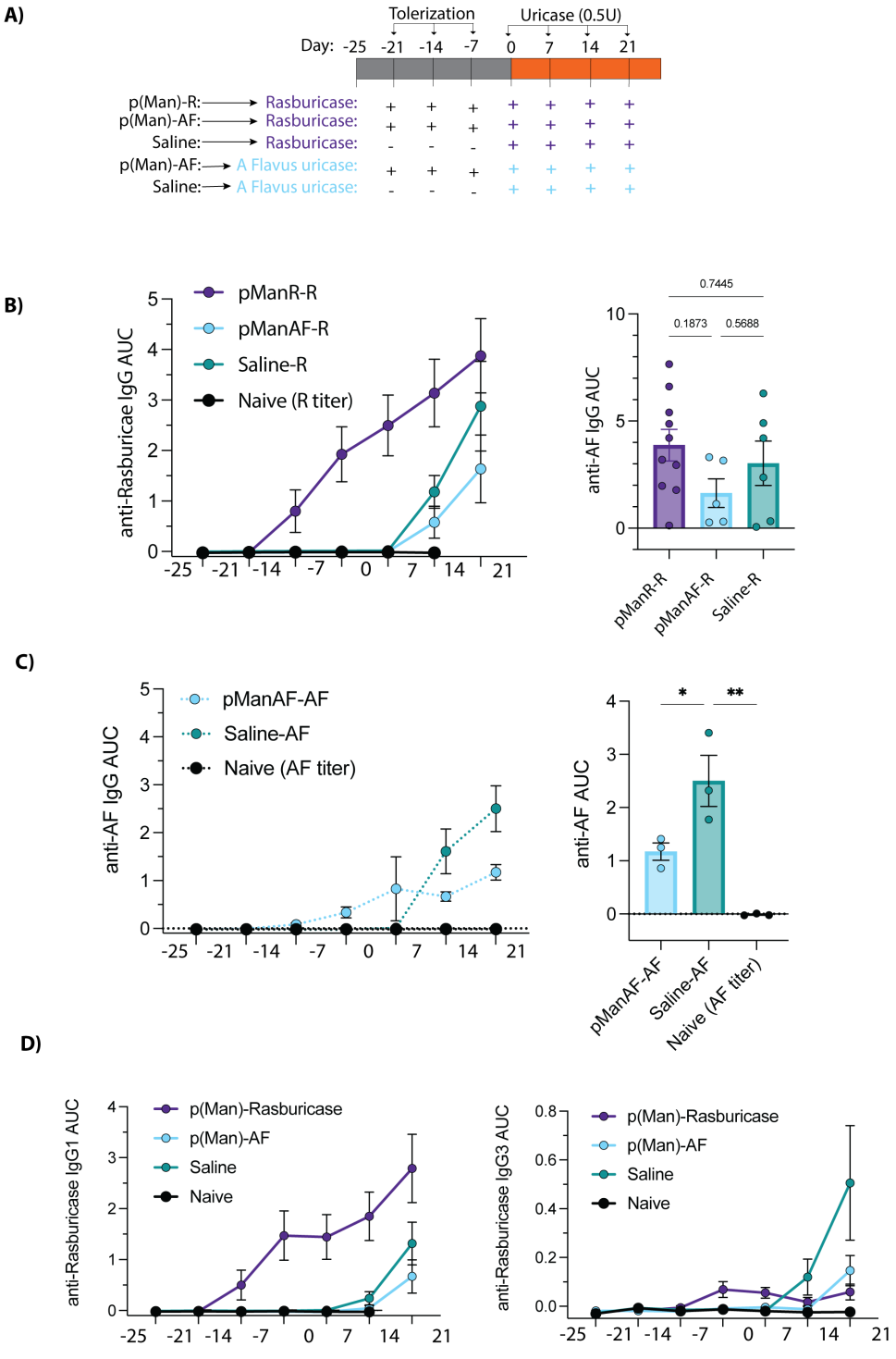

Figure 3.17: Native glycosylation of the protein antigen impacts p(Man)-antigen therapy. (A) Balb/c mice were treated weekly for 3 weeks as in Figure 3.8D followed by challenge with 0.5U of Rasburicase or *A Flavus* uricase as indicated.(Continued on the following page.)

Figure 3.17, continued: (B) Left, time course of the Rasburicase-specific IgG response represented as AUC. Symbols represent mean across n=5-10 mice. Right, the Rasburicase-specific IgG response at day 21 is highlighted. Each symbol represents an individual mouse.(C) Left, time course of the *A Flavus* uricase-specific IgG response represented as AUC. Symbols represent mean across n=3 mice. Right, the *A Flavus* uricase-specific IgG response at day 21 is highlighted. Each symbol represents an individual mouse. (D) Left, time course of the Rasburicase-specific IgG1 antibody response represented as AUC. Right, time course of the Rasburicase-specific IgG3 antibody response represented as AUC. Symbols represent mean across n=5-10 mice. Data are shown as mean±SEM. Unless otherwise stated symbols represent individual mice and statistical differences in all graphs were determined by one-way ANOVA with Tukey's *p<0.05, **p<0.01 and ***p<0.001

xanthine oxidase's conversion of allantoin, a more soluble metabolite, into uric acid. We treated mice weekly for three weeks with p(Man)-uricase, uricase or saline followed by twice-weekly injections of uric acid (Figure 3.18A). Throughout the course of the experiment serum uric acid levels and urine uric acid/creatine ratio was measured as readouts of hyperuricemia and kidney function respectively. *Uox-/-* mice exhibited increased serum uric acid levels compared to WT controls for the entire course of the experiment, which increased once allopurinol treatment was removed (Figure 3.18B). Kidney filtration capacity as a readout of uric acid/creatine in the urine was also consistently higher in *Uox-/-* mice compared to WT (Figure 3.18C). On day 42 *Uox-/-* mice were injected with uricase and blood was collected to measure the percent change in serum uric acid compared to baseline over time (Figure 3.18D). When the uricase-specific antibody AUC was plotted against the AUC of the change in serum uric acid, the mice with high levels of antibody trended towards a less negative AUC, indicating that anti-uricase antibody responses in this model may correlate with hyperuricemia pathology due to increased clearance of the therapeutic, uricase.

To evaluate the histological kidney pathology associated with the *Uox-/-* mutation, we performed PAS staining to look for morphological changes. We found increased damage to the glomerulus in the kidneys of *Uox-/-* mice compared to wild-type, however this did not seem to correlate with the anti-uricase antibody response (Figure 3.19).

We next analyzed the effects of p(Man)-antigen treatment in the *Uox-/-* model. The individual curves of percent change in serum uric acid over time after uricase treatment

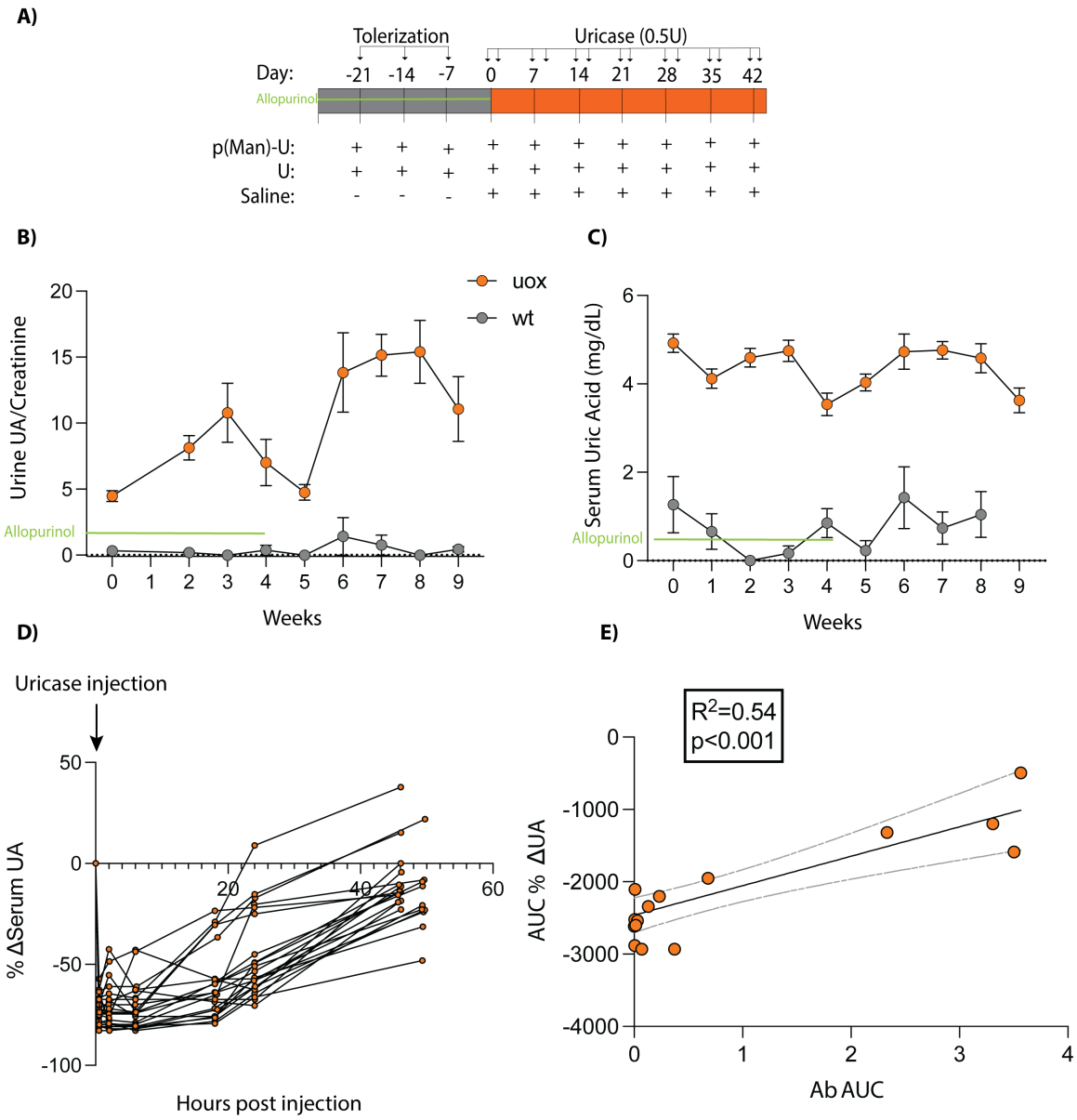

Figure 3.18: Uricase as a therapeutic for *Uox-/-* mice. (A) Uox-/- or age-matched WT mice were treated 3 times weekly with p(Man)-uricase followed by removal of allopurinol-supplemented water and subsequent twice-weekly treatment with 0.5U *Candida* uricase.(B) Time course of urine uric acid/creatinine in *Uox-/-* and WT mice across treatment groups. (C)Time course of serum uric acid (mg/dL) in *Uox-/-* and WT mice across treatment groups. (D) Time course of the change in serum uric acid from baseline across treatment groups after uricase treamtent on day 42. (E) Linear regression of the change in serum uric acid after uricase injection represented as area under the curve against the uricase-specific IgG response at day 42 represented as AUC. Data are shown as mean±SEM.

were plotted for each treatment group (Figure 3.20A). Wild-type mice did not exhibit much change in serum uric acid levels over time, likely as a result of the presence of the native

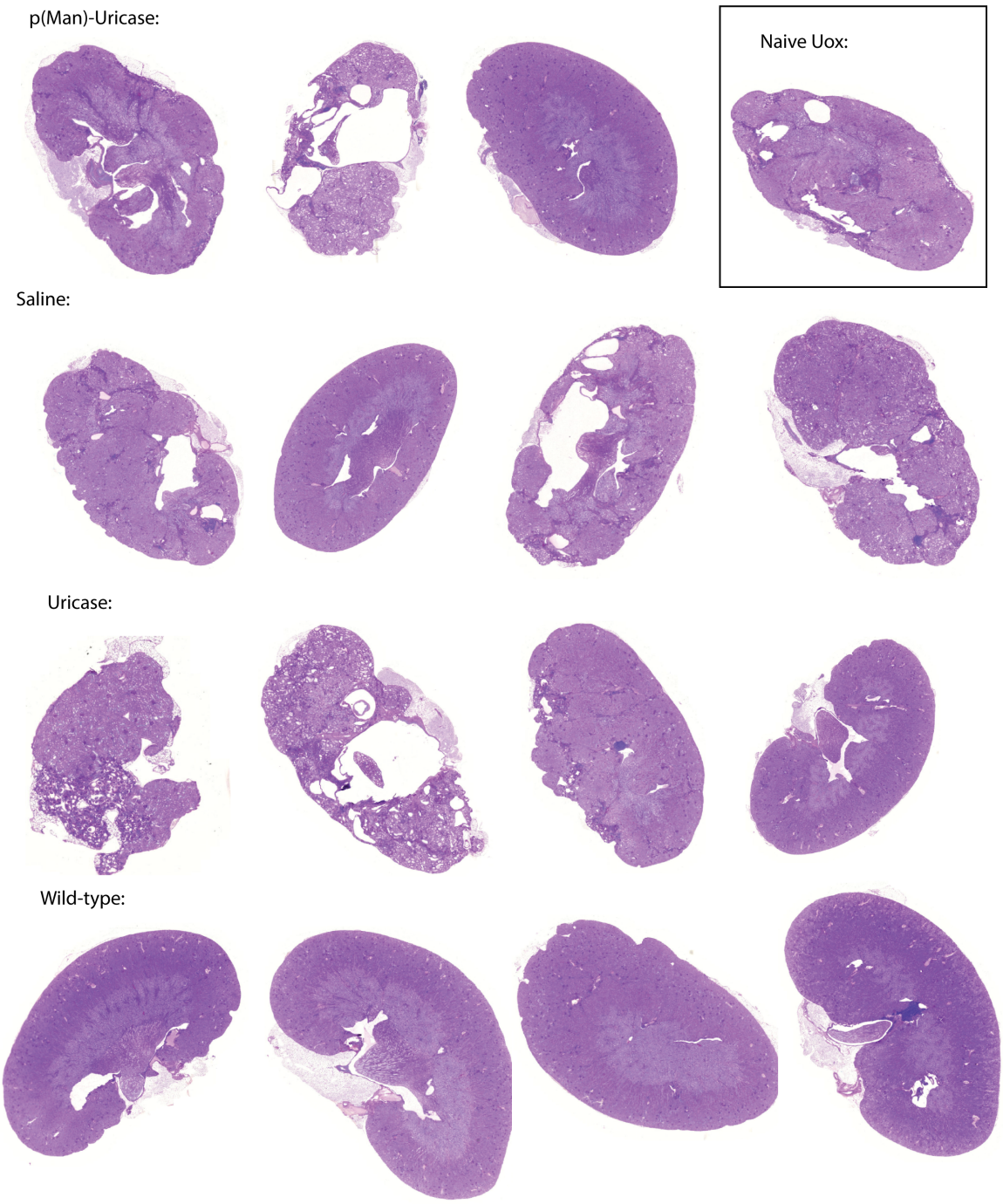

Figure 3.19: Mice were treated as in Figure 3.18. Kidneys were isolated and formalin-fixed followed by Periodic acid-Schiff staining to highlight glomerular changes and renal pathology.

enzyme allowing for the maintenance of uric acid control. Naïve *Uox-/-* who had never experienced uricase treatment maintained a lower serum uric acid level for the first 20 hours before it gradually rose back to baseline, however in the p(Man)-uricase and saline treatment

groups a subset of mice had levels begin to rise within the first 6 hours, resulting in a less negative AUC (Figure 3.20B). The rise in AUC seems to be bimodal with certain mice in the p(Man)-uricase and saline groups demonstrating lower therapeutic efficacy of uricase. There were however no statistical differences between groups. Similarly, there are not strong statistical differences in the uricase-specific antibody responses of the different treatment groups, although the saline-treated group is the only one to have statistically higher antibody response than naïve mice (Figure 3.20C). Bimodal responses are also seen in uricase-specific antibody responses the p(Man)-uricase and saline-treated mice. The individuals with high antibody AUC also exhibit lower therapeutic efficacy indicating that this model may have promise to evaluate negative effects of ADA, however the bimodal nature of the treatment efficacy, which may be the result of the outbred mouse strain, would necessitate much higher n in future experiments to fully evaluate the efficacy of the p(Man)-uricase therapeutic.

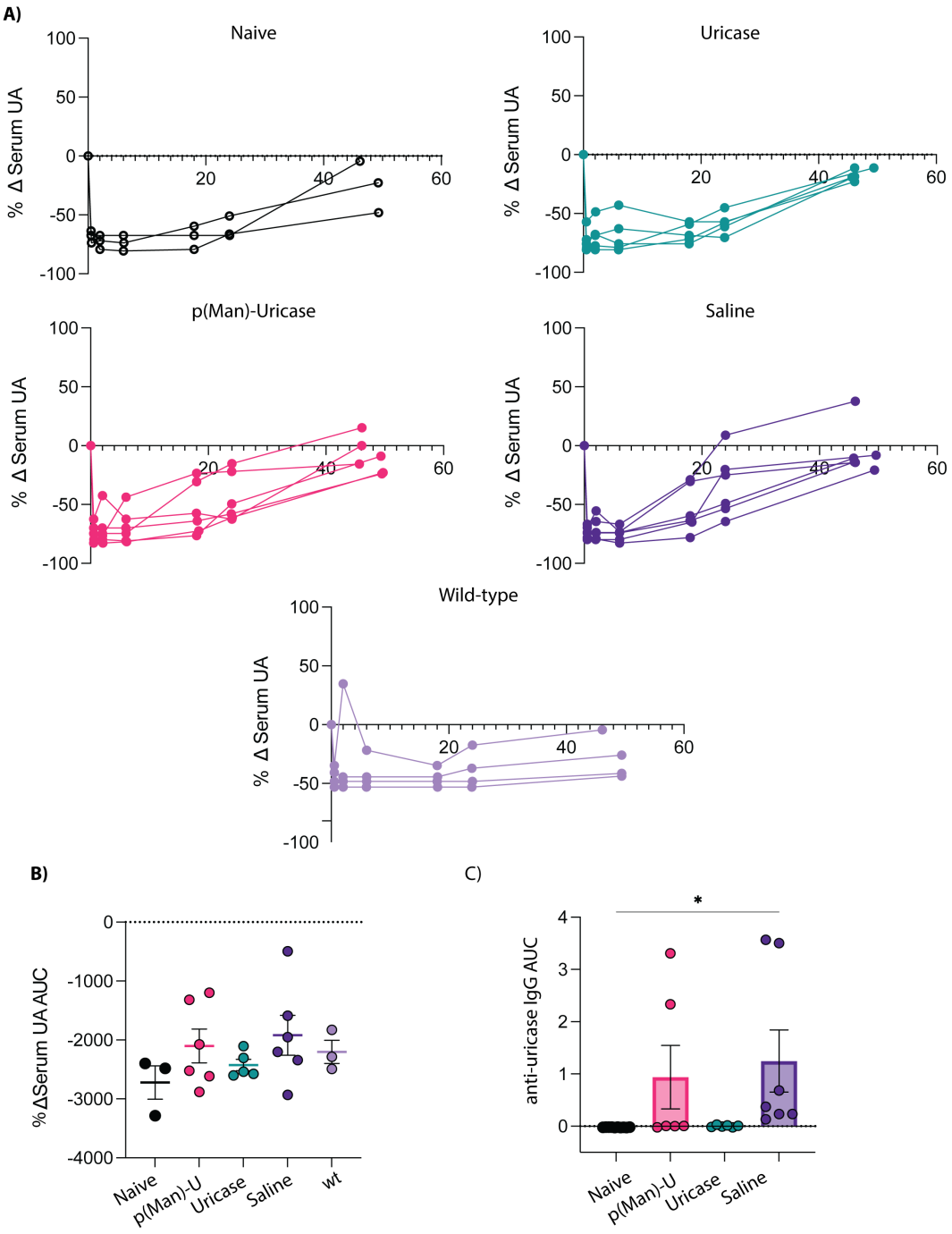

Figure 3.20: p(Man)-uricase treatment is insufficient to drive differences in the efficacy of uricase treatment in *Uox-/-* mice. A)Mice were treated as in Figure3.18A. Time course of the change in serum uric acid from baseline after uricase injection on day 42 for individual mice, plotted by treatment group.(Continued on the following page.)

Figure 3.20, continued: (B) The change in serum uric acid from baseline after uricase treatment from (A) represented as area under the curve. (C)The uricase-specific IgG response at day 42 represented as AUC.Data are shown as mean ± SEM. Unless otherwise stated symbols represent individual mice and statistical differences in all graphs were determined by one-way ANOVA with Tukey's *$p<0.05$, **$p<0.01$ and ***$p<0.001$

3.5 Discussion

In this study, we synthesized a novel mannose polymer, p(Man), that can be easily conjugated to any protein antigen in order to reduce the T follicular helper and resulting antibody response against the antigen upon future administration. We showed that pre-treatment with p(Man)-antigen was able to significantly reduce the antigen-specific antibody response to not only OVA but to a therapeutic doses of uricase, a highly immunogenic drug. We first demonstrated that p(Man) conjugation significantly increased the delivery of OVA to the liver to a greater extent than even our previously published liver-targeted glycopolymers(291; 293). This difference may be due to the more promiscuous binding of mannose residues to a wide variety of C-type lectins compared to GalNAc or GlcNAc resulting in increased endocytosis and cross-presentation(370; 381–383), or it may be mediated by signaling through a specific mannose-binding lectin in the liver we have yet to identify(384; 385). Like the previously published glycopolymers, pre-treatment with p(Man)-OVA resulted in an impaired CD4+ antigen-specific T cell response in the OT vaccination model, with an exceptional decrease in the number of T follicular helper (Tfh) cells within the OTII population. Once we saw this lack of Tfh cell help we confirmed that p(Man)-OVA pretreatment was sufficient to prevent an OVA-specific antibody response in an endogenous mouse. p(Man)-OVA treatment fully prevented a detectable OVA-specific antibody response while treatment with unmodified OVA, which contains native mannosylation did not(386). This provides evidence for the unique capacity of our linear p(Man) polymer to reduce humoral immune responses to an antigen over other forms of mannosylation.

While it generates an immune response, OVA is not an extremely immunogenic protein.

In order to investigate the capacity for p(Man)-antigen treatment to prevent antibody responses to a highly immunogenic therapeutic protein we conjugated it to uricase. Uricase is a tetrameric enzyme which degrades uric acid into the more easily excreted allantoin and is used as a therapeutic to treat hyperuricemia(387; 388). However even when pegylated, it elicits an immune response in the majority of patients, limiting therapeutic efficacy(379; 389; 390). When p(Man)-uricase was given as a pre-treatment prior to multiple doses of unconjugated therapeutic uricase doses, we found a significant reduction in the uricase-specific immune response via a reduction in uricase-specific antibodies, fewer uricase-specific antibody-secreting cells, and fewer uricase-specific B cells in the spleen indicating a broad reduction in the humoral response to this immunogenic antigen. The effect of p(Man) uricase treatment was different than OVA as the antibody response to uricase was not fully eliminated. Despite the presence of detectible antibodies after p(Man)-uricase treatment, they were significantly reduced compared to untreated mice. This reduction is clinically relevant as the magnitude of the ADA response effects the extent of clinical consequences(391). It is not yet clear how antigenic differences alter the efficacy of p(Man)-antigen treatment. The increased antibody response against uricase may be due to its enzymatic function. The enzymatic reaction produces hydrogen peroxide, a reactive oxygen species, as a by-product which may increase inflammation(392–394). Alternatively, or there may be differences in post-translational modifications between uricase and OVA which can alter immune response(395; 396) or differences between the natural affinity of an individual's T cell or B cell compartment to each antigen's epitopes(365; 397; 398).

To probe the immune mechanisms responsible for the effects of p(Man)-antigen delivery we performed an αCD25 depletion after p(Man) treatment. We found that pretreatment with p(Man)-uricase led to a significant reduction in the uricase-specific antibody response despite the depletion. αCD25 depletion has been shown to deplete Tregs in addition to other recently activated CD25 expressing cells(399). We interpret these data to suggest that Tregs likely do not play a predominant role in the reduction of antibodies we see after p(Man)

treatment. It is possible that the reduction of other CD25-expressing cells such as NK cells, B cells and activated T cells could confound this readout, but we do not expect the activated T cells or NK cells to have much of a role in maintaining the antibody response once germinal center activity has been initiated. If critical antibody-generating B cells were depleted we would have expected antibody responses to decrease after treatment with αCD25.

We recognized that the presence of non-protein p(Man) associated with the antigen during initial priming of B cells could affect downstream antibody responses though hapten immunodominance towards a p(Man)-dominated antibody response. This immunodominance has been shown with NP-OVA when more copies of NP are conjugated to an OVA protein, the B cells that are positively selected by T cells in the germinal center predominantly bind NP while expressing the OVA epitopes on their MHC after they endocytose the entire construct(400). To test for this effect we looked for antibody responses against the p(Man) polymer, but we saw no detectable response, making hapten immunodominance unlikely to account for the reduction in antibody response we see to uricase.

We performed transcriptional analysis on the OTII T cells after p(Man)-OVA treatment and found upregulation of signatures associated with TCR-signaling, apoptosis and exhaustion. These data suggest that p(Man) treatment increases presentation of the antigen to the T cells and resultant TCR signaling, however these T cells undergo non-Tfh fates of apoptosis, exhaustion or perhaps Th1-dominant responses limiting the Tfh help available to the B cells, ultimately preventing strong antibody responses against the antigen. Some other interesting gene signatures we identified include increased cytokine signaling including interferon and IL-23. The positive z score associated with these pathways may indicate that p(Man)-antigen treatment does not diminish T cell responses broadly but rather skews them away from an antibody-producing Tfh response to more Th1 or Th17 responses. We also saw upregulation of pathways associated with uptake such as endocytosis. This may be due to receptor endocytosis such as TCR and other surface receptor down-regulation associated with tolerance(401–403) which could also account for some reduced T cell responses we see

in the OT model.

Unexpectedly, p(Man)-rasburicase was unable to prevent high antibody titers against the heavily glycosylated FDA-approved therapeutic. The only difference between the Rasburicase and *A Flavus* uricase is the expression systems, resulting post-translational glycosylation patterns. The presence of native glycosylation may impact antigen uptake and delivery if the glycosylations bind different lectins on cells than would normally uptake p(Man)-antigen. Additionally, these lectins may act as PRRs and induce inflammation within the antigen presenting cell, leading to co-stimulation and activation of the antigen-specific T cell responses. The lectin binding array demonstrated that rasburicase likely has high-mannose structures, however these structures likely differ from p(Man). Natural mannosylations are likely branching, whereas p(Man) is a linear polymer with linkages between mannose residues and the backbone. A linear polymer is more likely to be recognized by lectins specific to terminal moities instead of those binding distinct forms of braching(404). p(Man) glycosylation also differs from native as p(Man) molecules will be released in the reducing conditions of the endosome. Native glycosylations, in contrast, will remain attached to peptide fragments and can be displayed to T cells on MHC, altering the displayed peptidome and resulting immune responses(405). Further investigation into the binding and signaling of p(Man) through c-type lectins as it compares to that of native glycosylations will futher inform the limits of p(Man)-mediated immune tolerance.

Lastly, we investigated the use of *Uox-/-* mice lacking a functional uricase enzyme as a model of anti-drug antibody-mediated loss of drug efficacy. We were able to demonstrate that the efficacy of exogenous uricase to lower uric acid levels was correlated to lower anti-uricase antibody responses. However, the mice in this model exhibited relatively weak and non-uniform antibody responses against i.v.-injected *Candida* uricase. This variabilty may be due to the outbred nature of the mouse strain and necessitates the use of a high n in future studies.

Here we investigated p(Man)-antigen therapy's capacity to prevent T cell dependent

IgG antibody responses specifically. Future work can inform how p(Man) may impact IgE responses relevant in a minority of ADA antibody responses(406; 407) and other diseases such as allergy and asthma(408). Since we hypothesize p(Man) acts through the abrogation of T cell help, it may not be able to reduce T cell independent antibody responses and further work should be done to investigate this application.

In conclusion we have demonstrated that p(Man)-antigen therapy can significantly diminish the resulting antibody response to an immunogenic antigen. This technology has the potential to be used with any immunogenic protein drug to prevent a patient from eliciting a strong ADA response to the drug and reduce the risk of adverse effects associated with ADAs including loss of therapeutic efficacy, infusion reactions and anaphylaxis. The ability the reduce antibodies in an antigen-specific manner may have other broad applications in the treatment of antibody-mediated diseases such as asthma, allergy and antibody mediated autoimmune diseases where specific antigens can be identified, such as pemphigus vulgaris and myasthenic gravis(409; 410). Further work should be done to see how p(Man)-antigen therapy might function in the therapeutic setting after an antibody response has already developed. It could potentially be combined with antibody reducing treatments such as αCD20 treatments, plasma cell depletion or IVIG to reduce an antibody response and use p(Man)-antigen therapy to keep the antigen-specific response of interest low once broad immunosuppressants are discontinued.

CHAPTER 4

DISCUSSION, FUTURE DIRECTIONS, AND CONCLUSION

4.1 Discussion and future directions in PEG-PPS polymersomes in vaccination

In the first study I presented a set of vaccines against SARS-CoV-2 using PEG-PPS polymersomes. Using the receptor binding domain (RBD) of the spike protein, I developed RBD encapsulated (RBDencap) and RBD surface-decorated (RBDsurf) polymersomes for antigen delivery and MPLA-encapsulated polymersomes for adjuvant delivery. Overall, I found that RBDsurf, RBDencap and free RBD formulations were able to induce strong RBD-specific IgG antibody titers, but only polymersome-formulated antigens RBDsurf and RBDencap resulted in increased antigen-specific Th1 T cell responses. Of the different antigen formulations, only RBDsurf polymersomes were able to elicit a neutralizing antibody response.

It would be interesting to further investigate the mechanisms by which antigen delivery via RBDsurf and RBDencap result in different immune responses. The increased neutralizing response found after RBDsurf vaccination was accompanied by a more limited epitope specificity, an increase in RBD-specific GC B cells and a lower IgG2b/IgG1 ratio. In contrast, the RBDencap vaccination did not result in neutralization, but elicited a faster antibody response, leading to a greater RBD-specific IgG signal than RBDsurf at day 7 after initial prime injection. RBDencap also resulted in higher frequency of RBD-specific plasmablasts and fewer RBD-specific GC B cells within the RBD-specific B cell compartment. These data suggest that RBDsurf may elicit a stronger GC response, while RBDencap results in more extrafollicular B cell responses. Extrafollicular responses are associated with rapid differentiation of the B cell into antibody-secreting plasmablasts, peaking 4-6 days after immunization. The antibodies secreted by these responses are typically lower affinity as the B cells were not able to undergo affinity-maturation and SHM in the germinal center(411). In contrast it is possible RBDsurf elicited a stronger germinal center response associated with

clonal selection and blasting resulting in the selection of B cells highly specific to a small number of epitopes. This high affinity and selectivity may explain the neutralization results and the limited epitopes identified via peptide array. Future work to investigate the localization of antigen and visualize GC formation after vaccination with RBDencap or RBDsurf via microscopy techniques may more definitively characterize these responses as GC or extrafollicular. It is not currently well understood why different antigens and pathogens elicit predominantly GC or extrafollicular B cell responses(411), delivery tools such as RBDsurf and RBDencap may be useful in further elucidating this mechanism.

One way in which antigen delivery via RBDsurf might differ from RBDencap is in the localization of the particles upon delivery. The presence of the protein on the surface of the RBDsurf polymersomes may interact differently with cells and tissues *in vivo*. The RBD contains the receptor binding motif which can bind to surface angiotensin-converting enzyme 2 (ACE2) expressed across a variety of tissues(412). Additionally, upon secondary boost administration, circulating RBD-specific antibodies may bind RBDsurf particles. Formation of immune complexes on the surface may lead to increased recognition and uptake through FcγR on various immune cells. As a mammalian-expressed recombinant protein, RBD may have surface glycosylations capable of binding lectins and increasing uptake. Future biodistribution studies using fluorescently labeled particles would be valuable to elucidate the cellular uptake and kinetics of administration of the different formulations.

In this study I demonstrated the utility of polymersomes as a delivery platform for vaccination. We were able to load antigen and adjuvant inside the polymersomes and conjugate antigen to the surface. Future studies may demonstrate the utility of polymersomes for delivery of multiple antigens from the same pathogen to improve vaccination and perhaps elicit an immune response against a variety of antigen sequences that may aid in protection against pathogens with multiple strains or a high frequency of mutation. It would be interesting to investigate how the immunodominance of different antigens may be altered if delivered on the surface vs. encapsulated or alongside another antigen. Having demonstrated that anti-

gen can be surface-conjugated to the polymersomes, it would be interesting to investigate how different molecular surface moieties could be used for more directed targeting of these polymersomes. Antibodies or Fabs could be used to target specific molecular signatures on target cells or organs of interest very specifically or carbohydrates such as mannose could be added to increase broad uptake through lectin-binding.

Overall, PEG-PPS polymersomes offer a versatile, biocompatible nanomaterial platform for the delivery of both hydrophobic and hydrophilic payloads. We have demonstrated their efficacy in mounting immune responses against antigens such as OVA(210; 213) and pathogens including Lassa virus(327) and now SARS-CoV-2. It may also prove useful in macromolecule delivery outside of the fields of vaccination such as tolerance or gene delivery.

4.2 Discussion and future directions in p(Man)-mediated humoral tolerance

In the second study I presented p(Man) conjugation as an antigen delivery strategy to increase localization to the liver, resulting in antigen-specific tolerance and diminished antigen-specific antibody responses. I was able to show that pretreatment with p(Man)-antigen was sufficient to impair downstream antibody responses to uricase, an immunogenic biologic and that this effect is most likely the result of an impaired Tfh response.

It is interesting to note the differential responses of p(Man)-antigen treatment to different antigens and identical antigens produced by different expression systems. While p(Man)-OVA treatment fully abolished anti-OVA antibody titers, p(Man)-uricase reduced, but did not eliminate antibodies. This difference likely corresponds to the different immunogenicity of the antigens or the natural repertoire. When comparing un-tolerized, saline treated mice, OVA elicited an antibody response peaking around a titer of 3 (Figure 3.5), whereas Candida uricase elicited an antibody response peaking around a tier of 5-6 (Figure 3.12). It is impossible to use titer measurement as a direct comparison between two antigens as the

exact concentration and affinity of each set of antibodies cannot be elucidated due to the polyclonal nature of the response, however, it does suggest a higher response to uricase as a function of concentration and affinity. The increased immunogenicity of uricase may be due to its multimeric structure, increasing the likelihood for BCR cross-linking. It may also be the result of the natural affinity of the naïve B cell repertoire to uricase-specific epitopes. Alternatively it might be due to the glycosylation of OVA as a chicken-produced protein compared to the aglycosylated *E Coli*-produced uricase. Further investigation into the role of valency, naïve B cell affinity, and glycosylation will offer additional insight into the utility of p(Man)-antigen treatment to induce humoral tolerance. Tools that offer precise control over antigen valency, such as eOD-GT constructs, which can be produced as 4-mers, 8-mers and 60-mers(69), could be used in future studies to further investigate the role of antigen valency on immunogenicity and the efficacy of p(Man) treatment. Investigating the natural affinity of the naïve B cell compartment offers a greater challenge. We use fluorescent antigen multimers in our studies to detect antigen-specific B cells, however binding to the multimers requires a sufficient affinity which may not capture all relevant naïve B cells prior to somatic hypermutation. Antigen-specific enrichment strategies have been used to capture up to 80% of the antigen-specific B cells(413; 414)and may help overcome this challenge. Due to the polyclonal nature of the B cell compartment, quantifying the affinity of the BCRs will require individual sorting, BCR sequencing and analysis of each BCR's binding affinity by techniques such as surface plasmon resonance (SPR).

We have shown in our experiments that antigen glycosylation alters the effects of p(Man)-antigen treatment. It would be interesting to determine what molecular patterns of glycosylation make an antigen more or less immunogenic to better understand the effects of p(Man)-antigen treatment. A better understanding of the immune effects of glycosylation may also to help guide the development of novel therapeutic glycopolymers. Mannose glycosylations have been used extensively to delivery antigen to APCs due to the affinity for the mannose receptor (MR; CD206). MR is expressed primarily on myeloid cells, including

macrophages and APCs(415). Binding to MR leads to uptake and delivery of its ligands to the early endosome, but does not trigger additional downstream signaling motifs(382). Targeting antigen to the MR leads to efficient cross-presentation and activation of CD8+ as well as CD4+ T cells for both vaccination and tolerance-inducing delivery approaches(291; 416). Despite its lack of signaling domain, some studies have associated MR cross-linking with initiating a tolerogenic DC and macrophage phenotypes(417; 418). In addition to MR, p(Man) likely also binds a number of other lectins such as Dectin-2, Mincle, DC-SIGN, SIGN-R1/3, and Langerin. Many of these lectins contain signaling domains. Dectin-2 contains an ITAM signaling motif, Mincle signals via FcRγ, DC-SIGN signals through an ITAM/ITIM independent pathway involving Raf recruitment(419). It would be interesting to further investigate the specificity for p(Man) to different lectins and the resulting downstream signaling. Future *in vivo* studies inhibiting these signaling pathways would give valuable insight to determine if the tolerance-inducing effects seen after p(Man) treatment can be attributed to its signaling capacity in addition to endosomal delivery of antigen.

Additional native antigen glycosylations were shown to alter the immune response, and p(Man)'s capacity to induce tolerance. It would be interesting to further study which glycosylations are associated with higher and lower antibody responses and which receptors they signal through to induce these immune signatures. C-type lectins are associated with both initiating immune responses and maintaining homeostasis and can typically bind a range of glycan signatures(370). High-throughput and computational analysis may offer insights into these patterns that could be utilized to design materials to co-opt these pathways to engineer vaccination and tolerance(420; 421)

I demonstrated that pre-treatment with p(Man)-antigen can elicit reduced antibody responses against subsequent exposure to an antigen. This type of prophylactic treatment has clinical utility primarily in the treatment of patients prior to their administration of an immunogenic biologic drug. In this scenario, patients will be prescribed a therapeutic with a known risk of immunogenicity and can undergo p(Man) treatment before beginning the

medication. Another scenario might be the pre-treatment of children at risk for developing allergy. It has been established that there is an 'atopic march' in the development of allergic diseases in which infants who develop atopic dermatitis, often in their first 6 months of life, will be at an increased risk for developing food allergies(422). If these children can be identified and treated prior to the development of food allergy, p(Man)-antigen therapy may be able to reduce food antigen-specific IgE and allergic responses. However, further investigation on the impact of p(Man)-antigen therapy on the development of antigen-specific IgE and allergic responses is warranted.

There are numerous clinical scenarios in which it would be beneficial to reduce an active antibody response. These include patients who have already developed ADAs or inhibitors against life-saving therapeutics, allergies or active antibody-mediated autoimmunity who will be diagnosed only after the development of the antibody response. Therefore it would be interesting to investigate the effects of p(Man)-antigen treatment after an antigen-specific antibody response is already established. We hypothesize that p(Man)-antigen therapy functions through the T cell compartment and it is thus unlikely that p(Man)-antigen treatment will have strong effects on an established long-lived antibody-secreting plasma cell response. Although regulatory T cells have been implicated in plasma cell homeostasis(423), it is likely that combination with B cell depletion and/ or plasma cell depletion strategies such as anti-CD20 and bortezomib would be required to eliminate an active humoral response sufficiently to enable treatment with p(Man)-antigen and subsequent immune tolerance. Even alongside B cell and plasma cell depletion, there may be danger in administering p(Man)-antigen to patients exhibiting active antibody responses. Intravenous administration of the antigen may lead to hypersensitivity responses and anaphylaxis if sufficient circulating antibodies remain and can bind the antigen despite some possible epitope shielding by the p(Man) polymer.

In conclusion, the p(Man) offers a modular platform to prophylactically reduce antigen-specific antibody responses. It is biocompatible and can be conjugated to any protein antigen. Future studies will offer valuable insight into the role of glycosylation in immune tolerance

and activation and an understanding of the scope in which p(Man)-antigen treatment is efficacious. Overall, p(Man)-antigen treatment may enhance tolerance to current and future biologics, enabling long-term therapeutic solutions for an ever-increasing healthcare problem.

4.3 Conclusion

In conclusion, this work seeks to contribute to the field of immunoengineering through the development of nanomaterials for the modulation of immunity, with a focus on antibody responses. I have developed and characterized tools for the delivery of antigen and studied how design features of these tools contribute to the resulting immune response. While Chapter 2 focuses on the development of polymersomes for immune activation in the context of vaccination and Chapter 3 focuses on the development of a glycopolymer for tolerogenic antigen-delivery, both studies offer valuable insights to inform future directions of the other. I have demonstrated that polymersomes can be used to encapsulate antigen for delivery. This may offer an advantage when developing novel delivery strategies for immune tolerance. In order to deliver an antigen to the tolerogenic microenvironment of the liver in an active immune response, it may be necessary to avoid recognition by circulating antigen-specific antibodies. Polymersomes may offer a way to shield the antigen from this recognition. I have also shown how p(Man) conjugation can increase accumulation of antigen in the liver likely through increased uptake via c-type lectins. In order to target the liver or increase uptake by DCs, it may prove beneficial to decorate the surface of polymersomes with p(Man) in order to increase uptake or target antigen and adjuvants for vaccination against liver-resident pathogens such as hepatitis. Overall, these and other design considerations may lead to improved vaccines and therapies for those suffering from immune dysregulation. Immunoengineering is a rapidly evolving and interdisciplinary field. My experience in this field has involved extensive collaborations between material scientists, chemists, engineers, immunologists and clinicians. I hope to utilize this incredible training and continue to work towards better understanding of the complexities of the immune system and improving

human health.

REFERENCES

[1] E. S. Vitetta, M. T. Berton, C. Burger, M. Kepron, W. T. Lee, and X. M. Yin. Memory B and T cells. *Annual Review of Immunology*, 9:193–217, 1991.

[2] Daniel L Hamilos. Antigen presenting cells. *Antigen Presenting Cells*.

[3] Petr Broz and Denise M. Monack. Newly described pattern recognition receptors team up against intracellular pathogens. *Nature Reviews Immunology*, 13(8):551–565, August 2013. Number: 8 Publisher: Nature Publishing Group.

[4] Danyang Li and Minghua Wu. Pattern recognition receptors in health and diseases. *Signal Transduction and Targeted Therapy*, 6(1):1–24, August 2021. Number: 1 Publisher: Nature Publishing Group.

[5] Gianna Elena Hammer and Averil Ma. Molecular Control of Steady-State Dendritic Cell Maturation and Immune Homeostasis. *Annual review of immunology*, 31:743–791, 2013.

[6] Olivier P. Joffre, Elodie Segura, Ariel Savina, and Sebastian Amigorena. Cross-presentation by dendritic cells. *Nature Reviews Immunology*, 12(8):557–569, August 2012. Number: 8 Publisher: Nature Publishing Group.

[7] Carl H June, Jeffrey A Ledbetter, Peter S Linsley, and Craig B Thompson. Role of the CD28 receptor in T-cell activation. *Immunology Today*, 11:211–216, January 1990.

[8] Jeong-Ryul Hwang, Yeongseon Byeon, Donghwan Kim, and Sung-Gyoo Park. Recent insights of T cell receptor-mediated signaling pathways for T cell activation and development. *Experimental & Molecular Medicine*, 52(5):750–761, May 2020. Number: 5 Publisher: Nature Publishing Group.

[9] Jinfang Zhu and William E. Paul. CD4 T cells: fates, functions, and faults. *Blood*, 112(5):1557–1569, September 2008.

[10] Dirk Wohlleber, Hamid Kashkar, Katja Gärtner, Marianne K. Frings, Margarete Odenthal, Silke Hegenbarth, Carolin Börner, Bernd Arnold, Günter Hämmerling, Bernd Nieswandt, Nico van Rooijen, Andreas Limmer, Karin Cederbrant, Mathias Heikenwalder, Manolis Pasparakis, Ulrike Protzer, Hans-Peter Dienes, Christian Kurts, Martin Krönke, and Percy A. Knolle. TNF-Induced Target Cell Killing by CTL Activated through Cross-Presentation. *Cell Reports*, 2(3):478–487, September 2012.

[11] Tazio Storni, Franziska Lechner, Iris Erdmann, Thomas Bächi, Andrea Jegerlehner, Tilman Dumrese, Thomas M. Kündig, Christiane Ruedl, and Martin F. Bachmann. Critical Role for Activation of Antigen-Presenting Cells in Priming of Cytotoxic T Cell Responses After Vaccination with Virus-Like Particles1. *The Journal of Immunology*, 168(6):2880–2886, March 2002.

[12] Julie M Curtsinger and Matthew F Mescher. Inflammatory cytokines as a third signal for T cell activation. *Current Opinion in Immunology*, 22(3):333–340, June 2010.

[13] Paul Ehrlich. Partial Cell Functions. *Nobel Lecture*, 31(1):4–13, 1908.

[14] Frank MacFarlane Burnet. The Nobel Prize in Physiology or Medicine 1960.

[15] Susumu Tonegawa. The Nobel Prize in Physiology or Medicine 1987, 1987.

[16] Bryan Briney, Anne Inderbitzin, Collin Joyce, and Dennis R. Burton. Commonality despite exceptional diversity in the baseline human antibody repertoire. *Nature*, 566(7744):393–397, February 2019.

[17] David G. Schatz, Marjorie A. Oettinger, and David Baltimore. The V(D)J recombination activating gene, RAG-1. *Cell*, 59(6):1035–1048, December 1989.

[18] Esil Aleyd, Marieke H. Heineke, and Marjolein van Egmond. The era of the immunoglobulin A Fc receptor FcαRI; its function and potential as target in disease. *Immunological Reviews*, 268(1):123–138, November 2015.

[19] J. P. Kinet. The high-affinity IgE receptor (Fc epsilon RI): from physiology to pathology. *Annual Review of Immunology*, 17:931–972, 1999.

[20] Stylianos Bournazos and Jeffrey V. Ravetch. Diversification of IgG effector functions. *International Immunology*, 29(7):303–310, July 2017.

[21] Christopher D. C. Allen and Jason G. Cyster. Follicular dendritic cell networks of primary follicles and germinal centers: Phenotype and function. *Seminars in Immunology*, 20(1):14–25, February 2008.

[22] Balthasar A. Heesters, Riley C. Myers, and Michael C. Carroll. Follicular dendritic cells: dynamic antigen libraries. *Nature Reviews Immunology*, 14(7):495–504, July 2014. Number: 7 Publisher: Nature Publishing Group.

[23] Mercedesz Balázs, Flavius Martin, Tong Zhou, and John F Kearney. Blood Dendritic Cells Interact with Splenic Marginal Zone B Cells to Initiate T-Independent Immune Responses. *Immunity*, 17(3):341–352, September 2002.

[24] David Allman, Joel R. Wilmore, and Brian T. Gaudette. The Continuing Story of T-cell Independent Antibodies. *Immunological reviews*, 288(1):128–135, March 2019.

[25] Ian C. M. MacLennan, Kai-Michael Toellner, Adam F. Cunningham, Karine Serre, Daniel M.-Y. Sze, Elina Zúñiga, Matthew C. Cook, and Carola G. Vinuesa. Extrafollicular antibody responses. *Immunological Reviews*, 194(1):8–18, 2003. _eprint: https://onlinelibrary.wiley.com/doi/pdf/10.1034/j.1600-065X.2003.00058.x.

[26] R. M. Perlmutter, D. Hansburg, D. E. Briles, R. A. Nicolotti, and J. M. Davie. Subclass restriction of murine anti-carbohydrate antibodies. *Journal of Immunology (Baltimore, Md.: 1950)*, 121(2):566–572, August 1978.

[27] Youn Soo Choi, Jessica A. Yang, Isharat Yusuf, Robert J. Johnston, Jason Greenbaum, Bjoern Peters, and Shane Crotty. Bcl6 expressing follicular helper CD4 T cells are fate committed early and have the capacity to form memory. *Journal of Immunology (Baltimore, Md.: 1950)*, 190(8):4014–4026, April 2013.

[28] André Ballesteros-Tato, Troy D. Randall, Frances E. Lund, Rosanne Spolski, Warren J. Leonard, and Beatriz León. T Follicular Helper Cell Plasticity Shapes Pathogenic T Helper 2 Cell-Mediated Immunity to Inhaled House Dust Mite. *Immunity*, 44(2):259–273, February 2016.

[29] Daniel DiToro, Colleen J. Winstead, Duy Pham, Steven Witte, Rakieb Andargachew, Jeffrey R. Singer, C. Garrett Wilson, Carlene L. Zindl, Rita J. Luther, Daniel J. Silberger, Benjamin T. Weaver, E. Motunrayo Kolawole, Ryan J. Martinez, Henrietta Turner, Robin D. Hatton, James J. Moon, Sing Sing Way, Brian D. Evavold, and Casey T. Weaver. Differential IL-2 expression defines developmental fates of follicular versus nonfollicular helper T cells. *Science*, 361(6407):eaao2933, September 2018. Publisher: American Association for the Advancement of Science.

[30] Shane Crotty. T Follicular Helper Cell Biology: A Decade of Discovery and Diseases. *Immunity*, 50(5):1132–1148, May 2019.

[31] Robbert Hoogeboom and Pavel Tolar. Molecular Mechanisms of B Cell Antigen Gathering and Endocytosis. In Tomohiro Kurosaki and Jürgen Wienands, editors, *B Cell Receptor Signaling*, Current Topics in Microbiology and Immunology, pages 45–63. Springer International Publishing, Cham, 2016.

[32] Sau K. Lee, Robert J. Rigby, Dimitra Zotos, Louis M. Tsai, Shimpei Kawamoto, Jennifer L. Marshall, Roybel R. Ramiscal, Tyani D. Chan, Dominique Gatto, Robert Brink, Di Yu, Sidonia Fagarasan, David M. Tarlinton, Adam F. Cunningham, and Carola G. Vinuesa. B cell priming for extrafollicular antibody responses requires Bcl-6 expression by T cells. *Journal of Experimental Medicine*, 208(7):1377–1388, June 2011.

[33] Dan Liu, Heping Xu, Changming Shih, Zurong Wan, Xiaopeng Ma, Weiwei Ma, Dan Luo, and Hai Qi. T–B-cell entanglement and ICOSL-driven feed-forward regulation of germinal centre reaction. *Nature*, 517(7533):214–218, January 2015. Number: 7533 Publisher: Nature Publishing Group.

[34] Gabriel D. Victora and Michel C. Nussenzweig. Germinal Centers. *Annual Review of Immunology*, 30(1):429–457, April 2012.

[35] Stephen L. Nutt, Philip D. Hodgkin, David M. Tarlinton, and Lynn M. Corcoran. The generation of antibody-secreting plasma cells. *Nature Reviews Immunology*, 15(3):160–171, March 2015. Number: 3 Publisher: Nature Publishing Group.

[36] Tanja A. Schwickert, Gabriel D. Victora, David R. Fooksman, Alice O. Kamphorst, Monica R. Mugnier, Alexander D. Gitlin, Michael L. Dustin, and Michel C. Nussenzweig. A dynamic T cell–limited checkpoint regulates affinity-dependent B cell entry

into the germinal center. *Journal of Experimental Medicine*, 208(6):1243–1252, May 2011.

[37] M.C. Woodruff, E.H. Kim, W. Luo, and B. Pulendran. B Cell Competition for Restricted T Cell Help Suppresses Rare-Epitope Responses. *Cell Reports*, 25(2):321–327.e3, 2018.

[38] T.-T. Zhang, D.G. Gonzalez, C.M. Cote, S.M. Kerfoot, S. Deng, Y. Cheng, M. Magari, and A.M. Haberman. Germinal center B cell development has distinctly regulated stages completed by disengagement from T cell help. *eLife*, 6, 2017.

[39] Luka Mesin, Jonatan Ersching, and Gabriel D. Victora. Germinal Center B Cell Dynamics. *Immunity*, 45(3):471–482, September 2016.

[40] Nike J. Kräutler, Dan Suan, Danyal Butt, Katherine Bourne, Jana R. Hermes, Tyani D. Chan, Christopher Sundling, Warren Kaplan, Peter Schofield, Jennifer Jackson, Antony Basten, Daniel Christ, and Robert Brink. Differentiation of germinal center B cells into plasma cells is initiated by high-affinity antigen and completed by Tfh cells. *Journal of Experimental Medicine*, 214(5):1259–1267, March 2017.

[41] Yuan Luo, Nihar B. Shah, Jianwei Huang, and Jean Walrand. Parametric Prediction from Parametric Agents. *Operations Research*, 66(2):313–326, April 2018. Publisher: INFORMS.

[42] Christopher D. C. Allen, Takaharu Okada, and Jason G. Cyster. Germinal-Center Organization and Cellular Dynamics. *Immunity*, 27(2):190–202, August 2007.

[43] J. Ersching, A. Efeyan, L. Mesin, J.T. Jacobsen, G. Pasqual, B.C. Grabiner, D. Dominguez-Sola, D.M. Sabatini, and G.D. Victora. Germinal Center Selection and Affinity Maturation Require Dynamic Regulation of mTORC1 Kinase. *Immunity*, 46(6):1045–1058.e6, 2017.

[44] Alexander D. Gitlin, Christian T. Mayer, Thiago Y. Oliveira, Ziv Shulman, Mathew J. K. Jones, Amnon Koren, and Michel C. Nussenzweig. T cell help controls the speed of the cell cycle in germinal center B cells. *Science*, 349(6248):643–646, August 2015. Publisher: American Association for the Advancement of Science.

[45] Gabriel D. Victora, Tanja A. Schwickert, David R. Fooksman, Alice O. Kamphorst, Michael Meyer-Hermann, Michael L. Dustin, and Michel C. Nussenzweig. Germinal Center Dynamics Revealed by Multiphoton Microscopy with a Photoactivatable Fluorescent Reporter. *Cell*, 143(4):592–605, November 2010.

[46] Christian T. Mayer, Anna Gazumyan, Ervin E. Kara, Alexander D. Gitlin, Jovana Golijanin, Charlotte Viant, Joy Pai, Thiago Y. Oliveira, Qiao Wang, Amelia Escolano, Max Medina-Ramirez, Rogier W. Sanders, and Michel C. Nussenzweig. The microanatomic segregation of selection by apoptosis in the germinal center. *Science*, 358(6360):eaao2602, October 2017. Publisher: American Association for the Advancement of Science.

[47] Alexander D. Gitlin, Ziv Shulman, and Michel C. Nussenzweig. Clonal selection in the germinal centre by regulated proliferation and hypermutation. *Nature*, 509(7502):637–640, May 2014. Number: 7502 Publisher: Nature Publishing Group.

[48] Tomohiro Kurosaki, Kohei Kometani, and Wataru Ise. Memory B cells. *Nature Reviews Immunology*, 15(3):149–159, March 2015. Number: 3 Publisher: Nature Publishing Group.

[49] Florian Weisel and Mark Shlomchik. Memory B Cells of Mice and Humans. *Annual Review of Immunology*, 35(1):255–284, 2017. _eprint: https://doi.org/10.1146/annurev-immunol-041015-055531.

[50] Adam F. Cunningham, Adriana Flores-Langarica, Saeeda Bobat, Carmen C. Dominguez Medina, Charlotte N. L. Cook, Ewan A. Ross, Constantino Lopez-Macias, and Ian R. Henderson. B1b Cells Recognize Protective Antigens after Natural Infection and Vaccination. *Frontiers in Immunology*, 5:535, October 2014.

[51] Vanessa Yenson and Nicole Baumgarth. Purification and immune phenotyping of B-1 cells from body cavities of mice. *Methods in Molecular Biology (Clifton, N.J.)*, 1190:17–34, 2014.

[52] John F. Kearney, Preeyam Patel, Emily K. Stefanov, and R. Glenn King. Natural Antibody Repertoires: Development and Functional Role in Inhibiting Allergic Airway Disease. *Annual Review of Immunology*, 33(1):475–504, 2015. _eprint: https://doi.org/10.1146/annurev-immunol-032713-120140.

[53] Mahboobeh Fereidan-Esfahani, Tarek Nayfeh, Arthur Warrington, Charles L. Howe, and Moses Rodriguez. IgM Natural Autoantibodies in Physiology and the Treatment of Disease. In Michael Steinitz, editor, *Human Monoclonal Antibodies: Methods and Protocols*, Methods in Molecular Biology, pages 53–81. Springer, New York, NY, 2019.

[54] Alexander E. Reynolds, Masayuki Kuraoka, and Garnett Kelsoe. Natural IgM Is Produced by CD5- Plasma Cells That Occupy a Distinct Survival Niche in Bone Marrow. *The Journal of Immunology*, 194(1):231–242, January 2015.

[55] Elizabeth C. Rosser and Claudia Mauri. Regulatory B Cells: Origin, Phenotype, and Function. *Immunity*, 42(4):607–612, April 2015.

[56] Susan D. Wolf, Bonnie N. Dittel, Fridrika Hardardottir, and Charles A. Janeway, Jr. Experimental Autoimmune Encephalomyelitis Induction in Genetically B Cell–deficient Mice. *Journal of Experimental Medicine*, 184(6):2271–2278, December 1996.

[57] Simon Fillatreau, Claire H. Sweenie, Mandy J. McGeachy, David Gray, and Stephen M. Anderton. B cells regulate autoimmunity by provision of IL-10. *Nature Immunology*, 3(10):944–950, October 2002.

[58] Atsushi Mizoguchi, Emiko Mizoguchi, Hidetoshi Takedatsu, Richard S Blumberg, and Atul K Bhan. Chronic Intestinal Inflammatory Condition Generates IL-10-Producing Regulatory B Cell Subset Characterized by CD1d Upregulation. *Immunity*, 16(2):219–230, February 2002.

[59] Claudia Mauri, David Gray, Naseem Mushtaq, and Marco Londei. Prevention of Arthritis by Interleukin 10–producing B Cells. *Journal of Experimental Medicine*, 197(4):489–501, February 2003.

[60] Masanori Matsumoto, Akemi Baba, Takafumi Yokota, Hiroyoshi Nishikawa, Yasuyuki Ohkawa, Hisako Kayama, Axel Kallies, Stephen L. Nutt, Shimon Sakaguchi, Kiyoshi Takeda, Tomohiro Kurosaki, and Yoshihiro Baba. Interleukin-10-Producing Plasmablasts Exert Regulatory Function in Autoimmune Inflammation. *Immunity*, 41(6):1040–1051, December 2014.

[61] Ping Shen, Toralf Roch, Vicky Lampropoulou, Richard A. O'Connor, Ulrik Stervbo, Ellen Hilgenberg, Stefanie Ries, Van Duc Dang, Yarúa Jaimes, Capucine Daridon, Rui Li, Luc Jouneau, Pierre Boudinot, Siska Wilantri, Imme Sakwa, Yusei Miyazaki, Melanie D. Leech, Rhoanne C. McPherson, Stefan Wirtz, Markus Neurath, Kai Hoehlig, Edgar Meinl, Andreas Grützkau, Joachim R. Grün, Katharina Horn, Anja A. Kühl, Thomas Dörner, Amit Bar-Or, Stefan H. E. Kaufmann, Stephen M. Anderton, and Simon Fillatreau. IL-35-producing B cells are critical regulators of immunity during autoimmune and infectious diseases. *Nature*, 507(7492):366–370, March 2014. Number: 7492 Publisher: Nature Publishing Group.

[62] Damian Maseda, Susan H. Smith, David J. DiLillo, Jacquelyn M. Bryant, Kathleen M. Candando, Casey T. Weaver, and Thomas F. Tedder. Regulatory B10 Cells Differentiate into Antibody-Secreting Cells After Transient IL-10 Production In Vivo. *The Journal of Immunology*, 188(3):1036–1048, February 2012.

[63] Jamie G. Evans, Karina A. Chavez-Rueda, Ayad Eddaoudi, Almut Meyer-Bahlburg, David J. Rawlings, Michael R. Ehrenstein, and Claudia Mauri. Novel Suppressive Function of Transitional 2 B Cells in Experimental Arthritis1. *The Journal of Immunology*, 178(12):7868–7878, June 2007.

[64] J.K. Hu, J.C. Crampton, A. Cupo, T. Ketas, M.J. van Gils, K. Sliepen, S.W. de Taeye, D. Sok, G. Ozorowski, I. Deresa, R. Stanfield, A.B. Ward, D.R. Burton, P.J. Klasse, R.W. Sanders, J.P. Moore, and S. Crotty. Murine antibody responses to cleaved soluble HIV-1 envelope trimers are highly restricted in specificity. *Journal of Virology*, 89(20):10383–10398, 2015.

[65] M. Pauthner, C. Havenar-Daughton, D. Sok, J.P. Nkolola, R. Bastidas, A.V. Boopathy, D.G. Carnathan, A. Chandrashekar, K.M. Cirelli, C.A. Cottrell, A.M. Eroshkin, J. Guenaga, K. Kaushik, D.W. Kulp, J. Liu, L.E. McCoy, A.L. Oom, G. Ozorowski, K.W. Post, S.K. Sharma, J.M. Steichen, S.W. de Taeye, T. Tokatlian, A. Torrents de la Peña, S.T. Butera, C.C. LaBranche, D.C. Montefiori, G. Silvestri, I.A. Wilson, D.J. Irvine, R.W. Sanders, W.R. Schief, A.B. Ward, R.T. Wyatt, D.H. Barouch, S. Crotty,

and D.R. Burton. Elicitation of Robust Tier 2 Neutralizing Antibody Responses in Nonhuman Primates by HIV Envelope Trimer Immunization Using Optimized Approaches. *Immunity*, 46(6):1073–1088.e6, 2017.

[66] H.H. Tam, M.B. Melo, M. Kang, J.M. Pelet, V.M. Ruda, M.H. Foley, J.K. Hu, S. Kumari, J. Crampton, A.D. Baldeon, R.W. Sanders, J.P. Moore, S. Crotty, R. Langer, D.G. Anderson, A.K. Chakraborty, and D.J. Irvine. Sustained antigen availability during germinal center initiation enhances antibody responses to vaccination. *Proceedings of the National Academy of Sciences of the United States of America*, 113(43):E6639–E6648, 2016.

[67] Robert K. Abbott, Jeong Hyun Lee, Sergey Menis, Patrick Skog, Meghan Rossi, Takayuki Ota, Daniel W. Kulp, Deepika Bhullar, Oleksandr Kalyuzhniy, Colin Havenar-Daughton, William R. Schief, David Nemazee, and Shane Crotty. Precursor Frequency and Affinity Determine B Cell Competitive Fitness in Germinal Centers, Tested with Germline-Targeting HIV Vaccine Immunogens. *Immunity*, 48(1):133–146.e6, January 2018.

[68] Pia Dosenovic, Ervin E. Kara, Anna-Klara Pettersson, Andrew T. McGuire, Matthew Gray, Harald Hartweger, Eddy S. Thientosapol, Leonidas Stamatatos, and Michel C. Nussenzweig. Anti–HIV-1 B cell responses are dependent on B cell precursor frequency and antigen-binding affinity. *Proceedings of the National Academy of Sciences*, 115(18):4743–4748, May 2018. Publisher: Proceedings of the National Academy of Sciences.

[69] Yu Kato, Robert K. Abbott, Brian L. Freeman, Sonya Haupt, Bettina Groschel, Murillo Silva, Sergey Menis, Darrell J. Irvine, William R. Schief, and Shane Crotty. Multifaceted Effects of Antigen Valency on B Cell Response Composition and Differentiation In Vivo. *Immunity*, 53(3):548–563.e8, September 2020.

[70] Masaru Kanekiyo, Chih-Jen Wei, Hadi M. Yassine, Patrick M. McTamney, Jeffrey C. Boyington, James R. R. Whittle, Srinivas S. Rao, Wing-Pui Kong, Lingshu Wang, and Gary J. Nabel. Self-assembling influenza nanoparticle vaccines elicit broadly neutralizing H1N1 antibodies. *Nature*, 499(7456):102–106, July 2013. Number: 7456 Publisher: Nature Publishing Group.

[71] Jessica Marcandalli, Brooke Fiala, Sebastian Ols, Michela Perotti, Willem de van der Schueren, Joost Snijder, Edgar Hodge, Mark Benhaim, Rashmi Ravichandran, Lauren Carter, Will Sheffler, Livia Brunner, Maria Lawrenz, Patrice Dubois, Antonio Lanzavecchia, Federica Sallusto, Kelly K. Lee, David Veesler, Colin E. Correnti, Lance J. Stewart, David Baker, Karin Loré, Laurent Perez, and Neil P. King. Induction of Potent Neutralizing Antibody Responses by a Designed Protein Nanoparticle Vaccine for Respiratory Syncytial Virus. *Cell*, 176(6):1420–1431.e17, March 2019.

[72] Joseph Jardine, Jean-Philippe Julien, Sergey Menis, Takayuki Ota, Oleksandr Kalyuzhniy, Andrew McGuire, Devin Sok, Po-Ssu Huang, Skye MacPherson, Meaghan

Jones, Travis Nieusma, John Mathison, David Baker, Andrew B. Ward, Dennis R. Burton, Leonidas Stamatatos, David Nemazee, Ian A. Wilson, and William R. Schief. Rational HIV Immunogen Design to Target Specific Germline B Cell Receptors. *Science*, 340(6133):711–716, May 2013. Publisher: American Association for the Advancement of Science.

[73] Talar Tokatlian, Benjamin J. Read, Christopher A. Jones, Daniel W. Kulp, Sergey Menis, Jason Y. H. Chang, Jon M. Steichen, Sudha Kumari, Joel D. Allen, Eric L. Dane, Alessia Liguori, Maya Sangesland, Daniel Lingwood, Max Crispin, William R. Schief, and Darrell J. Irvine. Innate immune recognition of glycans targets HIV nanoparticle immunogens to germinal centers. *Science*, 363(6427):649–654, February 2019. Publisher: American Association for the Advancement of Science.

[74] John C. Kraft, Minh N. Pham, Laila Shehata, Mitch Brinkkemper, Seyhan Boyoglu-Barnum, Kaitlin R. Sprouse, Alexandra C. Walls, Suna Cheng, Mike Murphy, Deleah Pettie, Maggie Ahlrichs, Claire Sydeman, Max Johnson, Alyssa Blackstone, Daniel Ellis, Rashmi Ravichandran, Brooke Fiala, Samuel Wrenn, Marcos Miranda, Kwinten Sliepen, Philip J. M. Brouwer, Aleksandar Antanasijevic, David Veesler, Andrew B. Ward, Masaru Kanekiyo, Marion Pepper, Rogier W. Sanders, and Neil P. King. Antigen- and scaffold-specific antibody responses to protein nanoparticle immunogens. *Cell Reports. Medicine*, 3(10):100780, October 2022.

[75] Seyhan Boyoglu-Barnum, Daniel Ellis, Rebecca A. Gillespie, Geoffrey B. Hutchinson, Young-Jun Park, Syed M. Moin, Oliver J. Acton, Rashmi Ravichandran, Mike Murphy, Deleah Pettie, Nick Matheson, Lauren Carter, Adrian Creanga, Michael J. Watson, Sally Kephart, Sila Ataca, John R. Vaile, George Ueda, Michelle C. Crank, Lance Stewart, Kelly K. Lee, Miklos Guttman, David Baker, John R. Mascola, David Veesler, Barney S. Graham, Neil P. King, and Masaru Kanekiyo. Quadrivalent influenza nanoparticle vaccines induce broad protection. *Nature*, 592(7855):623–628, April 2021. Number: 7855 Publisher: Nature Publishing Group.

[76] Kwinten Sliepen, Edith Schermer, Ilja Bontjer, Judith A. Burger, Réka Felfödiné Lévai, Philipp Mundsperger, Philip J. M. Brouwer, Monica Tolazzi, Attila Farsang, Dietmar Katinger, John P. Moore, Gabriella Scarlatti, Robin J. Shattock, Quentin J. Sattentau, and Rogier W. Sanders. Interplay of diverse adjuvants and nanoparticle presentation of native-like HIV-1 envelope trimers. *npj Vaccines*, 6(1):1–8, August 2021. Number: 1 Publisher: Nature Publishing Group.

[77] Darrell J Irvine and Benjamin J Read. Shaping humoral immunity to vaccines through antigen-displaying nanoparticles. *Current Opinion in Immunology*, 65:1–6, August 2020.

[78] Robert K. Abbott and Shane Crotty. Factors in B cell competition and immunodominance. *Immunological Reviews*, 296(1):120–131, 2020. _eprint: https://onlinelibrary.wiley.com/doi/pdf/10.1111/imr.12861.

[79] Aisha V. Sauer, Henner Morbach, Immacolata Brigida, Yen-Shing Ng, Alessandro Aiuti, and Eric Meffre. Defective B cell tolerance in adenosine deaminase deficiency is corrected by gene therapy. *The Journal of Clinical Investigation*, 122(6):2141–2152, June 2012. Publisher: American Society for Clinical Investigation.

[80] Eric Meffre and Hedda Wardemann. B-cell tolerance checkpoints in health and autoimmunity. *Current Opinion in Immunology*, 20(6):632–638, December 2008.

[81] Yen-Shing Ng, Hedda Wardemann, James Chelnis, Charlotte Cunningham-Rundles, and Eric Meffre. Bruton's Tyrosine Kinase Is Essential for Human B Cell Tolerance. *Journal of Experimental Medicine*, 200(7):927–934, October 2004.

[82] Isabelle Isnardi, Yen-Shing Ng, Iva Srdanovic, Roja Motaghedi, Sergei Rudchenko, Horst von Bernuth, Shen-Ying Zhang, Anne Puel, Emmanuelle Jouanguy, Capucine Picard, Ben-Zion Garty, Yildiz Camcioglu, Rainer Doffinger, Dinakantha Kumararatne, Graham Davies, John I. Gallin, Soichi Haraguchi, Noorbibi K. Day, Jean-Laurent Casanova, and Eric Meffre. IRAK-4- and MyD88-Dependent Pathways Are Essential for the Removal of Developing Autoreactive B Cells in Humans. *Immunity*, 29(5):746–757, November 2008.

[83] Laurence Menard, David Saadoun, Isabelle Isnardi, Yen-Shing Ng, Greta Meyers, Christopher Massad, Christina Price, Clara Abraham, Roja Motaghedi, Jane H. Buckner, Peter K. Gregersen, and Eric Meffre. The *PTPN22* allele encoding an R620W variant interferes with the removal of developing autoreactive B cells in humans. *The Journal of Clinical Investigation*, 121(9), August 2011. Publisher: American Society for Clinical Investigation.

[84] Joel Sng, Burcu Ayoglu, Jeff W. Chen, Jean-Nicolas Schickel, Elise M. N. Ferre, Salomé Glauzy, Neil Romberg, Manfred Hoenig, Charlotte Cunningham-Rundles, Paul J. Utz, Michail S. Lionakis, and Eric Meffre. AIRE expression controls the peripheral selection of autoreactive B cells. *Science Immunology*, 4(34):eaav6778, April 2019.

[85] Maxime Hervé, Isabelle Isnardi, Yen-shing Ng, James B. Bussel, Hans D. Ochs, Charlotte Cunningham-Rundles, and Eric Meffre. CD40 ligand and MHC class II expression are essential for human peripheral B cell tolerance. *Journal of Experimental Medicine*, 204(7):1583–1593, June 2007.

[86] Erin Janssen, Henner Morbach, Sumana Ullas, Jason M. Bannock, Christopher Massad, Laurence Menard, Isil Barlan, Gerard Lefranc, Helen Su, Majed Dasouki, Waleed Al-Herz, Sevgi Keles, Talal Chatila, Raif S. Geha, and Eric Meffre. Dedicator of cytokinesis 8-deficient patients have a breakdown in peripheral B-cell tolerance and defective regulatory T cells. *The Journal of Allergy and Clinical Immunology*, 134(6):1365–1374, December 2014.

[87] Maria Carmina Castiello, Marita Bosticardo, Francesca Pala, Marco Catucci, Nicolas Chamberlain, Menno C. van Zelm, Gertjan J. Driessen, Malgorzata Pac, Ewa Bernatowska, Samantha Scaramuzza, Alessandro Aiuti, Aisha V. Sauer, Elisabetta Traggiai,

Eric Meffre, Anna Villa, and Mirjam van der Burg. Wiskott–Aldrich Syndrome protein deficiency perturbs the homeostasis of B-cell compartment in humans. *Journal of Autoimmunity*, 50(100):42–50, May 2014.

[88] Masayuki Kuraoka, Pilar B. Snowden, Takuya Nojima, Laurent Verkoczy, Barton F. Haynes, Daisuke Kitamura, and Garnett Kelsoe. BCR and Endosomal TLR Signals Synergize to Increase AID Expression and Establish Central B Cell Tolerance. *Cell Reports*, 18(7):1627–1635, February 2017.

[89] Corey Tan, Mark Noviski, John Huizar, and Julie Zikherman. Self-reactivity on a spectrum: A sliding scale of peripheral B cell tolerance. *Immunological Reviews*, 292(1):37–60, November 2019.

[90] Julie Zikherman, Ramya Parameswaran, and Arthur Weiss. Endogenous antigen tunes the responsiveness of naive B cells but not T cells. *Nature*, 489(7414):160–164, September 2012. Number: 7414 Publisher: Nature Publishing Group.

[91] Danyal Butt, Tyani D. Chan, Katherine Bourne, Jana R. Hermes, Akira Nguyen, Aaron Statham, Lorraine A. O'Reilly, Andreas Strasser, Susan Price, Peter Schofield, Daniel Christ, Antony Basten, Cindy S. Ma, Stuart G. Tangye, Tri Giang Phan, V. Koneti Rao, and Robert Brink. FAS Inactivation Releases Unconventional Germinal Center B Cells that Escape Antigen Control and Drive IgE and Autoantibody Production. *Immunity*, 42(5):890–902, May 2015.

[92] Tyani D. Chan, Katherine Wood, Jana R. Hermes, Danyal Butt, Christopher J. Jolly, Antony Basten, and Robert Brink. Elimination of Germinal-Center-Derived Self-Reactive B Cells Is Governed by the Location and Concentration of Self-Antigen. *Immunity*, 37(5):893–904, November 2012.

[93] Tuure Kinnunen, Nicolas Chamberlain, Henner Morbach, Jinyoung Choi, Sangtaek Kim, Joseph Craft, Lloyd Mayer, Caterina Cancrini, Laura Passerini, Rosa Bacchetta, Hans D. Ochs, Troy R. Torgerson, and Eric Meffre. Accumulation of peripheral autoreactive B cells in the absence of functional human regulatory T cells. *Blood*, 121(9):1595–1603, February 2013.

[94] Yan Xing and Kristin A. Hogquist. T-Cell Tolerance: Central and Peripheral. *Cold Spring Harbor Perspectives in Biology*, 4(6):a006957, June 2012.

[95] Charles D. Surh and Jonathan Sprent. T-cell apoptosis detected in situ during positive and negative selection in the thymus. *Nature*, 372(6501):100–103, November 1994. Number: 6501 Publisher: Nature Publishing Group.

[96] Gretta L. Stritesky, Yan Xing, Jami R. Erickson, Lokesh A. Kalekar, Xiaodan Wang, Daniel L. Mueller, Stephen C. Jameson, and Kristin A. Hogquist. Murine thymic selection quantified using a unique method to capture deleted T cells. *Proceedings of the National Academy of Sciences*, 110(12):4679–4684, March 2013. Publisher: Proceedings of the National Academy of Sciences.

[97] Stephen R. Daley, Daniel Y. Hu, and Christopher C. Goodnow. Helios marks strongly autoreactive CD4+ T cells in two major waves of thymic deletion distinguished by induction of PD-1 or NF-B. *Journal of Experimental Medicine*, 210(2):269–285, January 2013.

[98] Ludger Klein, Ellen A. Robey, and Chyi-Song Hsieh. Central CD4+ T cell tolerance: deletion versus regulatory T cell differentiation. *Nature Reviews Immunology*, 19(1):7–18, January 2019. Number: 1 Publisher: Nature Publishing Group.

[99] Masashi Yano, Noriyuki Kuroda, Hongwei Han, Makiko Meguro-Horike, Yumiko Nishikawa, Hiroshi Kiyonari, Kentaro Maemura, Yuchio Yanagawa, Kunihiko Obata, Satoru Takahashi, Tomokatsu Ikawa, Rumi Satoh, Hiroshi Kawamoto, Yasuhiro Mouri, and Mitsuru Matsumoto. Aire controls the differentiation program of thymic epithelial cells in the medulla for the establishment of self-tolerance. *The Journal of Experimental Medicine*, 205(12):2827–2838, November 2008.

[100] Jason DeVoss, Yafei Hou, Kellsey Johannes, Wen Lu, Gregory I. Liou, John Rinn, Howard Chang, Rachel R. Caspi, Lawrence Fong, and Mark S. Anderson. Spontaneous autoimmunity prevented by thymic expression of a single self-antigen. *Journal of Experimental Medicine*, 203(12):2727–2735, November 2006.

[101] Mark S. Anderson, Emily S. Venanzi, Zhibin Chen, Stuart P. Berzins, Christophe Benoist, and Diane Mathis. The Cellular Mechanism of Aire Control of T Cell Tolerance. *Immunity*, 23(2):227–239, August 2005.

[102] Sven Malchow, Daniel S. Leventhal, Victoria Lee, Saki Nishi, Nicholas D. Socci, and Peter A. Savage. Aire Enforces Immune Tolerance by Directing Autoreactive T Cells into the Regulatory T Cell Lineage. *Immunity*, 44(5):1102–1113, May 2016.

[103] Justin S. A. Perry, Chan-Wang J. Lio, Andrew L. Kau, Katherine Nutsch, Zhuo Yang, Jeffrey I. Gordon, Kenneth M. Murphy, and Chyi-Song Hsieh. Distinct Contributions of Aire and Antigen-Presenting-Cell Subsets to the Generation of Self-Tolerance in the Thymus. *Immunity*, 41(3):414–426, September 2014.

[104] Sanjeev Mariathasan, Arsen Zakarian, Denis Bouchard, Alison M. Michie, Juan Carlos Zúñiga-Pflücker, and Pamela S. Ohashi. Duration and Strength of Extracellular Signal-Regulated Kinase Signals Are Altered During Positive Versus Negative Thymocyte Selection1. *The Journal of Immunology*, 167(9):4966–4973, November 2001.

[105] Mark A. Daniels, Emma Teixeiro, Jason Gill, Barbara Hausmann, Dominique Roubaty, Kaisa Holmberg, Guy Werlen, Georg A. Holländer, Nicholas R. J. Gascoigne, and Ed Palmer. Thymic selection threshold defined by compartmentalization of Ras/MAPK signalling. *Nature*, 444(7120):724–729, December 2006. Number: 7120 Publisher: Nature Publishing Group.

[106] Byron B. Au-Yeung, Heather J. Melichar, Jenny O. Ross, Debra A. Cheng, Julie Zikherman, Kevan M. Shokat, Ellen A. Robey, and Arthur Weiss. Quantitative and temporal requirements revealed for Zap70 catalytic activity during T cell development.

Nature Immunology, 15(7):687–694, July 2014. Number: 7 Publisher: Nature Publishing Group.

[107] Peter J. R. Ebert, Lauren I. Richie Ehrlich, and Mark M. Davis. Low Ligand Requirement for Deletion and Lack of Synapses in Positive Selection Enforce the Gauntlet of Thymic T Cell Maturation. *Immunity*, 29(5):734–745, November 2008.

[108] Daniel A. Peterson, Richard J. DiPaolo, Osami Kanagawa, and Emil R. Unanue. Cutting Edge: Negative Selection of Immature Thymocytes by a Few Peptide-MHC Complexes: Differential Sensitivity of Immature and Mature T Cells1. *The Journal of Immunology*, 162(6):3117–3120, March 1999.

[109] Jason D. Fontenot, James L. Dooley, Andrew G. Farr, and Alexander Y. Rudensky. Developmental regulation of Foxp3 expression during ontogeny. *Journal of Experimental Medicine*, 202(7):901–906, October 2005.

[110] Sahamoddin Khailaie, Philippe A. Robert, Aras Toker, Jochen Huehn, and Michael Meyer-Hermann. A Signal Integration Model of Thymic Selection and Natural Regulatory T Cell Commitment. *The Journal of Immunology*, 193(12):5983–5996, December 2014.

[111] Mohamed A. ElTanbouly and Randolph J. Noelle. Rethinking peripheral T cell tolerance: checkpoints across a T cell's journey. *Nature Reviews. Immunology*, 21(4):257–267, April 2021.

[112] D. R. DeSilva, W. S. Feeser, E. J. Tancula, and P. A. Scherle. Anergic T cells are defective in both jun NH2-terminal kinase and mitogen-activated protein kinase signaling pathways. *The Journal of Experimental Medicine*, 183(5):2017–2023, May 1996.

[113] P. E. Fields, T. F. Gajewski, and F. W. Fitch. Blocked Ras activation in anergic CD4+ T cells. *Science (New York, N.Y.)*, 271(5253):1276–1278, March 1996.

[114] W. Li, C. D. Whaley, A. Mondino, and D. L. Mueller. Blocked signal transduction to the ERK and JNK protein kinases in anergic CD4+ T cells. *Science (New York, N.Y.)*, 271(5253):1272–1276, March 1996.

[115] Yuanyuan Zha, Reinhard Marks, Allen W. Ho, Amy C. Peterson, Sujit Janardhan, Ian Brown, Kesavannair Praveen, Stacey Stang, James C. Stone, and Thomas F. Gajewski. T cell anergy is reversed by active Ras and is regulated by diacylglycerol kinase-alpha. *Nature Immunology*, 7(11):1166–1173, November 2006.

[116] B. Rocha, A. Grandien, and A. A. Freitas. Anergy and exhaustion are independent mechanisms of peripheral T cell tolerance. *The Journal of Experimental Medicine*, 181(3):993–1003, March 1995.

[117] B. Rocha, C. Tanchot, and H. Von Boehmer. Clonal anergy blocks in vivo growth of mature T cells and can be reversed in the absence of antigen. *The Journal of Experimental Medicine*, 177(5):1517–1521, May 1993.

[118] K. A. Pape, R. Merica, A. Mondino, A. Khoruts, and M. K. Jenkins. Direct evidence that functionally impaired CD4+ T cells persist in vivo following induction of peripheral tolerance. *Journal of Immunology (Baltimore, Md.: 1950)*, 160(10):4719–4729, May 1998.

[119] Lokesh A. Kalekar, Shirdi E. Schmiel, Sarada L. Nandiwada, Wing Y. Lam, Laura O. Barsness, Na Zhang, Gretta L. Stritesky, Deepali Malhotra, Kristen E. Pauken, Jonathan L. Linehan, M. Gerard O'Sullivan, Brian T. Fife, Kristin A. Hogquist, Marc K. Jenkins, and Daniel L. Mueller. CD4(+) T cell anergy prevents autoimmunity and generates regulatory T cell precursors. *Nature Immunology*, 17(3):304–314, March 2016.

[120] Jason B. Williams, Brendan L. Horton, Yan Zheng, Yukan Duan, Jonathan D. Powell, and Thomas F. Gajewski. The EGR2 targets LAG-3 and 4-1BB describe and regulate dysfunctional antigen-specific CD8+ T cells in the tumor microenvironment. *The Journal of Experimental Medicine*, 214(2):381–400, February 2017.

[121] E. John Wherry. T cell exhaustion. *Nature Immunology*, 12(6):492–499, June 2011. Number: 6 Publisher: Nature Publishing Group.

[122] E. John Wherry, Daniel L. Barber, Susan M. Kaech, Joseph N. Blattman, and Rafi Ahmed. Antigen-independent memory CD8 T cells do not develop during chronic viral infection. *Proceedings of the National Academy of Sciences of the United States of America*, 101(45):16004–16009, November 2004.

[123] Michael J. Fuller, David A. Hildeman, Steffanie Sabbaj, Dalia E. Gaddis, Anne E. Tebo, Liang Shang, Paul A. Goepfert, and Allan J. Zajac. Cutting edge: emergence of CD127high functionally competent memory T cells is compromised by high viral loads and inadequate T cell help. *Journal of Immunology (Baltimore, Md.: 1950)*, 174(10):5926–5930, May 2005.

[124] Omar Khan, Josephine R. Giles, Sierra McDonald, Sasikanth Manne, Shin Foong Ngiow, Kunal P. Patel, Michael T. Werner, Alexander C. Huang, Katherine A. Alexander, Jennifer E. Wu, John Attanasio, Patrick Yan, Sangeeth M. George, Bertram Bengsch, Ryan P. Staupe, Greg Donahue, Wei Xu, Ravi K. Amaravadi, Xiaowei Xu, Giorgos C. Karakousis, Tara C. Mitchell, Lynn M. Schuchter, Jonathan Kaye, Shelley L. Berger, and E. John Wherry. TOX transcriptionally and epigenetically programs CD8+ T cell exhaustion. *Nature*, 571(7764):211–218, July 2019. Number: 7764 Publisher: Nature Publishing Group.

[125] Francesca Alfei, Kristiyan Kanev, Maike Hofmann, Ming Wu, Hazem E. Ghoneim, Patrick Roelli, Daniel T. Utzschneider, Madlaina von Hoesslin, Jolie G. Cullen, Yiping Fan, Vasyl Eisenberg, Dirk Wohlleber, Katja Steiger, Doron Merkler, Mauro Delorenzi, Percy A. Knolle, Cyrille J. Cohen, Robert Thimme, Benjamin Youngblood, and Dietmar Zehn. TOX reinforces the phenotype and longevity of exhausted T cells in chronic viral infection. *Nature*, 571(7764):265–269, July 2019.

[126] C. Kurts, H. Kosaka, F. R. Carbone, J. F. Miller, and W. R. Heath. Class I-restricted cross-presentation of exogenous self-antigens leads to deletion of autoreactive CD8(+) T cells. *The Journal of Experimental Medicine*, 186(2):239–245, July 1997.

[127] D. Kyburz, P. Aichele, D. E. Speiser, H. Hengartner, R. M. Zinkernagel, and H. Pircher. T cell immunity after a viral infection versus T cell tolerance induced by soluble viral peptides. *European Journal of Immunology*, 23(8):1956–1962, August 1993.

[128] R. S. Liblau, R. Tisch, K. Shokat, X. Yang, N. Dumont, C. C. Goodnow, and H. O. McDevitt. Intravenous injection of soluble antigen induces thymic and peripheral T-cells apoptosis. *Proceedings of the National Academy of Sciences of the United States of America*, 93(7):3031–3036, April 1996.

[129] David A. Hildeman, Yanan Zhu, Thomas C. Mitchell, John Kappler, and Philippa Marrack. Molecular mechanisms of activated T cell death in vivo. *Current Opinion in Immunology*, 14(3):354–359, June 2002.

[130] Gayle M. Davey, Christian Kurts, Jacques F. A. P. Miller, Philippe Bouillet, Andreas Strasser, Andrew G. Brooks, Francis R. Carbone, and William R. Heath. Peripheral deletion of autoreactive CD8 T cells by cross presentation of self-antigen occurs by a Bcl-2-inhibitable pathway mediated by Bim. *The Journal of Experimental Medicine*, 196(7):947–955, October 2002.

[131] Ethan M. Shevach. Mechanisms of foxp3+ T regulatory cell-mediated suppression. *Immunity*, 30(5):636–645, May 2009.

[132] Ethan M. Shevach and Angela M. Thornton. tTregs, pTregs, and iTregs: similarities and differences. *Immunological Reviews*, 259(1):88–102, 2014. _eprint: https://onlinelibrary.wiley.com/doi/pdf/10.1111/imr.12160.

[133] Lauren W. Collison, Creg J. Workman, Timothy T. Kuo, Kelli Boyd, Yao Wang, Kate M. Vignali, Richard Cross, David Sehy, Richard S. Blumberg, and Dario A. A. Vignali. The inhibitory cytokine IL-35 contributes to regulatory T-cell function. *Nature*, 450(7169):566–569, November 2007. Number: 7169 Publisher: Nature Publishing Group.

[134] Craig L. Maynard, Laurie E. Harrington, Karen M. Janowski, James R. Oliver, Carlene L. Zindl, Alexander Y. Rudensky, and Casey T. Weaver. Regulatory T cells expressing interleukin 10 develop from Foxp3+ and Foxp3- precursor cells in the absence of interleukin 10. *Nature Immunology*, 8(9):931–941, September 2007. Number: 9 Publisher: Nature Publishing Group.

[135] Pushpa Pandiyan, Lixin Zheng, Satoru Ishihara, Jennifer Reed, and Michael J. Lenardo. CD4+CD25+Foxp3+ regulatory T cells induce cytokine deprivation–mediated apoptosis of effector CD4+ T cells. *Nature Immunology*, 8(12):1353–1362, December 2007. Number: 12 Publisher: Nature Publishing Group.

[136] Silvia Deaglio, Karen M. Dwyer, Wenda Gao, David Friedman, Anny Usheva, Anna Erat, Jiang-Fan Chen, Keiichii Enjyoji, Joel Linden, Mohamed Oukka, Vijay K. Kuchroo, Terry B. Strom, and Simon C. Robson. Adenosine generation catalyzed by CD39 and CD73 expressed on regulatory T cells mediates immune suppression. *Journal of Experimental Medicine*, 204(6):1257–1265, May 2007.

[137] David C. Gondek, Li-Fan Lu, Sergio A. Quezada, Shimon Sakaguchi, and Randolph J. Noelle. Cutting Edge: Contact-Mediated Suppression by CD4+CD25+ Regulatory Cells Involves a Granzyme B-Dependent, Perforin-Independent Mechanism1. *The Journal of Immunology*, 174(4):1783–1786, February 2005.

[138] Dong-Mei Zhao, Angela M. Thornton, Richard J. DiPaolo, and Ethan M. Shevach. Activated CD4+CD25+ T cells selectively kill B lymphocytes. *Blood*, 107(10):3925–3932, May 2006.

[139] Hyung W. Lim, Peter Hillsamer, Allison H. Banham, and Chang H. Kim. Cutting Edge: Direct Suppression of B Cells by CD4+CD25+ Regulatory T Cells1. *The Journal of Immunology*, 175(7):4180–4183, October 2005.

[140] Mary E. Morgan, Roger P. M. Sutmuller, Hendrik J. Witteveen, Leonie M. van Duivenvoorde, Eric Zanelli, Cornelis J. M. Melief, Alies Snijders, Rienk Offringa, René R. P. de Vries, and René E. M. Toes. CD25+ cell depletion hastens the onset of severe disease in collagen-induced arthritis. *Arthritis & Rheumatism*, 48(5):1452–1460, 2003. _eprint: https://onlinelibrary.wiley.com/doi/pdf/10.1002/art.11063.

[141] Su-jean Seo, Michele L Fields, Jodi L Buckler, Amy J Reed, Laura Mandik-Nayak, Simone A Nish, Randolph J Noelle, Laurence A Turka, Fred D Finkelman, Andrew J Caton, and Jan Erikson. The Impact of T Helper and T Regulatory Cells on the Regulation of Anti-Double-Stranded DNA B Cells. *Immunity*, 16(4):535–546, April 2002.

[142] Frank Fenner, Donald A. Henderson, Isao Arita, Zdenek Jezek, Ivan Danilovich Ladnyi, and World Health Organization. Smallpox and its eradication. Technical report, World Health Organization, 1988. ISBN: 9789241561105 number-of-pages: 1460.

[143] Sandra W. Roush, Trudy V. Murphy, and Vaccine-Preventable Disease Table Working Group. Historical comparisons of morbidity and mortality for vaccine-preventable diseases in the United States. *JAMA*, 298(18):2155–2163, November 2007.

[144] Center for Biologics Evaluation and FDA. Vaccines Licensed for Use in the United States. *FDA*, October 2022. Publisher: FDA.

[145] Stanley A. Plotkin. Correlates of Protection Induced by Vaccination. *Clinical and Vaccine Immunology : CVI*, 17(7):1055–1065, July 2010.

[146] Anna-Karin E. Palm and Carole Henry. Remembrance of Things Past: Long-Term B Cell Memory After Infection and Vaccination. *Frontiers in Immunology*, 10, 2019.

[147] Sarah C. Gilbert. T-cell-inducing vaccines – what's the future. *Immunology*, 135(1):19–26, 2012. _eprint: https://onlinelibrary.wiley.com/doi/pdf/10.1111/j.1365-2567.2011.03517.x.

[148] William D. Phillips and Angela Vincent. Pathogenesis of myasthenia gravis: update on disease types, models, and mechanisms. *F1000Research*, 5:F1000 Faculty Rev–1513, June 2016.

[149] Edgar Carnero Contentti and Jorge Correale. Neuromyelitis optica spectrum disorders: from pathophysiology to therapeutic strategies. *Journal of Neuroinflammation*, 18(1):208, September 2021.

[150] Jinyoung Choi, Sang Taek Kim, and Joe Craft. The Pathogenesis of Systemic Lupus Erythematosus – An Update. *Current opinion in immunology*, 24(6):651–657, December 2012.

[151] Mia J. Smith, Kimber M. Simmons, and John C. Cambier. B cells in type 1 diabetes mellitus and diabetic kidney disease. *Nature reviews. Nephrology*, 13(11):712–720, October 2017.

[152] Andrea Matucci, Francesca Nencini, Emanuele Vivarelli, Susanna Bormioli, Enrico Maggi, and Alessandra Vultaggio. Immunogenicity-unwanted immune responses to biological drugs – can we predict them? *Expert Review of Clinical Pharmacology*, 14(1):47–53, January 2021. Publisher: Taylor & Francis _eprint: https://doi.org/10.1080/17512433.2020.1772053.

[153] Walter A. Orenstein and Rafi Ahmed. Simply put: Vaccination saves lives. *Proceedings of the National Academy of Sciences*, 114(16):4031–4033, April 2017. Publisher: Proceedings of the National Academy of Sciences.

[154] S. J. Olshansky, L. Hayflick, S. J. Olshansky, and L. Hayflick. The Role of the WI-38 Cell Strain in Saving Lives and Reducing Morbidity. *AIMS Public Health*, 4(2):127–138, 2017. Cc_license_type: cc_by Primary_atype: AIMS Public Health Subject_term: Perspective Subject_term_id: Perspective.

[155] Rebecca J. Loomis and Philip R. Johnson. Emerging Vaccine Technologies. *Vaccines*, 3(2):429–447, May 2015.

[156] Natalie J. Carter and Monique P. Curran. Live Attenuated Influenza Vaccine (FluMist®; Fluenz™). *Drugs*, 71(12):1591–1622, August 2011.

[157] Albert B. Sabin. PROPERTIES AND BEHAVIOR OF ORALLY ADMINISTERED ATTENUATED POLIOVIRUS VACCINE. *Journal of the American Medical Association*, 164(11):1216–1223, July 1957.

[158] David Baxter. Active and passive immunity, vaccine types, excipients and licensing. *Occupational Medicine*, 57(8):552–556, December 2007.

[159] Abhishek Vartak and Steven J. Sucheck. Recent Advances in Subunit Vaccine Carriers. *Vaccines*, 4(2):12, April 2016.

[160] Andrew D. Murdin, Luis Barreto, and Stanley Plotkin. Inactivated poliovirus vaccine: past and present experience. *Vaccine*, 14(8):735–746, June 1996.

[161] Ralf Clemens, Assad Safary, Anne Hepburn, Ceara Roche, William J. Stanbury, and Francis E. André. Clinical Experience With An Inactivated Hepatitis A Vaccine. *The Journal of Infectious Diseases*, 171(Supplement_1):S44–S49, March 1995.

[162] Dong-Kun Yang, Ha-Hyun Kim, Kyung-Woo Lee, and Jae-Young Song. The present and future of rabies vaccine in animals. *Clinical and Experimental Vaccine Research*, 2(1):19–25, January 2013. Publisher: The Korean Vaccine Society.

[163] K. L. Seib, X. Zhao, and R. Rappuoli. Developing vaccines in the era of genomics: a decade of reverse vaccinology. *Clinical Microbiology and Infection*, 18:109–116, October 2012. Publisher: Elsevier.

[164] Rino Rappuoli. Reverse vaccinology. *Current Opinion in Microbiology*, 3(5):445–450, October 2000.

[165] Binbin Chen, Michael S. Khodadoust, Niclas Olsson, Lisa E. Wagar, Ethan Fast, Chih Long Liu, Yagmur Muftuoglu, Brian J. Sworder, Maximilian Diehn, Ronald Levy, Mark M. Davis, Joshua E. Elias, Russ B. Altman, and Ash A. Alizadeh. Predicting HLA class II antigen presentation through integrated deep learning. *Nature Biotechnology*, 37(11):1332–1343, November 2019. Publisher: Nature Publishing Group.

[166] Brett N. Bowman, Paul R. McAdam, Sandro Vivona, Jin X. Zhang, Tiffany Luong, Richard K. Belew, Harpal Sahota, Donald Guiney, Faramarz Valafar, Joshua Fierer, and Christopher H. Woelk. Improving reverse vaccinology with a machine learning approach. *Vaccine*, 29(45):8156–8164, October 2011.

[167] Zikun Yang, Paul Bogdan, and Shahin Nazarian. An in silico deep learning approach to multi-epitope vaccine design: a SARS-CoV-2 case study. *Scientific Reports*, 11(1):3238, February 2021. Number: 1 Publisher: Nature Publishing Group.

[168] Fernando Aleman, Netanel Tzarum, Leopold Kong, Kenna Nagy, Jiang Zhu, Ian A. Wilson, and Mansun Law. Immunogenetic and structural analysis of a class of HCV broadly neutralizing antibodies and their precursors. *Proceedings of the National Academy of Sciences*, 115(29):7569–7574, July 2018. Publisher: Proceedings of the National Academy of Sciences.

[169] Maxwell T. Finkelstein, Adam G. Mermelstein, Emma Parker Miller, Paul C. Seth, Erik-Stephane D. Stancofski, and Daniela Fera. Structural Analysis of Neutralizing Epitopes of the SARS-CoV-2 Spike to Guide Therapy and Vaccine Design Strategies. *Viruses*, 13(1):134, January 2021.

[170] Fazren Azmi, Abdullah Al Hadi Ahmad Fuaad, Mariusz Skwarczynski, and Istvan Toth. Recent progress in adjuvant discovery for peptide-based subunit vaccines. *Human Vaccines & Immunotherapeutics*, 10(3):778–796, March 2014. Publisher: Taylor & Francis _eprint: https://doi.org/10.4161/hv.27332.

[171] Sarah Schillie. Recommendations of the Advisory Committee on Immunization Practices for Use of a Hepatitis B Vaccine with a Novel Adjuvant. *MMWR. Morbidity and Mortality Weekly Report*, 67, 2018.

[172] Vladimir P. Torchilin. Recent advances with liposomes as pharmaceutical carriers. *Nature Reviews Drug Discovery*, 4(2):145–160, February 2005. Number: 2 Publisher: Nature Publishing Group.

[173] Malou Henriksen-Lacey, Andrew Devitt, and Yvonne Perrie. The vesicle size of DDA:TDB liposomal adjuvants plays a role in the cell-mediated immune response but has no significant effect on antibody production. *Journal of Controlled Release: Official Journal of the Controlled Release Society*, 154(2):131–137, September 2011.

[174] Randip Kaur, Vincent W Bramwell, Daniel J Kirby, and Yvonne Perrie. Manipulation of the surface pegylation in combination with reduced vesicle size of cationic liposomal adjuvants modifies their clearance kinetics from the injection site, and the rate and type of T cell response. *Journal of controlled release*, 164(3):331–337, December 2012.

[175] Preety Sahdev, Lukasz J. Ochyl, and James J. Moon. Biomaterials for Nanoparticle Vaccine Delivery Systems. *Pharmaceutical Research*, 31(10):2563–2582, October 2014.

[176] Takashi Nakamura, Daiki Yamazaki, Jun Yamauchi, and Hideyoshi Harashima. The nanoparticulation by octaarginine-modified liposome improves α-galactosylceramide-mediated antitumor therapy via systemic administration. *Journal of Controlled Release: Official Journal of the Controlled Release Society*, 171(2):216–224, October 2013.

[177] Ali Badiee, Ali Khamesipour, Afshin Samiei, Dina Soroush, Vahid Heravi Shargh, Masoumeh Tavassoti Kheiri, Farzaneh Barkhordari, W. Robert Mc Master, Fereidoun Mahboudi, and Mahmoud R. Jaafari. The role of liposome size on the type of immune response induced in BALB/c mice against leishmaniasis: rgp63 as a model antigen. *Experimental Parasitology*, 132(4):403–409, December 2012.

[178] Takashi Nakamura, Rumiko Moriguchi, Kentaro Kogure, Nilabh Shastri, and Hideyoshi Harashima. Efficient MHC class I presentation by controlled intracellular trafficking of antigens in octaarginine-modified liposomes. *Molecular Therapy: The Journal of the American Society of Gene Therapy*, 16(8):1507–1514, August 2008.

[179] Douglas S. Watson, Aaron N. Endsley, and Leaf Huang. Design considerations for liposomal vaccines: influence of formulation parameters on antibody and cell-mediated immune responses to liposome associated antigens. *Vaccine*, 30(13):2256–2272, March 2012.

[180] Theresa M. Allen, Davis R. Mumbengegwi, and Gregory J. R. Charrois. Anti-CD19-targeted liposomal doxorubicin improves the therapeutic efficacy in murine B-cell lymphoma and ameliorates the toxicity of liposomes with varying drug release rates. *Clinical Cancer Research: An Official Journal of the American Association for Cancer Research*, 11(9):3567–3573, May 2005.

[181] Rumiana Tenchov, Robert Bird, Allison E. Curtze, and Qiongqiong Zhou. Lipid NanoparticlesFrom Liposomes to mRNA Vaccine Delivery, a Landscape of Research Diversity and Advancement. *ACS Nano*, 15(11):16982–17015, November 2021.

[182] Xingfang Su, Jennifer Fricke, Daniel G. Kavanagh, and Darrell J. Irvine. In vitro and in vivo mRNA delivery using lipid-enveloped pH-responsive polymer nanoparticles. *Molecular Pharmaceutics*, 8(3):774–787, June 2011.

[183] Lindsey R. Baden, Hana M. El Sahly, Brandon Essink, Karen Kotloff, Sharon Frey, Rick Novak, David Diemert, Stephen A. Spector, Nadine Rouphael, C. Buddy Creech, John McGettigan, Shishir Khetan, Nathan Segall, Joel Solis, Adam Brosz, Carlos Fierro, Howard Schwartz, Kathleen Neuzil, Lawrence Corey, Peter Gilbert, Holly Janes, Dean Follmann, Mary Marovich, John Mascola, Laura Polakowski, Julie Ledgerwood, Barney S. Graham, Hamilton Bennett, Rolando Pajon, Conor Knightly, Brett Leav, Weiping Deng, Honghong Zhou, Shu Han, Melanie Ivarsson, Jacqueline Miller, and Tal Zaks. Efficacy and Safety of the mRNA-1273 SARS-CoV-2 Vaccine. *New England Journal of Medicine*, 384(5):403–416, February 2021. Publisher: Massachusetts Medical Society _eprint: https://doi.org/10.1056/NEJMoa2035389.

[184] Fernando P. Polack, Stephen J. Thomas, Nicholas Kitchin, Judith Absalon, Alejandra Gurtman, Stephen Lockhart, John L. Perez, Gonzalo Pérez Marc, Edson D. Moreira, Cristiano Zerbini, Ruth Bailey, Kena A. Swanson, Satrajit Roychoudhury, Kenneth Koury, Ping Li, Warren V. Kalina, David Cooper, Robert W. Frenck, Laura L. Hammitt, Özlem Türeci, Haylene Nell, Axel Schaefer, Serhat Ünal, Dina B. Tresnan, Susan Mather, Philip R. Dormitzer, Uğur Şahin, Kathrin U. Jansen, and William C. Gruber. Safety and Efficacy of the BNT162b2 mRNA Covid-19 Vaccine. *New England Journal of Medicine*, 383(27):2603–2615, December 2020. Publisher: Massachusetts Medical Society _eprint: https://doi.org/10.1056/NEJMoa2034577.

[185] Nicole Doria-Rose, Mehul S. Suthar, Mat Makowski, Sarah O'Connell, Adrian B. McDermott, Britta Flach, Julie E. Ledgerwood, John R. Mascola, Barney S. Graham, Bob C. Lin, Sijy O'Dell, Stephen D. Schmidt, Alicia T. Widge, Venkata-Viswanadh Edara, Evan J. Anderson, Lilin Lai, Katharine Floyd, Nadine G. Rouphael, Veronika Zarnitsyna, Paul C. Roberts, Mamodikoe Makhene, Wendy Buchanan, Catherine J. Luke, John H. Beigel, Lisa A. Jackson, Kathleen M. Neuzil, Hamilton Bennett, Brett Leav, Jim Albert, Pratap Kunwar, and mRNA-1273 Study Group. Antibody Persistence through 6 Months after the Second Dose of mRNA-1273 Vaccine for Covid-19. *The New England Journal of Medicine*, 384(23):2259–2261, June 2021.

[186] Amarendra Pegu, Sarah E. O'Connell, Stephen D. Schmidt, Sijy O'Dell, Chloe A. Talana, Lilin Lai, Jim Albert, Evan Anderson, Hamilton Bennett, Kizzmekia S. Corbett,

Britta Flach, Lisa Jackson, Brett Leav, Julie E. Ledgerwood, Catherine J. Luke, Mat Makowski, Martha C. Nason, Paul C. Roberts, Mario Roederer, Paulina A. Rebolledo, Christina A. Rostad, Nadine G. Rouphael, Wei Shi, Lingshu Wang, Alicia T. Widge, Eun Sung Yang, The mRNA-1273 Study Group, John H. Beigel, Barney S. Graham, John R. Mascola, Mehul S. Suthar, Adrian B. McDermott, and Nicole A. Doria-Rose. Durability of mRNA-1273 vaccine–induced antibodies against SARS-CoV-2 variants. *Science*, 373(6561):1372–1377, September 2021. Publisher: American Association for the Advancement of Science.

[187] Mohamad-Gabriel Alameh, István Tombácz, Emily Bettini, Katlyn Lederer, Sonia Ndeupen, Chutamath Sittplangkoon, Joel R. Wilmore, Brian T. Gaudette, Ousamah Y. Soliman, Matthew Pine, Philip Hicks, Tomaz B. Manzoni, James J. Knox, John L. Johnson, Dorottya Laczkó, Hiromi Muramatsu, Benjamin Davis, Wenzhao Meng, Aaron M. Rosenfeld, Shirin Strohmeier, Paulo J.C. Lin, Barbara L. Mui, Ying K. Tam, Katalin Karikó, Alain Jacquet, Florian Krammer, Paul Bates, Michael P. Cancro, Drew Weissman, Eline T. Luning Prak, David Allman, Botond Z. Igyártó, Michela Locci, and Norbert Pardi. Lipid nanoparticles enhance the efficacy of mRNA and protein subunit vaccines by inducing robust T follicular helper cell and humoral responses. *Immunity*, 54(12):2877–2892.e7, December 2021.

[188] Siddhartha Jain, Derek T. O'Hagan, and Manmohan Singh. The long-term potential of biodegradable poly(lactide-co-glycolide) microparticles as the next-generation vaccine adjuvant. *Expert Review of Vaccines*, 10(12):1731–1742, December 2011.

[189] Jayanth Panyam and Vinod Labhasetwar. Biodegradable nanoparticles for drug and gene delivery to cells and tissue. *Advanced Drug Delivery Reviews*, 55(3):329–347, February 2003.

[190] James J. Moon, Heikyung Suh, Mark E. Polhemus, Christian F. Ockenhouse, Anjali Yadava, and Darrell J. Irvine. Antigen-displaying lipid-enveloped PLGA nanoparticles as delivery agents for a Plasmodium vivax malaria vaccine. *PloS One*, 7(2):e31472, 2012.

[191] Dilip Pawar, Sharad Mangal, Roshan Goswami, and K. S. Jaganathan. Development and characterization of surface modified PLGA nanoparticles for nasal vaccine delivery: effect of mucoadhesive coating on antigen uptake and immune adjuvant activity. *European Journal of Pharmaceutics and Biopharmaceutics: Official Journal of Arbeitsgemeinschaft Fur Pharmazeutische Verfahrenstechnik e.V*, 85(3 Pt A):550–559, November 2013.

[192] Qing Zhu, James Talton, Guofeng Zhang, Tshaka Cunningham, Zijian Wang, Robert C. Waters, James Kirk, Bärbel Eppler, Klinman Dennis M, Yongjun Sui, Susan Gagnon, Igor M. Belyakov, Russell J. Mumper, and Jay A. Berzofsky. Large intestine-targeted nanoparticle-releasing oral vaccine to control genitorectal viral infection. *Nature medicine*, 18(8):1291–1296, August 2012.

[193] Omar A. Ali, Nathaniel Huebsch, Lan Cao, Glenn Dranoff, and David J. Mooney. Infection-mimicking materials to program dendritic cells in situ. *Nature Materials*, 8(2):151–158, February 2009.

[194] Marie-Luce De Temmerman, Joanna Rejman, Roosmarijn E. Vandenbroucke, Stefaan De Koker, Claude Libert, Johan Grooten, Jo Demeester, Bruno Gander, and Stefaan C. De Smedt. Polyelectrolyte LbL microcapsules versus PLGA microparticles for immunization with a protein antigen. *Journal of Controlled Release: Official Journal of the Controlled Release Society*, 158(2):233–239, March 2012.

[195] Stacey L. Demento, Weiguo Cui, Jason M. Criscione, Eric Stern, Jacob Tulipan, Susan M. Kaech, and Tarek M. Fahmy. Role of sustained antigen release from nanoparticle vaccines in shaping the T cell memory phenotype. *Biomaterials*, 33(19):4957–4964, June 2012.

[196] P. Johansen, F. Estevez, R. Zurbriggen, H. P. Merkle, R. Glück, G. Corradin, and B. Gander. Towards clinical testing of a single-administration tetanus vaccine based on PLA/PLGA microspheres. *Vaccine*, 19(9-10):1047–1054, December 2000.

[197] P. Johansen, L. Moon, H. Tamber, H. P. Merkle, B. Gander, and D. Sesardic. Immunogenicity of single-dose diphtheria vaccines based on PLA/PLGA microspheres in guinea pigs. *Vaccine*, 18(3-4):209–215, September 1999.

[198] Federica Sarti, Glen Perera, Fabian Hintzen, Katerina Kotti, Vassilis Karageorgiou, Olga Kammona, Costas Kiparissides, and Andreas Bernkop-Schnürch. In vivo evidence of oral vaccination with PLGA nanoparticles containing the immunostimulant monophosphoryl lipid A. *Biomaterials*, 32(16):4052–4057, June 2011.

[199] Frank Wegmann, Kate H. Gartlan, Ali M. Harandi, Sarah A. Brinckmann, Margherita Coccia, William R. Hillson, Wai Ling Kok, Suzanne Cole, Ling-Pei Ho, Teresa Lambe, Manoj Puthia, Catharina Svanborg, Erin M. Scherer, George Krashias, Adam Williams, Joseph N. Blattman, Philip D. Greenberg, Richard A. Flavell, Amin E. Moghaddam, Neil C. Sheppard, and Quentin J. Sattentau. Polyethyleneimine is a potent mucosal adjuvant for viral glycoprotein antigens. *Nature Biotechnology*, 30(9):883–888, September 2012.

[200] Shao-Min Zou, Patrick Erbacher, Jean-Serge Remy, and Jean-Paul Behr. Systemic linear polyethylenimine (L-PEI)-mediated gene delivery in the mouse. *The Journal of Gene Medicine*, 2(2):128–134, 2000. _eprint: https://onlinelibrary.wiley.com/doi/pdf/10.1002/%28SICI%291521-2254%28200003/04%292%3A2%3C128%3A%3AAID-JGM95%3E3.0.CO%3B2-W.

[201] Akin Akinc, Mini Thomas, Alexander M. Klibanov, and Robert Langer. Exploring polyethylenimine-mediated DNA transfection and the proton sponge hypothesis. *The Journal of Gene Medicine*, 7(5):657–663, 2005. _eprint: https://onlinelibrary.wiley.com/doi/pdf/10.1002/jgm.696.

[202] Evita V. Grant, Mini Thomas, Jennifer Fortune, Alexander M. Klibanov, and Norman L. Letvin. Enhancement of plasmid DNA immunogenicity with linear polyethylenimine. *European Journal of Immunology*, 42(11):2937–2948, November 2012.

[203] Yi-Fan Ma and Ya-Wun Yang. Delivery of DNA-based cancer vaccine with polyethylenimine. *European Journal of Pharmaceutical Sciences: Official Journal of the European Federation for Pharmaceutical Sciences*, 40(2):75–83, May 2010.

[204] S. Moein Moghimi, Peter Symonds, J. Clifford Murray, A. Christy Hunter, Grazyna Debska, and Adam Szewczyk. A two-stage poly(ethylenimine)-mediated cytotoxicity: implications for gene transfer/therapy. *Molecular Therapy*, 11(6):990–995, June 2005.

[205] J Kreuter and P P Speiser. New adjuvants on a polymethylmethacrylate base. *Infection and Immunity*, 13(1):204–210, January 1976.

[206] J. Kreuter, R. Mauler, H. Gruschkau, and P. P. Speiser. The use of new polymethylmethacrylate adjuvants for split influenza vaccines. *Experimental Cell Biology*, 44(1):12–19, 1976.

[207] Suzanne Flanary, Allan S. Hoffman, and Patrick S. Stayton. Antigen Delivery with Poly(Propylacrylic Acid) Conjugation Enhances MHC-1 Presentation and T-Cell Activation. *Bioconjugate chemistry*, 20(2):241–248, February 2009.

[208] Suzanne Foster, Craig L. Duvall, Emily F. Crownover, Allan S. Hoffman, and Patrick S. Stayton. Intracellular delivery of a protein antigen with an endosomal-releasing polymer enhances CD8 T-cell production and prophylactic vaccine efficacy. *Bioconjugate Chemistry*, 21(12):2205–2212, December 2010.

[209] André J. van der Vlies, Conlin P. O'Neil, Urara Hasegawa, Nathan Hammond, and Jeffrey A. Hubbell. Synthesis of Pyridyl Disulfide-Functionalized Nanoparticles for Conjugating Thiol-Containing Small Molecules, Peptides, and Proteins. *Bioconjugate Chemistry*, 21(4):653–662, April 2010. Publisher: American Chemical Society.

[210] Armando Stano, Evan A. Scott, Karen Y. Dane, Melody A. Swartz, and Jeffrey A. Hubbell. Tunable T cell immunity towards a protein antigen using polymersomes vs. solid-core nanoparticles. *Biomaterials*, 34(17):4339–4346, June 2013.

[211] B. M. Discher, Y. Y. Won, D. S. Ege, J. C. Lee, F. S. Bates, D. E. Discher, and D. A. Hammer. Polymersomes: tough vesicles made from diblock copolymers. *Science (New York, N.Y.)*, 284(5417):1143–1146, May 1999.

[212] Eric P. Holowka, Victor Z. Sun, Daniel T. Kamei, and Timothy J. Deming. Polyarginine segments in block copolypeptides drive both vesicular assembly and intracellular delivery. *Nature Materials*, 6(1):52–57, January 2007. Number: 1 Publisher: Nature Publishing Group.

[213] Evan A. Scott, Armando Stano, Morgane Gillard, Alexandra C. Maio-Liu, Melody A. Swartz, and Jeffrey A. Hubbell. Dendritic cell activation and T cell priming

with adjuvant- and antigen-loaded oxidation-sensitive polymersomes. *Biomaterials*, 33(26):6211–6219, September 2012.

[214] Wenqian Tao and Harvinder S. Gill. M2e-immobilized gold nanoparticles as influenza A vaccine: role of soluble M2e and longevity of protection. *Vaccine*, 33(20):2307–2315, May 2015.

[215] Carlos H. Villa, Tao Dao, Ian Ahearn, Nicole Fehrenbacher, Emily Casey, Diego A. Rey, Tatyana Korontsvit, Victoriya Zakhaleva, Carl A. Batt, Mark R. Philips, and David A. Scheinberg. Single-walled carbon nanotubes deliver peptide antigen into dendritic cells and enhance IgG responses to tumor-associated antigens. *ACS nano*, 5(7):5300–5311, July 2011.

[216] Stephanie M. Curley and David Putnam. Biological Nanoparticles in Vaccine Development. *Frontiers in Bioengineering and Biotechnology*, 10, 2022.

[217] Jesús Zepeda-Cervantes, Josué Orlando Ramírez-Jarquín, and Luis Vaca. Interaction Between Virus-Like Particles (VLPs) and Pattern Recognition Receptors (PRRs) From Dendritic Cells (DCs): Toward Better Engineering of VLPs. *Frontiers in Immunology*, 11, 2020.

[218] Lukai Zhai, Julianne Peabody, Yuk-Ying Susana Pang, John Schiller, Bryce Chackerian, and Ebenezer Tumban. A novel candidate HPV vaccine: MS2 phage VLP displaying a tandem HPV L2 peptide offers similar protection in mice to Gardasil-9. *Antiviral Research*, 147:116–123, November 2017.

[219] Rupsa Basu, Lukai Zhai, Alice Contreras, and Ebenezer Tumban. Immunization with phage virus-like particles displaying Zika virus potential B-cell epitopes neutralizes Zika virus infection of monkey kidney cells. *Vaccine*, 36(10):1256–1264, February 2018.

[220] Steven M. Opal. Endotoxins and Other Sepsis Triggers. *Endotoxemia and Endotoxin Shock*, 167:14–24, 2010. Publisher: Karger Publishers.

[221] C. Garrett Rappazzo, Hannah C. Watkins, Cassandra M. Guarino, Annie Chau, Jody L. Lopez, Matthew P. DeLisa, Cynthia A. Leifer, Gary R. Whittaker, and David Putnam. Recombinant M2e outer membrane vesicle vaccines protect against lethal influenza A challenge in BALB/c mice. *Vaccine*, 34(10):1252–1258, March 2016.

[222] Hannah C. Watkins, C. Garrett Rappazzo, Jaclyn S. Higgins, Xiangjie Sun, Nicole Brock, Annie Chau, Aditya Misra, Joseph P. B. Cannizzo, Michael R. King, Taronna R. Maines, Cynthia A. Leifer, Gary R. Whittaker, Matthew P. DeLisa, and David Putnam. Safe Recombinant Outer Membrane Vesicles that Display M2e Elicit Heterologous Influenza Protection. *Molecular Therapy*, 25(4):989–1002, April 2017. Publisher: Elsevier.

[223] Puthupparampil V. Scaria, Christopher G. Rowe, Beth B. Chen, Olga V. Muratova, Elizabeth R. Fischer, Emma K. Barnafo, Charles F. Anderson, Irfan U. Zaidi, Lynn E. Lambert, Bob J. Lucas, Debbie D. Nahas, David L. Narum, and Patrick E. Duffy.

Outer membrane protein complex as a carrier for malaria transmission blocking antigen Pfs230. *npj Vaccines*, 4(1):1–10, July 2019. Number: 1 Publisher: Nature Publishing Group.

[224] René H. M. Raeven, Naomi van Vlies, Merijn L. M. Salverda, Larissa van der Maas, Joost P. Uittenbogaard, Tim H. E. Bindels, Jolanda Rigters, Lisa M. Verhagen, Sabine Kruijer, Elly van Riet, Bernard Metz, and Arno A. J. van der Ark. The Role of Virulence Proteins in Protection Conferred by Bordetella pertussis Outer Membrane Vesicle Vaccines. *Vaccines*, 8(3):429, September 2020. Number: 3 Publisher: Multidisciplinary Digital Publishing Institute.

[225] Francisco Carriquiriborde, Pablo Martin Aispuro, Nicolás Ambrosis, Eugenia Zurita, Daniela Bottero, María Emilia Gaillard, Celina Castuma, Erika Rudi, Aníbal Lodeiro, and Daniela F. Hozbor. Pertussis Vaccine Candidate Based on Outer Membrane Vesicles Derived From Biofilm Culture. *Frontiers in Immunology*, 12, 2021.

[226] M. J. Klouwens, M. L. M. Salverda, J. J. Trentelman, J. I. Ersoz, A. Wagemakers, M. J. H. Gerritzen, P. A. van der Ley, and J. W. Hovius. Vaccination with meningococcal outer membrane vesicles carrying Borrelia OspA protects against experimental Lyme borreliosis. *Vaccine*, 39(18):2561–2567, April 2021.

[227] Xiuran Wang, Amit K. Singh, Xiangmin Zhang, and Wei Sun. Induction of Protective Antiplague Immune Responses by Self-Adjuvanting Bionanoparticles Derived from Engineered Yersinia pestis. *Infection and Immunity*, 88(5):e00081–20, April 2020. Publisher: American Society for Microbiology.

[228] A L Carvalho, A Miquel-Clopés, U Wegmann, E Jones, R Stentz, A Telatin, N J Walker, W A Butcher, P J Brown, S Holmes, M J Dennis, E D Williamson, S G P Funnell, M Stock, and S R Carding. Use of bioengineered human commensal gut bacteria-derived microvesicles for mucosal plague vaccine delivery and immunization. *Clinical and Experimental Immunology*, 196(3):287–304, June 2019.

[229] Emanuelle B. Gaspar, Carlos Roberto Prudencio, and Elizabeth De Gaspari. Experimental studies using OMV in a new platform of SARS-CoV-2 vaccines. *Human Vaccines & Immunotherapeutics*, 17(9):2965–2968, September 2021. Publisher: Taylor & Francis _eprint: https://doi.org/10.1080/21645515.2021.1920272.

[230] Himadri B. Thapa, Anna M. Müller, Andrew Camilli, and Stefan Schild. An Intranasal Vaccine Based on Outer Membrane Vesicles Against SARS-CoV-2. *Frontiers in Microbiology*, 12, November 2021. Publisher: Frontiers.

[231] Peter A. van der Ley, Afshin Zariri, Elly van Riet, Dinja Oosterhoff, and Corine P. Kruiswijk. An Intranasal OMV-Based Vaccine Induces High Mucosal and Systemic Protecting Immunity Against a SARS-CoV-2 Infection. *Frontiers in Immunology*, 12, 2021.

[232] Na Kyeong Lee, Seongeon Cho, and In-San Kim. Ferritin – a multifaceted protein scaffold for biotherapeutics. *Experimental & Molecular Medicine*, 54(10):1652–1657, October 2022. Number: 10 Publisher: Nature Publishing Group.

[233] Tatianna Travieso, Jenny Li, Sneha Mahesh, Juliana Da Fonzeca Redenze E. Mello, and Maria Blasi. The use of viral vectors in vaccine development. *npj Vaccines*, 7(1):1–10, July 2022. Number: 1 Publisher: Nature Publishing Group.

[234] Shabir A. Madhi, Vicky Baillie, Clare L. Cutland, Merryn Voysey, Anthonet L. Koen, Lee Fairlie, Sherman D. Padayachee, Keertan Dheda, Shaun L. Barnabas, Qasim E. Bhorat, Carmen Briner, Gaurav Kwatra, Khatija Ahmed, Parvinder Aley, Sutika Bhikha, Jinal N. Bhiman, As'ad E. Bhorat, Jeanine du Plessis, Aliasgar Esmail, Marisa Groenewald, Elizea Horne, Shi-Hsia Hwa, Aylin Jose, Teresa Lambe, Matt Laubscher, Mookho Malahleha, Masebole Masenya, Mduduzi Masilela, Shakeel McKenzie, Kgaogelo Molapo, Andrew Moultrie, Suzette Oelofse, Faeezah Patel, Sureshnee Pillay, Sarah Rhead, Hylton Rodel, Lindie Rossouw, Carol Taoushanis, Houriiyah Tegally, Asha Thombrayil, Samuel van Eck, Constantinos K. Wibmer, Nicholas M. Durham, Elizabeth J. Kelly, Tonya L. Villafana, Sarah Gilbert, Andrew J. Pollard, Tulio de Oliveira, Penny L. Moore, Alex Sigal, and Alane Izu. Efficacy of the ChAdOx1 nCoV-19 Covid-19 Vaccine against the B.1.351 Variant. *New England Journal of Medicine*, 384(20):1885–1898, May 2021. Publisher: Massachusetts Medical Society _eprint: https://doi.org/10.1056/NEJMoa2102214.

[235] Christopher R. Piszczatoski and John G. Gums. Ervebo (Ebola Zaire Vaccine, Live/rVSVG-ZEBOV-GP): The First Licensed Vaccine for the Prevention of Ebola Virus Disease. *Journal of Pharmacy Technology*, 36(6):243–250, December 2020. Publisher: SAGE Publications Inc.

[236] J. Braun, P. Kästner, P. Flaxenberg, J. Währisch, P. Hanke, W. Demary, U. von Hinüber, K. Rockwitz, W. Heitz, U. Pichlmeier, C. Guimbal-Schmolck, A. Brandt, and MC-MTX.6/RH Study Group. Comparison of the clinical efficacy and safety of subcutaneous versus oral administration of methotrexate in patients with active rheumatoid arthritis: results of a six-month, multicenter, randomized, double-blind, controlled, phase IV trial. *Arthritis and Rheumatism*, 58(1):73–81, January 2008.

[237] Rüdiger B. Müller, Johannes von Kempis, Sarah R. Haile, and Michael H. Schiff. Effectiveness, tolerability, and safety of subcutaneous methotrexate in early rheumatoid arthritis: A retrospective analysis of real-world data from the St. Gallen cohort. *Seminars in Arthritis and Rheumatism*, 45(1):28–34, August 2015.

[238] Jasvinder A. Singh, Chris Cameron, Shahrzad Noorbaloochi, Tyler Cullis, Matthew Tucker, Robin Christensen, Elizabeth Tanjong Ghogomu, Doug Coyle, Tammy Clifford, Peter Tugwell, and George A. Wells. Risk of serious infection in biological treatment of patients with rheumatoid arthritis: a systematic review and meta-analysis. *Lancet (London, England)*, 386(9990):258–265, July 2015.

[239] Jin Kyun Park, Min Ah Lee, Eun Young Lee, Yeong Wook Song, Yunhee Choi, Kevin L. Winthrop, and Eun Bong Lee. Effect of methotrexate discontinuation on efficacy of seasonal influenza vaccination in patients with rheumatoid arthritis: a randomised clinical trial. *Annals of the Rheumatic Diseases*, 76(9):1559–1565, September 2017.

[240] Charlotte Hua, Thomas Barnetche, Bernard Combe, and Jacques Morel. Effect of methotrexate, anti-tumor necrosis factor α, and rituximab on the immune response to influenza and pneumococcal vaccines in patients with rheumatoid arthritis: a systematic review and meta-analysis. *Arthritis Care & Research*, 66(7):1016–1026, July 2014.

[241] William Maidhof and Olga Hilas. Lupus: An Overview of the Disease And Management Options. *Pharmacy and Therapeutics*, 37(4):240–249, April 2012.

[242] Ashok K. Dubey, Shailendra S. Handu, Suparna Dubey, Prashant Sharma, K. K. Sharma, and Qazi M. Ahmed. Belimumab: First targeted biological treatment for systemic lupus erythematosus. *Journal of Pharmacology & Pharmacotherapeutics*, 2(4):317–319, 2011.

[243] Joan T. Merrill, C. Michael Neuwelt, Daniel J. Wallace, Joseph C. Shanahan, Kevin M. Latinis, James C. Oates, Tammy O. Utset, Caroline Gordon, David A. Isenberg, Hsin-Ju Hsieh, David Zhang, and Paul G. Brunetta. Efficacy and Safety of Rituximab in Moderately-to-Severely Active Systemic Lupus Erythematosus. *Arthritis and rheumatism*, 62(1):222–233, January 2010.

[244] Christopher M. Warren, Jialing Jiang, and Ruchi S. Gupta. Epidemiology and Burden of Food Allergy. *Current allergy and asthma reports*, 20(2):6, February 2020.

[245] Benjamin L. Wright, Madeline Walkner, Brian P. Vickery, and Ruchi S. Gupta. Clinical Management of Food Allergy. *Pediatric clinics of North America*, 62(6):1409–1424, December 2015.

[246] Konstantinos Samitas, Vasiliki Delimpoura, Eleftherios Zervas, and Mina Gaga. Anti-IgE treatment, airway inflammation and remodelling in severe allergic asthma: current knowledge and future perspectives. *European Respiratory Review*, 24(138):594–601, December 2015. Publisher: European Respiratory Society Section: Reviews.

[247] Jonathan Corren, Mario Castro, Thomas O'Riordan, Nicola A. Hanania, Ian D. Pavord, Santiago Quirce, Bradley E. Chipps, Sally E. Wenzel, Karthinathan Thangavelu, Megan S. Rice, Sivan Harel, Alexandre Jagerschmidt, Asif H. Khan, Siddhesh Kamat, Jaman Maroni, Paul Rowe, Yufang Lu, Nikhil Amin, Gianluca Pirozzi, Marcella Ruddy, Neil M. H. Graham, and Ariel Teper. Dupilumab Efficacy in Patients with Uncontrolled, Moderate-to-Severe Allergic Asthma. *The Journal of Allergy and Clinical Immunology: In Practice*, 8(2):516–526, February 2020.

[248] Ann-Marie Malby Schoos, Dominique Bullens, Bo Lund Chawes, Joana Costa, Liselot De Vlieger, Audrey DunnGalvin, Michelle M. Epstein, Johan Garssen, Christiane Hilger, Karen Knipping, Annette Kuehn, Dragan Mijakoski, Daniel Munblit, Nikita A.

Nekliudov, Cevdet Ozdemir, Karine Patient, Diego Peroni, Sasho Stoleski, Eva Stylianou, Mirjana Tukalj, Kitty Verhoeckx, Mihaela Zidarn, and Willem van de Veen. Immunological Outcomes of Allergen-Specific Immunotherapy in Food Allergy. *Frontiers in Immunology*, 11:568598, November 2020.

[249] Sophia Tsabouri, Antigoni Mavroudi, Gavriela Feketea, and George V. Guibas. Subcutaneous and Sublingual Immunotherapy in Allergic Asthma in Children. *Frontiers in Pediatrics*, 5, 2017.

[250] Shannon L. Meeks and Glaivy Batsuli. Hemophilia and inhibitors: current treatment options and potential new therapeutic approaches. *Hematology: the American Society of Hematology Education Program*, 2016(1):657–662, December 2016.

[251] Roberto Zori, Janet A. Thomas, Natasha Shur, William B. Rizzo, Celeste Decker, Orli Rosen, Mingjin Li, Becky Schweighardt, Kevin Larimore, and Nicola Longo. Induction, titration, and maintenance dosing regimen in a phase 2 study of pegvaliase for control of blood phenylalanine in adults with phenylketonuria. *Molecular Genetics and Metabolism*, 125(3):217–227, November 2018.

[252] John K. Botson, John R. P. Tesser, Ralph Bennett, Howard M. Kenney, Paul M. Peloso, Katie Obermeyer, Brian LaMoreaux, Michael E. Weinblatt, and Jeff Peterson. Pegloticase in Combination With Methotrexate in Patients With Uncontrolled Gout: A Multicenter, Open-label Study (MIRROR). *The Journal of Rheumatology*, 48(5):767–774, May 2021. Publisher: The Journal of Rheumatology Section: Gout.

[253] Hans H. Herfarth, Michael D Kappelman, Millie D Long, and Kim L Isaacs. Use of methotrexate in the treatment of inflammatory bowel diseases (IBD). *Inflammatory bowel diseases*, 22(1):224–233, January 2016.

[254] Marco Sebastiani, Maria Grazia Anelli, Fabiola Atzeni, Chiara Bazzani, Ilaria Farina, Anna Laura Fedele, Ennio Giulio Favalli, Irene Fineschi, Nicolò Cino, Ilaria Dal Forno, Stefania Gasparini, Emanuele Cassarà, Rita Giardina, Eleonora Bruschi, Olga Addimanda, Giulia Cassone, Simona Lopriore, Piercarlo Sarzi-Puttini, Matteo Filippini, Federica Pignatti, Elisa Gremese, Martina Biggioggero, Stefania Manganelli, Giorgio Amato, Cristian Caimmi, Fausto Salaffi, Florenzo Iannone, Clodoveo Ferri, Gilda Sandri, Giovanni Lapadula, Roberto Gorla, Marcello Govoni, Gianfranco Ferraccioli, Antonio Marchesoni, Mauro Galeazzi, Rosario Foti, Antonio Carletto, Fabrizio Cantini, Giovanni Triolo, Oscar Massimiliano Epis, Carlo Salvarani, and Italian Study Group on Early Arthritides (GISEA). Efficacy and safety of rituximab with and without methotrexate in the treatment of rheumatoid arthritis patients: results from the GISEA register. *Joint Bone Spine*, 81(6):508–512, December 2014.

[255] Suhrad G. Banugaria, Sean N. Prater, Judeth K. McGann, Jonathan D. Feldman, Jesse A. Tannenbaum, Carrie Bailey, Renuka Gera, Robert L. Conway, David Viskochil, Joyce A. Kobori, Amy S. Rosenberg, and Priya S. Kishnani. Bortezomib in the rapid reduction of high sustained antibody titers in disorders treated with therapeutic protein: lessons learned from Pompe disease. *Genetics in Medicine: Official Journal of the American College of Medical Genetics*, 15(2):123–131, February 2013.

[256] Zoheb B. Kazi, Ankit K. Desai, R. Bradley Troxler, David Kronn, Seymour Packman, Marta Sabbadini, William B. Rizzo, Katalin Scherer, Omar Abdul-Rahman, Pranoot Tanpaiboon, Sheela Nampoothiri, Neerja Gupta, Annette Feigenbaum, Dmitriy M. Niyazov, Langston Sherry, Reeval Segel, Alison McVie-Wylie, Crystal Sung, Alexandra M. Joseph, Susan Richards, and Priya S. Kishnani. An immune tolerance approach using transient low-dose methotrexate in the ERT-naïve setting of patients treated with a therapeutic protein: experience in infantile-onset Pompe disease. *Genetics in Medicine*, 21(4):887–895, April 2019. Publisher: Nature Publishing Group.

[257] A. Kandiel, A. G. Fraser, B. I. Korelitz, C. Brensinger, and J. D. Lewis. Increased risk of lymphoma among inflammatory bowel disease patients treated with azathioprine and 6-mercaptopurine. *Gut*, 54(8):1121–1125, August 2005.

[258] Karin Ekström Smedby, Eva Baecklund, and Johan Askling. Malignant lymphomas in autoimmunity and inflammation: A review of risks, risk factors, and lymphoma characteristics. *Cancer Epidemiology Biomarkers and Prevention*, 15(11):2069–2077, November 2006.

[259] David S. Kotlyar, James D. Lewis, Laurent Beaugerie, Ann Tierney, Colleen M. Brensinger, Javier P. Gisbert, Edward V. Loftus, Laurent Peyrin-Biroulet, Wojciech C. Blonski, Manuel Van Domselaar, Maria Chaparro, Sandipani Sandilya, Meenakshi Bewtra, Florian Beigel, Livia Biancone, and Gary R. Lichtenstein. Risk of lymphoma in patients with inflammatory bowel disease treated with azathioprine and 6-mercaptopurine: A meta-analysis. *Clinical Gastroenterology and Hepatology*, 13(5):847–858.e4, May 2015. Publisher: W.B. Saunders.

[260] Paula A. Agudelo Garcia and Shelley L. Berger. Genetics Meets Epigenetics in Treg Cells and Autoimmunity. *Immunity*, 52(6):897, June 2020. Publisher: NIH Public Access.

[261] Eric A. Engels, James R. Cerhan, Martha S. Linet, Wendy Cozen, Joanne S. Colt, Scott Davis, Gloria Gridley, Richard K. Severson, and Patricia Hartge. Immune-related conditions and immune-modulating medications as risk factors for non-Hodgkin's lymphoma: a case-control study. *American Journal of Epidemiology*, 162(12):1153–1161, December 2005.

[262] Makoto Miyara, Yumiko Yoshioka, Akihiko Kitoh, Tomoko Shima, Kajsa Wing, Akira Niwa, Christophe Parizot, Cécile Taflin, Toshio Heike, Dominique Valeyre, Alexis Mathian, Tatsutoshi Nakahata, Tomoyuki Yamaguchi, Takashi Nomura, Masahiro Ono, Zahir Amoura, Guy Gorochov, and Shimon Sakaguchi. Functional delineation and differentiation dynamics of human CD4+ T cells expressing the FoxP3 transcription factor. *Immunity*, 30(6):899–911, June 2009.

[263] Jeffrey A. Bluestone, Jane H. Buckner, Mark Fitch, Stephen E. Gitelman, Shipra Gupta, Marc K. Hellerstein, Kevan C. Herold, Angela Lares, Michael R. Lee, Kelvin Li, Weihong Liu, S. Alice Long, Lisa M. Masiello, Vinh Nguyen, Amy L. Putnam, Mary

Rieck, Peter H. Sayre, and Qizhi Tang. Type 1 diabetes immunotherapy using polyclonal regulatory T cells. *Science Translational Medicine*, 7(315):315ra189–315ra189, November 2015. Publisher: American Association for the Advancement of Science.

[264] Claudio G. Brunstein, Jeffrey S. Miller, David H. McKenna, Keli L. Hippen, Todd E. DeFor, Darin Sumstad, Julie Curtsinger, Michael R. Verneris, Margaret L. MacMillan, Bruce L. Levine, James L. Riley, Carl H. June, Chap Le, Daniel J. Weisdorf, Philip B. McGlave, Bruce R. Blazar, and John E. Wagner. Umbilical cord blood–derived T regulatory cells to prevent GVHD: kinetics, toxicity profile, and clinical effect. *Blood*, 127(8):1044–1051, February 2016.

[265] Eleonora Trotta, Paul H. Bessette, Stephanie L. Silveria, Lauren K. Ely, Kevin M. Jude, Duy T. Le, Charles R. Holst, Anthony Coyle, Marc Potempa, Lewis L. Lanier, K. Christopher Garcia, Natasha K. Crellin, Isaac J. Rondon, and Jeffrey A. Bluestone. A human anti-IL-2 antibody that potentiates regulatory T cells by a structure-based mechanism. *Nature Medicine*, 24(7):1005–1014, July 2018. Number: 7 Publisher: Nature Publishing Group.

[266] Ana Luisa Perdigoto, Lucienne Chatenoud, Jeffrey A. Bluestone, and Kevan C. Herold. Inducing and Administering Tregs to Treat Human Disease. *Frontiers in Immunology*, 6, 2015. Publisher: Frontiers Media SA.

[267] Christoph T. Ellebrecht, Vijay G. Bhoj, Arben Nace, Eun Jung Choi, Xuming Mao, Michael Jeffrey Cho, Giovanni Di Zenzo, Antonio Lanzavecchia, John T. Seykora, George Cotsarelis, Michael C. Milone, and Aimee S. Payne. Reengineering chimeric antigen receptor T cells for targeted therapy of autoimmune disease. *Science*, 353(6295):179–184, July 2016. Publisher: American Association for the Advancement of Science.

[268] Divya J. Mekala and Terrence L. Geiger. Immunotherapy of autoimmune encephalomyelitis with redirected CD4+CD25+ T lymphocytes. *Blood*, 105(5):2090–2092, March 2005.

[269] Ioana Moisini, Phuong Nguyen, Lars Fugger, and Terrence L. Geiger. Redirecting therapeutic T cells against myelin-specific T lymphocytes using a humanized myelin basic protein-HLA-DR2-zeta chimeric receptor. *Journal of Immunology (Baltimore, Md.: 1950)*, 180(5):3601–3611, March 2008.

[270] Zhaohui Qian, Kary A. Latham, Karen B. Whittington, David C. Miller, David D. Brand, and Edward F. Rosloniec. Engineered regulatory T cells coexpressing MHC class II:peptide complexes are efficient inhibitors of autoimmune T cell function and prevent the development of autoimmune arthritis. *Journal of Immunology (Baltimore, Md.: 1950)*, 190(11):5382–5391, June 2013.

[271] Carl H. June, Stanley R. Riddell, and Ton N. Schumacher. Adoptive cellular therapy: a race to the finish line. *Science Translational Medicine*, 7(280):280ps7, March 2015.

[272] D. E. Goodkin, M. Shulman, J. Winkelhake, E. Waubant, P. Andersson, T. Stewart, S. Nelson, N. Fischbein, P. K. Coyle, E. Frohman, L. Jacobs, J. Holcenberg, M. Lee, and S. Mocci. A phase I trial of solubilized DR2:MBP84-102 (AG284) in multiple sclerosis. *Neurology*, 54(7):1414–1420, April 2000.

[273] Vijayshree Yadav, Dennis N. Bourdette, James D. Bowen, Sharon G. Lynch, David Mattson, Jana Preiningerova, Christopher T. Bever, Jack Simon, Andrew Goldstein, Gregory G. Burrows, Halina Offner, Al J. Ferro, and Arthur A. Vandenbark. Recombinant T-Cell Receptor Ligand (RTL) for Treatment of Multiple Sclerosis: A Double-Blind, Placebo-Controlled, Phase 1, Dose-Escalation Study. *Autoimmune Diseases*, 2012:954739, 2012.

[274] M. S. Freedman, A. Bar-Or, J. Oger, A. Traboulsee, D. Patry, C. Young, T. Olsson, D. Li, H.-P. Hartung, M. Krantz, L. Ferenczi, T. Verco, and MAESTRO-01 Investigators. A phase III study evaluating the efficacy and safety of MBP8298 in secondary progressive MS. *Neurology*, 77(16):1551–1560, October 2011.

[275] Eva C. Koffeman, Mark Genovese, Diane Amox, Elissa Keogh, Ernesto Santana, Eric L. Matteson, Arthur Kavanaugh, Jerry A. Molitor, Michael H. Schiff, James O. Posever, Joan M. Bathon, Alan J. Kivitz, Rodrigo Samodal, Francis Belardi, Carolyn Dennehey, Theo van den Broek, Femke van Wijk, Xiao Zhang, Peter Zieseniss, Tho Le, Berent A. Prakken, Gary C. Cutter, and Salvatore Albani. Epitope-specific immunotherapy of rheumatoid arthritis: clinical responsiveness occurs with immune deviation and relies on the expression of a cluster of molecules associated with T cell tolerance in a double-blind, placebo-controlled, pilot phase II trial. *Arthritis and Rheumatism*, 60(11):3207–3216, November 2009.

[276] Gautam Goel, Tim King, A. James Daveson, Jane M. Andrews, Janakan Krishnarajah, Richard Krause, Gregor J. E. Brown, Ronald Fogel, Charles F. Barish, Roger Epstein, Timothy P. Kinney, Philip B. Miner, Jason A. Tye-Din, Adam Girardin, Juha Taavela, Alina Popp, John Sidney, Markku Mäki, Kaela E. Goldstein, Patrick H. Griffin, Suyue Wang, John L. Dzuris, Leslie J. Williams, Alessandro Sette, Ramnik J. Xavier, Ludvig M. Sollid, Bana Jabri, and Robert P. Anderson. Epitope-specific immunotherapy targeting CD4-positive T cells in coeliac disease: two randomised, double-blind, placebo-controlled phase 1 studies. *The Lancet. Gastroenterology & Hepatology*, 2(7):479–493, July 2017.

[277] A. James M. Daveson, Hooi C. Ee, Jane M. Andrews, Timothy King, Kaela E. Goldstein, John L. Dzuris, James A. MacDougall, Leslie J. Williams, Anita Treohan, Michael P. Cooreman, and Robert P. Anderson. Epitope-Specific Immunotherapy Targeting CD4-Positive T Cells in Celiac Disease: Safety, Pharmacokinetics, and Effects on Intestinal Histology and Plasma Cytokines with Escalating Dose Regimens of Nexvax2 in a Randomized, Double-Blind, Placebo-Controlled Phase 1 Study. *EBioMedicine*, 26:78–90, December 2017.

[278] B. Bielekova, B. Goodwin, N. Richert, I. Cortese, T. Kondo, G. Afshar, B. Gran, J. Eaton, J. Antel, J. A. Frank, H. F. McFarland, and R. Martin. Encephalitogenic

potential of the myelin basic protein peptide (amino acids 83-99) in multiple sclerosis: results of a phase II clinical trial with an altered peptide ligand. *Nature Medicine*, 6(10):1167–1175, October 2000.

[279] L. Kappos, G. Comi, H. Panitch, J. Oger, J. Antel, P. Conlon, and L. Steinman. Induction of a non-encephalitogenic type 2 T helper-cell autoimmune response in multiple sclerosis after administration of an altered peptide ligand in a placebo-controlled, randomized phase II trial. The Altered Peptide Ligand in Relapsing MS Study Group. *Nature Medicine*, 6(10):1176–1182, October 2000.

[280] Edwin Liu, Hiroaki Moriyama, Norio Abiru, Dongmei Miao, Liping Yu, Robert M. Taylor, Fred D. Finkelman, and George S. Eisenbarth. Anti-peptide autoantibodies and fatal anaphylaxis in NOD mice in response to insulin self-peptides B:9-23 and B:13-23. *The Journal of Clinical Investigation*, 110(7):1021–1027, October 2002.

[281] Christelle Capini, Montree Jaturanpinyo, Hsin-I. Chang, Srinivas Mutalik, Alice McNally, Shayna Street, Raymond Steptoe, Brendan O'Sullivan, Nigel Davies, and Ranjeny Thomas. Antigen-specific suppression of inflammatory arthritis using liposomes. *Journal of Immunology (Baltimore, Md.: 1950)*, 182(6):3556–3565, March 2009.

[282] Roberto A. Maldonado, Robert A. LaMothe, Joseph D. Ferrari, Ai-Hong Zhang, Robert J. Rossi, Pallavi N. Kolte, Aaron P. Griset, Conlin O'Neil, David H. Altreuter, Erica Browning, Lloyd Johnston, Omid C. Farokhzad, Robert Langer, David W. Scott, Ulrich H. von Andrian, and Takashi Kei Kishimoto. Polymeric synthetic nanoparticles for the induction of antigen-specific immunological tolerance. *Proceedings of the National Academy of Sciences*, 112(2):E156–E165, January 2015. Publisher: Proceedings of the National Academy of Sciences.

[283] Robert A. LaMothe, Pallavi N. Kolte, Trinh Vo, Joseph D. Ferrari, Tracy C. Gelsinger, Jodie Wong, Victor T. Chan, Sinthia Ahmed, Aditi Srinivasan, Patrick Deitemeyer, Roberto A. Maldonado, and Takashi K. Kishimoto. Tolerogenic Nanoparticles Induce Antigen-Specific Regulatory T Cells and Provide Therapeutic Efficacy and Transferrable Tolerance against Experimental Autoimmune Encephalomyelitis. *Frontiers in Immunology*, 9, 2018.

[284] Buvana Ravishankar, Rahul Shinde, Haiyun Liu, Kapil Chaudhary, Jillian Bradley, Henrique P. Lemos, Phillip Chandler, Masato Tanaka, David H. Munn, Andrew L. Mellor, and Tracy L. McGaha. Marginal zone CD169+ macrophages coordinate apoptotic cell-driven cellular recruitment and tolerance. *Proceedings of the National Academy of Sciences*, 111(11):4215–4220, March 2014. Publisher: Proceedings of the National Academy of Sciences.

[285] Suchitra Prasad, Adam P. Kohm, Jeffrey S. McMahon, Xunrong Luo, and Stephen D. Miller. Pathogenesis of NOD Diabetes is Initiated by Reactivity to the Insulin B Chain 9–23 Epitope and Involves Functional Epitope Spreading. *Journal of autoimmunity*, 39(4):347–353, December 2012.

[286] Daniel R. Getts, Danielle M. Turley, Cassandra E. Smith, Christopher T. Harp, Derrick McCarthy, Emma M. Feeney, Meghann Teague Getts, Aaron J. Martin, Xunrong Luo, Rachael L. Terry, Nicholas J. C. King, and Stephen D. Miller. Tolerance induced by apoptotic antigen-coupled leukocytes is induced by PD-L1+ and IL-10-producing splenic macrophages and maintained by T regulatory cells. *Journal of Immunology (Baltimore, Md.: 1950)*, 187(5):2405–2417, September 2011.

[287] Alizée J. Grimm, Stephan Kontos, Giacomo Diaceri, Xavier Quaglia-Thermes, and Jeffrey A. Hubbell. Memory of tolerance and induction of regulatory T cells by erythrocyte-targeted antigens. *Scientific Reports*, 5(1):15907, October 2015. Number: 1 Publisher: Nature Publishing Group.

[288] Kristen M. Lorentz, Stephan Kontos, Giacomo Diaceri, Hugues Henry, and Jeffrey A. Hubbell. Engineered binding to erythrocytes induces immunological tolerance to E. coli asparaginase. *Science Advances*, 1(6):e1500112, July 2015.

[289] Angus W. Thomson and Percy A. Knolle. Antigen-presenting cell function in the tolerogenic liver environment. *Nature Reviews. Immunology*, 10(11):753–766, November 2010.

[290] Antonella Carambia, Barbara Freund, Dorothee Schwinge, Oliver T. Bruns, Sunhild C. Salmen, Harald Ittrich, Rudolph Reimer, Markus Heine, Samuel Huber, Christian Waurisch, Alexander Eychmüller, David C. Wraith, Thomas Korn, Peter Nielsen, Horst Weller, Christoph Schramm, Stefan Lüth, Ansgar W. Lohse, Joerg Heeren, and Johannes Herkel. Nanoparticle-based autoantigen delivery to Treg-inducing liver sinusoidal endothelial cells enables control of autoimmunity in mice. *Journal of Hepatology*, 62(6):1349–1356, June 2015.

[291] D Scott Wilson, Martina Damo, Sachiko Hirosue, Michal M Raczy, Kym Brünggel, Giacomo Diaceri, Xavier Quaglia-Thermes, and Jeffrey A Hubbell. Synthetically glycosylated antigens induce antigen-specific tolerance and prevent the onset of diabetes. *Nature Biomedical Engineering*, 3(10):817–829, 2019.

[292] Chitavi D. Maulloo, Shijie Cao, Elyse A. Watkins, Michal M. Raczy, Ani S. Solanki, Mindy Nguyen, Joseph W. Reda, Ha Na Shim, D. Scott Wilson, Melody A. Swartz, and Jeffrey A. Hubbell. Lymph Node-Targeted Synthetically Glycosylated Antigen Leads to Antigen-Specific Immunological Tolerance. *Frontiers in Immunology*, 12(September):1–17, 2021.

[293] Martina Damo, D. Scott Wilson, Elyse A. Watkins, and Jeffrey A. Hubbell. Soluble N-Acetylgalactosamine-Modified Antigens Enhance Hepatocyte-Dependent Antigen Cross-Presentation and Result in Antigen-Specific CD8+ T Cell Tolerance Development. *Frontiers in Immunology*, 12(March):1–15, 2021.

[294] D. Scott Wilson, Sachiko Hirosue, Michal M. Raczy, Leonardo Bonilla-Ramirez, Laura Jeanbart, Ruyi Wang, Marcin Kwissa, Jean-Francois Franetich, Maria A. S. Broggi, Giacomo Diaceri, Xavier Quaglia-Thermes, Dominique Mazier, Melody A. Swartz,

and Jeffrey A. Hubbell. Antigens reversibly conjugated to a polymeric glyco-adjuvant induce protective humoral and cellular immunity. *Nature Materials*, 18(February):175–185, 2019. Publisher: Springer US.

[295] Tung Thanh Le, Jakob P. Cramer, Robert Chen, and Stephen Mayhew. Evolution of the COVID-19 vaccine development landscape. *Nature Reviews Drug Discovery*, 19(10):667–668, September 2020. Bandiera_abtest: a Cg_type: From The Analyst's Couch Number: 10 Publisher: Nature Publishing Group.

[296] Nikolaos C. Kyriakidis, Andrés López-Cortés, Eduardo Vásconez González, Alejandra Barreto Grimaldos, and Esteban Ortiz Prado. SARS-CoV-2 vaccines strategies: a comprehensive review of phase 3 candidates. *npj Vaccines*, 6(1):1–17, February 2021. Number: 1 Publisher: Nature Publishing Group.

[297] Peter Richmond, Lara Hatchuel, Min Dong, Brenda Ma, Branda Hu, Igor Smolenov, Ping Li, Peng Liang, Htay Htay Han, Joshua Liang, and Ralf Clemens. Safety and immunogenicity of S-Trimer (SCB-2019), a protein subunit vaccine candidate for COVID-19 in healthy adults: a phase 1, randomised, double-blind, placebo-controlled trial. *The Lancet*, 397(10275):682–694, February 2021.

[298] Cheryl Keech, Gary Albert, Iksung Cho, Andreana Robertson, Patricia Reed, Susan Neal, Joyce S. Plested, Mingzhu Zhu, Shane Cloney-Clark, Haixia Zhou, Gale Smith, Nita Patel, Matthew B. Frieman, Robert E. Haupt, James Logue, Marisa McGrath, Stuart Weston, Pedro A. Piedra, Chinar Desai, Kathleen Callahan, Maggie Lewis, Patricia Price-Abbott, Neil Formica, Vivek Shinde, Louis Fries, Jason D. Lickliter, Paul Griffin, Bethanie Wilkinson, and Gregory M. Glenn. Phase 1–2 Trial of a SARS-CoV-2 Recombinant Spike Protein Nanoparticle Vaccine. *New England Journal of Medicine*, 383(24):2320–2332, December 2020. Publisher: Massachusetts Medical Society.

[299] Peng Zhou, Xing-Lou Yang, Xian-Guang Wang, Ben Hu, Lei Zhang, Wei Zhang, Hao-Rui Si, Yan Zhu, Bei Li, Chao-Lin Huang, Hui-Dong Chen, Jing Chen, Yun Luo, Hua Guo, Ren-Di Jiang, Mei-Qin Liu, Ying Chen, Xu-Rui Shen, Xi Wang, Xiao-Shuang Zheng, Kai Zhao, Quan-Jiao Chen, Fei Deng, Lin-Lin Liu, Bing Yan, Fa-Xian Zhan, Yan-Yi Wang, Geng-Fu Xiao, and Zheng-Li Shi. A pneumonia outbreak associated with a new coronavirus of probable bat origin. *Nature*, 579(7798):270–273, March 2020. Number: 7798 Publisher: Nature Publishing Group.

[300] Jun Lan, Jiwan Ge, Jinfang Yu, Sisi Shan, Huan Zhou, Shilong Fan, Qi Zhang, Xuanling Shi, Qisheng Wang, Linqi Zhang, and Xinquan Wang. Structure of the SARS-CoV-2 spike receptor-binding domain bound to the ACE2 receptor. *Nature*, 581(7807):215–220, May 2020. Number: 7807 Publisher: Nature Publishing Group.

[301] Yunlong Cao, Bin Su, Xianghua Guo, Wenjie Sun, Yongqiang Deng, Linlin Bao, Qinyu Zhu, Xu Zhang, Yinghui Zheng, Chenyang Geng, Xiaoran Chai, Runsheng He, Xiaofeng Li, Qi Lv, Hua Zhu, Wei Deng, Yanfeng Xu, Yanjun Wang, Luxin Qiao, Yafang Tan, Liyang Song, Guopeng Wang, Xiaoxia Du, Ning Gao, Jiangning Liu, Junyu Xiao, Xiao-dong Su, Zongmin Du, Yingmei Feng, Chuan Qin, Chengfeng Qin, Ronghua Jin,

and X. Sunney Xie. Potent Neutralizing Antibodies against SARS-CoV-2 Identified by High-Throughput Single-Cell Sequencing of Convalescent Patients' B Cells. *Cell*, 182(1):73–84.e16, July 2020.

[302] Seth J. Zost, Pavlo Gilchuk, James Brett Case, Elad Binshtein, Rita E. Chen, Joseph P. Nkolola, Alexandra Schäfer, Joseph X. Reidy, Andrew Trivette, Rachel S. Nargi, Rachel E. Sutton, Naveenchandra Suryadevara, David R. Martinez, Lauren E. Williamson, Elaine C. Chen, Taylor Jones, Samuel Day, Luke Myers, Ahmed O. Hassan, Natasha M. Kafai, Emma S. Winkler, Julie M. Fox, Swathi Shrihari, Benjamin K. Mueller, Jens Meiler, Abishek Chandrashekar, Noe B. Mercado, James J. Steinhardt, Kuishu Ren, Yueh-Ming Loo, Nicole L. Kallewaard, Broc T. McCune, Shamus P. Keeler, Michael J. Holtzman, Dan H. Barouch, Lisa E. Gralinski, Ralph S. Baric, Larissa B. Thackray, Michael S. Diamond, Robert H. Carnahan, and James E. Crowe. Potently neutralizing and protective human antibodies against SARS-CoV-2. *Nature*, 584(7821):443–449, August 2020. Number: 7821 Publisher: Nature Publishing Group.

[303] Rui Shi, Chao Shan, Xiaomin Duan, Zhihai Chen, Peipei Liu, Jinwen Song, Tao Song, Xiaoshan Bi, Chao Han, Lianao Wu, Ge Gao, Xue Hu, Yanan Zhang, Zhou Tong, Weijin Huang, William Jun Liu, Guizhen Wu, Bo Zhang, Lan Wang, Jianxun Qi, Hui Feng, Fu-Sheng Wang, Qihui Wang, George Fu Gao, Zhiming Yuan, and Jinghua Yan. A human neutralizing antibody targets the receptor-binding site of SARS-CoV-2. *Nature*, 584(7819):120–124, August 2020. Number: 7819 Publisher: Nature Publishing Group.

[304] Lihong Liu, Pengfei Wang, Manoj S. Nair, Jian Yu, Micah Rapp, Qian Wang, Yang Luo, Jasper F.-W. Chan, Vincent Sahi, Amir Figueroa, Xinzheng V. Guo, Gabriele Cerutti, Jude Bimela, Jason Gorman, Tongqing Zhou, Zhiwei Chen, Kwok-Yung Yuen, Peter D. Kwong, Joseph G. Sodroski, Michael T. Yin, Zizhang Sheng, Yaoxing Huang, Lawrence Shapiro, and David D. Ho. Potent neutralizing antibodies against multiple epitopes on SARS-CoV-2 spike. *Nature*, 584(7821):450–456, August 2020. Number: 7821 Publisher: Nature Publishing Group.

[305] Ariane Sternberg and Cord Naujokat. Structural features of coronavirus SARS-CoV-2 spike protein: Targets for vaccination. *Life Sciences*, 257:118056, September 2020.

[306] Lianpan Dai and George F. Gao. Viral targets for vaccines against COVID-19. *Nature Reviews Immunology*, 21(2):73–82, February 2021. Number: 2 Publisher: Nature Publishing Group.

[307] Yunfei Wang, Lichun Wang, Han Cao, and Cunbao Liu. SARS-CoV-2 S1 is superior to the RBD as a COVID-19 subunit vaccine antigen. *Journal of Medical Virology*, 93(2):892–898, 2021. _eprint: https://onlinelibrary.wiley.com/doi/pdf/10.1002/jmv.26320.

[308] Matthew D. Shin, Sourabh Shukla, Young Hun Chung, Veronique Beiss, Soo Khim Chan, Oscar A. Ortega-Rivera, David M. Wirth, Angela Chen, Markus Sack, Jonathan K. Pokorski, and Nicole F. Steinmetz. COVID-19 vaccine development and a

potential nanomaterial path forward. *Nature Nanotechnology*, 15(8):646–655, August 2020. Number: 8 Publisher: Nature Publishing Group.

[309] Ankur Singh. Eliciting B cell immunity against infectious diseases using nanovaccines. *Nature Nanotechnology*, 16(1):16–24, January 2021. Number: 1 Publisher: Nature Publishing Group.

[310] Tiong Kit Tan, Pramila Rijal, Rolle Rahikainen, Anthony H. Keeble, Lisa Schimanski, Saira Hussain, Ruth Harvey, Jack W. P. Hayes, Jane C. Edwards, Rebecca K. McLean, Veronica Martini, Miriam Pedrera, Nazia Thakur, Carina Conceicao, Isabelle Dietrich, Holly Shelton, Anna Ludi, Ginette Wilsden, Clare Browning, Adrian K. Zagrajek, Dagmara Bialy, Sushant Bhat, Phoebe Stevenson-Leggett, Philippa Hollinghurst, Matthew Tully, Katy Moffat, Chris Chiu, Ryan Waters, Ashley Gray, Mehreen Azhar, Valerie Mioulet, Joseph Newman, Amin S. Asfor, Alison Burman, Sylvia Crossley, John A. Hammond, Elma Tchilian, Bryan Charleston, Dalan Bailey, Tobias J. Tuthill, Simon P. Graham, Helen M. E. Duyvesteyn, Tomas Malinauskas, Jiandong Huo, Julia A. Tree, Karen R. Buttigieg, Raymond J. Owens, Miles W. Carroll, Rodney S. Daniels, John W. McCauley, David I. Stuart, Kuan-Ying A. Huang, Mark Howarth, and Alain R. Townsend. A COVID-19 vaccine candidate using SpyCatcher multimerization of the SARS-CoV-2 spike protein receptor-binding domain induces potent neutralising antibody responses. *Nature Communications*, 12(1):542, January 2021. Number: 1 Publisher: Nature Publishing Group.

[311] Yin-Feng Kang, Cong Sun, Zhen Zhuang, Run-Yu Yuan, Qingbing Zheng, Jiang-Ping Li, Ping-Ping Zhou, Xin-Chun Chen, Zhe Liu, Xiao Zhang, Xiao-Hui Yu, Xiang-Wei Kong, Qian-Ying Zhu, Qian Zhong, Miao Xu, Nan-Shan Zhong, Yi-Xin Zeng, Guo-Kai Feng, Changwen Ke, Jin-Cun Zhao, and Mu-Sheng Zeng. Rapid Development of SARS-CoV-2 Spike Protein Receptor-Binding Domain Self-Assembled Nanoparticle Vaccine Candidates. *ACS Nano*, 15(2):2738–2752, February 2021. Publisher: American Chemical Society.

[312] Alexandra C. Walls, Brooke Fiala, Alexandra Schäfer, Samuel Wrenn, Minh N. Pham, Michael Murphy, Longping V. Tse, Laila Shehata, Megan A. O'Connor, Chengbo Chen, Mary Jane Navarro, Marcos C. Miranda, Deleah Pettie, Rashmi Ravichandran, John C. Kraft, Cassandra Ogohara, Anne Palser, Sara Chalk, E-Chiang Lee, Kathryn Guerriero, Elizabeth Kepl, Cameron M. Chow, Claire Sydeman, Edgar A. Hodge, Brieann Brown, Jim T. Fuller, Kenneth H. Dinnon, Lisa E. Gralinski, Sarah R. Leist, Kendra L. Gully, Thomas B. Lewis, Miklos Guttman, Helen Y. Chu, Kelly K. Lee, Deborah H. Fuller, Ralph S. Baric, Paul Kellam, Lauren Carter, Marion Pepper, Timothy P. Sheahan, David Veesler, and Neil P. King. Elicitation of Potent Neutralizing Antibody Responses by Designed Protein Nanoparticle Vaccines for SARS-CoV-2. *Cell*, 183(5):1367–1382.e17, November 2020.

[313] Alexander A. Cohen, Priyanthi N. P. Gnanapragasam, Yu E. Lee, Pauline R. Hoffman, Susan Ou, Leesa M. Kakutani, Jennifer R. Keeffe, Hung-Jen Wu, Mark Howarth, Anthony P. West, Christopher O. Barnes, Michel C. Nussenzweig, and Pamela J. Bjork-

man. Mosaic nanoparticles elicit cross-reactive immune responses to zoonotic coronaviruses in mice. *Science*, 371(6530):735–741, February 2021. Publisher: American Association for the Advancement of Science.

[314] Mangalakumari Jeyanathan, Sam Afkhami, Fiona Smaill, Matthew S. Miller, Brian D. Lichty, and Zhou Xing. Immunological considerations for COVID-19 vaccine strategies. *Nature Reviews Immunology*, 20(10):615–632, October 2020. Number: 10 Publisher: Nature Publishing Group.

[315] Rebecca J. Cox and Karl A. Brokstad. Not just antibodies: B cells and T cells mediate immunity to COVID-19. *Nature Reviews Immunology*, 20(10):581–582, October 2020. Number: 10 Publisher: Nature Publishing Group.

[316] Alessandro Sette and Shane Crotty. Adaptive immunity to SARS-CoV-2 and COVID-19. *Cell*, 184(4):861–880, February 2021.

[317] Zeyu Chen and E. John Wherry. T cell responses in patients with COVID-19. *Nature Reviews Immunology*, 20(9):529–536, September 2020. Number: 9 Publisher: Nature Publishing Group.

[318] Takuya Sekine, André Perez-Potti, Olga Rivera-Ballesteros, Kristoffer Strålin, Jean-Baptiste Gorin, Annika Olsson, Sian Llewellyn-Lacey, Habiba Kamal, Gordana Bogdanovic, Sandra Muschiol, David J. Wullimann, Tobias Kammann, Johanna Emgård, Tiphaine Parrot, Elin Folkesson, Mira Akber, Lena Berglin, Helena Bergsten, Susanna Brighenti, Demi Brownlie, Marta Butrym, Benedict Chambers, Puran Chen, Martin Cornillet Jeannin, Jonathan Grip, Angelica Cuapio Gomez, Lena Dillner, Isabel Diaz Lozano, Majda Dzidic, Malin Flodström Tullberg, Anna Färnert, Hedvig Glans, Alvaro Haroun-Izquierdo, Elizabeth Henriksson, Laura Hertwig, Sadaf Kalsum, Efthymia Kokkinou, Egle Kvedaraite, Marco Loreti, Magalini Lourda, Kimia Maleki, Karl-Johan Malmberg, Nicole Marquardt, Christopher Maucourant, Jakob Michaelsson, Jenny Mjösberg, Kirsten Moll, Jagadees Muva, Johan Mårtensson, Pontus Nauclér, Anna Norrby-Teglund, Laura Palma Medina, Björn Persson, Lena Radler, Emma Ringqvist, John Tyler Sandberg, Ebba Sohlberg, Tea Soini, Mattias Svensson, Janne Tynell, Renata Varnaite, Andreas Von Kries, Christian Unge, Olav Rooyackers, Lars I. Eriksson, Jan-Inge Henter, Anders Sönnerborg, Tobias Allander, Jan Albert, Morten Nielsen, Jonas Klingström, Sara Gredmark-Russ, Niklas K. Björkström, Johan K. Sandberg, David A. Price, Hans-Gustaf Ljunggren, Soo Aleman, and Marcus Buggert. Robust T Cell Immunity in Convalescent Individuals with Asymptomatic or Mild COVID-19. *Cell*, 183(1):158–168.e14, October 2020.

[319] Alba Grifoni, Daniela Weiskopf, Sydney I. Ramirez, Jose Mateus, Jennifer M. Dan, Carolyn Rydyznski Moderbacher, Stephen A. Rawlings, Aaron Sutherland, Lakshmanane Premkumar, Ramesh S. Jadi, Daniel Marrama, Aravinda M. de Silva, April Frazier, Aaron F. Carlin, Jason A. Greenbaum, Bjoern Peters, Florian Krammer, Davey M. Smith, Shane Crotty, and Alessandro Sette. Targets of T Cell Responses to SARS-CoV-2 Coronavirus in Humans with COVID-19 Disease and Unexposed Individuals. *Cell*, 181(7):1489–1501.e15, June 2020.

[320] Yanchun Peng, Alexander J. Mentzer, Guihai Liu, Xuan Yao, Zixi Yin, Danning Dong, Wanwisa Dejnirattisai, Timothy Rostron, Piyada Supasa, Chang Liu, César López-Camacho, Jose Slon-Campos, Yuguang Zhao, David I. Stuart, Guido C. Paesen, Jonathan M. Grimes, Alfred A. Antson, Oliver W. Bayfield, Dorothy E. D. P. Hawkins, De-Sheng Ker, Beibei Wang, Lance Turtle, Krishanthi Subramaniam, Paul Thomson, Ping Zhang, Christina Dold, Jeremy Ratcliff, Peter Simmonds, Thushan de Silva, Paul Sopp, Dannielle Wellington, Ushani Rajapaksa, Yi-Ling Chen, Mariolina Salio, Giorgio Napolitani, Wayne Paes, Persephone Borrow, Benedikt M. Kessler, Jeremy W. Fry, Nikolai F. Schwabe, Malcolm G. Semple, J. Kenneth Baillie, Shona C. Moore, Peter J. M. Openshaw, M. Azim Ansari, Susanna Dunachie, Eleanor Barnes, John Frater, Georgina Kerr, Philip Goulder, Teresa Lockett, Robert Levin, Yonghong Zhang, Ronghua Jing, Ling-Pei Ho, Richard J. Cornall, Christopher P. Conlon, Paul Klenerman, Gavin R. Screaton, Juthathip Mongkolsapaya, Andrew McMichael, Julian C. Knight, Graham Ogg, and Tao Dong. Broad and strong memory CD4+ and CD8+ T cells induced by SARS-CoV-2 in UK convalescent individuals following COVID-19. *Nature Immunology*, 21(11):1336–1345, November 2020. Number: 11 Publisher: Nature Publishing Group.

[321] Agnes Bonifacius, Sabine Tischer-Zimmermann, Anna C. Dragon, Daniel Gussarow, Alexander Vogel, Ulrike Krettek, Nina Gödecke, Mustafa Yilmaz, Anke R. M. Kraft, Marius M. Hoeper, Isabell Pink, Julius J. Schmidt, Yang Li, Tobias Welte, Britta Maecker-Kolhoff, Jörg Martens, Marc Moritz Berger, Corinna Lobenwein, Metodi V. Stankov, Markus Cornberg, Sascha David, Georg M. N. Behrens, Oliver Witzke, Rainer Blasczyk, and Britta Eiz-Vesper. COVID-19 immune signatures reveal stable antiviral T cell function despite declining humoral responses. *Immunity*, 54(2):340–354.e6, February 2021.

[322] Bo Diao, Chenhui Wang, Yingjun Tan, Xiewan Chen, Ying Liu, Lifen Ning, Li Chen, Min Li, Yueping Liu, Gang Wang, Zilin Yuan, Zeqing Feng, Yi Zhang, Yuzhang Wu, and Yongwen Chen. Reduction and Functional Exhaustion of T Cells in Patients With Coronavirus Disease 2019 (COVID-19). *Frontiers in Immunology*, 11, 2020.

[323] Guang Chen, Di Wu, Wei Guo, Yong Cao, Da Huang, Hongwu Wang, Tao Wang, Xiaoyun Zhang, Huilong Chen, Haijing Yu, Xiaoping Zhang, Minxia Zhang, Shiji Wu, Jianxin Song, Tao Chen, Meifang Han, Shusheng Li, Xiaoping Luo, Jianping Zhao, and Qin Ning. Clinical and immunological features of severe and moderate coronavirus disease 2019. *The Journal of Clinical Investigation*, 130(5):2620–2629, May 2020. Publisher: American Society for Clinical Investigation.

[324] Daniel M. Altmann and Rosemary J. Boyton. SARS-CoV-2 T cell immunity: Specificity, function, durability, and role in protection. *Science Immunology*, 5(49):eabd6160, July 2020. Publisher: American Association for the Advancement of Science.

[325] Alessandro Napoli, Massimiliano Valentini, Nicola Tirelli, Martin Müller, and Jeffrey A. Hubbell. Oxidation-responsive polymeric vesicles. *Nature Materials*, 3(3):183–189, March 2004. Number: 3 Publisher: Nature Publishing Group.

[326] Simona Cerritelli, Conlin P. O'Neil, Diana Velluto, Antonella Fontana, Marc Adrian, Jacques Dubochet, and Jeffrey A. Hubbell. Aggregation Behavior of Poly(ethylene glycol-bl-propylene sulfide) Di- and Triblock Copolymers in Aqueous Solution. *Langmuir*, 25(19):11328–11335, October 2009. Publisher: American Chemical Society.

[327] Clara Galan-Navarro, Marcela Rincon-Restrepo, Gert Zimmer, Erica Ollmann Saphire, Jeffrey A. Hubbell, Sachiko Hirosue, Melody A. Swartz, and Stefan Kunz. Oxidation-sensitive polymersomes as vaccine nanocarriers enhance humoral responses against Lassa virus envelope glycoprotein. *Virology*, 512:161–171, December 2017.

[328] Fatima Amanat, Daniel Stadlbauer, Shirin Strohmeier, Thi H. O. Nguyen, Veronika Chromikova, Meagan McMahon, Kaijun Jiang, Guha Asthagiri Arunkumar, Denise Jurczyszak, Jose Polanco, Maria Bermudez-Gonzalez, Giulio Kleiner, Teresa Aydillo, Lisa Miorin, Daniel S. Fierer, Luz Amarilis Lugo, Erna Milunka Kojic, Jonathan Stoever, Sean T. H. Liu, Charlotte Cunningham-Rundles, Philip L. Felgner, Thomas Moran, Adolfo García-Sastre, Daniel Caplivski, Allen C. Cheng, Katherine Kedzierska, Olli Vapalahti, Jussi M. Hepojoki, Viviana Simon, and Florian Krammer. A serological assay to detect SARS-CoV-2 seroconversion in humans. *Nature Medicine*, 26(7):1033–1036, July 2020. Number: 7 Publisher: Nature Publishing Group.

[329] Sean Allen, Omar Osorio, Yu-Gang Liu, and Evan Scott. Facile assembly and loading of theranostic polymersomes via multi-impingement flash nanoprecipitation. *Journal of Controlled Release: Official Journal of the Controlled Release Society*, 262:91–103, September 2017.

[330] Samar Hamdy, Azita Haddadi, Vishwa Somayaji, David Ruan, and John Samuel. Pharmaceutical analysis of synthetic lipid A-based vaccine adjuvants in poly (D,L-lactic-co-glycolic acid) nanoparticle formulations. *Journal of Pharmaceutical and Biomedical Analysis*, 44(4):914–923, August 2007.

[331] M. B. Lutz, N. Kukutsch, A. L. Ogilvie, S. Rössner, F. Koch, N. Romani, and G. Schuler. An advanced culture method for generating large quantities of highly pure dendritic cells from mouse bone marrow. *Journal of Immunological Methods*, 223(1):77–92, February 1999.

[332] Na Zhu, Dingyu Zhang, Wenling Wang, Xingwang Li, Bo Yang, Jingdong Song, Xiang Zhao, Baoying Huang, Weifeng Shi, Roujian Lu, Peihua Niu, Faxian Zhan, Xuejun Ma, Dayan Wang, Wenbo Xu, Guizhen Wu, George F. Gao, and Wenjie Tan. A Novel Coronavirus from Patients with Pneumonia in China, 2019. *New England Journal of Medicine*, 382(8):727–733, February 2020. Publisher: Massachusetts Medical Society.

[333] Tracy L. Stevens, Alexis Bossie, Virginia M. Sanders, Rafael Fernandez-Botran, Robert L. Coffman, Timothy R. Mosmann, and Ellen S. Vitetta. Regulation of antibody isotype secretion by subsets of antigen-specific helper T cells. *Nature*, 334(6179):255–258, July 1988. Number: 6179 Publisher: Nature Publishing Group.

[334] D. M. Hinton. Convalescent Plasma EUA Letter of Authorization, March 2021.

[335] Chunyan Yi, Xiaoyu Sun, Jing Ye, Longfei Ding, Meiqin Liu, Zhuo Yang, Xiao Lu, Yaguang Zhang, Liyang Ma, Wangpeng Gu, Aidong Qu, Jianqing Xu, Zhengli Shi, Zhiyang Ling, and Bing Sun. Key residues of the receptor binding motif in the spike protein of SARS-CoV-2 that interact with ACE2 and neutralizing antibodies. *Cellular & Molecular Immunology*, 17(6):621–630, June 2020. Number: 6 Publisher: Nature Publishing Group.

[336] Jian Shang, Gang Ye, Ke Shi, Yushun Wan, Chuming Luo, Hideki Aihara, Qibin Geng, Ashley Auerbach, and Fang Li. Structural basis of receptor recognition by SARS-CoV-2. *Nature*, 581(7807):221–224, May 2020. Number: 7807 Publisher: Nature Publishing Group.

[337] Youn Soo Choi, Robin Kageyama, Danelle Eto, Tania C. Escobar, Robert J. Johnston, Laurel Monticelli, Christopher Lao, and Shane Crotty. ICOS Receptor Instructs T Follicular Helper Cell versus Effector Cell Differentiation via Induction of the Transcriptional Repressor Bcl6. *Immunity*, 34(6):932–946, June 2011.

[338] Munir Akkaya, Kihyuck Kwak, and Susan K. Pierce. B cell memory: building two walls of protection against pathogens. *Nature Reviews Immunology*, 20(4):229–238, April 2020. Number: 4 Publisher: Nature Publishing Group.

[339] Hirochika Toyama, Seiji Okada, Masahiko Hatano, Yoshimasa Takahashi, Nobue Takeda, Hirohito Ichii, Toshitada Takemori, Yoshikazu Kuroda, and Takeshi Tokuhisa. Memory B Cells without Somatic Hypermutation Are Generated from Bcl6-Deficient B Cells. *Immunity*, 17(3):329–339, September 2002.

[340] Simone Mocellin, Francesco M. Marincola, and Howard A. Young. Interleukin-10 and the immune response against cancer: a counterpoint. *Journal of Leukocyte Biology*, 78(5):1043–1051, November 2005.

[341] Tadamitsu Kishimoto. Interleukin-6: discovery of a pleiotropic cytokine. *Arthritis Research & Therapy*, 8(2):S2, July 2006.

[342] Jason G. Cyster and Christopher D. C. Allen. B Cell Responses: Cell Interaction Dynamics and Decisions. *Cell*, 177(3):524–540, April 2019.

[343] Mona O. Mohsen, Lisha Zha, Gustavo Cabral-Miranda, and Martin F. Bachmann. Major findings and recent advances in virus–like particle (VLP)-based vaccines. *Seminars in Immunology*, 34:123–132, December 2017.

[344] Hsueh-Ling Janice Oh, Samuel Ken-En Gan, Antonio Bertoletti, and Yee-Joo Tan. Understanding the T cell immune response in SARS coronavirus infection. *Emerging Microbes & Infections*, 1(1):1–6, July 2012. Publisher: Taylor & Francis _eprint: https://doi.org/10.1038/emi.2012.26.

[345] Hyoung-Shik Shin, Yeonjae Kim, Gayeon Kim, Ji Yeon Lee, Ina Jeong, Joon-Sung Joh, Hana Kim, Eunjin Chang, Soo Yeon Sim, Jun-Sun Park, and Dong-Gyun Lim. Immune Responses to Middle East Respiratory Syndrome Coronavirus During the Acute and

Convalescent Phases of Human Infection. *Clinical Infectious Diseases: An Official Publication of the Infectious Diseases Society of America*, 68(6):984–992, March 2019.

[346] Fumihiko Yasui, Chieko Kai, Masahiro Kitabatake, Shingo Inoue, Misako Yoneda, Shoji Yokochi, Ryoichi Kase, Satoshi Sekiguchi, Kouichi Morita, Tsunekazu Hishima, Hidenori Suzuki, Katsuo Karamatsu, Yasuhiro Yasutomi, Hisatoshi Shida, Minoru Kidokoro, Kyosuke Mizuno, Kouji Matsushima, and Michinori Kohara. Prior Immunization with Severe Acute Respiratory Syndrome (SARS)-Associated Coronavirus (SARS-CoV) Nucleocapsid Protein Causes Severe Pneumonia in Mice Infected with SARS-CoV1. *The Journal of Immunology*, 181(9):6337–6348, November 2008.

[347] Li Liu, Qiang Wei, Qingqing Lin, Jun Fang, Haibo Wang, Hauyee Kwok, Hangying Tang, Kenji Nishiura, Jie Peng, Zhiwu Tan, Tongjin Wu, Ka-Wai Cheung, Kwok-Hung Chan, Xavier Alvarez, Chuan Qin, Andrew Lackner, Stanley Perlman, Kwok-Yung Yuen, and Zhiwei Chen. Anti–spike IgG causes severe acute lung injury by skewing macrophage responses during acute SARS-CoV infection. *JCI Insight*, 4(4), February 2019. Publisher: American Society for Clinical Investigation.

[348] C. R. Casella and T. C. Mitchell. Putting endotoxin to work for us: Monophosphoryl lipid A as a safe and effective vaccine adjuvant. pages 3231–40, October 2008. Num Pages: 3231-40 Publisher: Springer Nature B.V.

[349] F Sallusto, M Cella, C Danieli, and A Lanzavecchia. Dendritic cells use macropinocytosis and the mannose receptor to concentrate macromolecules in the major histocompatibility complex class II compartment: downregulation by cytokines and bacterial products. *Journal of Experimental Medicine*, 182(2):389–400, August 1995.

[350] Víctor Gabriel Morón, Paloma Rueda, Christine Sedlik, and Claude Leclerc. In Vivo, Dendritic Cells Can Cross-Present Virus-Like Particles Using an Endosome-to-Cytosol Pathway 1. *The Journal of Immunology*, 171(5):2242–2250, September 2003.

[351] Martin F. Bachmann and Gary T. Jennings. Vaccine delivery: a matter of size, geometry, kinetics and molecular patterns. *Nature Reviews Immunology*, 10(11):787–796, November 2010. Number: 11 Publisher: Nature Publishing Group.

[352] Anita Gamvrellis, David Leong, Jennifer C Hanley, Sue D Xiang, Patricia Mottram, and Magdalena Plebanski. Vaccines that facilitate antigen entry into dendritic cells. *Immunology & Cell Biology*, 82(5):506–516, 2004. _eprint: https://onlinelibrary.wiley.com/doi/pdf/10.1111/j.0818-9641.2004.01271.x.

[353] Eleni Panagioti, Paul Klenerman, Lian N. Lee, Sjoerd H. van der Burg, and Ramon Arens. Features of Effective T Cell-Inducing Vaccines against Chronic Viral Infections. *Frontiers in Immunology*, 9, 2018.

[354] Beatriz G. de la Torre and Fernando Albericio. The pharmaceutical industry in 2020. An analysis of fda drug approvals from the perspective of molecules. *Molecules*, 26(3):1–14, 2021.

[355] Anne S. De Groot and David W. Scott. Immunogenicity of protein therapeutics. *Trends in Immunology*, 28(11):482–490, 2007.

[356] Vibha Jawa, Frances Terry, Jochem Gokemeijer, Shibani Mitra-Kaushik, Brian J. Roberts, Sophie Tourdot, and Anne S. De Groot. T-cell dependent immunogenicity of protein therapeutics pre-clinical assessment and mitigation–updated consensus and review 2020. *Frontiers in Immunology*, 11, 2020. Publisher: Frontiers Media S.A.

[357] Trevor T. Hansel, Harald Kropshofer, Thomas Singer, Jane A. Mitchell, and Andrew J.T. George. The safety and side effects of monoclonal antibodies. *Nature Reviews Drug Discovery*, 9(4):325–338, 2010. Publisher: Nature Publishing Group.

[358] Lloyd Mayer and Yuki Young. Infusion reactions and their management. *Gastroenterology Clinics of North America*, 35(4):857–866, 2006.

[359] Huub Schellekens and Nicole Casadevall. Immunogenicity of recombinant human proteins: Causes and consequences. *Journal of Neurology, Supplement*, 251(2):4–9, 2004.

[360] Geertje M. Bartelds, Carla A. Wijbrandts, Michael T. Nurmohamed, Steven Stapel, Willem F. Lems, Lucien Aarden, Ben A.C. Dijkmans, Paul Peter Tak, and Gerrit Jan Wolbink. Clinical response to adalimumab: Relationship to anti-adalimumab antibodies and serum adalimumab concentrations in rheumatoid arthritis. *Annals of the Rheumatic Diseases*, 66(7):921–926, 2007.

[361] Gerrit J. Wolbink, Lucien A. Aarden, and B. A.C. Dijkmans. Dealing with immunogenicity of biologicals: Assessment and clinical relevance. *Current Opinion in Rheumatology*, 21(3):211–215, 2009.

[362] I. C. Büttel, P. Chamberlain, Y. Chowers, F. Ehmann, A. Greinacher, R. Jefferis, D. Kramer, H. Kropshofer, P. Lloyd, A. Lubiniecki, R. Krause, A. Mire-Sluis, T. Platts-Mills, J. A. Ragheb, B. M. Reipert, H. Schellekens, R. Seitz, P. Stas, M. Subramanyam, R. Thorpe, J.-H. Trouvin, M. Weise, J. Windisch, and C. K. Schneider. Taking immunogenicity assessment of therapeutic proteins to the next level. *Biologicals: Journal of the International Association of Biological Standardization*, 39(2):100–109, March 2011.

[363] Fda, Cder, and pritzlaffo. Guidance for Industry Immunogenicity Assessment for Therapeutic Protein Products. Technical report, 2014.

[364] Kasper Lamberth, Stine Louise Reedtz-Runge, Jonathan Simon, Ksenia Klementyeva, Gouri Shankar Pandey, Søren Berg Padkjaer, Véronique Pascal, Ileana R León, Charlotte Nini Gudme, Søren Buus, and Zuben E Sauna. Post hoc assessment of the immunogenicity of bioengineered factor VIIa demonstrates the use of preclinical tools. Technical report.

[365] Moustafa Hamze, Sylvain Meunier, Anette Karle, Abdelaziz Gdoura, Amélie Goudet, Natacha Szely, Marc Pallardy, Franck Carbonnel, Sebastian Spindeldreher, Xavier Mariette, Corinne Miceli-Richard, and Bernard Maillère. Characterization of CD4 T

Cell Epitopes of Infliximab and Rituximab Identified from Healthy Donors. *Frontiers in Immunology*, 8, 2017.

[366] Anette Karle, Sebastian Spindeldreher, and Frank Kolbinger. Secukinumab, a novel anti–IL-17A antibody, shows low immunogenicity potential in human in vitro assays comparable to other marketed biotherapeutics with low clinical immunogenicity. *mAbs*, 8(3):536–550, April 2016. Publisher: Taylor and Francis Inc.

[367] Jennifer G. Abelin, Dewi Harjanto, Matthew Malloy, Prerna Suri, Tyler Colson, Scott P. Goulding, Amanda L. Creech, Lia R. Serrano, Gibran Nasir, Yusuf Nasrullah, Christopher D. McGann, Diana Velez, Ying S. Ting, Asaf Poran, Daniel A. Rothenberg, Sagar Chhangawala, Alex Rubinsteyn, Jeff Hammerbacher, Richard B. Gaynor, Edward F. Fritsch, Joel Greshock, Rob C. Oslund, Dominik Barthelme, Terri A. Addona, Christina M. Arieta, and Michael S. Rooney. Defining HLA-II Ligand Processing and Binding Rules with Mass Spectrometry Enhances Cancer Epitope Prediction. *Immunity*, 51(4):766–779.e17, October 2019. Publisher: Cell Press.

[368] Julien Racle, Justine Michaux, Georg Alexander Rockinger, Marion Arnaud, Sara Bobisse, Chloe Chong, Philippe Guillaume, George Coukos, Alexandre Harari, Camilla Jandus, Michal Bassani-Sternberg, and David Gfeller. Robust prediction of HLA class II epitopes by deep motif deconvolution of immunopeptidomes. *Nature Biotechnology*, 37(11):1283–1286, November 2019. Publisher: Nature Publishing Group.

[369] Kurt Drickamer and Maureen E. Taylor. Recent insights into structures and functions of C-type lectins in the immune system. *Current Opinion in Structural Biology*, 34:26–34, October 2015. Publisher: Elsevier Ltd.

[370] Gordon D. Brown, Janet A. Willment, and Lauren Whitehead. C-type lectins in immunity and homeostasis. *Nature Reviews Immunology*, 18(6):374–389, June 2018. Number: 6 Publisher: Nature Publishing Group.

[371] Anna J. Slezak, Aslan Mansurov, Michal M. Raczy, Kevin Chang, Aaron T. Alpar, Abigail L. Lauterbach, Rachel P. Wallace, Rachel K. Weathered, Jorge E.G. Medellin, Claudia Battistella, Laura T. Gray, Tiffany M. Marchell, Suzana Gomes, Melody A. Swartz, and Jeffrey A. Hubbell. Tumor Cell-Surface Binding of Immune Stimulating Polymeric Glyco-Adjuvant via Cysteine-Reactive Pyridyl Disulfide Promotes Antitumor Immunity. *ACS Central Science*, 8(10):1435–1446, October 2022.

[372] Alexander Dobin, Carrie A. Davis, Felix Schlesinger, Jorg Drenkow, Chris Zaleski, Sonali Jha, Philippe Batut, Mark Chaisson, and Thomas R. Gingeras. STAR: Ultrafast universal RNA-seq aligner. *Bioinformatics*, 29(1), 2013.

[373] Artem Tarasov, Albert J. Vilella, Edwin Cuppen, Isaac J. Nijman, and Pjotr Prins. Sambamba: Fast processing of NGS alignment formats. *Bioinformatics*, 31(12), 2015.

[374] Yang Liao, Gordon K. Smyth, and Wei Shi. The Subread aligner: Fast, accurate and scalable read mapping by seed-and-vote. *Nucleic Acids Research*, 41(10), 2013.

[375] Nicolas L. Bray, Harold Pimentel, Páll Melsted, and Lior Pachter. Near-optimal probabilistic RNA-seq quantification. *Nature Biotechnology*, 34(5):525–527, May 2016. Number: 5 Publisher: Nature Publishing Group.

[376] Syed Nisar Hussain Bukhari, Amit Jain, Ehtishamul Haq, Abolfazl Mehbodniya, and Julian Webber. Machine Learning Techniques for the Prediction of B-Cell and T-Cell Epitopes as Potential Vaccine Targets with a Specific Focus on SARS-CoV-2 Pathogen: A Review. *Pathogens*, 11(2):146, January 2022.

[377] Christian M Harding and Mario F Feldman. Glycoengineering bioconjugate vaccines, therapeutics, and diagnostics in E. coli. *Glycobiology*, 29(7):519–529, July 2019.

[378] Albert M. Wu, June H. Wu, Tanuja Singh, Li-Ju Lai, Zhangung Yang, and Anthony Herp. Recognition factors of Ricinus communis agglutinin 1 (RCA1). *Molecular Immunology*, 43(10):1700–1715, April 2006.

[379] Susan J Kelly, Marielle Delnomdedieu, Michael I Oliverio, L David Williams, Mark G P Saifer, Merry R Sherman, Thomas M Coffman, G Allan Johnson, and Michael S Hershfield. Diabetes Insipidus in Uricase-Deficient Mice : A Model for Evaluating Therapy with Poly (Ethylene Glycol) -Modified Uricase. *Journal of the American Society of Nephrology*, 12:1001–1009, 2001. ISBN: 1046-6673 (Print)\r1046-6673 (Linking).

[380] X Wu, M Wakamiya, S Vaishnav, R Geske, C Montgomery, P Jones, A Bradley, and C T Caskey. Hyperuricemia and urate nephropathy in urate oxidase-deficient mice. *Proceedings of the National Academy of Sciences of the United States of America*, 91(2):742–746, January 1994.

[381] Yiling Mi, Marcy Coonce, Dorothy Fiete, Lindsay Steirer, Gabriela Dveksler, R. Reid Townsend, and Jacques U. Baenziger. Functional Consequences of Mannose and Asialoglycoprotein Receptor Ablation*. *Journal of Biological Chemistry*, 291(36):18700–18717, September 2016.

[382] Sven Burgdorf, Andreas Kautz, Volker Böhnert, Percy A. Knolle, and Christian Kurts. Distinct Pathways of Antigen Uptake and Intracellular Routing in CD4 and CD8 T Cell Activation. *Science*, 316(5824):612–616, April 2007. Publisher: American Association for the Advancement of Science.

[383] M. C. Agnes A. Tan, A. Mieke Mommaas, Jan Wouter Drijfhout, Reina Jordens, Jos J. M. Onderwater, Desiree Verwoerd, Aat A. Mulder, Annette N. van der Heiden, Doris Scheidegger, Lauran C. J. M. Oomen, Tom H. M. Ottenhoff, Abraham Tulp, Jacques J. Neefjes, and Frits Koning. Mannose receptor-mediated uptake of antigens strongly enhances HLA class II-restricted antigen presentation by cultured dendritic cells. *European Journal of Immunology*, 27(9):2426–2435, 1997. _eprint: https://onlinelibrary.wiley.com/doi/pdf/10.1002/eji.1830270942.

[384] Verena Schuette, Maria Embgenbroich, Thomas Ulas, Meike Welz, Jonas Schulte-Schrepping, Astrid M. Draffehn, Thomas Quast, Katharina Koch, Melanie Nehring,

Jessica König, Annegret Zweynert, Frederike L. Harms, Nancy Steiner, Andreas Limmer, Irmgard Förster, Friederike Berberich-Siebelt, Percy A. Knolle, Dirk Wohlleber, Waldemar Kolanus, Marc Beyer, Joachim L. Schultze, and Sven Burgdorf. Mannose receptor induces T-cell tolerance via inhibition of CD45 and up-regulation of CTLA-4. *Proceedings of the National Academy of Sciences of the United States of America*, 2016.

[385] Yvette van Kooyk and Teunis B. H. Geijtenbeek. DC-SIGN: escape mechanism for pathogens. *Nature Reviews. Immunology*, 3(9):697–709, September 2003.

[386] Yang Yang, Arjan Barendregt, Johannis P. Kamerling, and Albert J. R. Heck. Analyzing Protein Micro-Heterogeneity in Chicken Ovalbumin by High-Resolution Native Mass Spectrometry Exposes Qualitatively and Semi-Quantitatively 59 Proteoforms. *Analytical Chemistry*, 85(24):12037–12045, December 2013. Publisher: American Chemical Society.

[387] S. Vadhan-Raj, L. E. Fayad, M. A. Fanale, B. Pro, A. Rodriguez, F. B. Hagemeister, C. E. Bueso-Ramos, X. Zhou, P. W. McLaughlin, N. Fowler, J. Shah, R. Z. Orlowski, F. Samaniego, M. Wang, J. E. Cortes, A. Younes, L. W. Kwak, N. J. Sarlis, and J. E. Romaguera. A randomized trial of a single-dose rasburicase versus five-daily doses in patients at risk for tumor lysis syndrome. *Annals of Oncology*, 23(6):1640–1645, June 2012.

[388] John S. Sundy, Herbert S. B. Baraf, Robert A. Yood, N. Lawrence Edwards, Sergio R. Gutierrez-Urena, Edward L. Treadwell, Janitzia Vázquez-Mellado, William B. White, Peter E. Lipsky, Zeb Horowitz, William Huang, Allan N. Maroli, Royce W. Waltrip, II, Steven A. Hamburger, and Michael A. Becker. Efficacy and Tolerability of Pegloticase for the Treatment of Chronic Gout in Patients Refractory to Conventional Treatment: Two Randomized Controlled Trials. *JAMA*, 306(7):711–720, August 2011.

[389] Peter E. Lipsky, Leonard H. Calabrese, Arthur Kavanaugh, John S. Sundy, David Wright, Marsha Wolfson, and Michael A. Becker. Pegloticase immunogenicity: the relationship between efficacy and antibody development in patients treated for refractory chronic gout. *Arthritis Research & Therapy*, 16(2):R60, March 2014.

[390] John A. Albert, Tony Hosey, and Brian LaMoreaux. Increased Efficacy and Tolerability of Pegloticase in Patients With Uncontrolled Gout Co-Treated With Methotrexate: A Retrospective Study. *Rheumatology and Therapy*, 7(3):639–648, September 2020.

[391] G. Shankar, S. Arkin, L. Cocea, V. Devanarayan, S. Kirshner, A. Kromminga, V. Quarmby, S. Richards, C. K. Schneider, M. Subramanyam, S. Swanson, D. Verthelyi, and S. Yim. Assessment and Reporting of the Clinical Immunogenicity of Therapeutic Proteins and Peptides—Harmonized Terminology and Tactical Recommendations. *The AAPS Journal*, 16(4):658–673, July 2014.

[392] Ronald Bentley and A. Neuberger. The mechanism of the action of uricase. *Biochemical Journal*, 52(4):694–699, December 1952.

[393] Philipp Niethammer, Clemens Grabher, A. Thomas Look, and Timothy J. Mitchison. A tissue-scale gradient of hydrogen peroxide mediates rapid wound detection in zebrafish. *Nature*, 459(7249):996–999, June 2009. Number: 7249 Publisher: Nature Publishing Group.

[394] Asmaa El-Kenawi and Brian Ruffell. Inflammation, ROS, and Mutagenesis. *Cancer Cell*, 32(6):727–729, December 2017.

[395] Ana I Fernandes and Gregory Gregoriadis. The effect of polysialylation on the immunogenicity and antigenicity of asparaginase: implication in its pharmacokinetics. *International Journal of Pharmaceutics*, 217(1):215–224, April 2001.

[396] Roy Jefferis. Posttranslational Modifications and the Immunogenicity of Biotherapeutics. *Journal of Immunology Research*, 2016:5358272, 2016.

[397] Ronit Mazor, Masanori Onda, Dong Park, Selamawit Addissie, Laiman Xiang, Jingli Zhang, Raffit Hassan, and Ira Pastan. Dual B- and T-cell de-immunization of recombinant immunotoxin targeting mesothelin with high cytotoxic activity. *Oncotarget*, 7(21):29916–29926, May 2016.

[398] Antonino Cassotta, Vincent Mikol, Thomas Bertrand, Stéphanie Pouzieux, Josiane Le Parc, Paul Ferrari, Jacques Dumas, Michael Auer, Florian Deisenhammer, Matteo Gastaldi, Diego Franciotta, Chiara Silacci-Fregni, Blanca Fernandez Rodriguez, Isabella Giacchetto-Sasselli, Mathilde Foglierini, David Jarrossay, Roger Geiger, Federica Sallusto, Antonio Lanzavecchia, and Luca Piccoli. A single T cell epitope drives the neutralizing anti-drug antibody response to natalizumab in multiple sclerosis patients. *Nature Medicine*, 25(9):1402–1407, September 2019. Number: 9 Publisher: Nature Publishing Group.

[399] S Sakaguchi, N Sakaguchi, M Asano, M Itoh, and M Toda. Immunologic self-tolerance maintained by activated T cells expressing IL-2 receptor alpha-chains (CD25). Breakdown of a single mechanism of self-tolerance causes various autoimmune diseases. *The Journal of Immunology*, 155(3):1151–1164, August 1995.

[400] Jeremy F. Brooks, Corey Tan, James L. Mueller, Kenta Hibiya, Ryosuke Hiwa, Vivasvan Vykunta, and Julie Zikherman. Negative feedback by NUR77/Nr4a1 restrains B cell clonal dominance during early T-dependent immune responses. *Cell Reports*, 36(9):109645, August 2021.

[401] Claude Boyer, Nathalie Auphan, Frédéric Luton, Jean-Marc Malburet, Marc Barad, Jean-Pierre Bizozzero, Hubert Reggio, and Anne-Marie Schmitt-Verhulst. T cell receptor/CD3 complex internalization following activation of a cytolytic T cell clone: Evidence for a protein kinase C-independent staurosporine-sensitive step. *European Journal of Immunology*, 21(7):1623–1634, 1991. _eprint: https://onlinelibrary.wiley.com/doi/pdf/10.1002/eji.1830210707.

[402] Lakshmi Balagopalan, Valarie A. Barr, and Lawrence E. Samelson. Endocytic events in TCR signaling: focus on adapters in microclusters. *Immunological reviews*, 232(1):84–98, November 2009.

[403] A. Subtil, A. Hemar, and A. Dautry-Varsat. Rapid endocytosis of interleukin 2 receptors when clathrin-coated pit endocytosis is inhibited. *Journal of Cell Science*, 107(12):3461–3468, December 1994.

[404] Masamichi Nagae, Sushil K Mishra, Shinya Hanashima, Hiroaki Tateno, and Yoshiki Yamaguchi. Distinct roles for each N-glycan branch interacting with mannose-binding type Jacalin-related lectins Orysata and Calsepa. *Glycobiology*, 27(12):1120–1133, December 2017.

[405] Pauline M. Rudd, Tim Elliott, Peter Cresswell, Ian A. Wilson, and Raymond A. Dwek. Glycosylation and the Immune System. *Science*, 291(5512):2370–2376, March 2001. Publisher: American Association for the Advancement of Science.

[406] A. Vultaggio, A. Matucci, F. Nencini, S. Pratesi, P. Parronchi, O. Rossi, S. Romagnani, and E. Maggi. Anti-infliximab IgE and non-IgE antibodies and induction of infusion-related severe anaphylactic reactions. *Allergy*, 65(5):657–661, May 2010.

[407] Christine H. Chung, Beloo Mirakhur, Emily Chan, Quynh-Thu Le, Jordan Berlin, Michael Morse, Barbara A. Murphy, Shama M. Satinover, Jacob Hosen, David Mauro, Robbert J. Slebos, Qinwei Zhou, Diane Gold, Tina Hatley, Daniel J. Hicklin, and Thomas A.E. Platts-Mills. Cetuximab-Induced Anaphylaxis and IgE Specific for Galactose-α-1,3-Galactose. *New England Journal of Medicine*, 358(11):1109–1117, March 2008. Publisher: Massachusetts Medical Society _eprint: https://doi.org/10.1056/NEJMoa074943.

[408] Hannah J. Gould and Brian J. Sutton. IgE in allergy and asthma today. *Nature Reviews Immunology*, 8(3):205–217, March 2008. Number: 3 Publisher: Nature Publishing Group.

[409] Thomas Sajda and Animesh A. Sinha. Autoantibody Signaling in Pemphigus Vulgaris: Development of an Integrated Model. *Frontiers in Immunology*, 9:692, April 2018.

[410] Nils Erik Gilhus, Geir Olve Skeie, Fredrik Romi, Konstantinos Lazaridis, Paraskevi Zisimopoulou, and Socrates Tzartos. Myasthenia gravis — autoantibody characteristics and their implications for therapy. *Nature Reviews Neurology*, 12(5):259–268, May 2016. Number: 5 Publisher: Nature Publishing Group.

[411] Rebecca A. Elsner and Mark J. Shlomchik. Germinal Center and Extrafollicular B Cell Responses in vaccination, immunity and autoimmunity. *Immunity*, 53(6):1136–1150, December 2020.

[412] Francesca Salamanna, Melania Maglio, Maria Paola Landini, and Milena Fini. Body Localization of ACE-2: On the Trail of the Keyhole of SARS-CoV-2. *Frontiers in Medicine*, 7, 2020.

[413] Kathryn A. Pape, Justin J. Taylor, Robert W. Maul, Patricia J. Gearhart, and Marc K. Jenkins. Different B Cell Populations Mediate Early and Late Memory During an Endogenous Immune Response. *Science*, 331(6021):1203–1207, March 2011. Publisher: American Association for the Advancement of Science.

[414] Justin J. Taylor, Kathryn A. Pape, Holly R. Steach, and Marc K. Jenkins. Apoptosis and antigen affinity limit effector cell differentiation of a single naïve B cell. *Science*, 347(6223):784–787, February 2015. Publisher: American Association for the Advancement of Science.

[415] Ann M. Kerrigan and Gordon D. Brown. C-type lectins and phagocytosis. *Immunobiology*, 214(7):562–575, 2009.

[416] Mariken E. Luca, Junda M. Kel, Wouter van Rijs, Jan Wouter Drijfhout, Frits Koning, and Lex Nagelkerken. Mannosylated PLP139–151 induces peptide-specific tolerance to experimental autoimmune encephalomyelitis. *Journal of Neuroimmunology*, 160(1):178–187, March 2005.

[417] Marcello Chieppa, Giancarlo Bianchi, Andrea Doni, Annalisa Del Prete, Marina Sironi, Gordana Laskarin, Paolo Monti, Lorenzo Piemonti, Andrea Biondi, Alberto Mantovani, Martino Introna, and Paola Allavena. Cross-Linking of the Mannose Receptor on Monocyte-Derived Dendritic Cells Activates an Anti-Inflammatory Immunosuppressive Program 1. *The Journal of Immunology*, 171(9):4552–4560, November 2003.

[418] P. Allavena, M. Chieppa, G. Bianchi, G. Solinas, M. Fabbri, G. Laskarin, and A. Mantovani. Engagement of the Mannose Receptor by Tumoral Mucins Activates an Immune Suppressive Phenotype in Human Tumor-Associated Macrophages. *Journal of Immunology Research*, 2010:e547179, February 2011. Publisher: Hindawi.

[419] Amy J. Foster, Jessie H. Bird, Mattie S. M. Timmer, and Bridget L. Stocker. The Ligands of C-Type Lectins. *C-Type Lectin Receptors in Immunity*, pages 191–215, December 2015.

[420] Mirat Sojitra, Susmita Sarkar, Jasmine Maghera, Emily Rodrigues, Eric J. Carpenter, Shaurya Seth, Daniel Ferrer Vinals, Nicholas J. Bennett, Revathi Reddy, Amira Khalil, Xiaochao Xue, Michael R. Bell, Ruixiang Blake Zheng, Ping Zhang, Corwin Nycholat, Justin J. Bailey, Chang-Chun Ling, Todd L. Lowary, James C. Paulson, Matthew S. Macauley, and Ratmir Derda. Genetically encoded multivalent liquid glycan array displayed on M13 bacteriophage. *Nature Chemical Biology*, 17(7):806–816, July 2021. Number: 7 Publisher: Nature Publishing Group.

[421] Simon Wisnovsky and Carolyn R. Bertozzi. Reading the glyco-code: New approaches to studying protein–carbohydrate interactions. *Current Opinion in Structural Biology*, 75:102395, August 2022.

[422] David A. Hill and Jonathan M. Spergel. The Atopic March: Critical Evidence and Clinical Relevance. *Annals of allergy, asthma & immunology : official publication of*

the American College of Allergy, Asthma, & Immunology, 120(2):131–137, February 2018.

[423] Arielle Glatman Zaretsky, Christoph Konradt, Fabien Dépis, James B. Wing, Radhika Goenka, Daniela Gomez Atria, Jonathan S. Silver, Sunglim Cho, Amaya I. Wolf, William J. Quinn, Julie B. Engiles, Dorothy C. Brown, Daniel Beiting, Jan Erikson, David Allman, Michael P. Cancro, Shimon Sakaguchi, Lifan Lu, Christophe O. Benoist, and Christopher A. Hunter. T Regulatory Cells Support Plasma Cell Populations in the Bone Marrow. *Cell reports*, 18(8):1906–1916, February 2017.